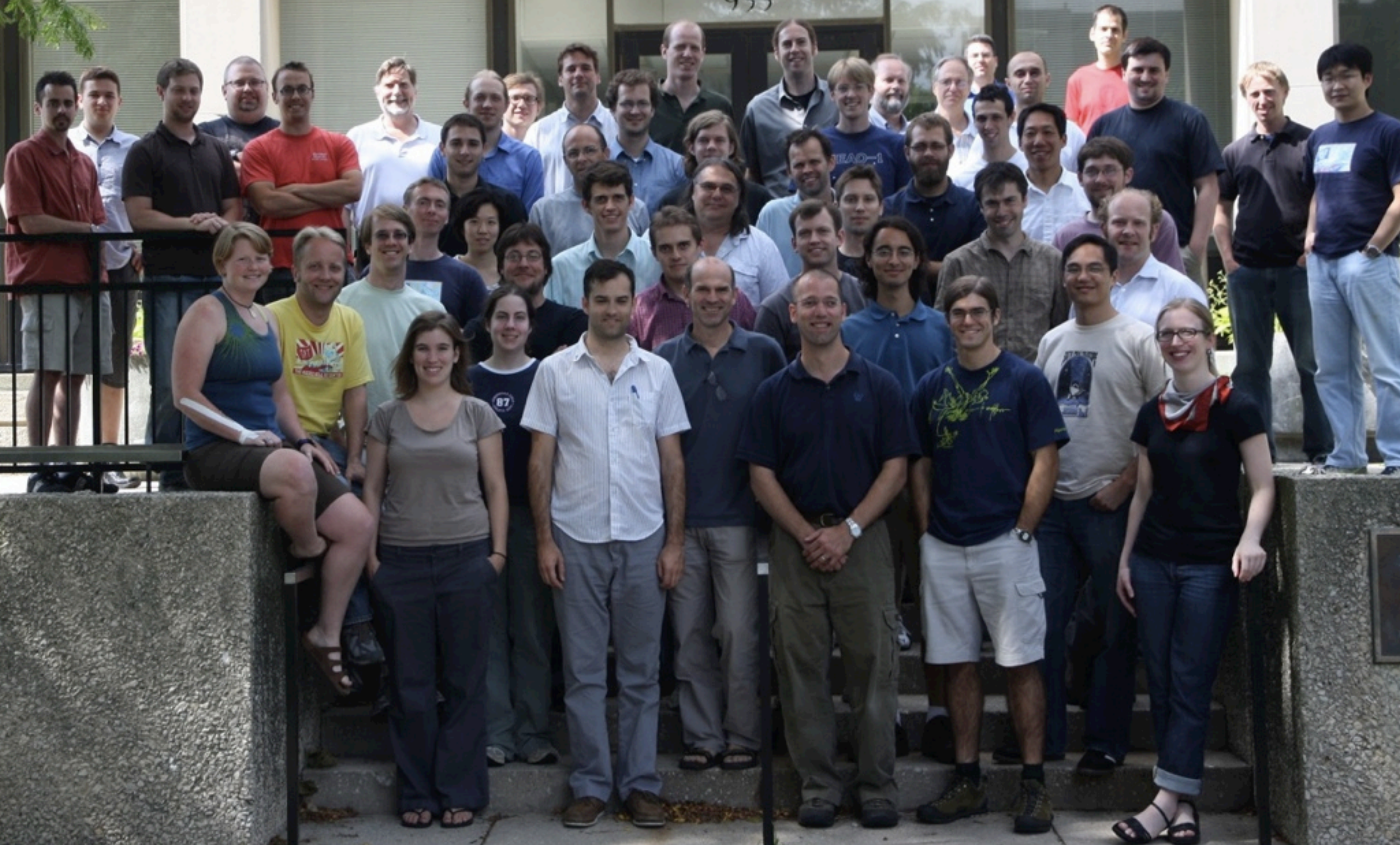
A large radio telescope dish is mounted on a snowy mountain peak. The dish is white and has a complex, lattice-like structure. It is positioned on a concrete base. The background shows a vast, snow-covered landscape under a clear sky with a soft orange glow from the setting or rising sun. The overall scene is serene and remote.

Cluster Cosmology with the South Pole Telescope

Lindsey Bleem

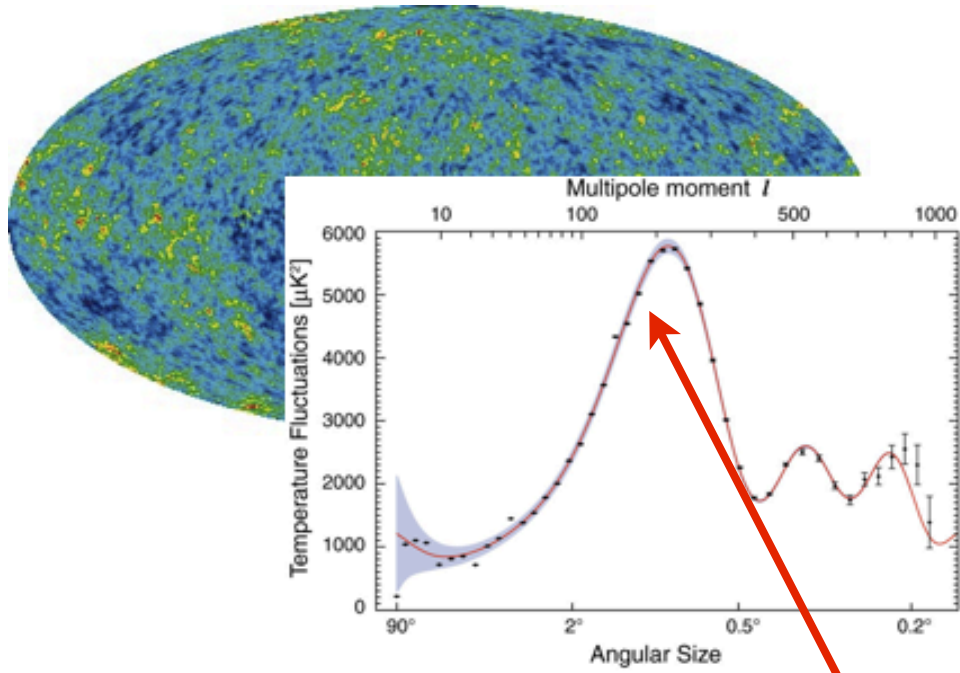
July 1, 2013

SPT Team July 2010

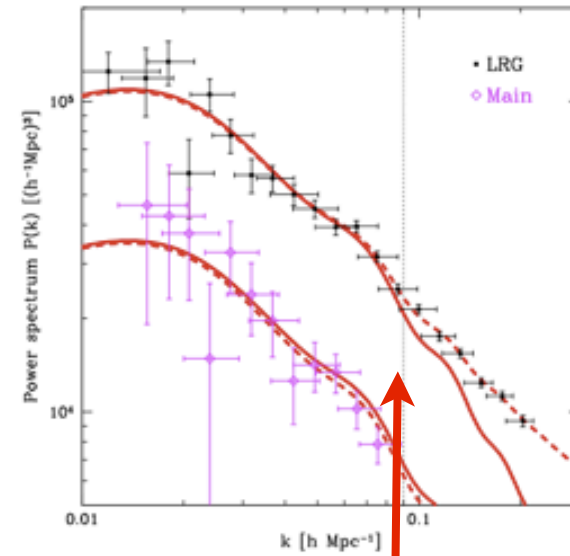


Outline

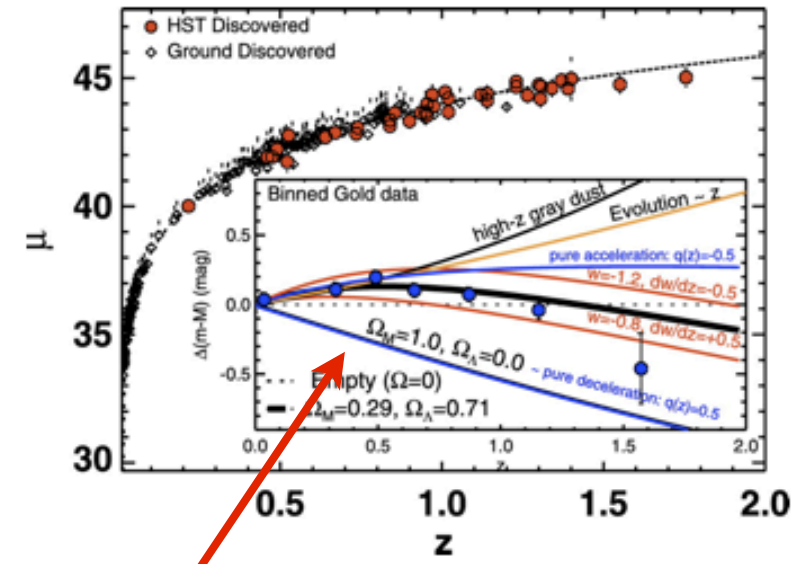
- Brief Introduction
- The SPT Cluster Sample
- Example Joint Optical-SZ Study



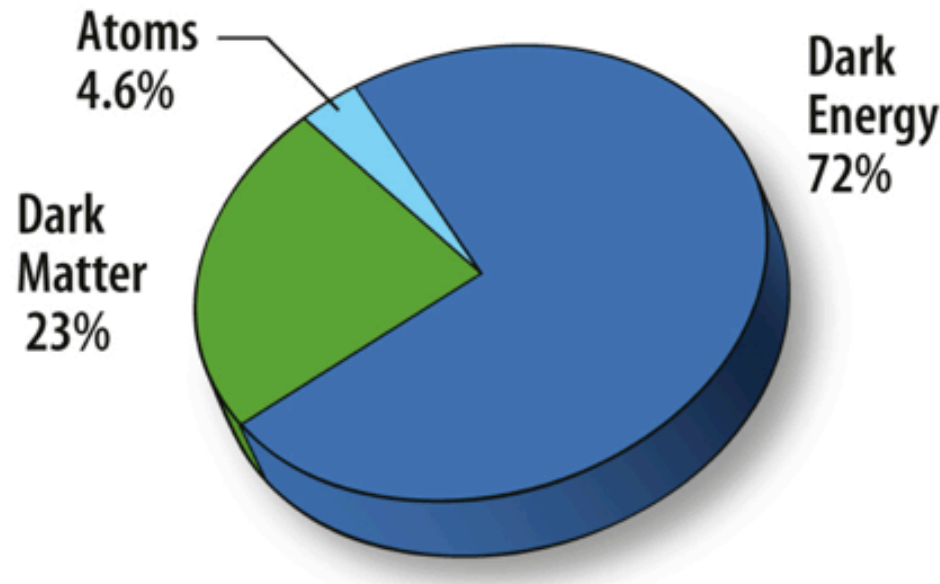
Tegmark et al 2006



Riess et al 2007

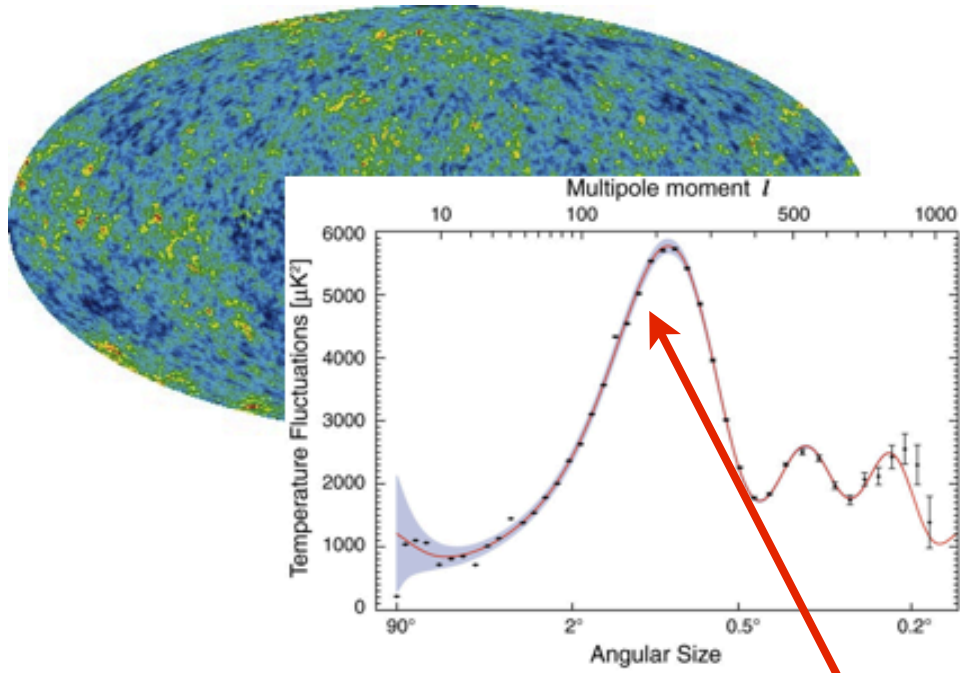


CMB + Large Scale Structure + SNe Ia

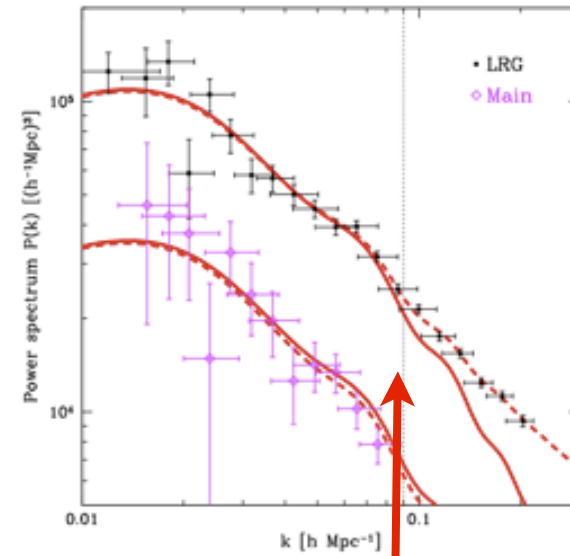


We live in a flat universe whose density is dominated by dark energy

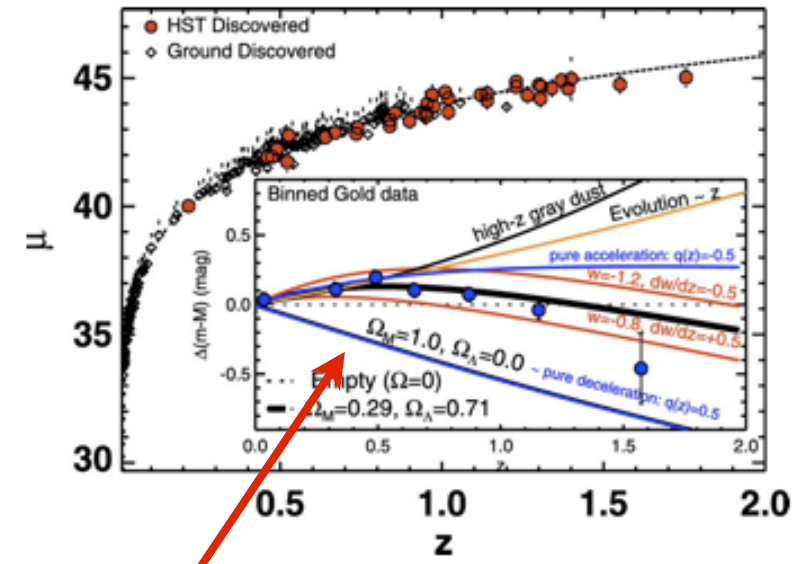
... but what is dark energy?



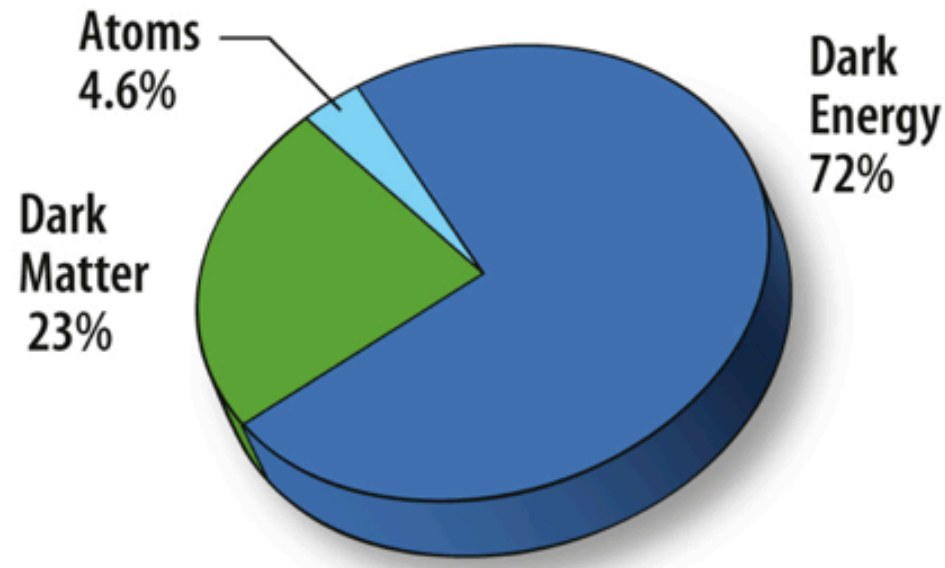
Tegmark et al 2006



Riess et al 2007

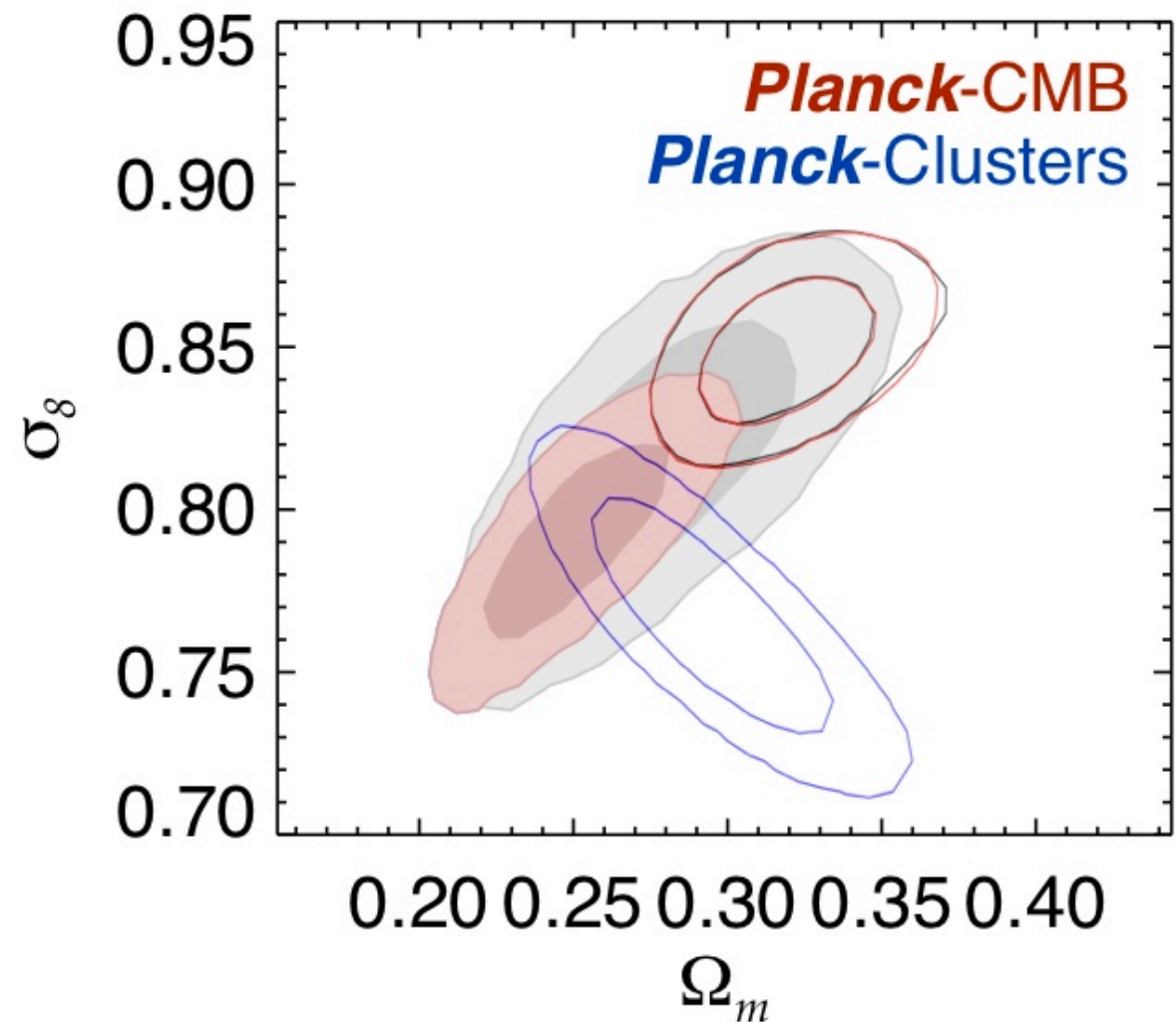
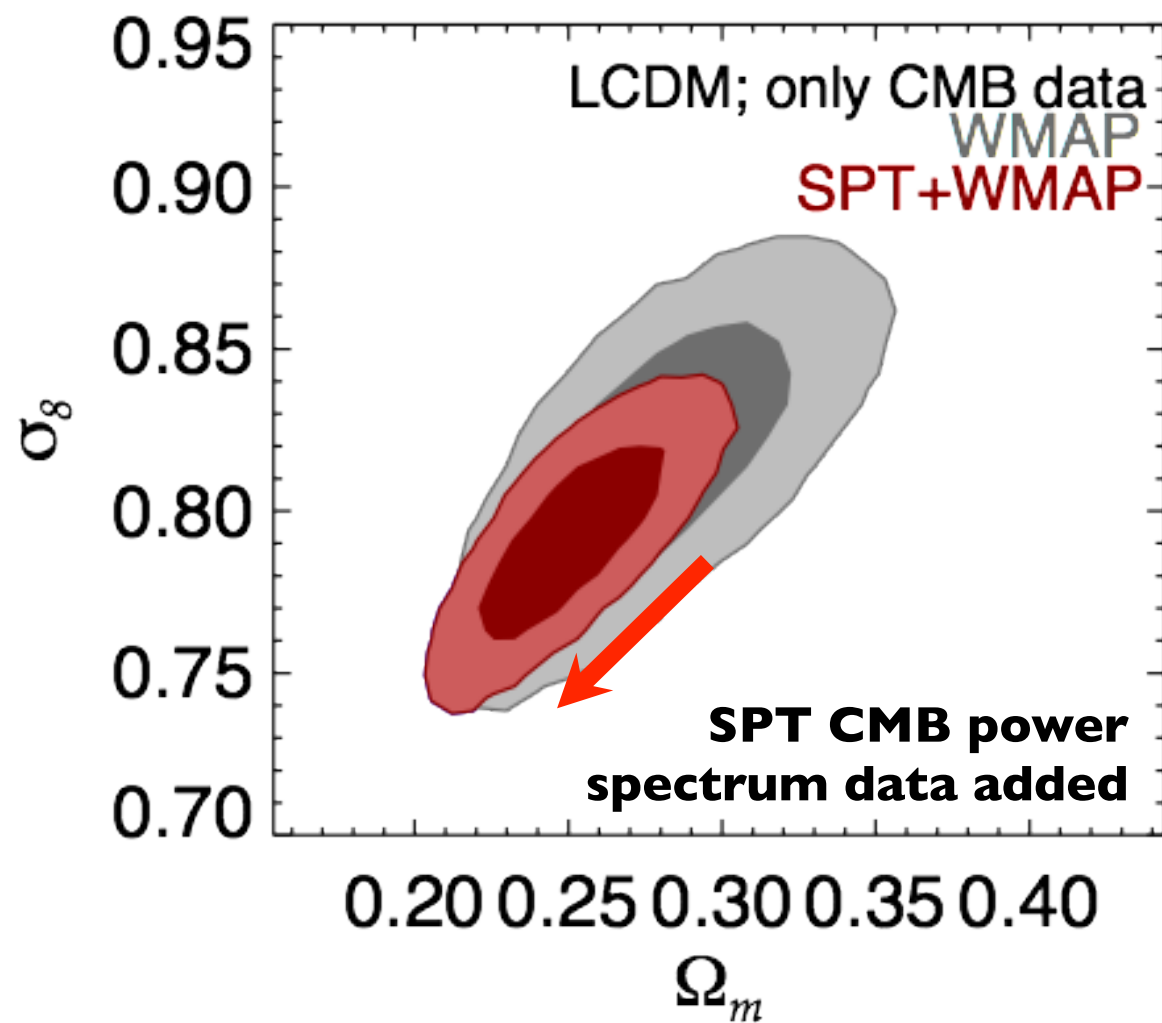


CMB + Large Scale Structure + SNe Ia



Galaxy clusters, as a probes of the growth of structure, can be used to study Dark Energy.

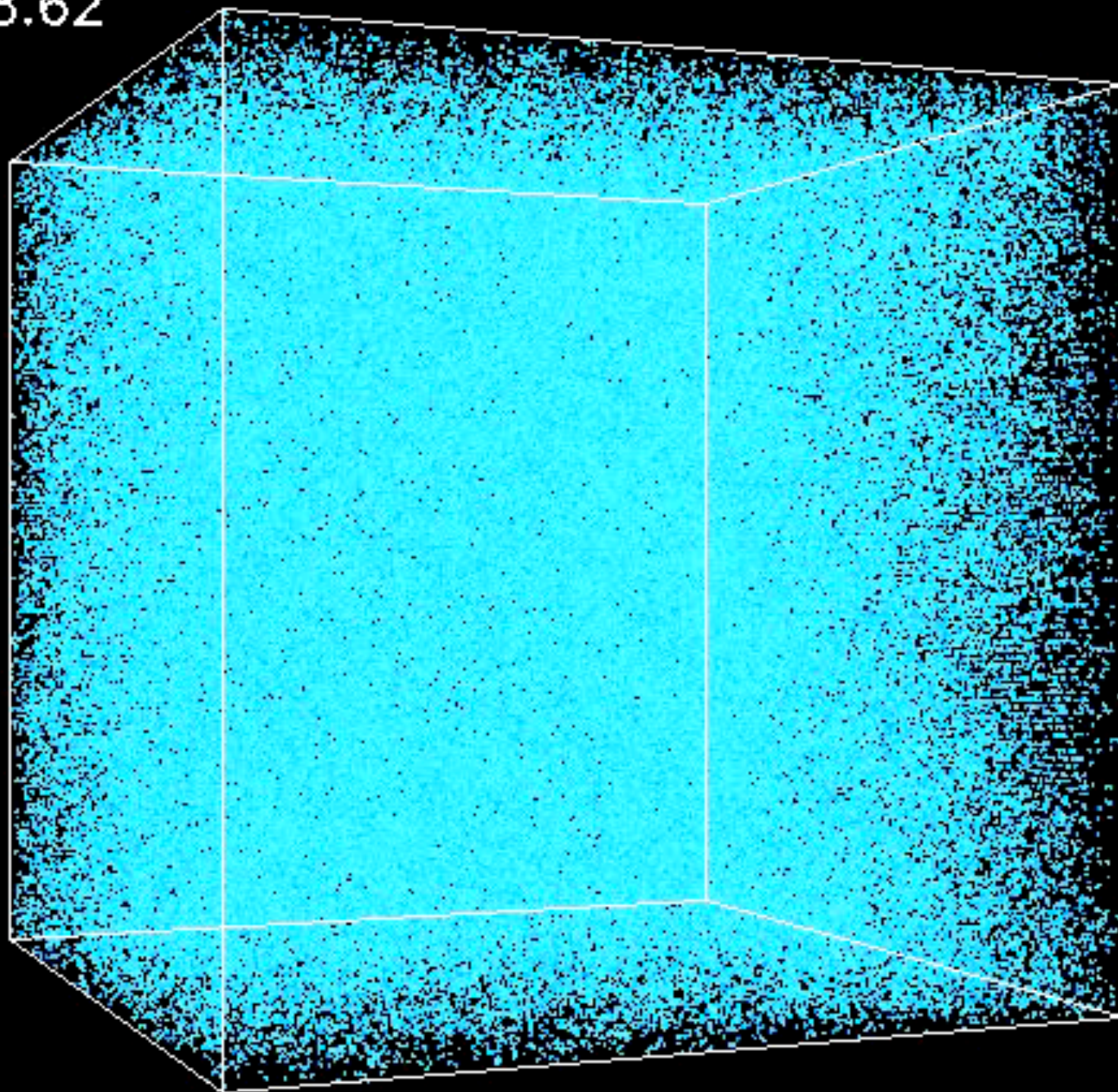
CMB Constraints on σ_8 , Ω_m



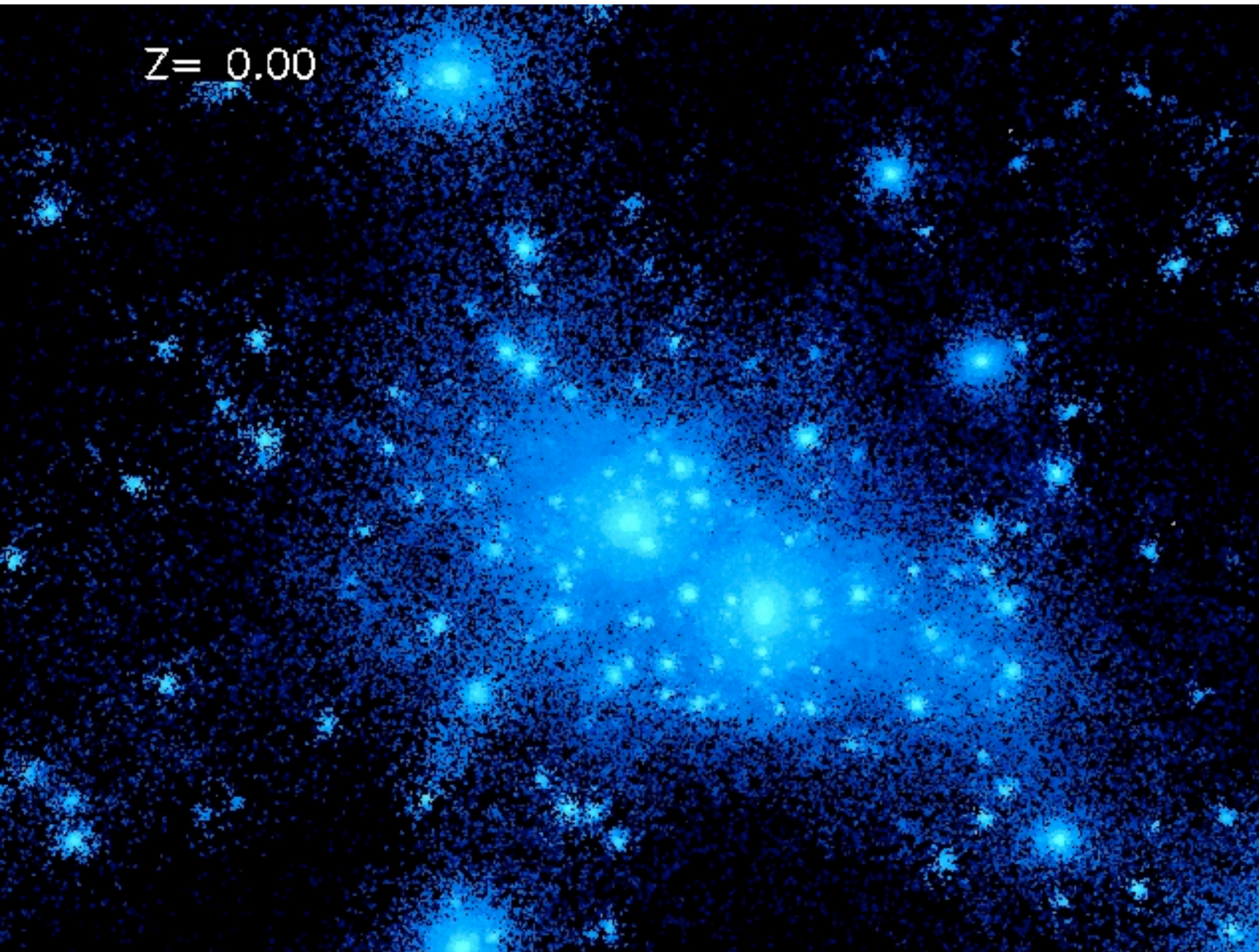
	WMAP7	WMAP7+SPT	Planck-CMB
σ_8	0.819 +/- 0.031	0.795 +/- 0.022	0.829 +/- 0.012
Ω_m	0.276 +/- 0.029	0.250 +/- 0.020	0.315 +/- 0.016

(WMAP7) Komatsu
+2011
(SPT) Story+2012
Planck XX 2013
Planck XVI 2013

$Z=28.62$

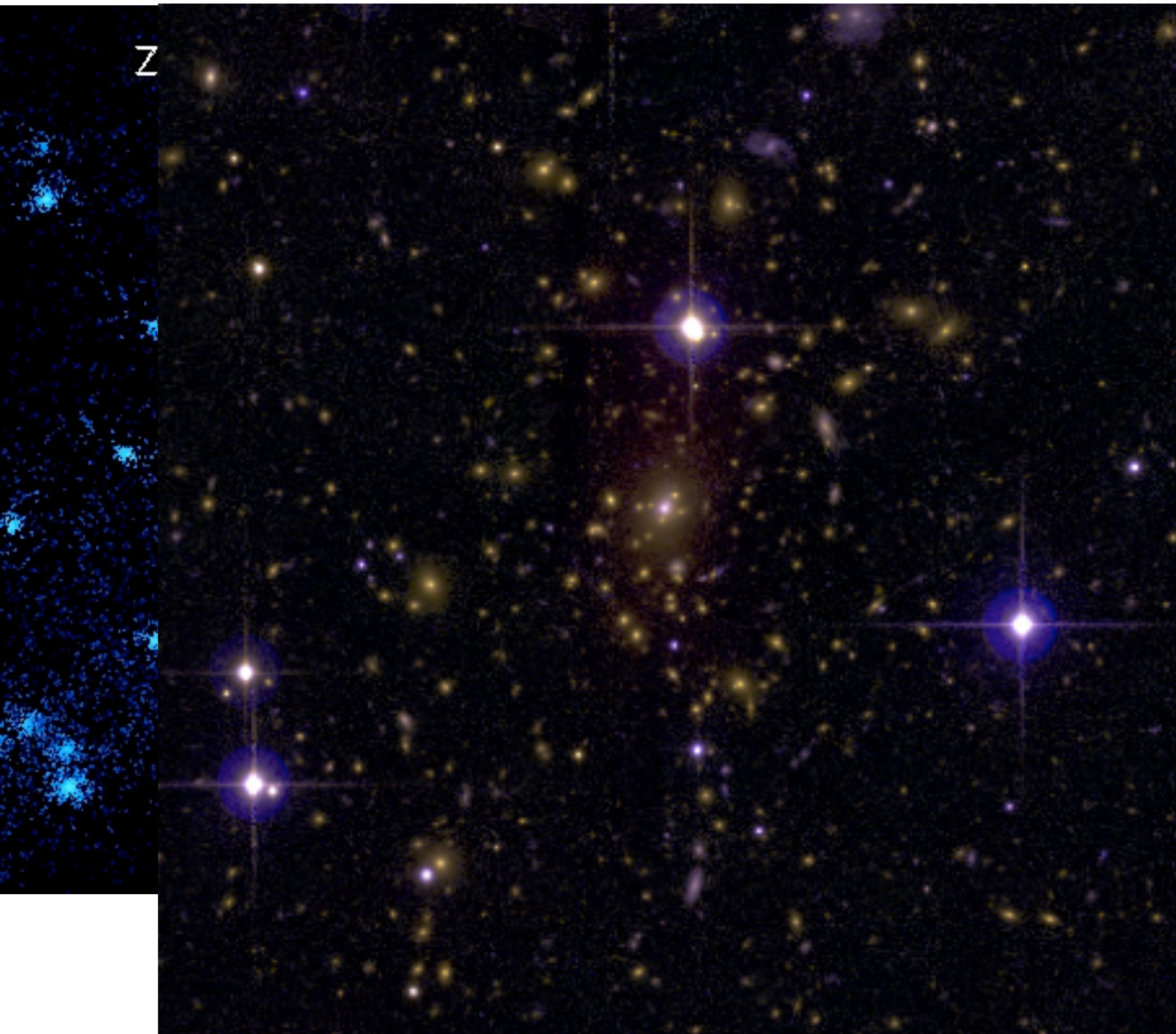


$Z = 0.00$



Simulations
Scale: 4Mpc

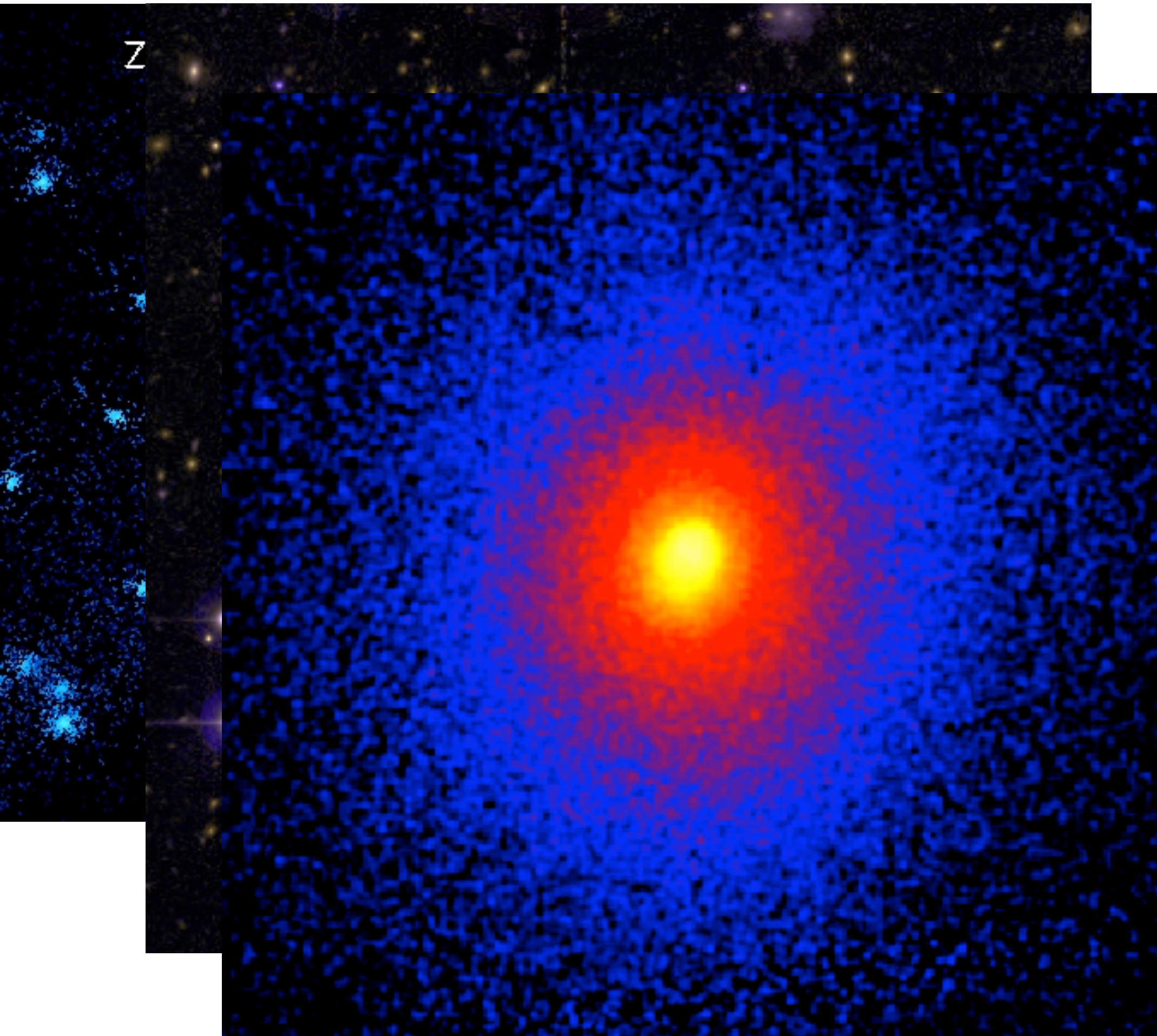
Kravtsov et al.



Optical

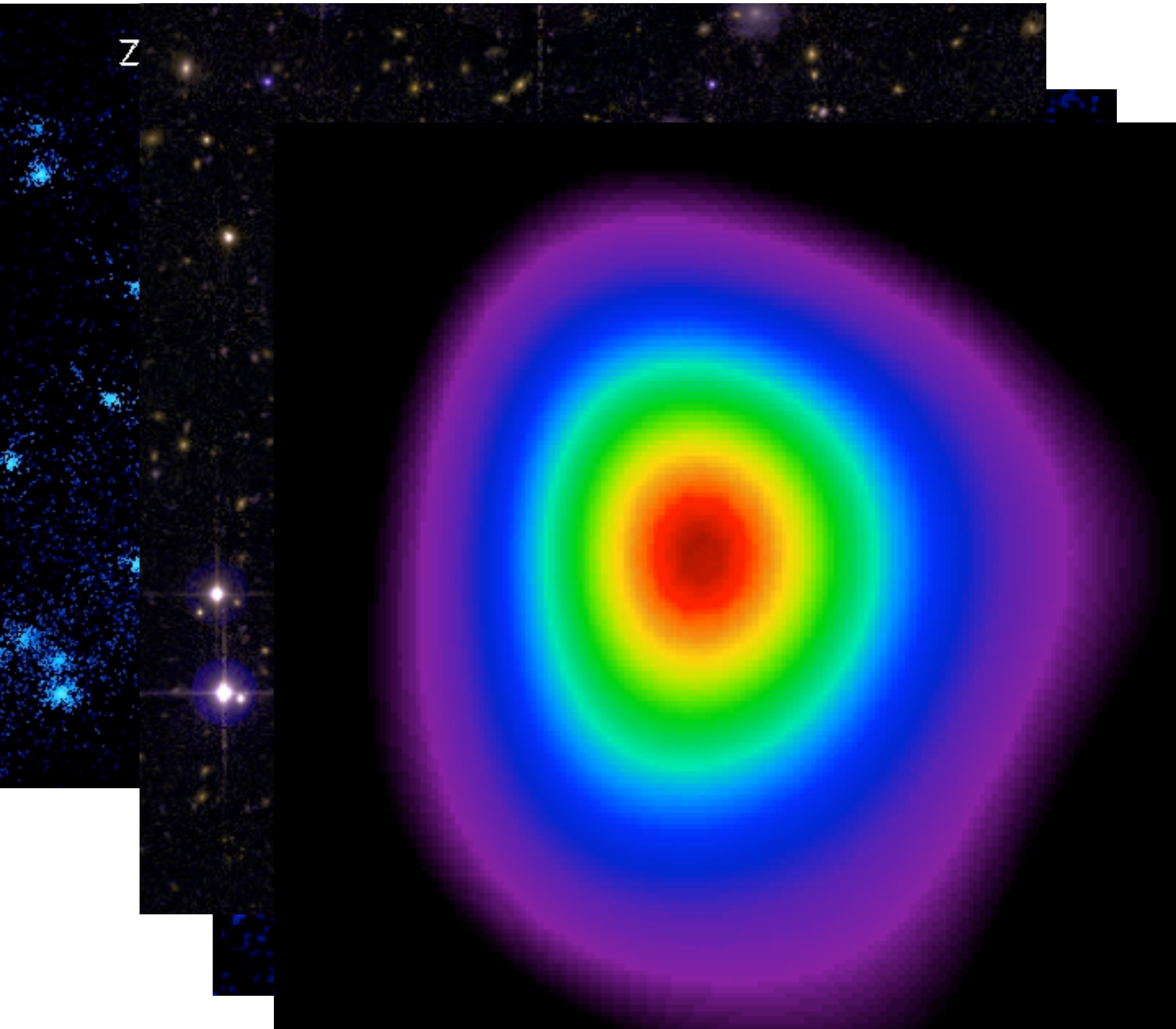
Scale 1.2 Mpc
(5', $z=0.23$)

Allen et al.



X-ray

Allen et al.



z

mm

Allen et al.

We can use the abundance of clusters to probe dark energy.

Cluster Abundance, dN/dz

$$\frac{dN}{d\Omega dz} = n(z) \frac{dV}{d\Omega dz}$$

Depends on:

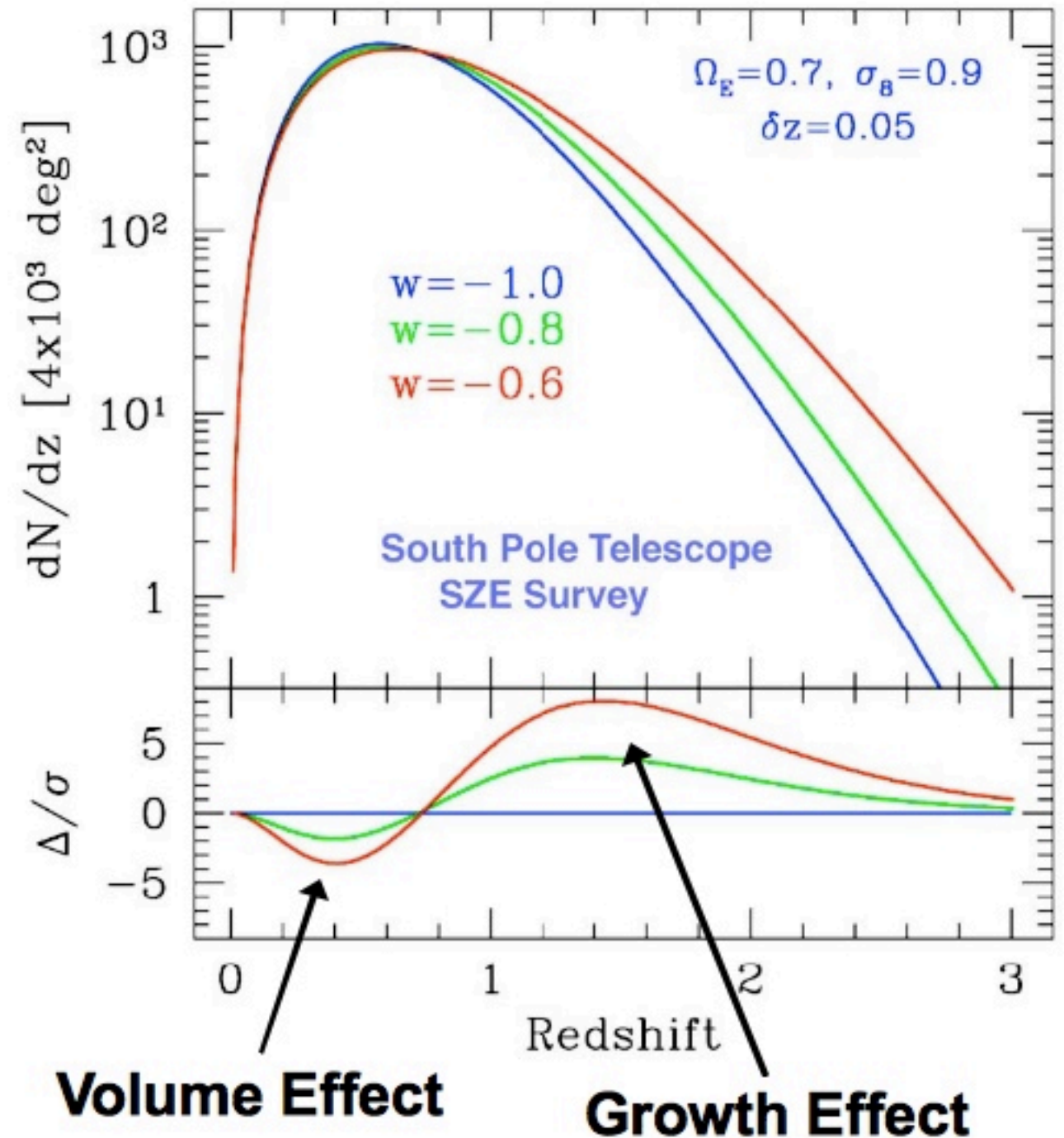
Matter Power Spectrum, $P(k)$
& exponentially on the
Growth Rate of Structure, $D(z)$

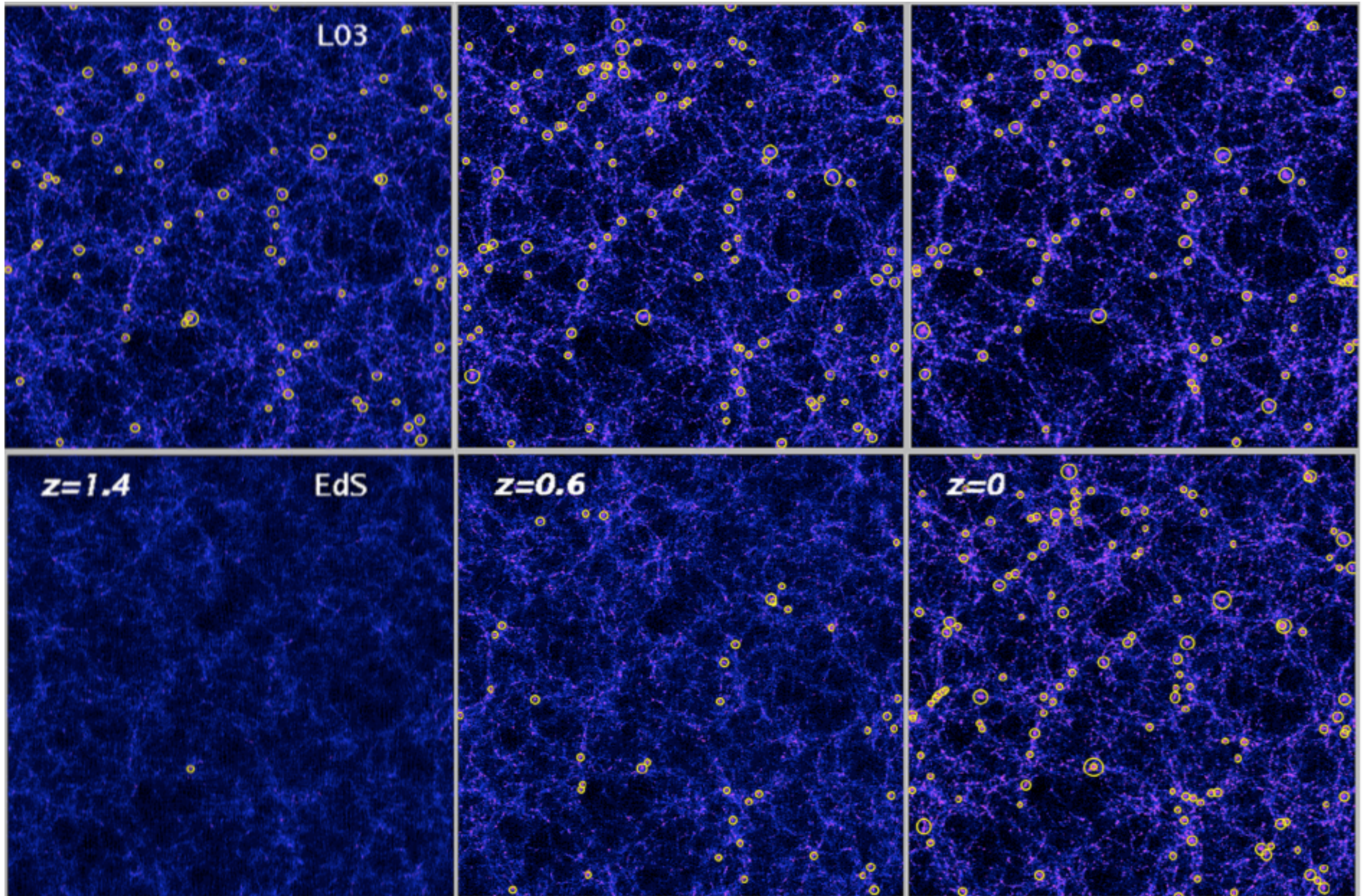
Depends on:

Rate of Expansion, $H(z)$

$$\rho \propto a^{-3(1+w)}$$

Credit: Joe Mohr





Source Borgani and Guzzo 2001

The cluster mass budget

Matter component	% total mass	% baryonic mass
<i>Dark matter</i>	85-90 %	(na)
<i>Baryons</i>	10-15 %	100 %
Hot gas	7-14 %	70-95%
Stars	0.5-5 %	5-30 %
Galaxies	0.5-4 %	4-27 %

For Cosmology with Clusters We Need To

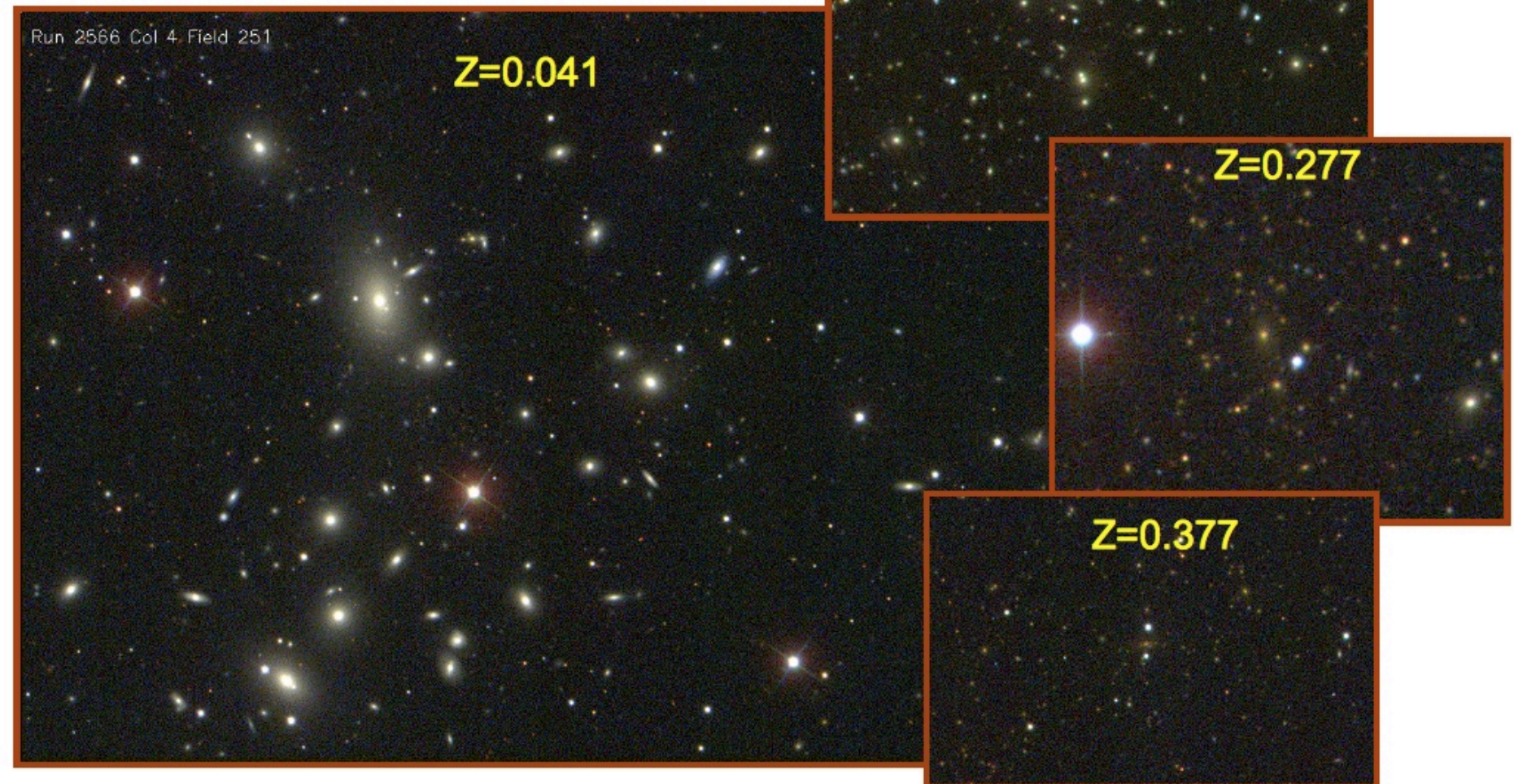


“Weigh” Them.

Find Them.

Optical Cluster Surveys: find lots of clusters!

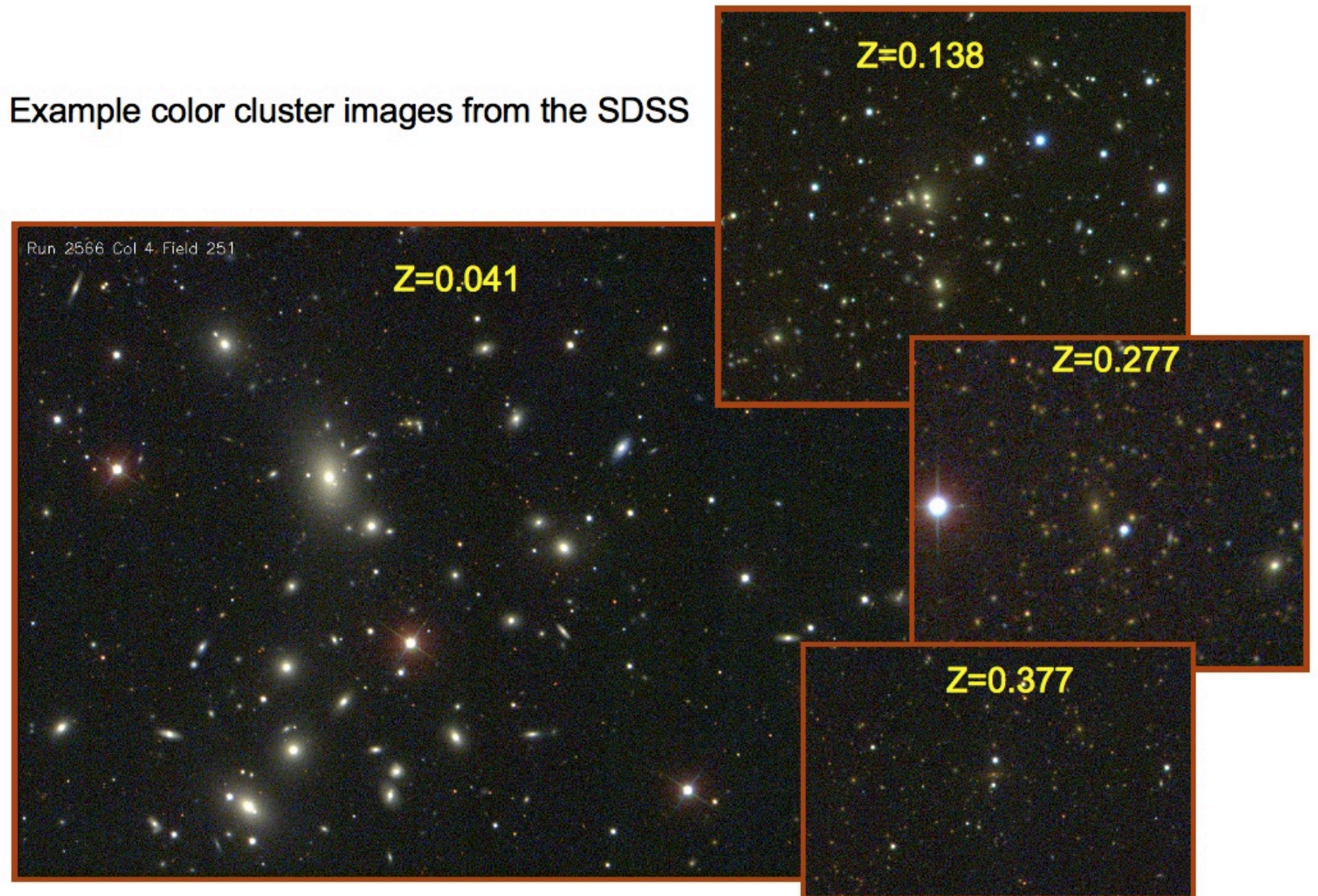
Example color cluster images from the SDSS



- MaxBCG (SDSS) 13,823 clusters

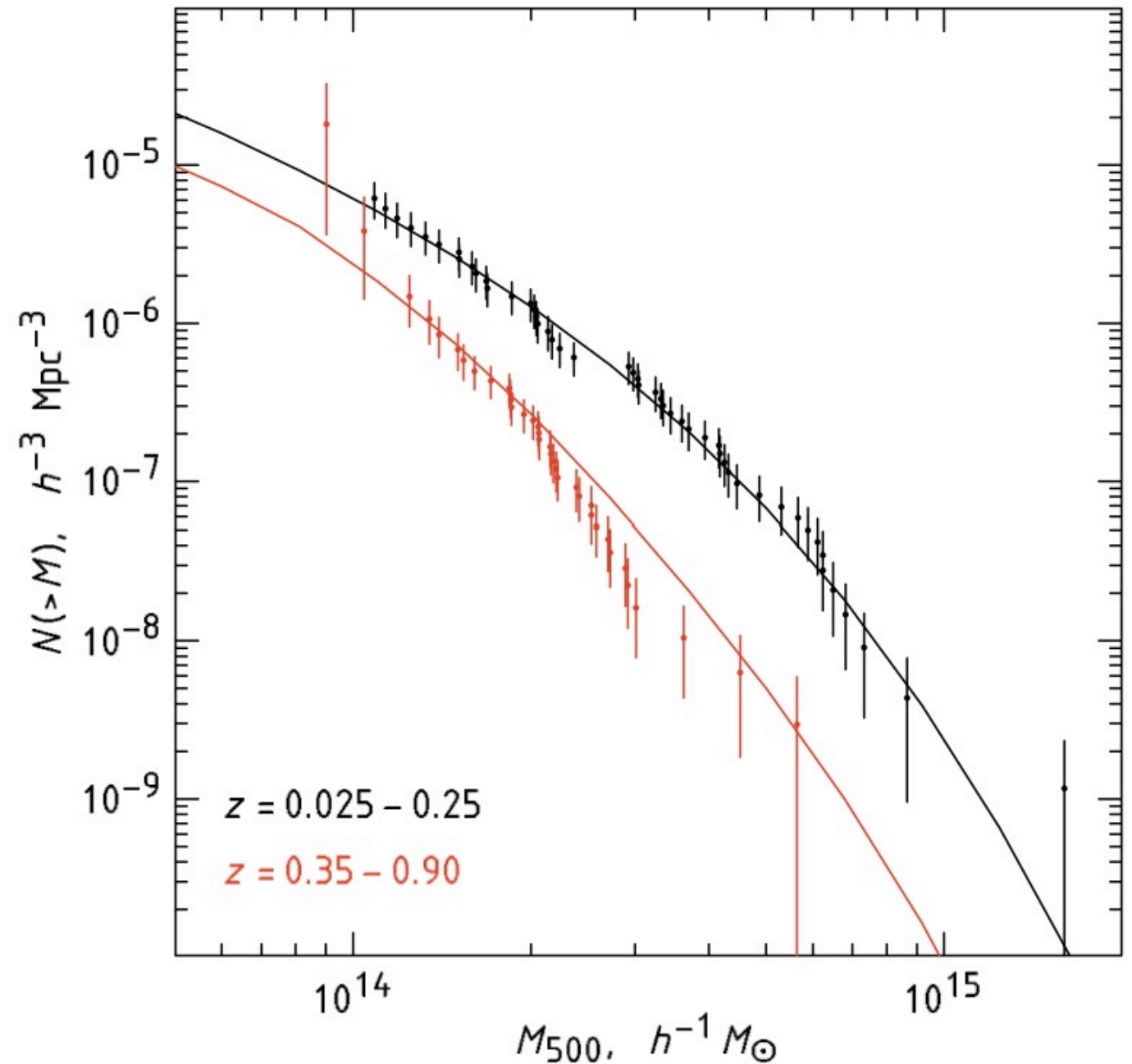
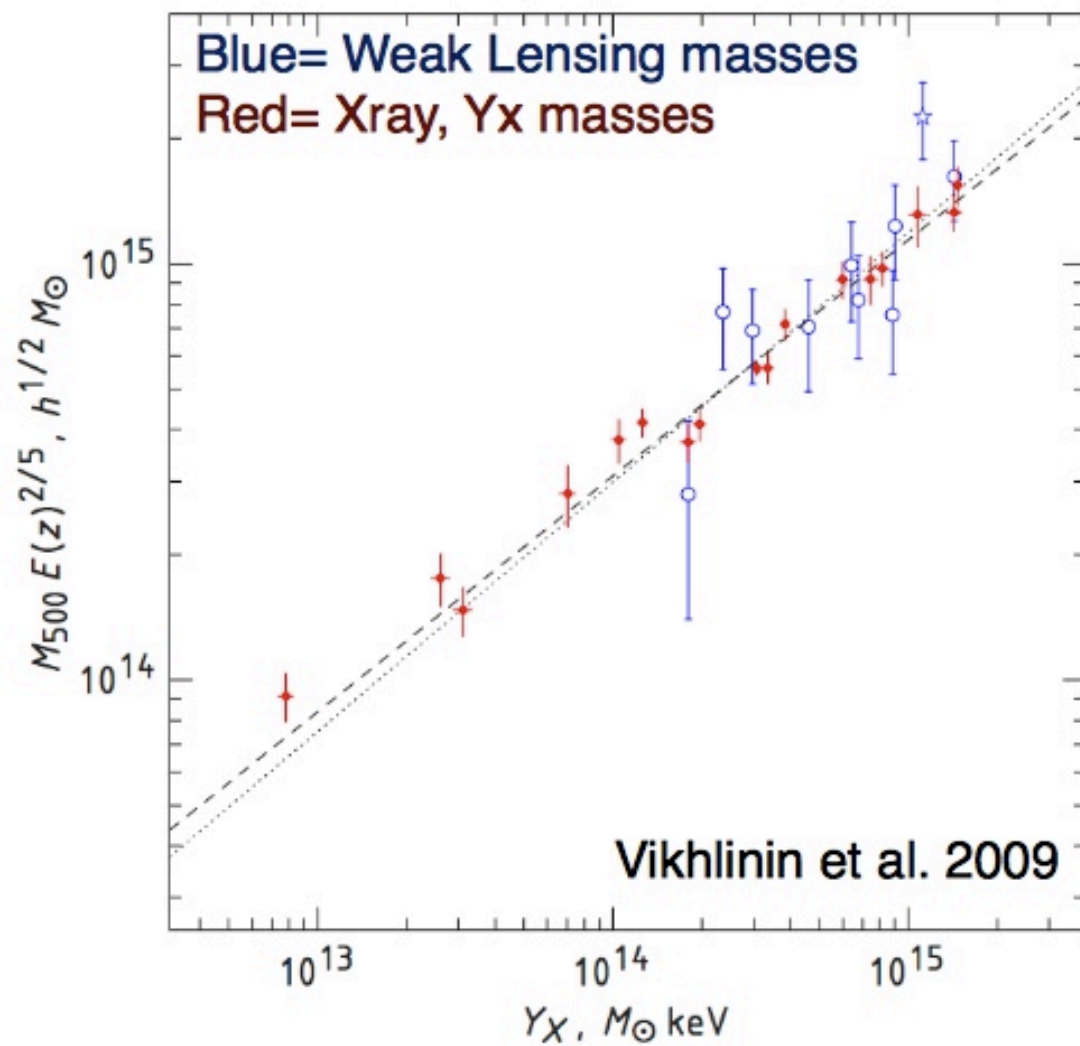
But have large scatter mass proxies.

Example color cluster images from the SDSS

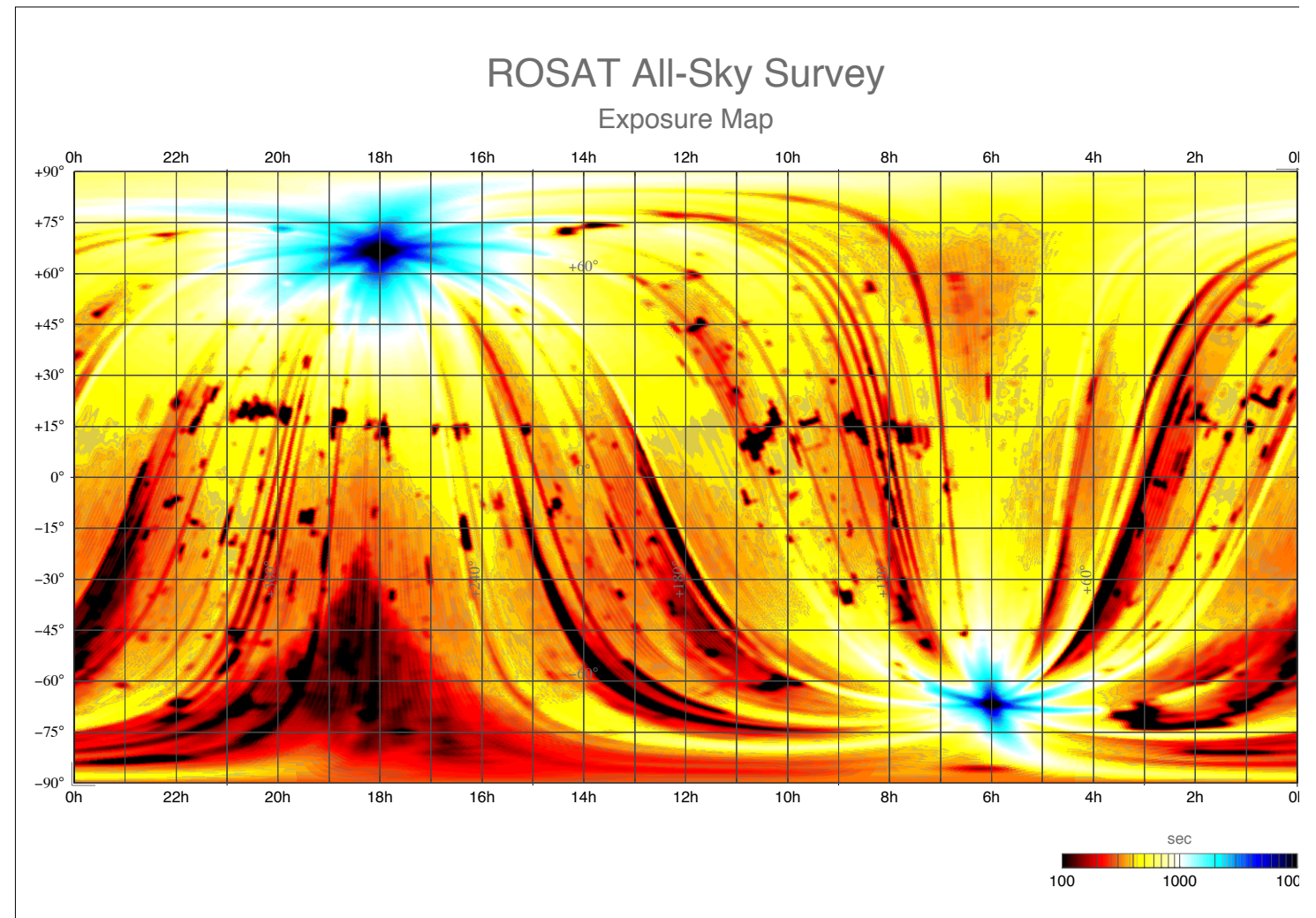
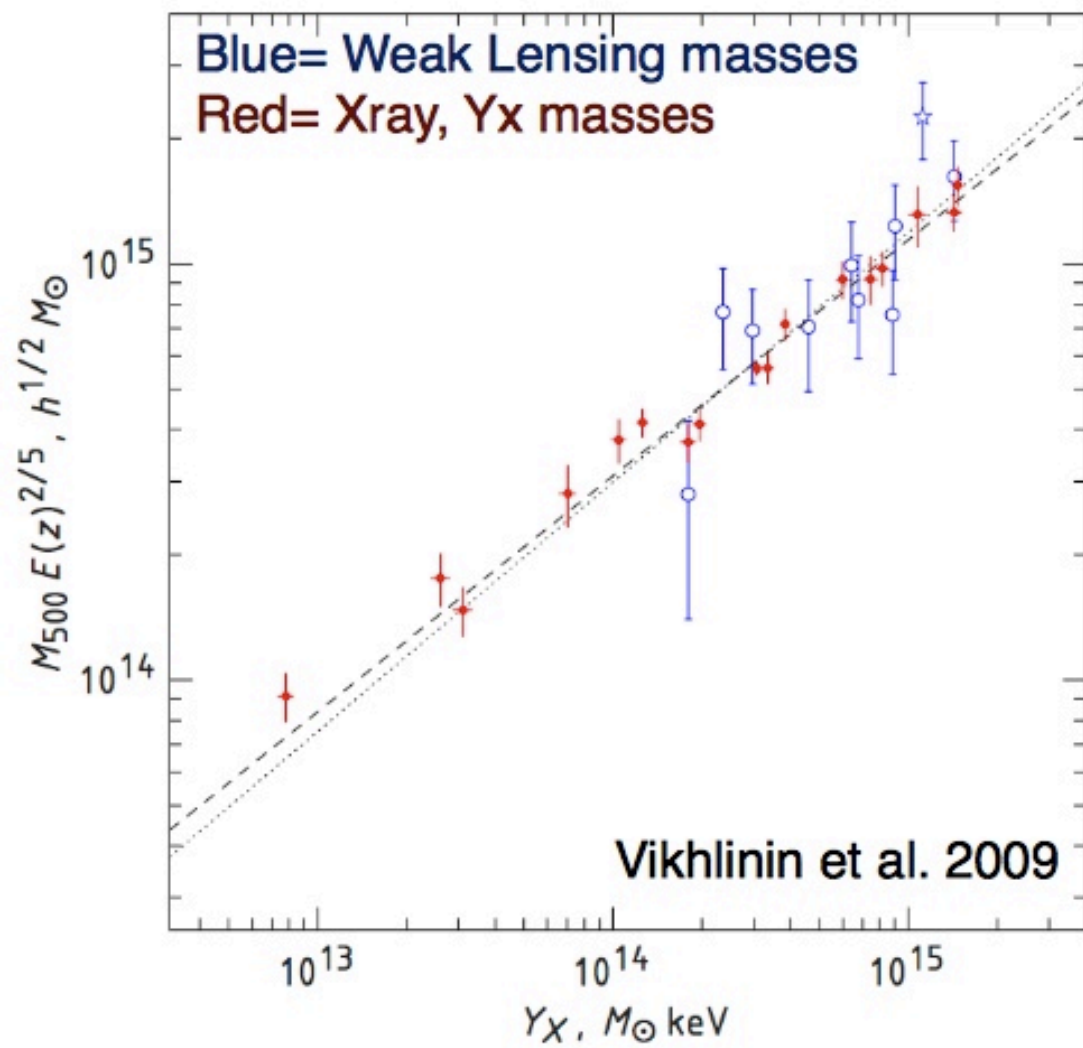


- MaxBCG (SDSS) 13,823 clusters

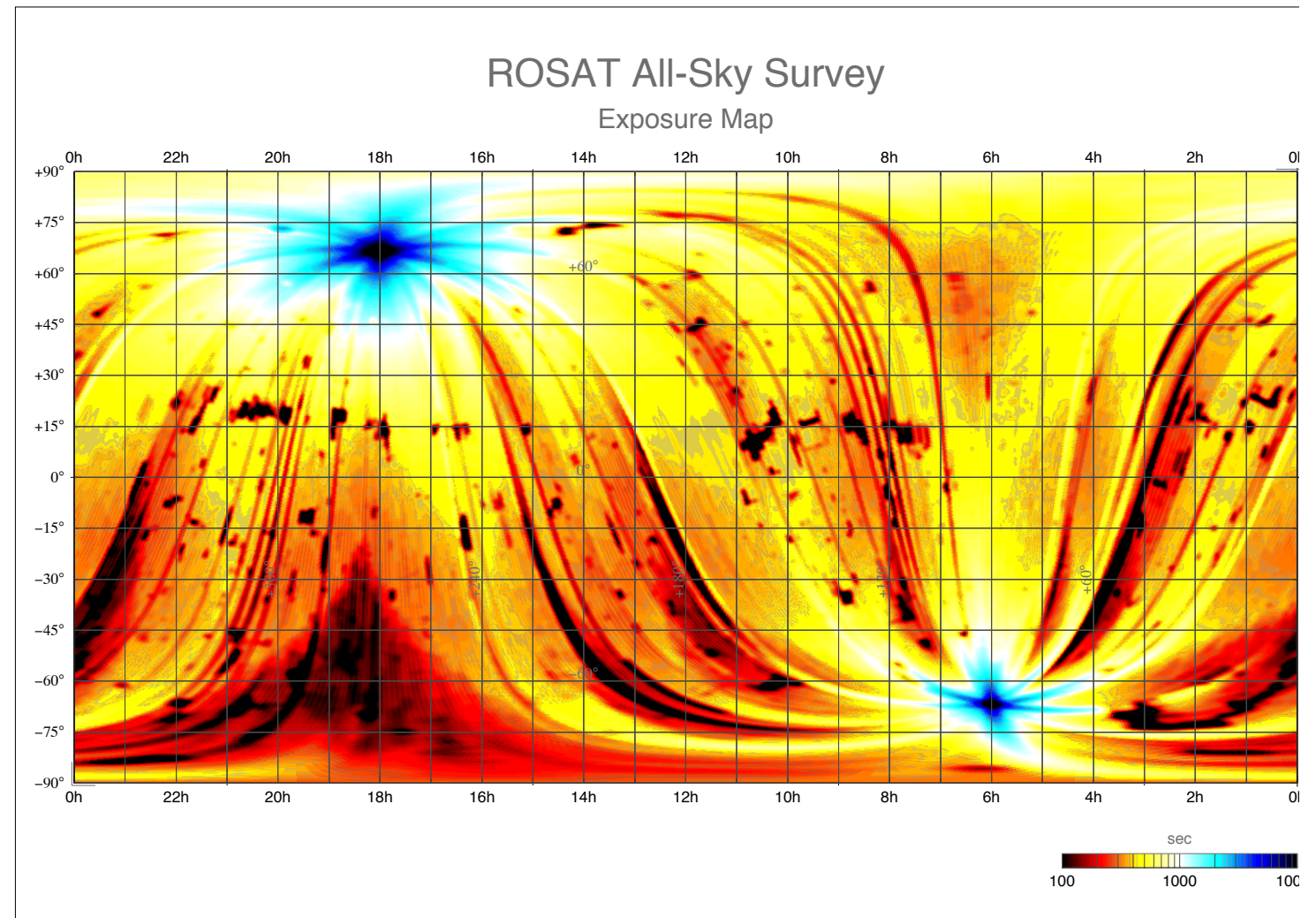
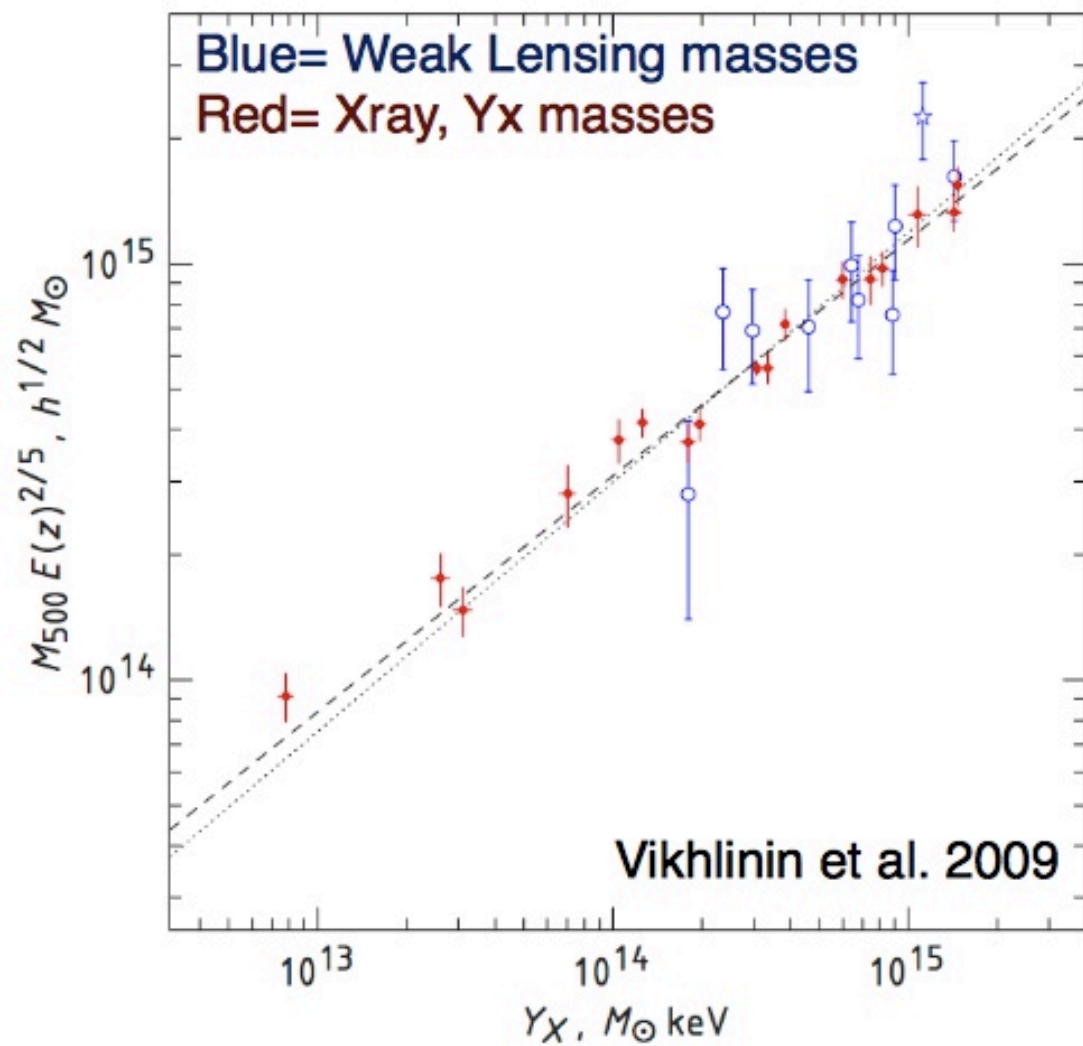
X-Ray Cluster Surveys have clean selection and tight mass proxies ...



.... but are expensive to do on large areas.

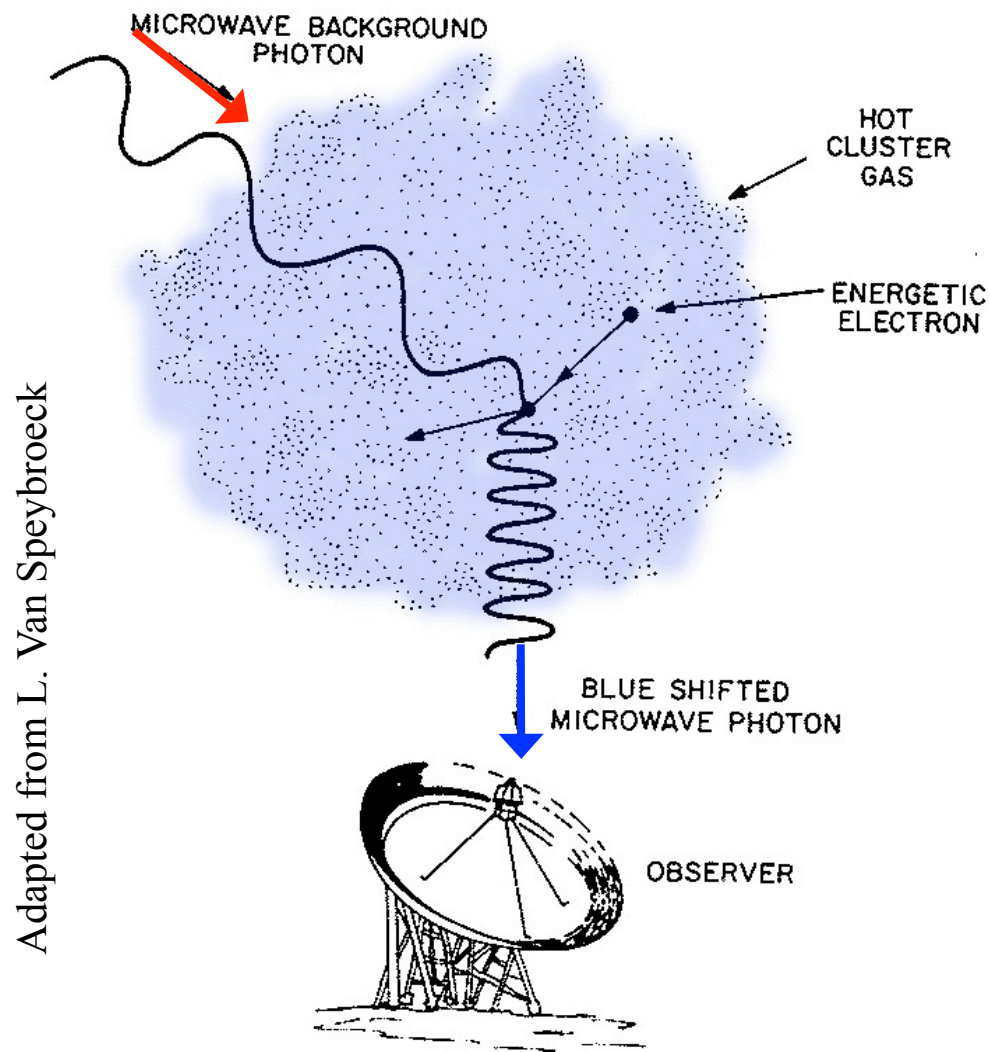


.... but are expensive to do on large areas.

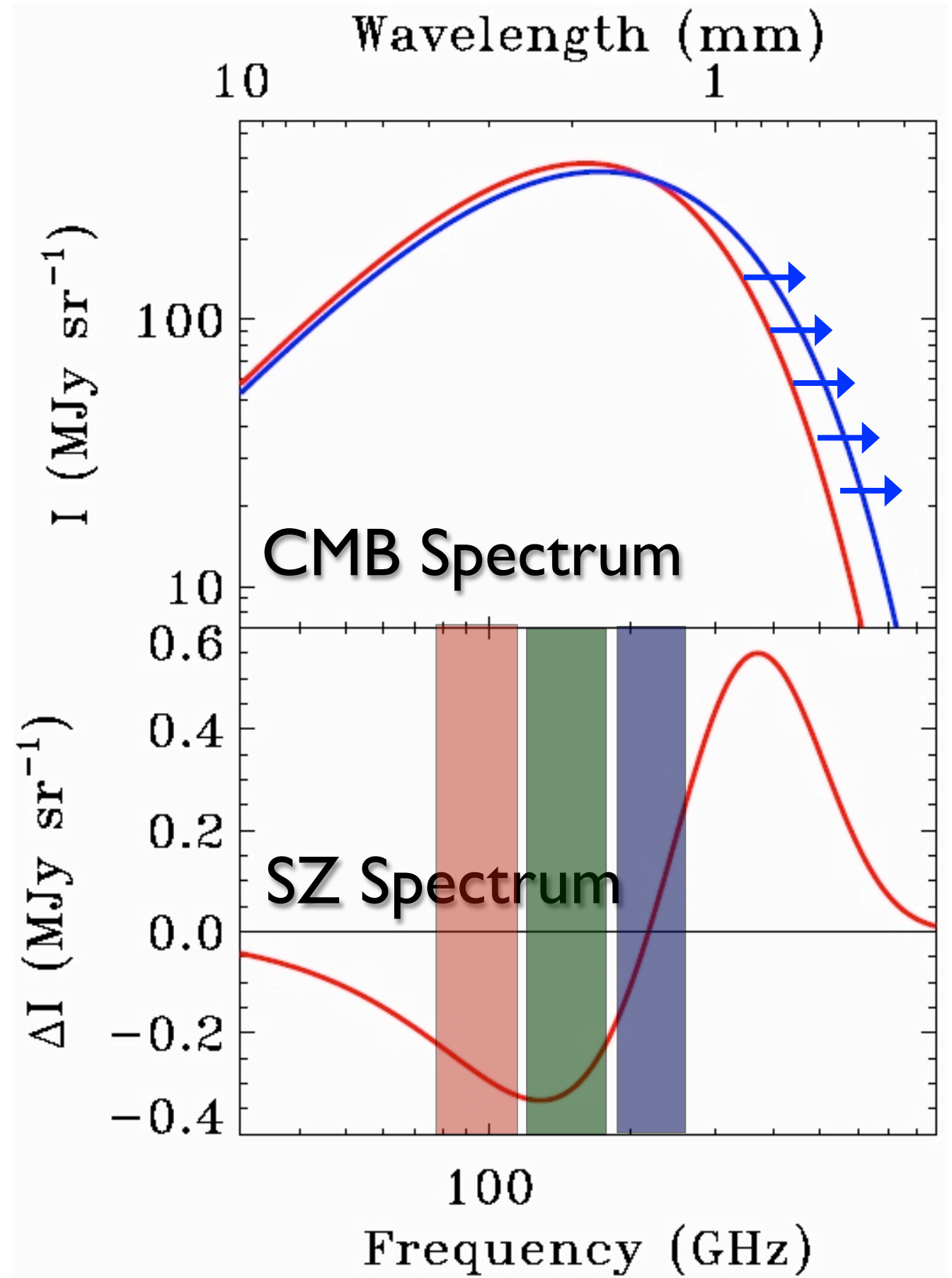


eRosita launch next year!

The Sunyaev Zel'dovich (SZ) Effect



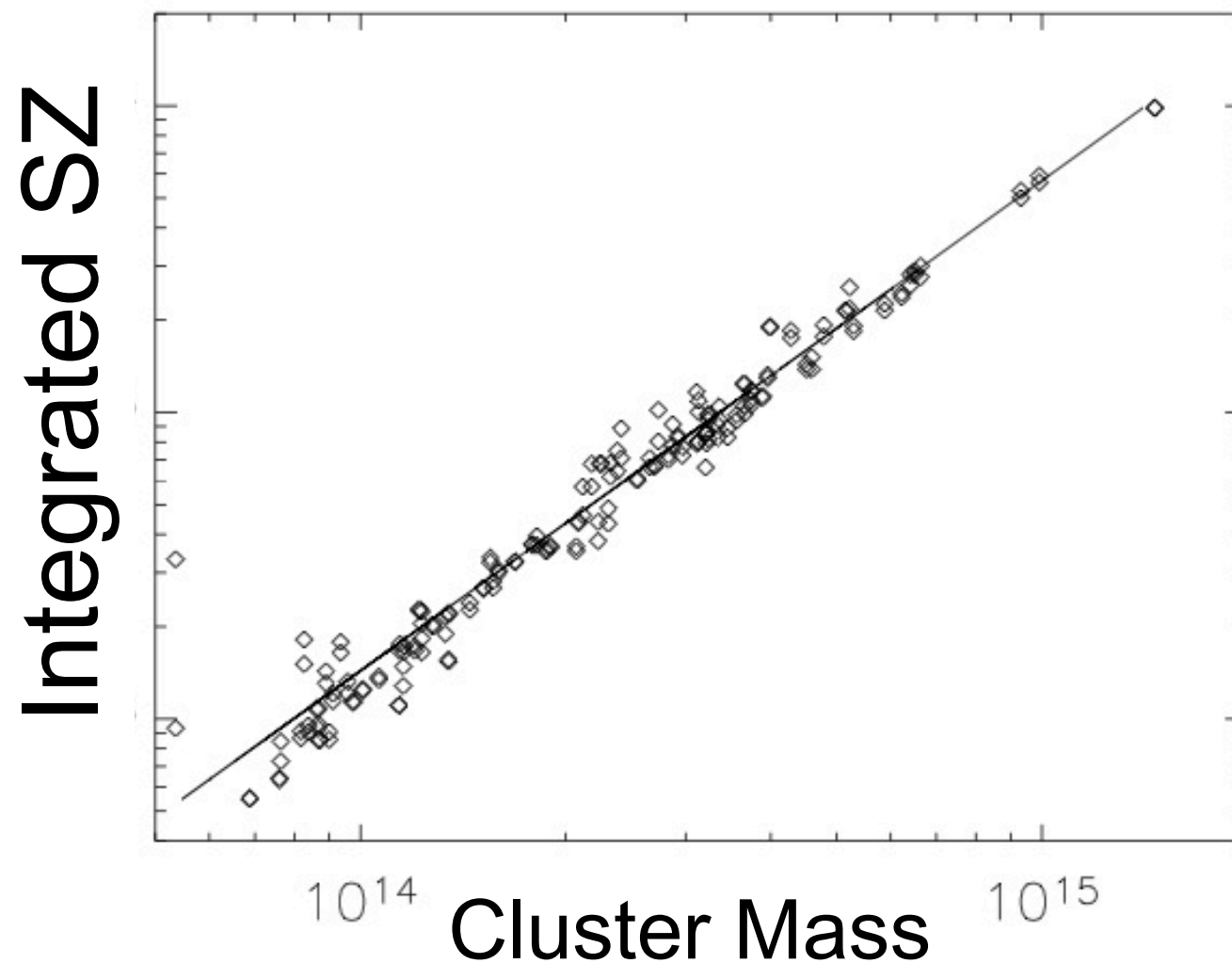
Towards a massive cluster, $\sim 1\%$ of CMB photons scatter off of intra-cluster gas



The SZ-observable is tightly correlated with mass.

$$\int y \, d\Omega \propto \frac{kT_e}{m_e c^2} \sigma_T \frac{N_e}{D_A^2}$$

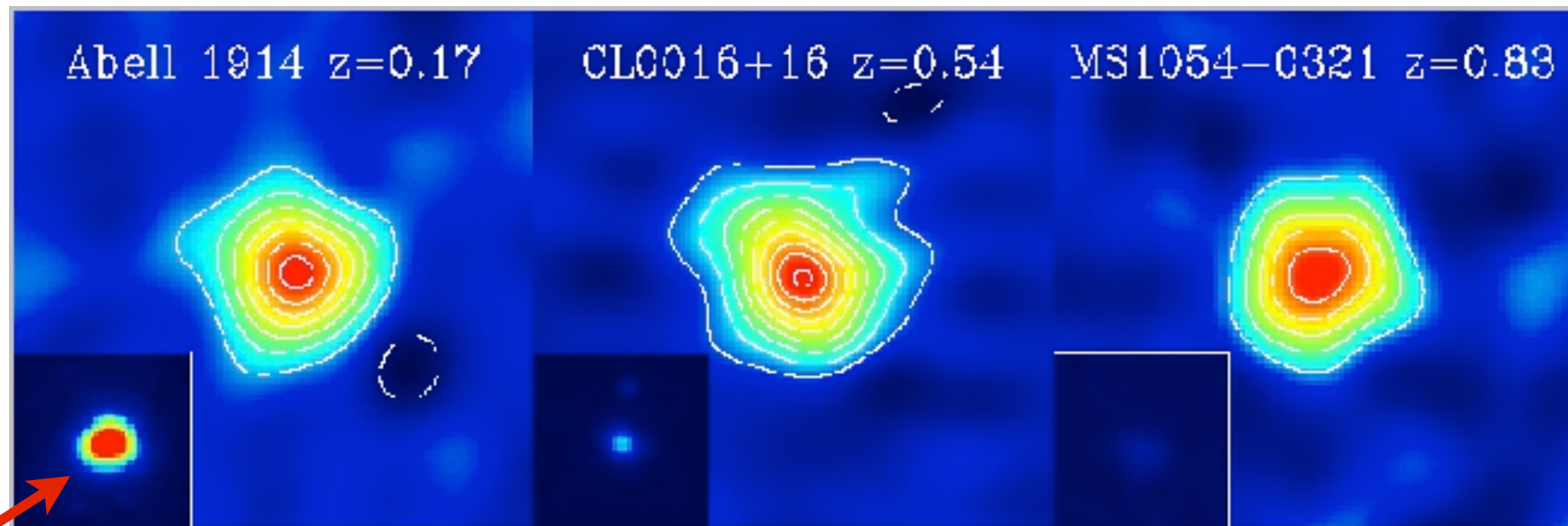
← Integrated Signal proportional to total thermal energy, should faithfully track cluster mass



The SZ-observable is tightly correlated with mass.

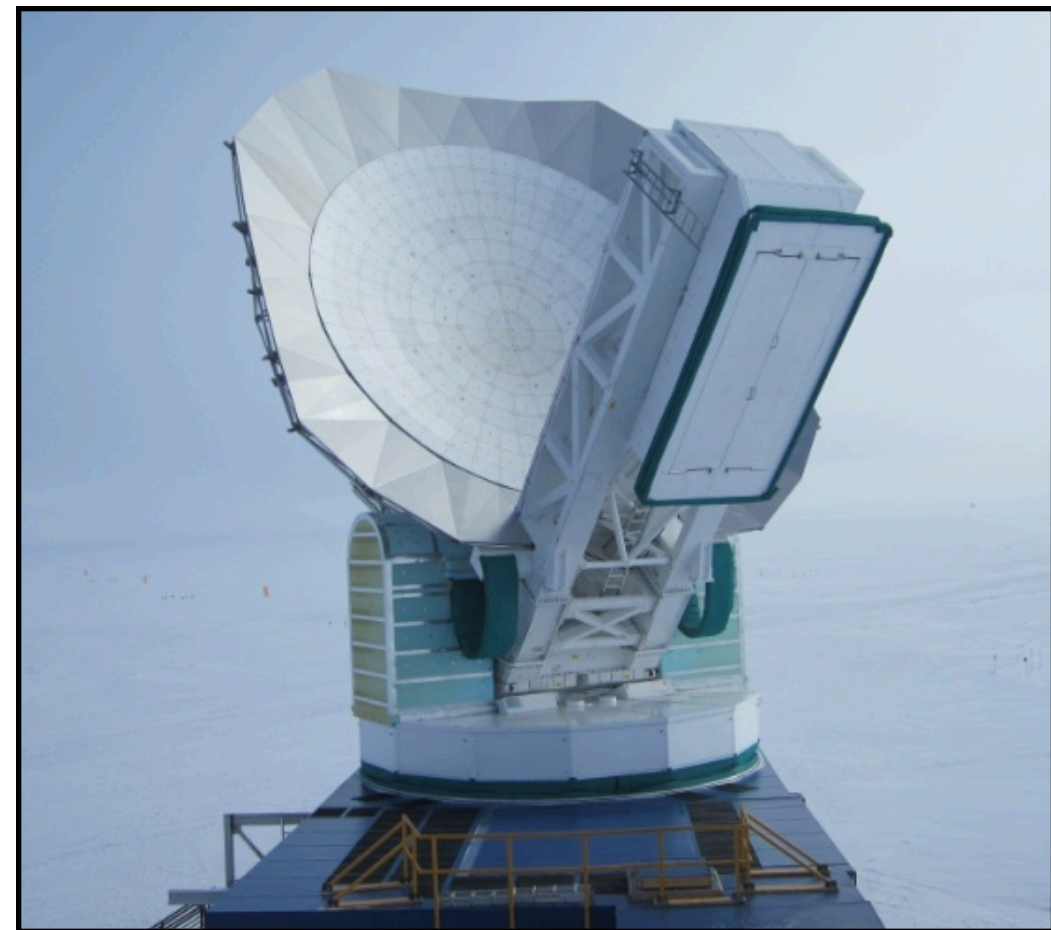
$$\int y \, d\Omega \propto \frac{kT_e}{m_e c^2} \sigma_T \frac{N_e}{D_A^2}$$

Integrated Signal proportional to total thermal energy, should faithfully track cluster mass



X-Ray

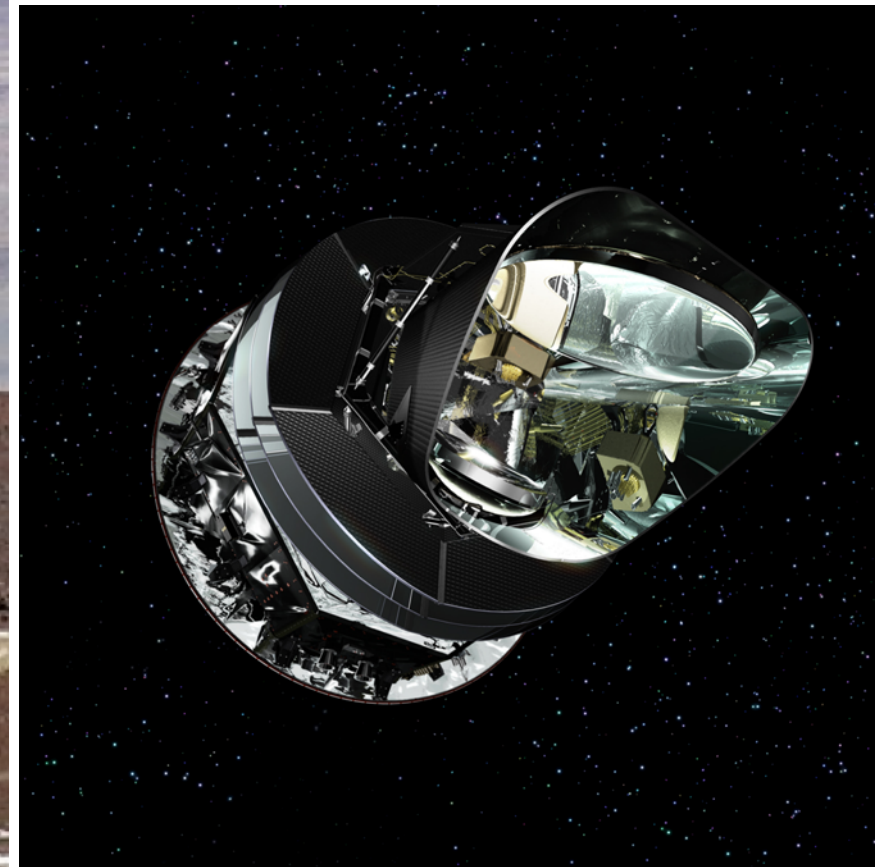
High resolution, low noise observations are required to detect clusters.



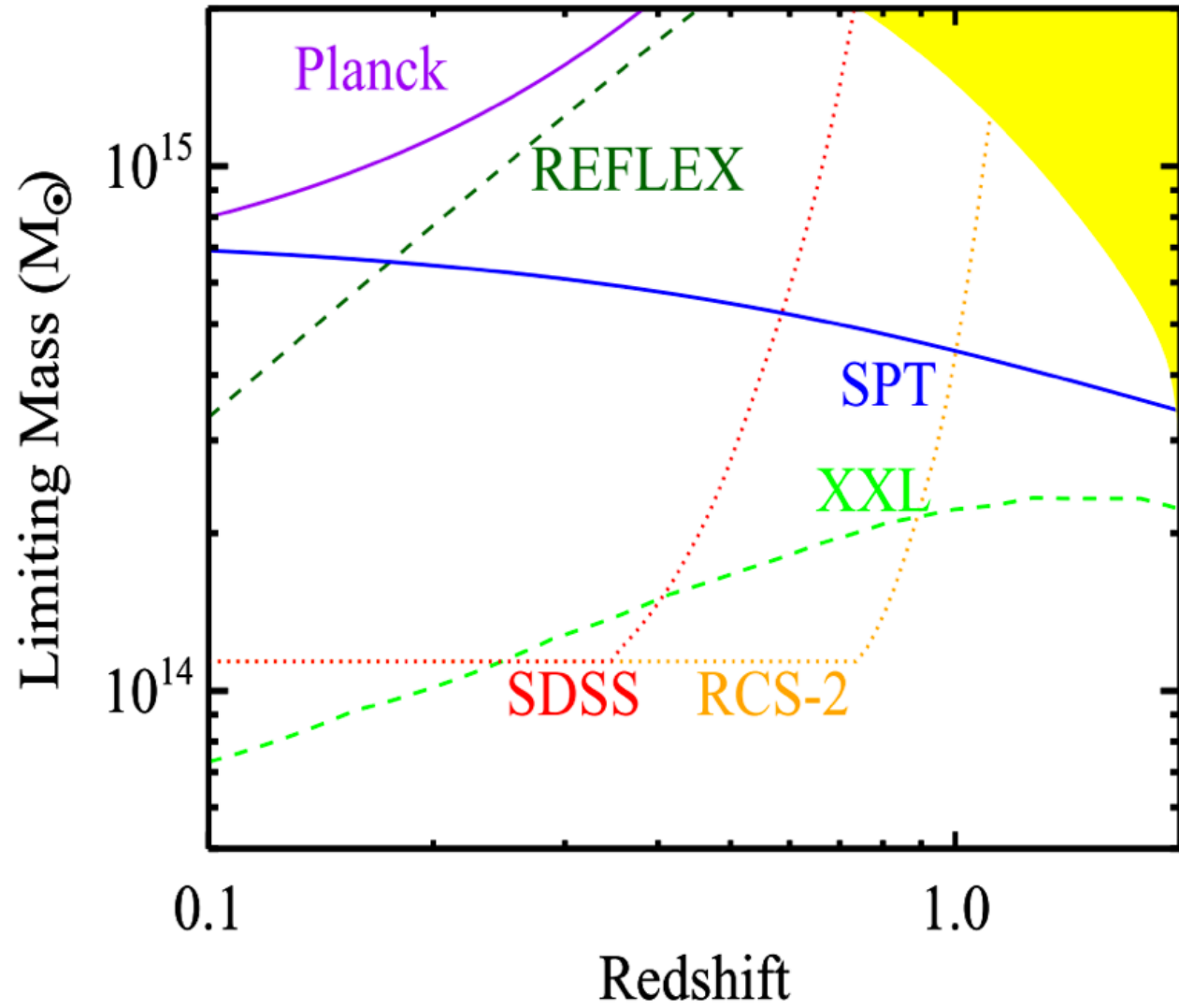
South Pole
Telescope



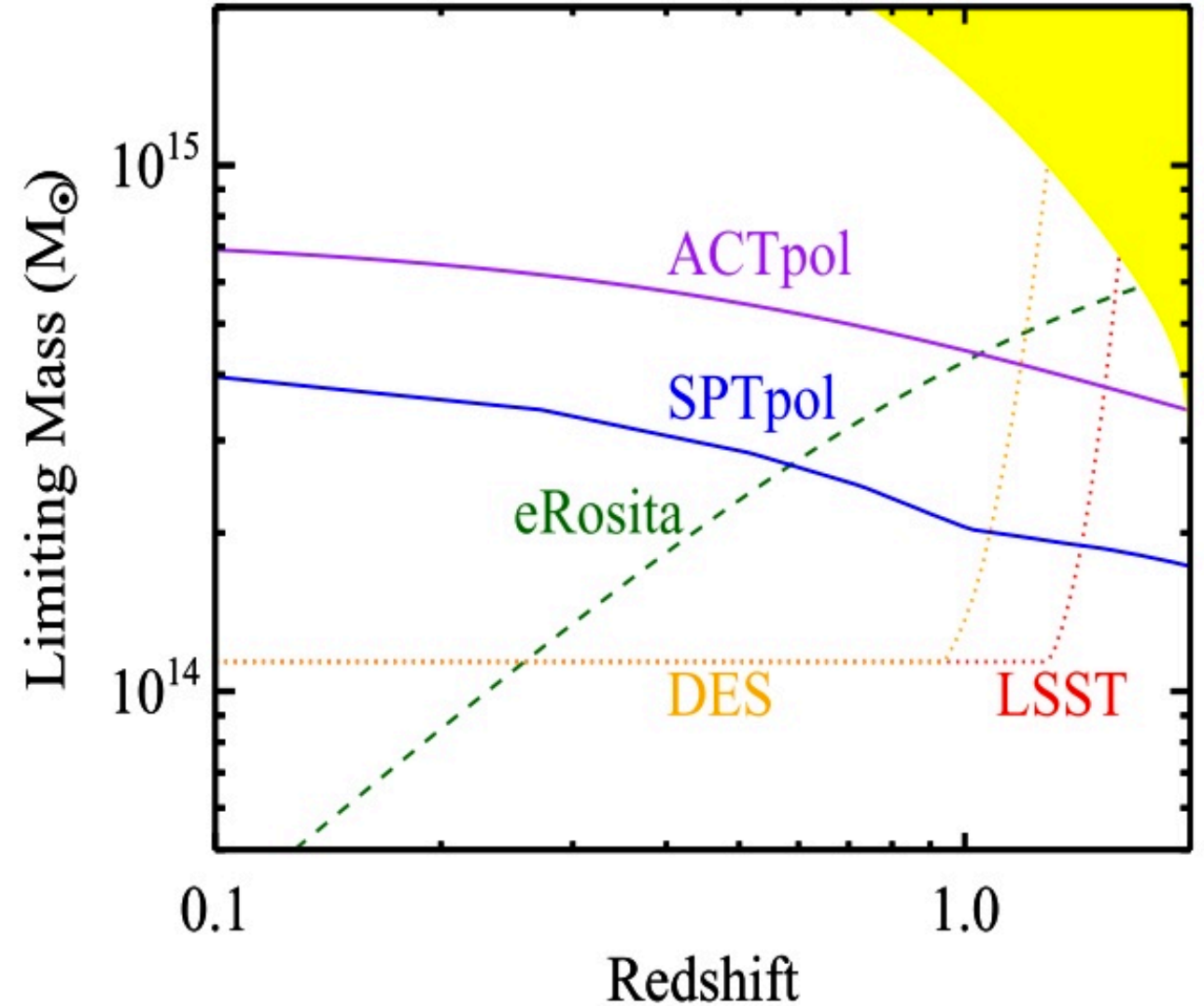
Atacama Cosmology
Telescope



Planck

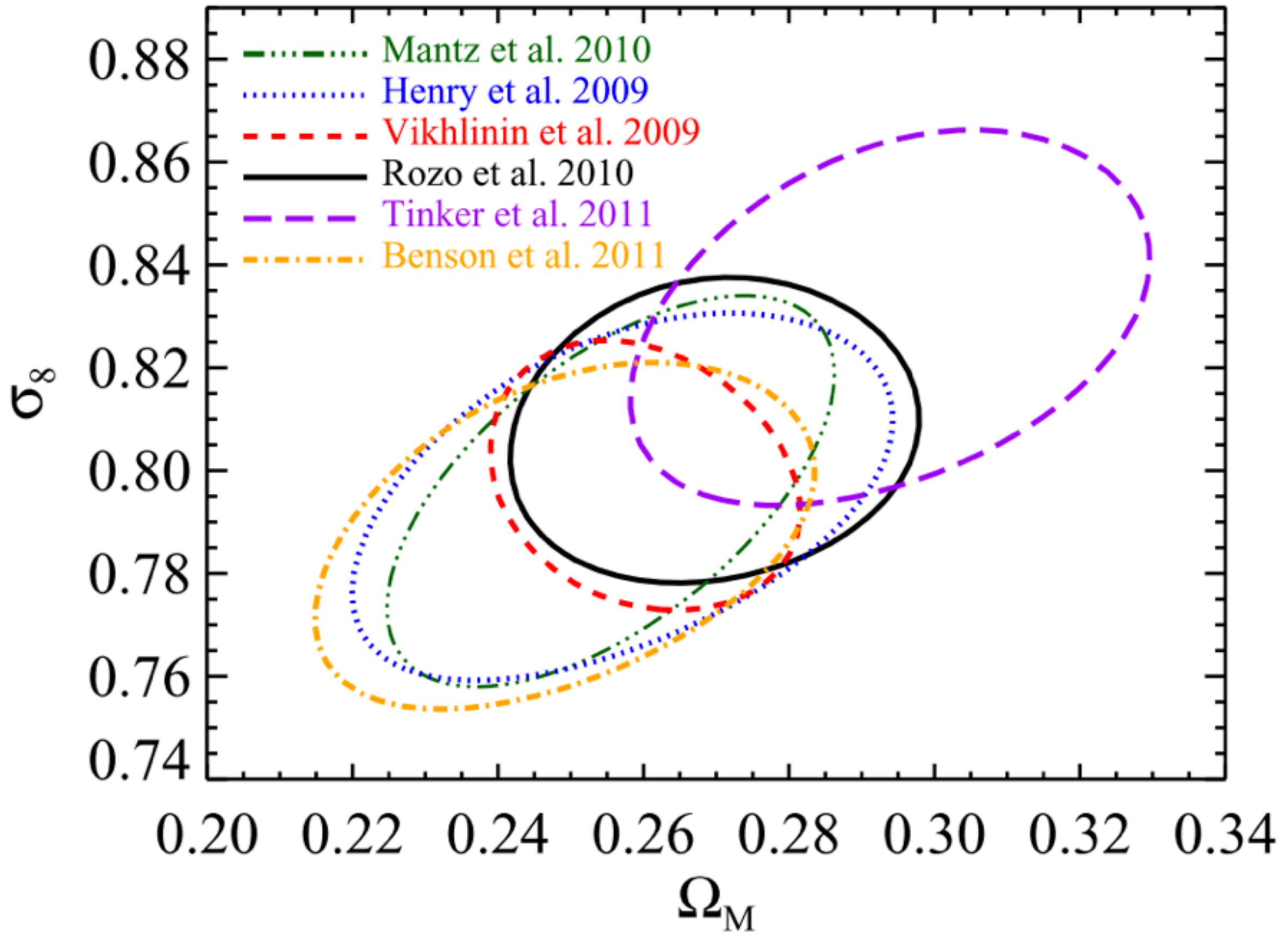


Current



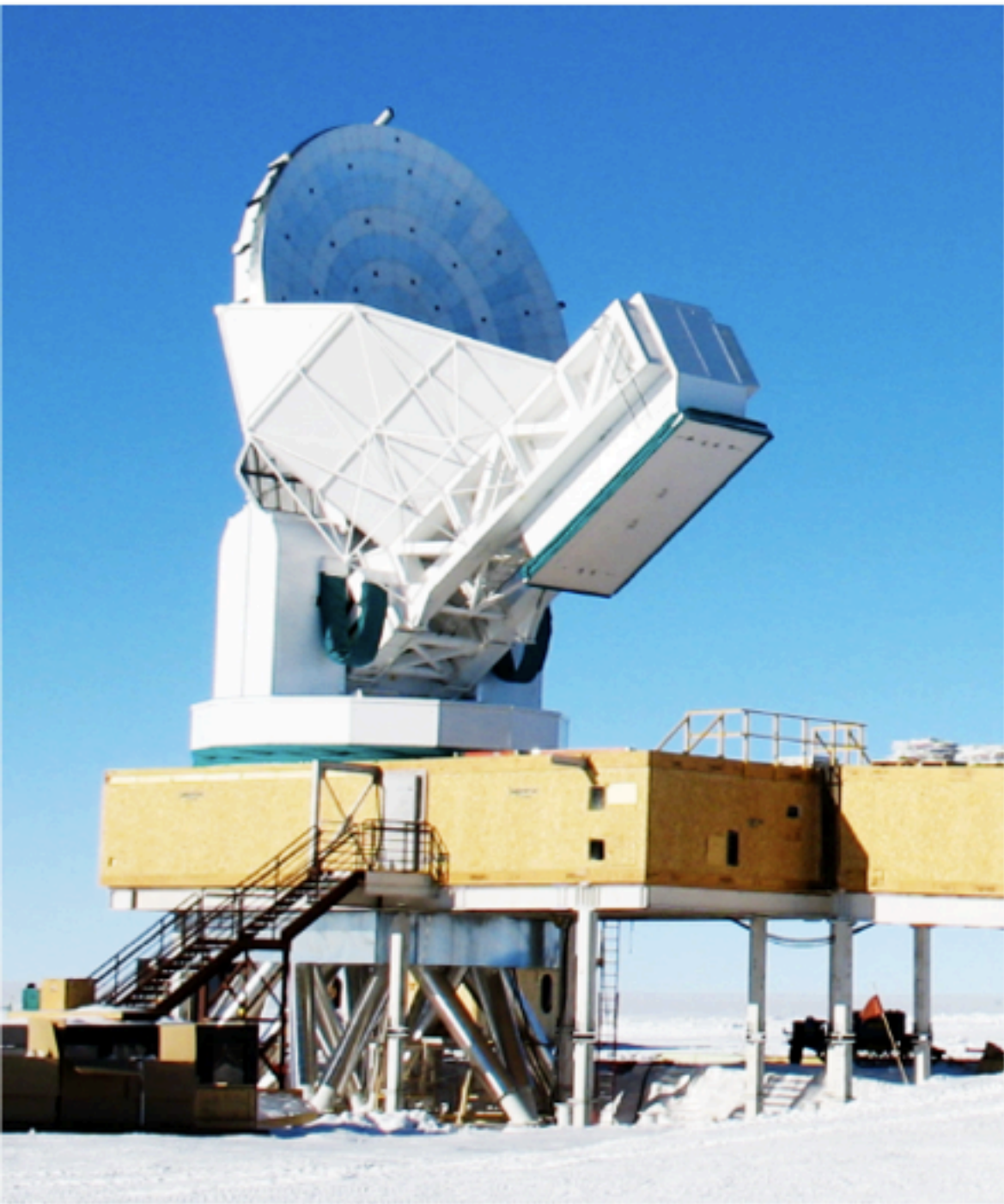
Online/Near Future

Weinberg et al. 1201.2434



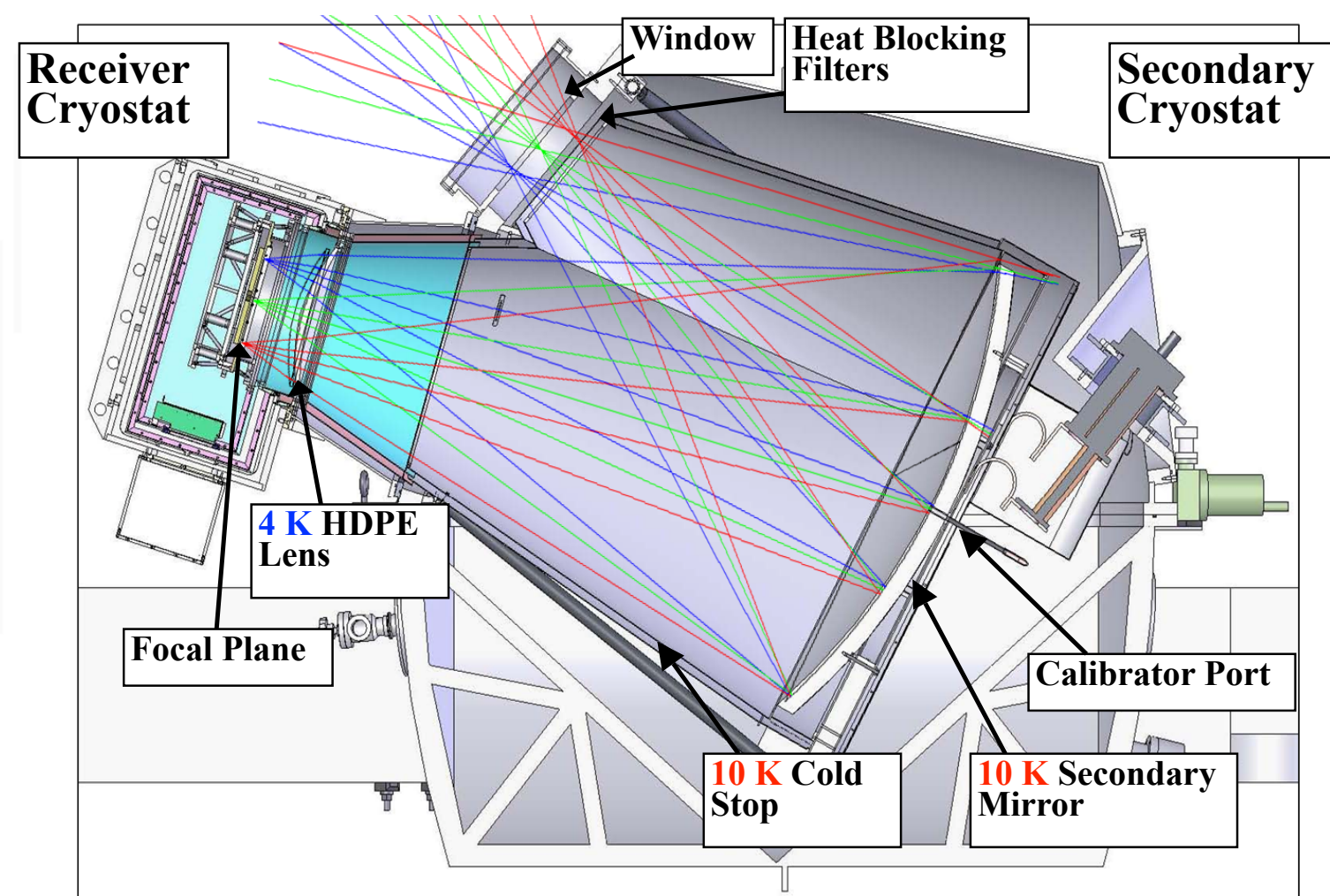
Weinberg et al. 1201.2434

The South Pole Telescope (SPT)



Sub-millimeter Wavelength Telescope:

- 10 meter telescope
- Off-axis Gregorian optics design
- 20 microns RMS surface accuracy
- 1 arc-second pointing
- Fast scanning (up to 4 deg/sec in azimuth)



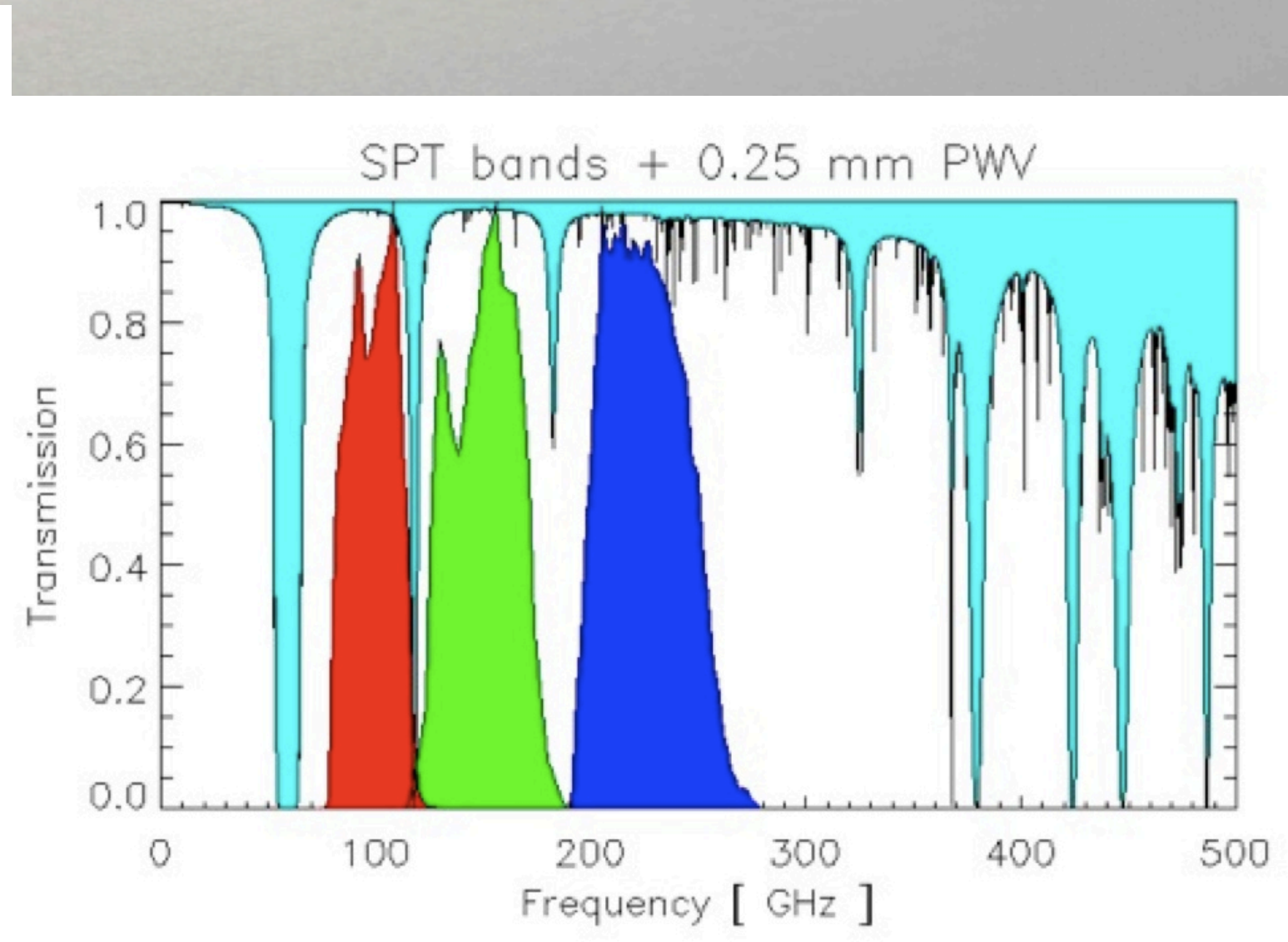
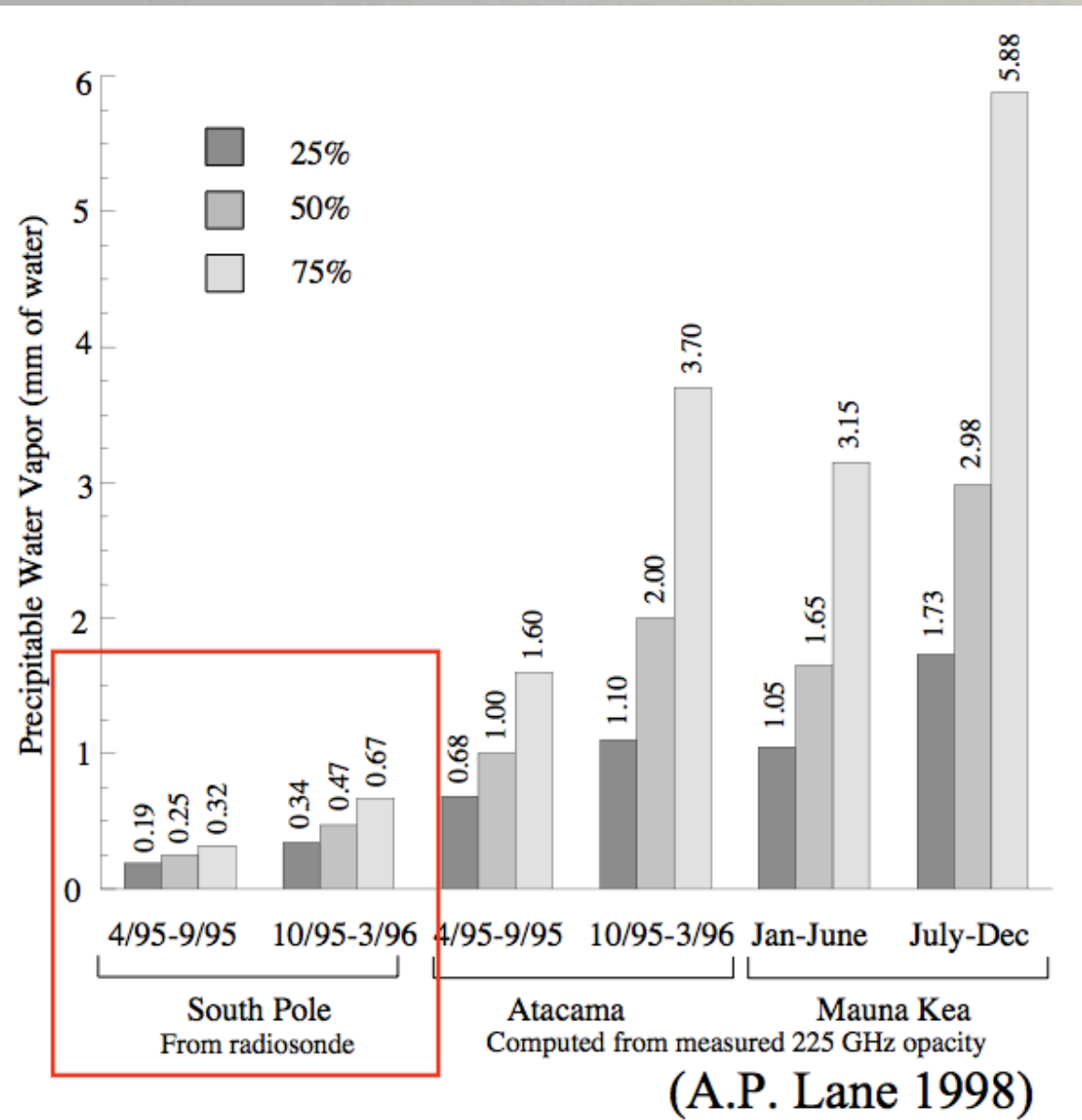
Funded
by NSF



We go to the South Pole for the weather.



We go to the South Pole for the weather.

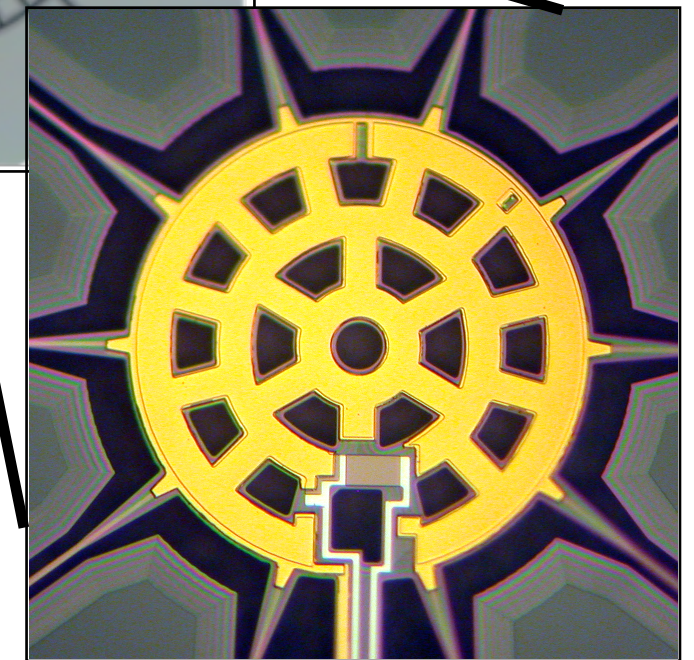
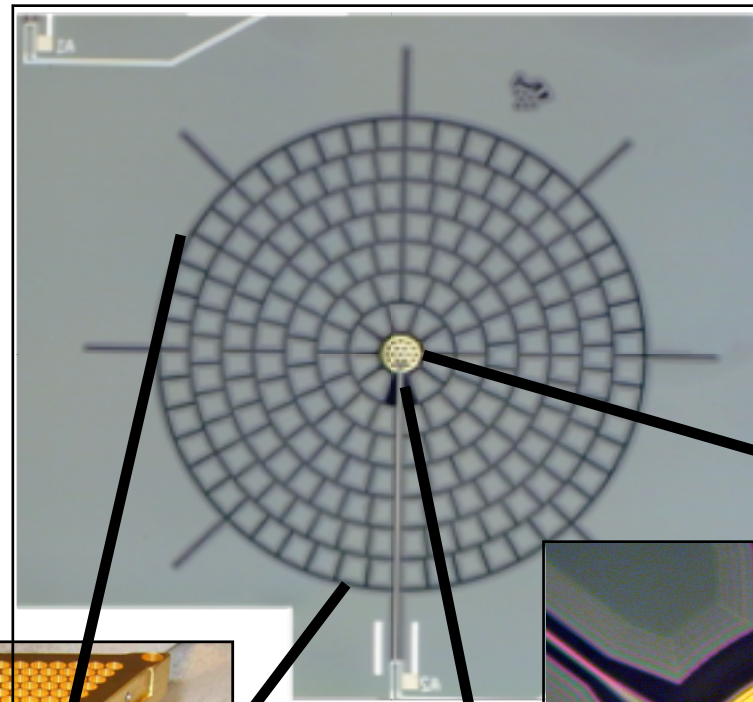


SPT Focal Plane

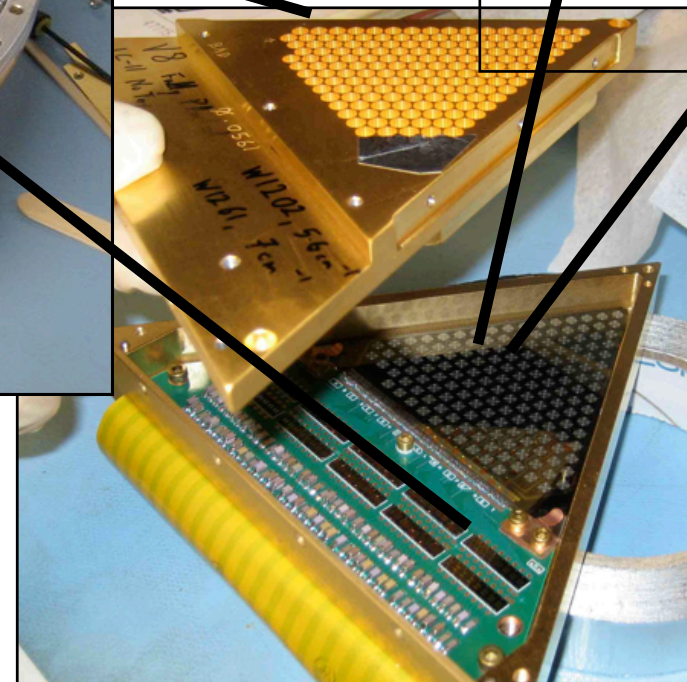
Each detector is a 4mm diameter gold web that absorbs microwaves

SPT Focal Plane

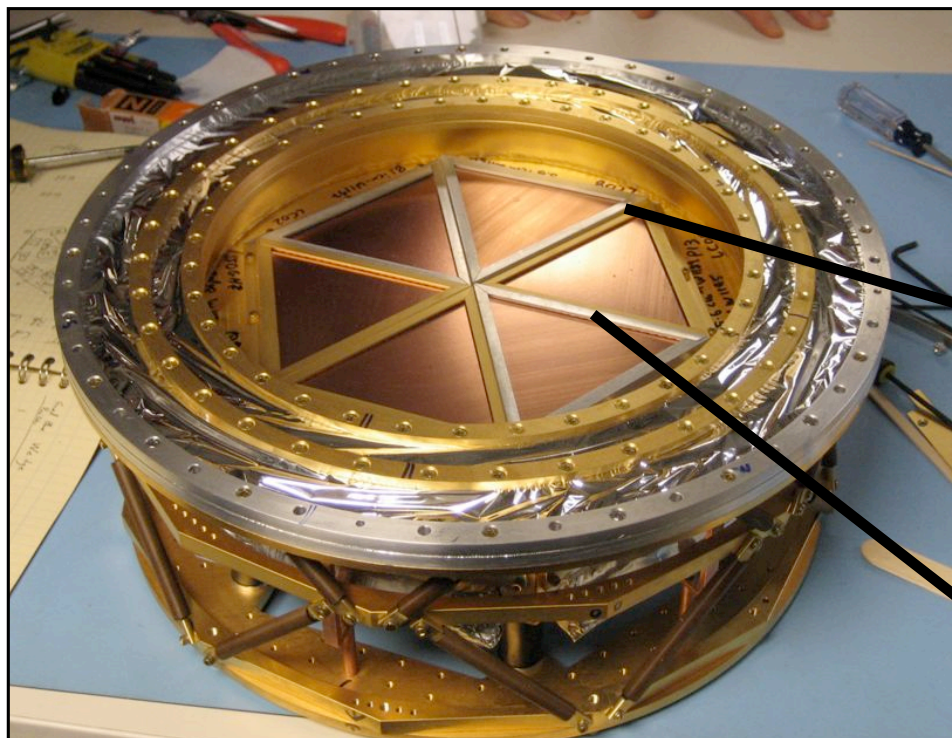
- 6 wedges of 160 detectors
- 90, 150, 220 GHz



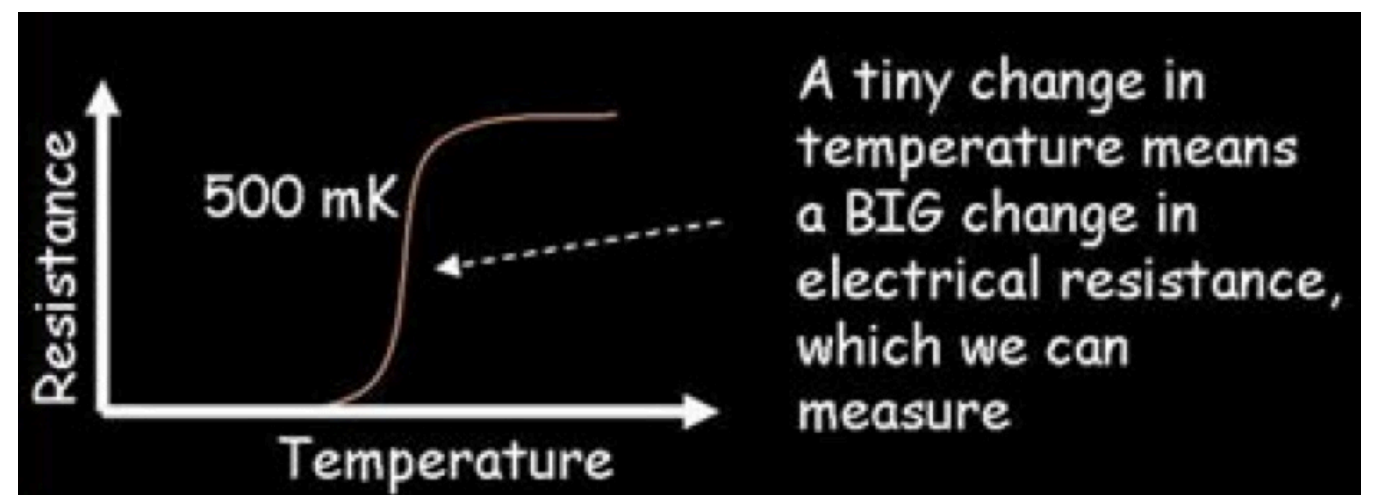
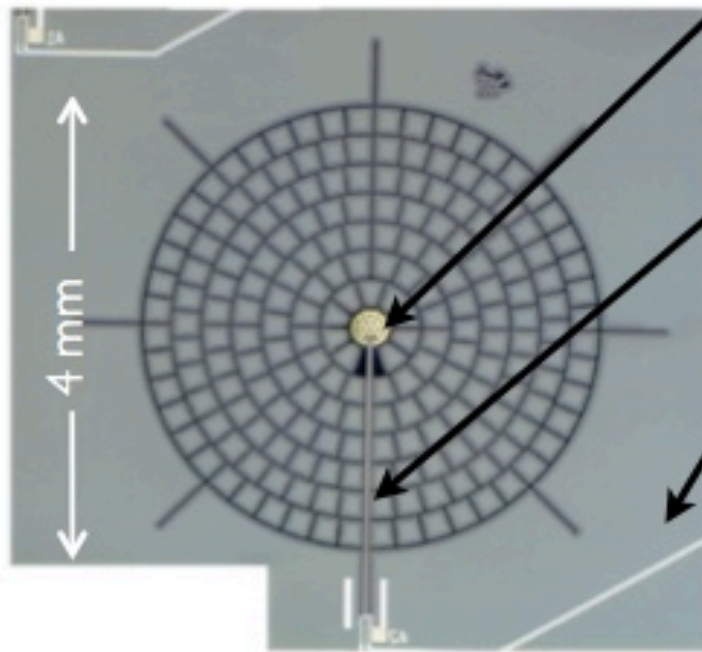
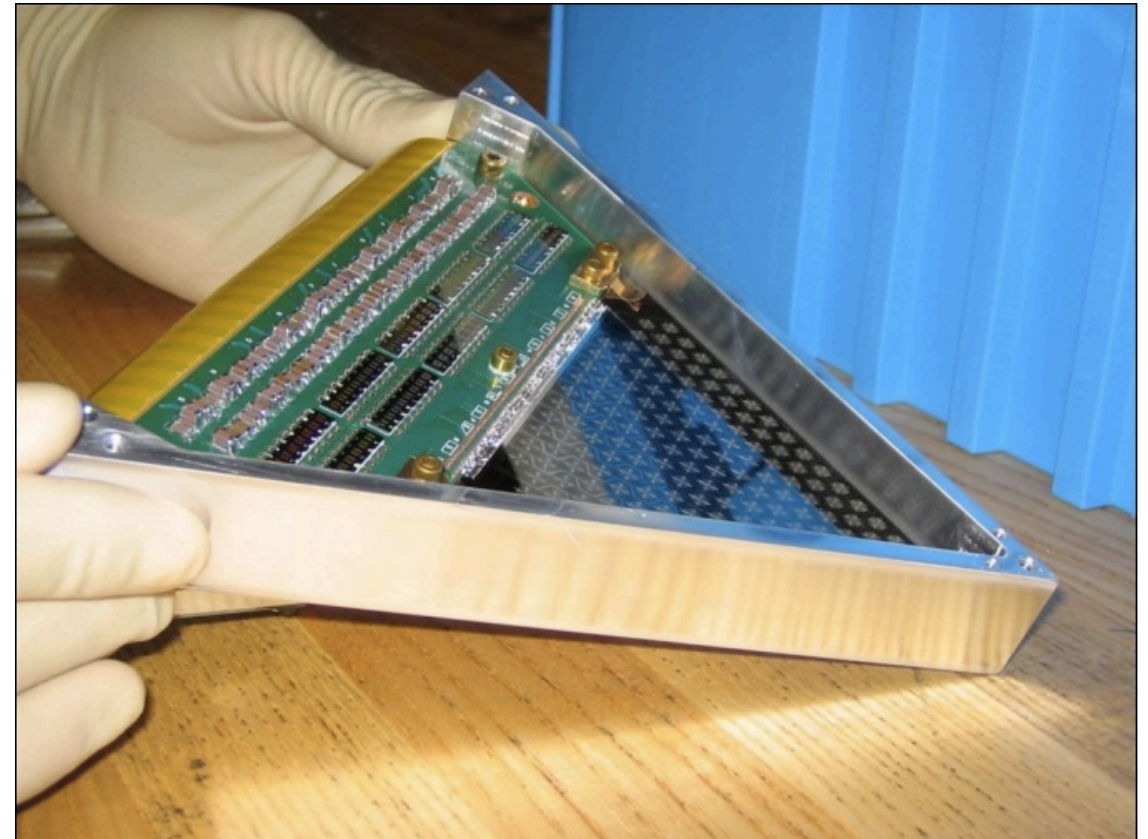
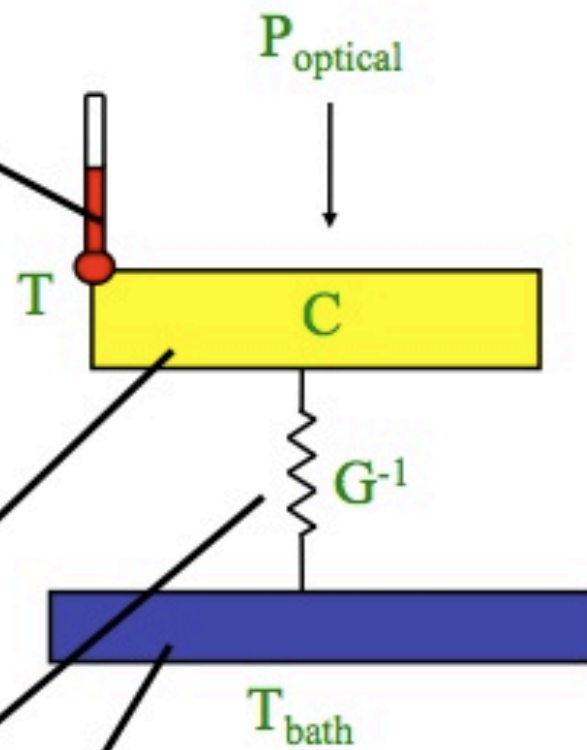
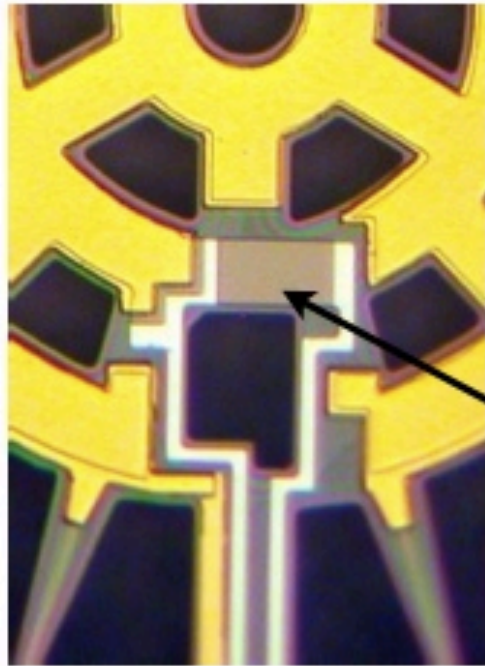
Al-Ti bi-layer Transition Edge Sensor (TES) with $T_c = 0.55$ K



Wedge of 160 detectors

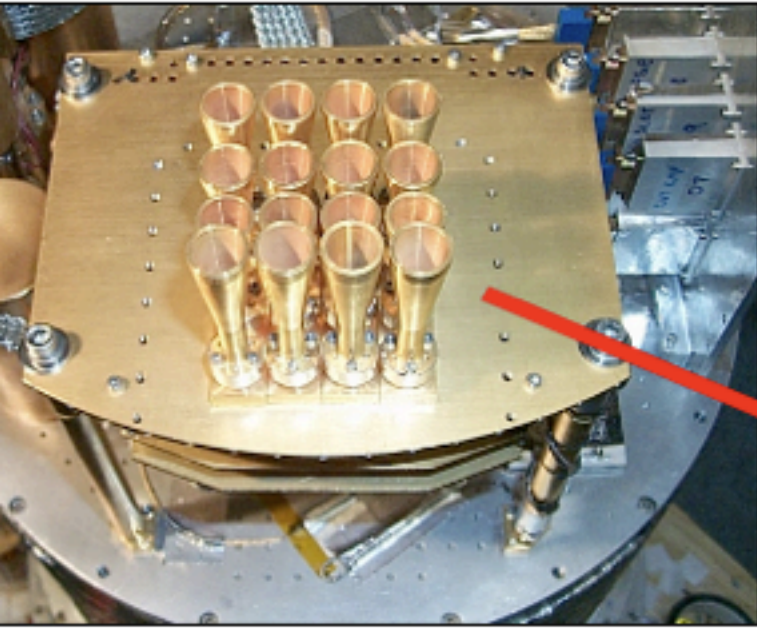


Our detectors are bolometers.

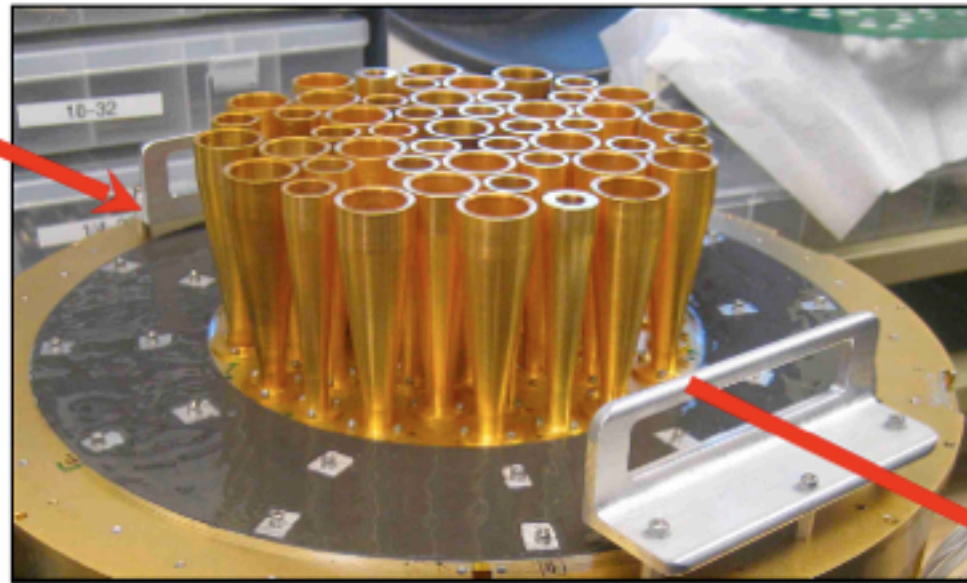


History of Recent CMB Focal Planes

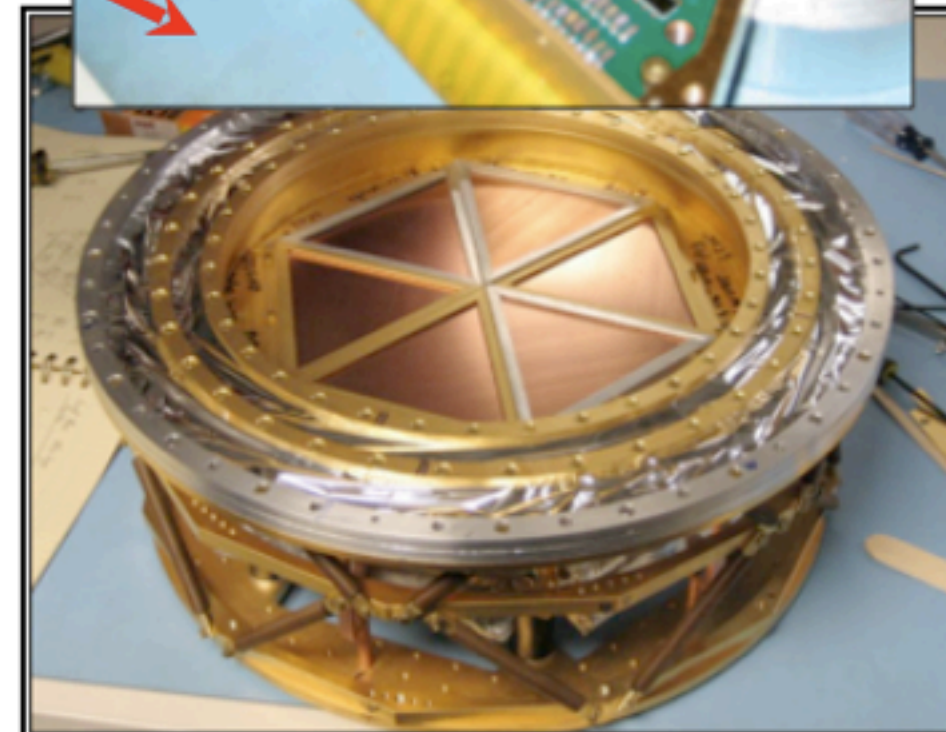
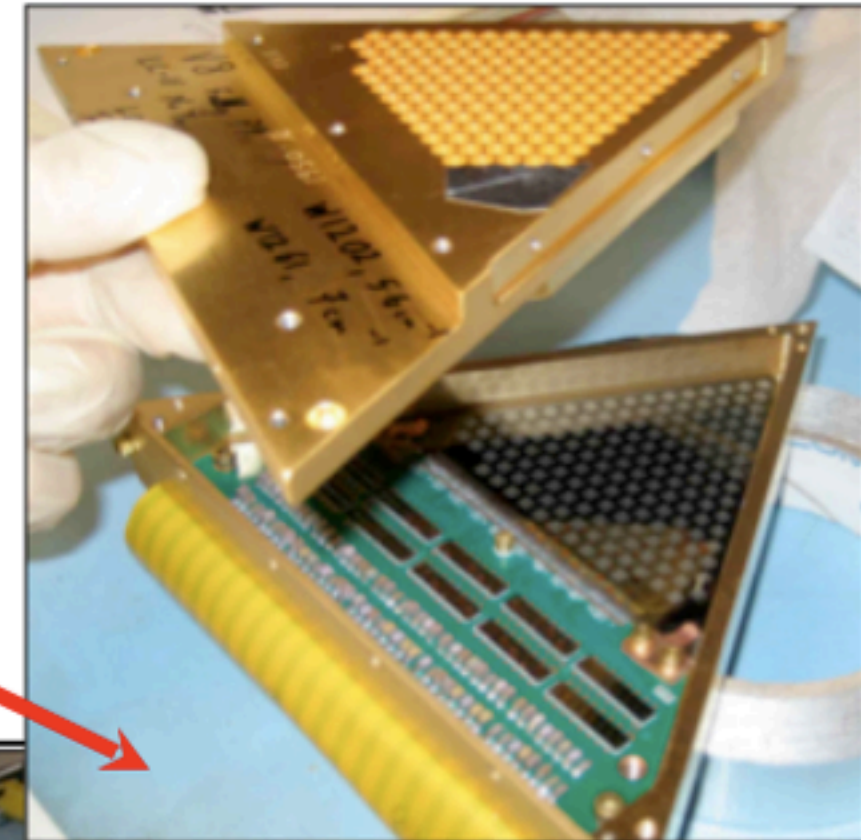
2001: ACBAR
16 detectors



2005: BICEP
~50 detectors

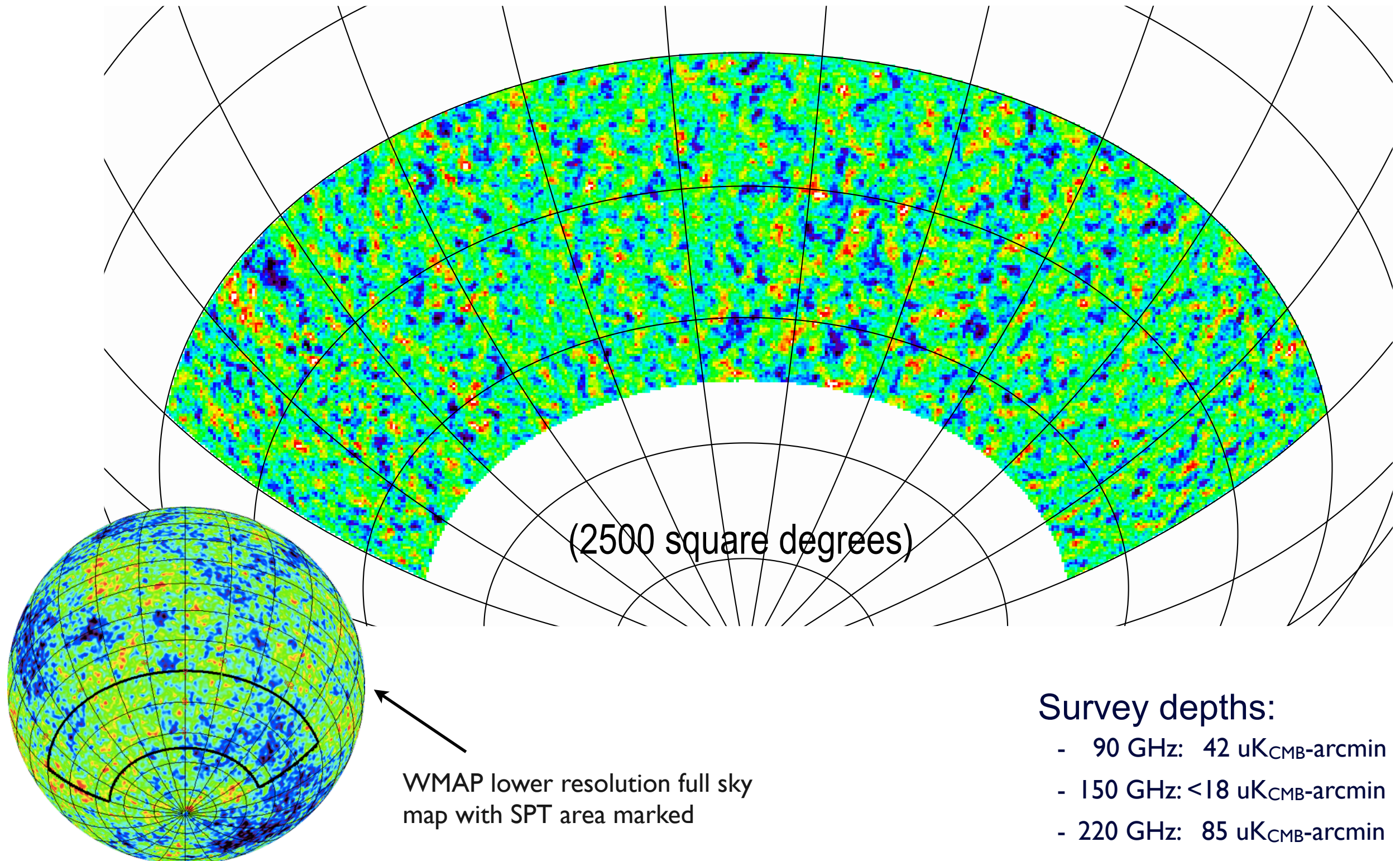
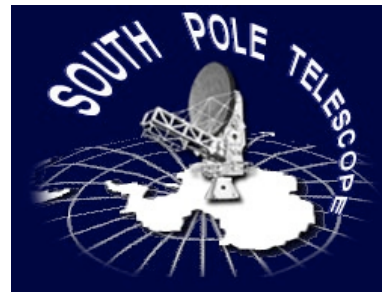


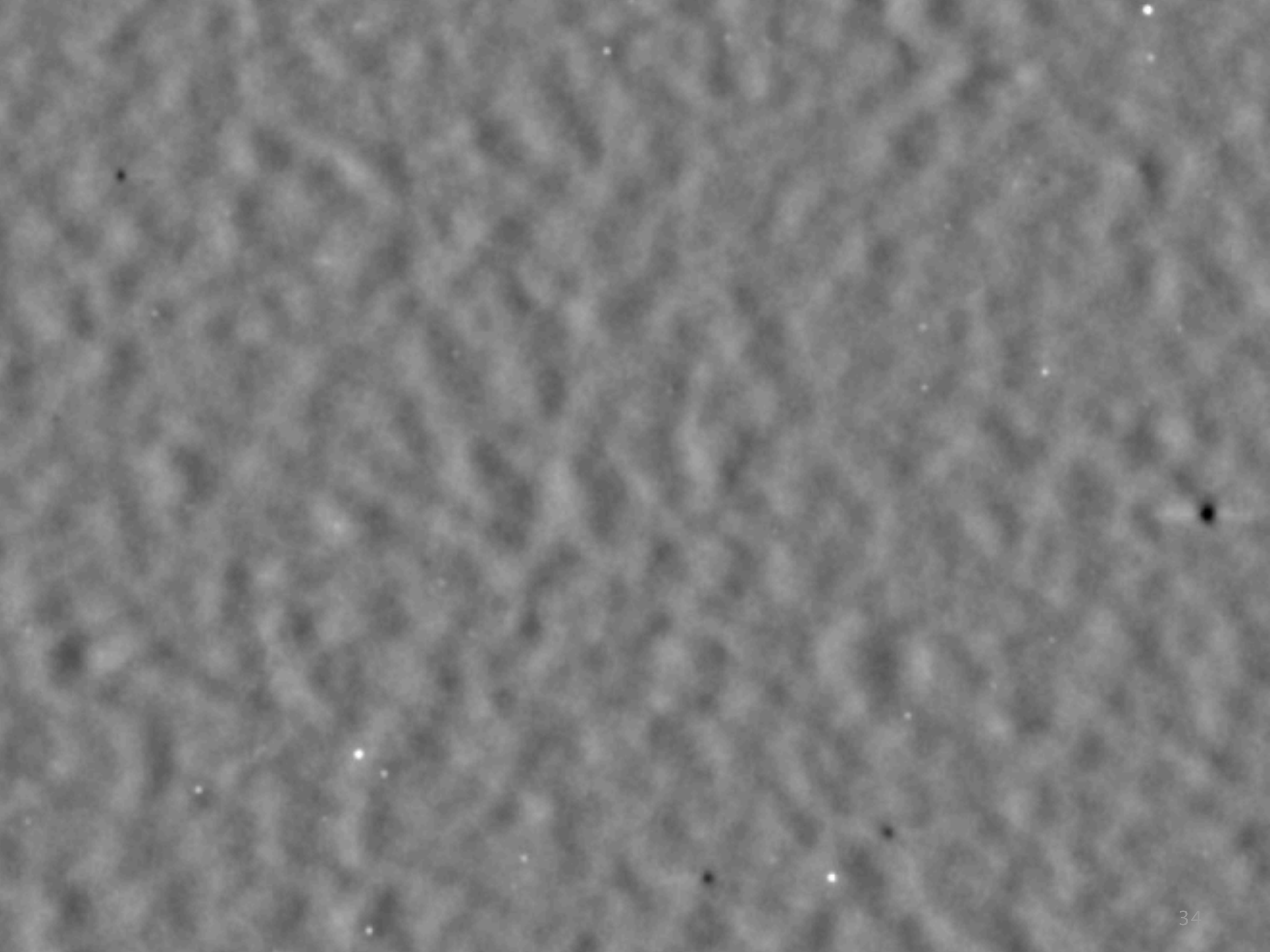
2007: SPT
~1000 detectors



- ACBAR was the first experiment to make a “background limited” detector (limited by random arrival time of photons)
- To make these measurements, we need more detectors

SPT has produced the *highest resolution and sensitivity map of the CMB*



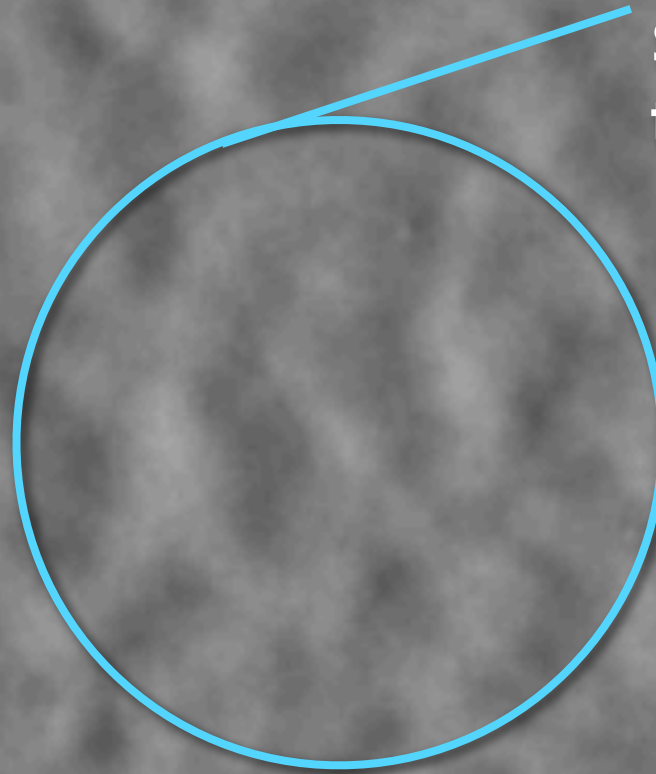


Zoom in on highpass filtered SPT map

~50 square degrees from
2500 square degree survey

CMB Anisotropy

– Primordial and
secondary anisotropy in
the CMB

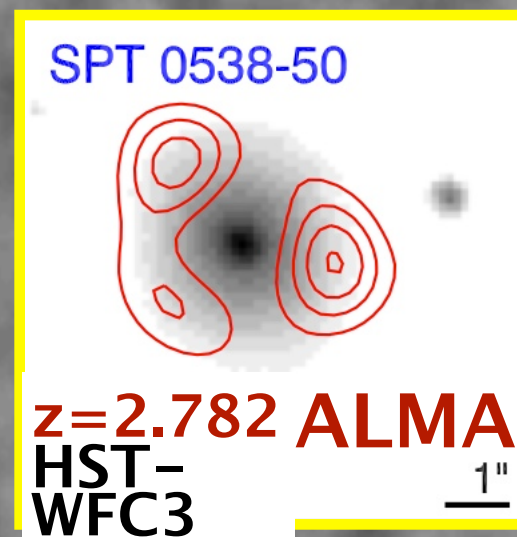
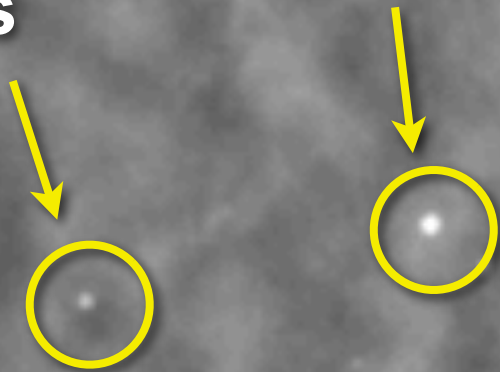


Story et al. astro-ph/1210.7231
Hou et al. astro-ph/1212.6267
Reichardt et al. 2012 ApJ, 755, 70
van Engelen et al. 2012 ApJ 756, 142
and more!

Zoom in on highpass filtered SPT map

~50 square degrees from
2500 square degree survey

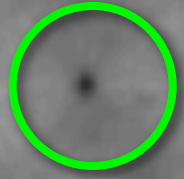
Point Sources – Bright radio galaxies, AGN, and discovery of rare lensed, high redshift dusty star forming galaxies



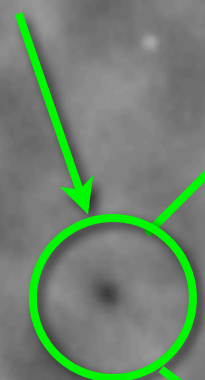
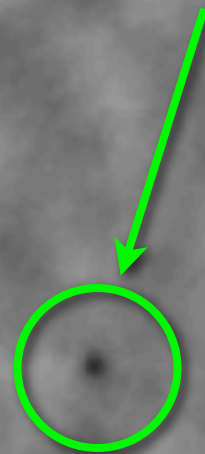
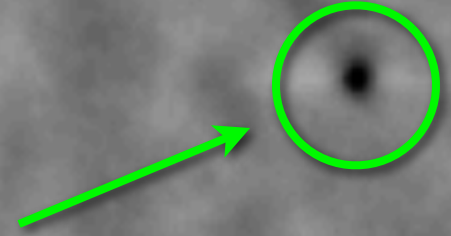
Hezaveh et al. ApJ 767, (2013) ,132
Weiss et al. ApJ, 767, (2013), 88
Vieira et al. Nature, 495 (2013), 344
and more!

Zoom in on highpass filtered SPT map

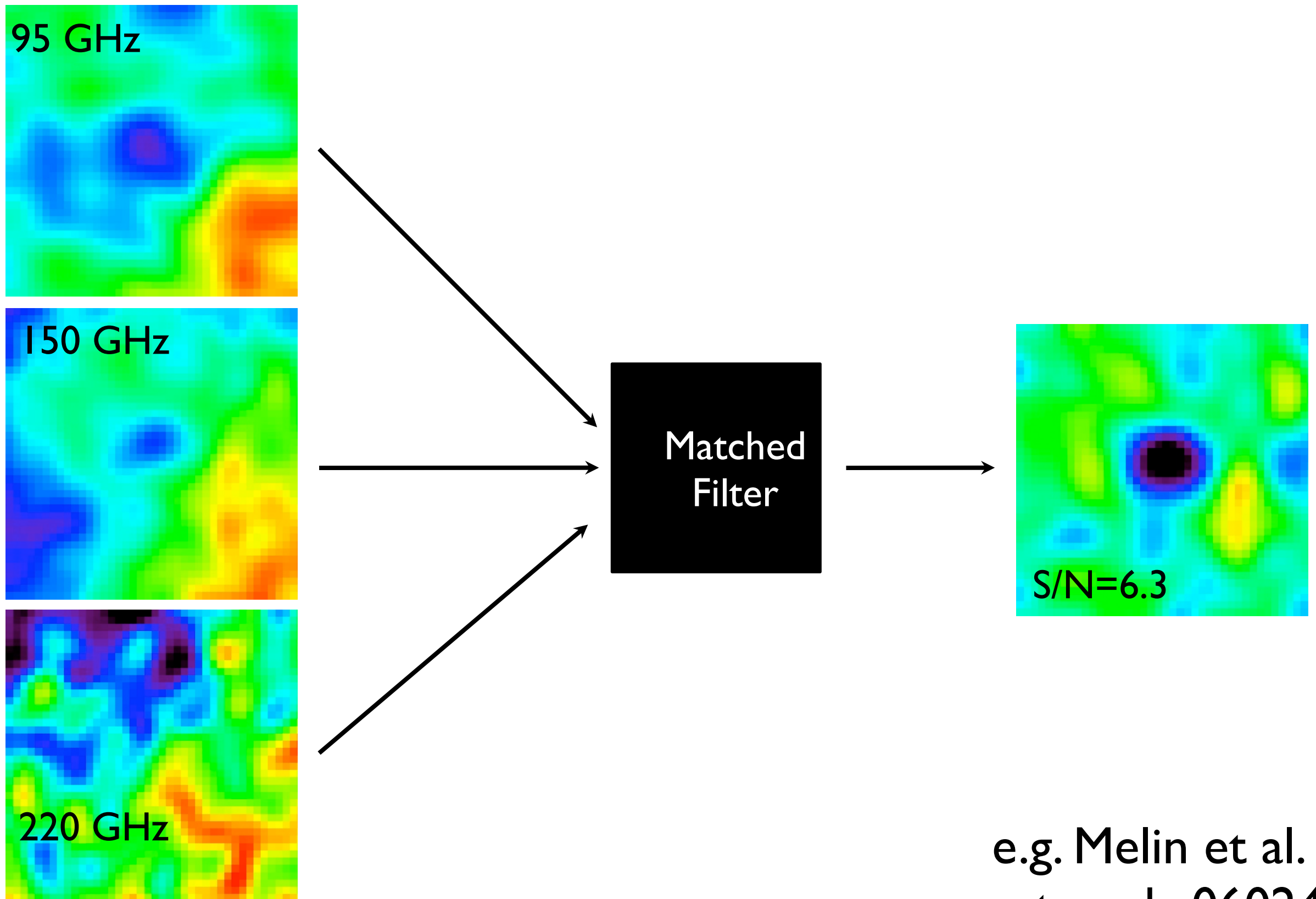
~50 square degrees from
2500 square degree survey



Galaxy Clusters – High
signal-to-noise SZ galaxy
cluster detections appear as
“shadows” against the CMB!



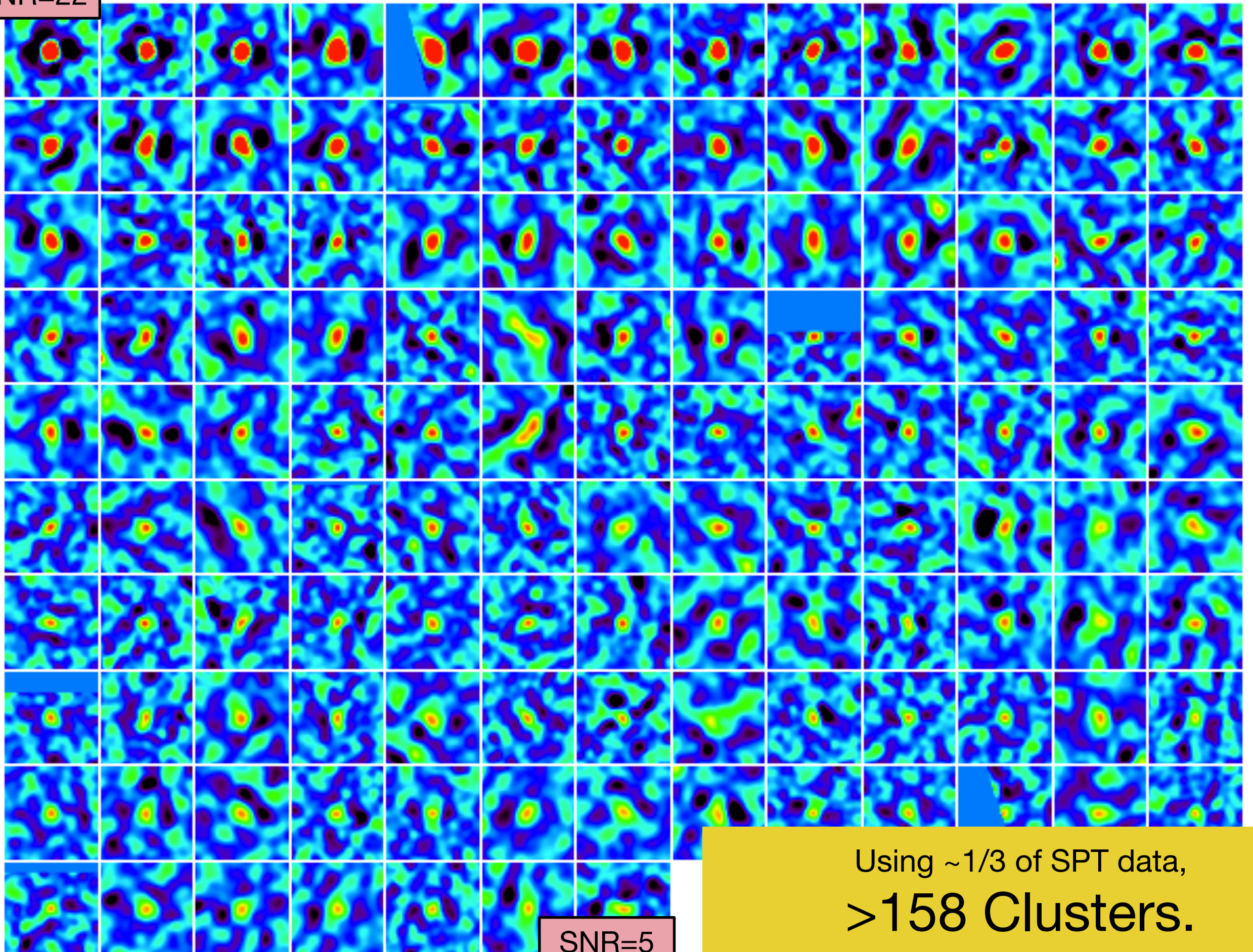
Finding Clusters in the SPT Survey



e.g. Melin et al.
astro-ph: 0602424

SPT Discovered Clusters from first 720 deg²

SNR=22



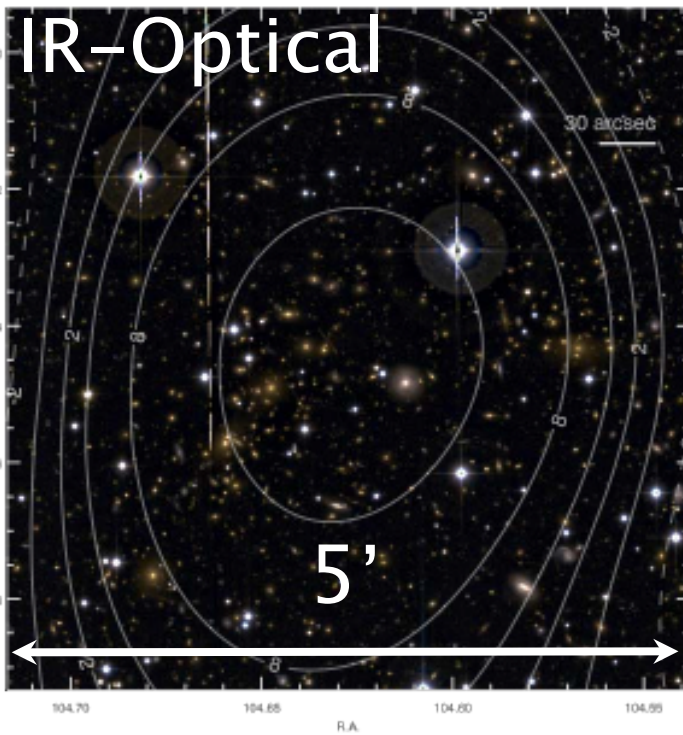
Reichardt et al 2013

Using ~1/3 of SPT data,
>158 Clusters.

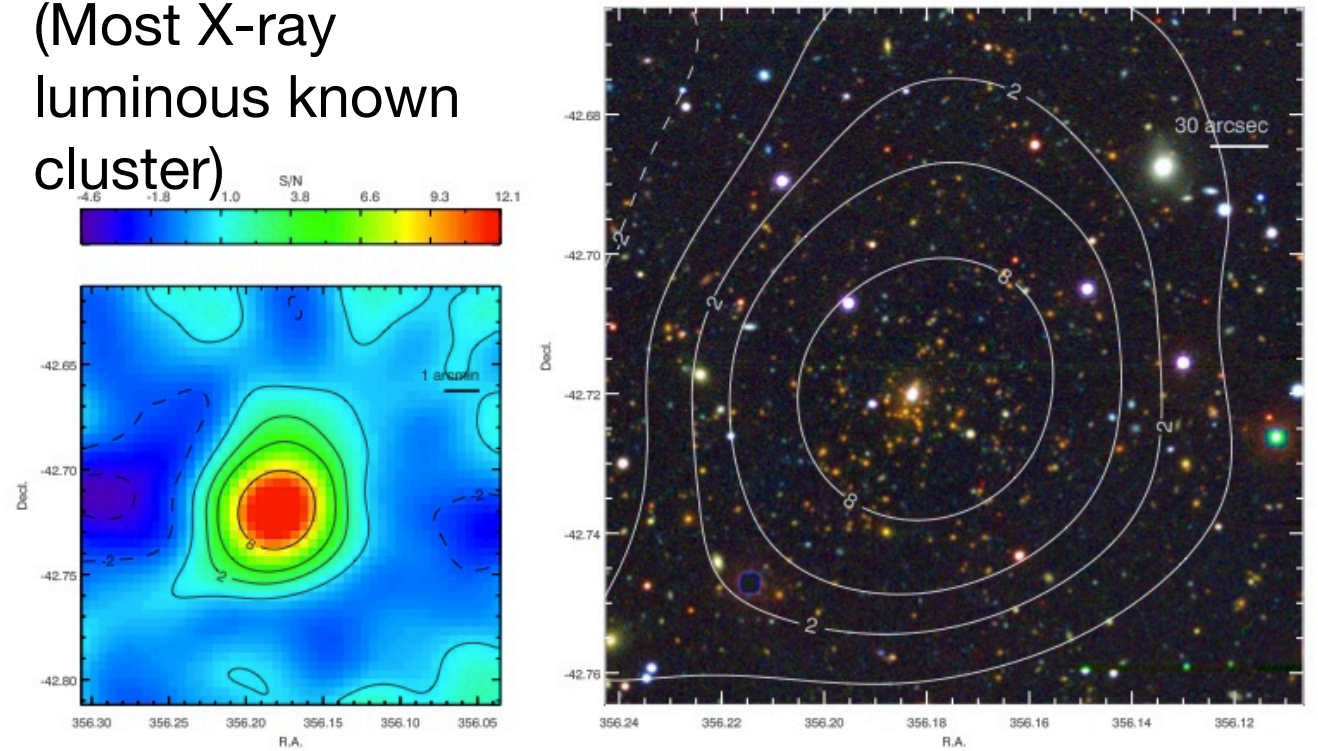
SNR=5

Example Massive SPT Clusters

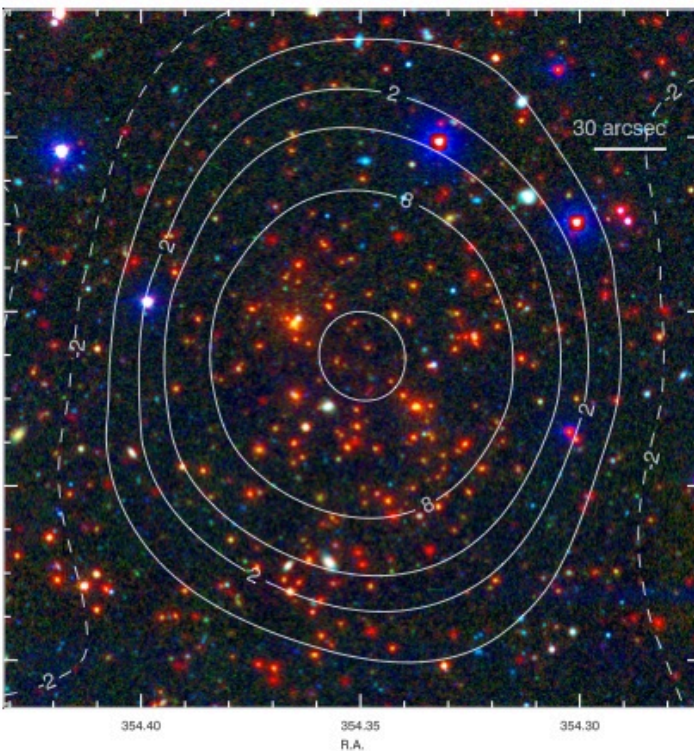
0658-5358 ($z=0.30$)
(Bullet)



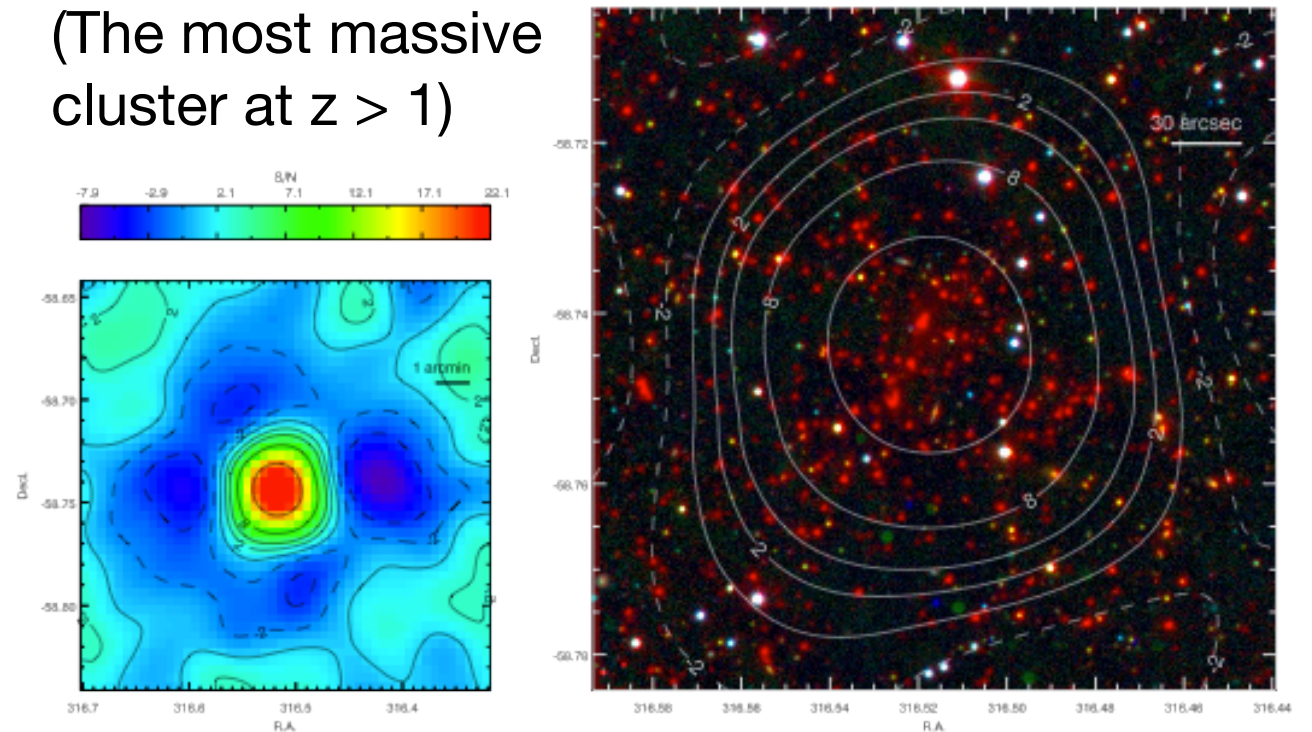
2344-4243 ($z=0.62$)
(Most X-ray
luminous known
cluster)



2337-5942 ($z=0.78$)



2106-5844 ($z=1.13$)
(The most massive
cluster at $z > 1$)



Cosmological Analysis:

Combine X-ray Measurements with SZ Cluster Survey

Developed Markov-Chain Monte Carlo (MCMC) method to vary cosmology and cluster observable-mass relation simultaneously, while accounting for SZ selection in a self-consistent way

6 Cosmology Parameters (plus extension parameters)

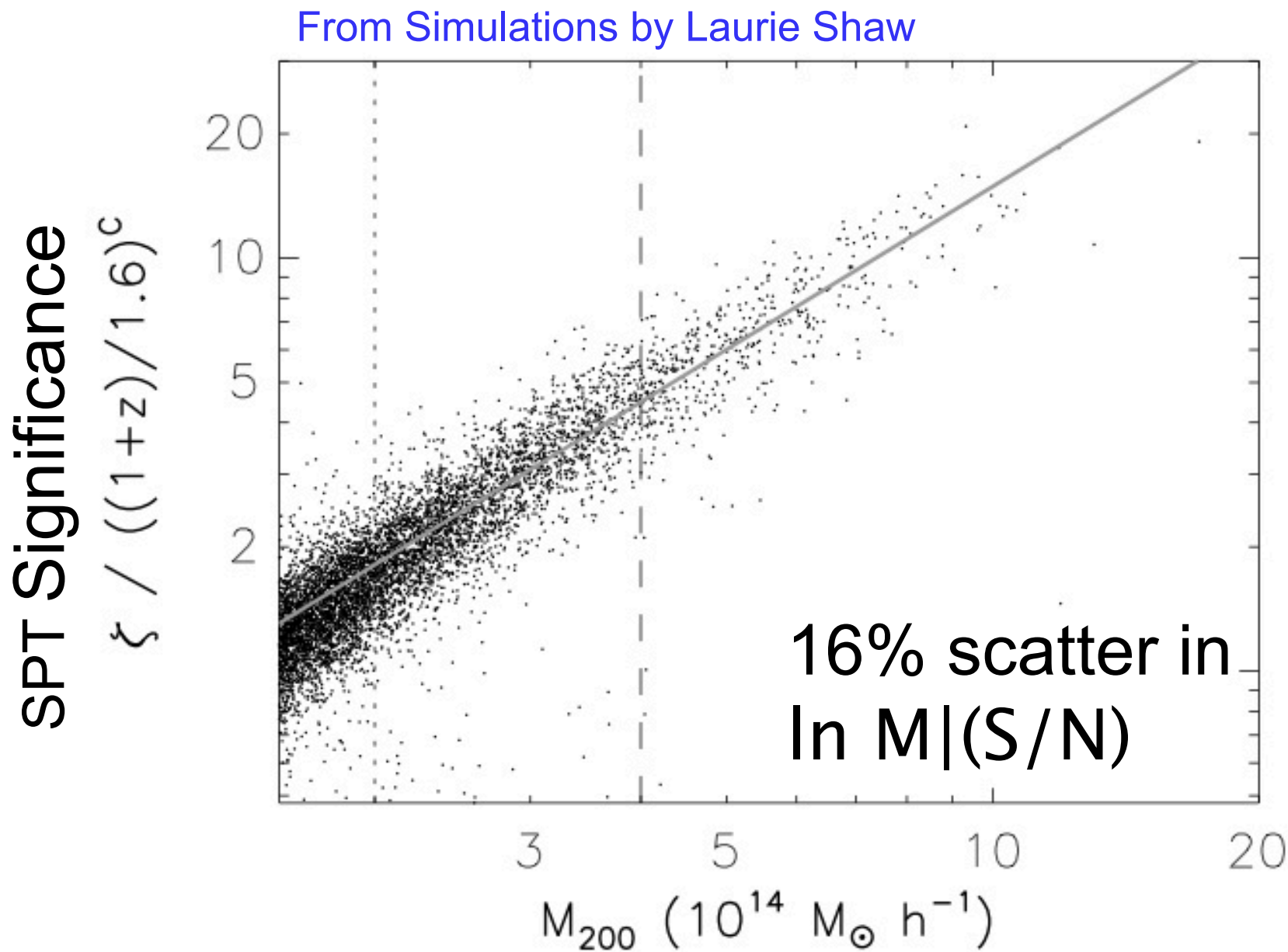
- Λ CDM Cosmology
 - $\Omega_m h^2, \Omega_b h^2, A_s, n_s, \tau, \theta_s$
- Extension Cosmology
 - $w, \Sigma m_\nu, f_{NL}, N_{eff}$

9 Scaling Relation Parameters

- X-ray (Y_x - M) and SZ (ζ - M) relations (4 and 5 parameters):
 - A) normalization,
 - B) slope,
 - C) redshift evolution,
 - D) scatter,
 - F) correlated scatter

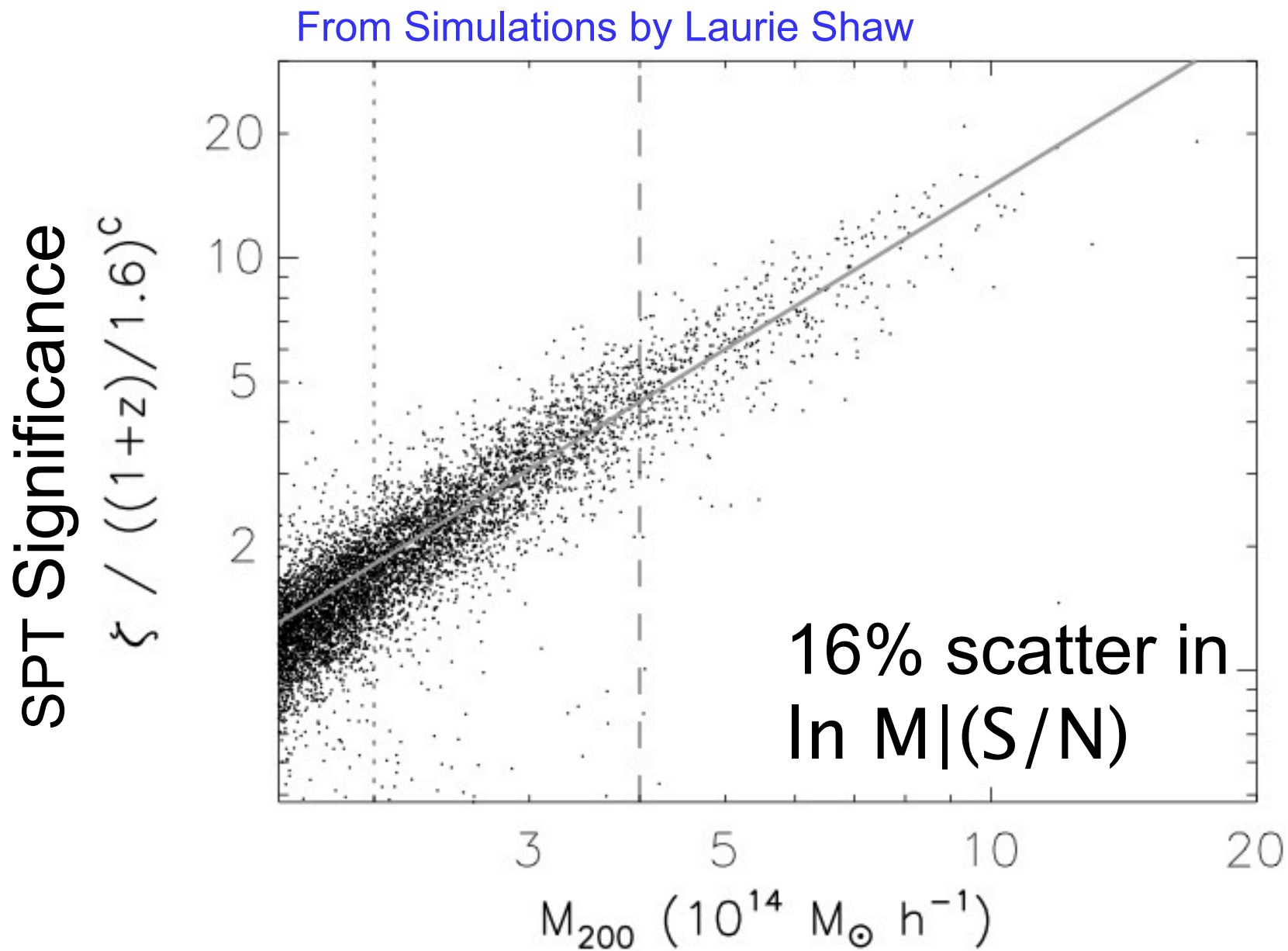
Benson et al 2013,
arXiv: 1112.5435

SPT Significance as a Mass Proxy



- For any cluster survey, challenge is to link cluster “observable” to cluster mass
- YSZ should have low scatter (Kravstov 2006, Battaglia 2012)
- From simulations, signal-to-noise in spatial filtered SPT map is a relatively good mass proxy (Vanderlinde et al 2010)
- **Need to calibrate SZ significance to cluster mass!**

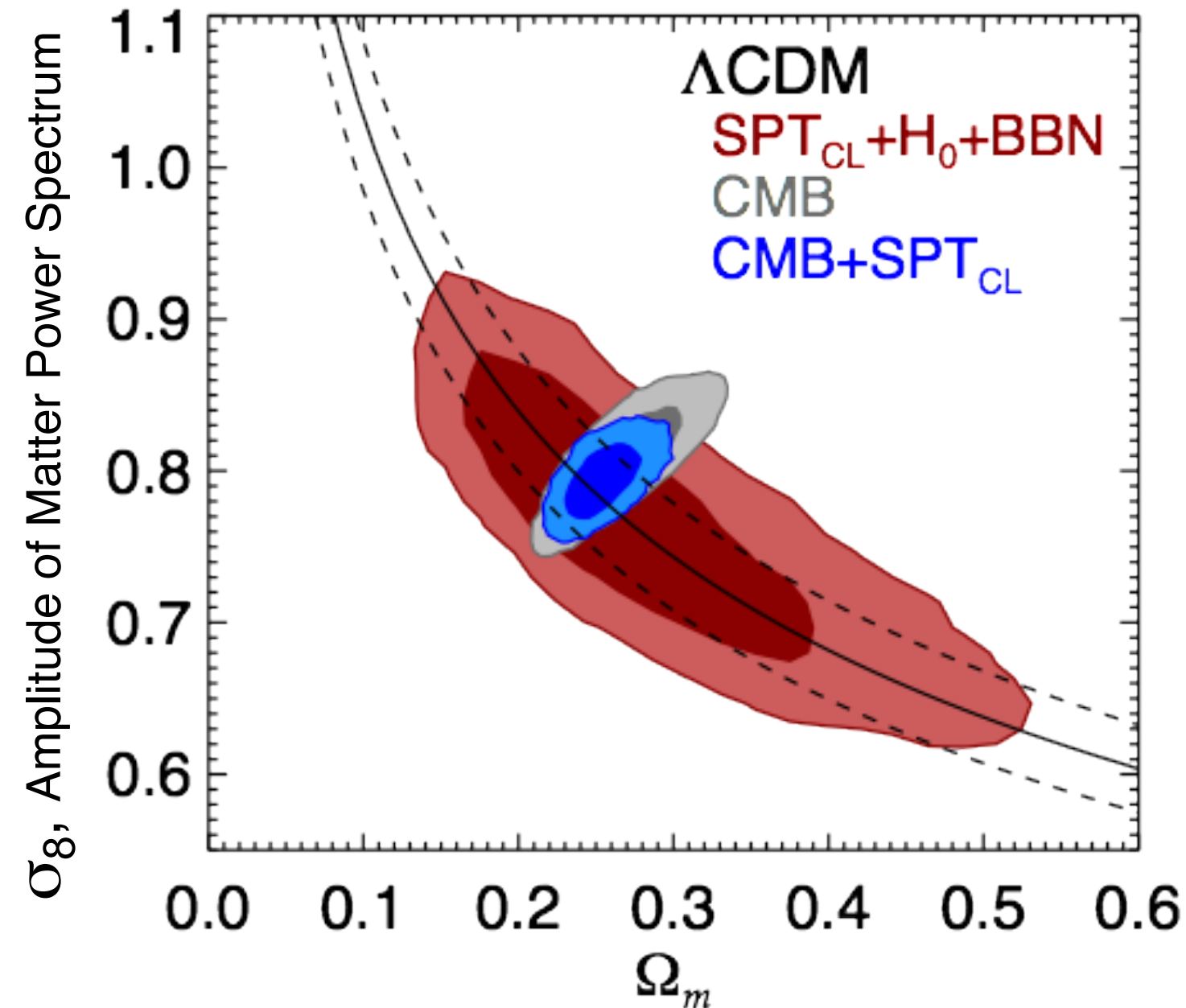
SPT Significance as a Mass Proxy



- For any cluster survey, challenge is to link cluster “observable” to cluster mass
- YSZ should have low scatter (Kravstov 2006, Battaglia 2012)
- From simulations, signal-to-noise in spatial filtered SPT map is a relatively good mass proxy (Vanderlinde et al 2010)
- **Need to calibrate SZ significance to cluster mass!**

Λ CDM Constraints:

Test X-ray Mass Calibration on 18 clusters (Benson et al. 2011)



σ_8, Ω_m - 68, 95% Confidence Contours

$H_0 = 73.8 \pm 2.4$ km / s Mpc (Riess et al 2011)

CMB: WMAP7 + SPT (Komatsu et al 2011, Keisler et al. 2011)

BBN: $\Omega_b h^2 = 0.022 \pm 0.002$ (Kirkman et al. 2003)

- SPT_{CL}+H₀+BBN Λ CDM fit best constrains:

$$-\sigma_8(\Omega_m/0.25)^{0.30} = 0.785 \pm 0.037$$

– *Limited by accuracy of cluster mass calibration!*

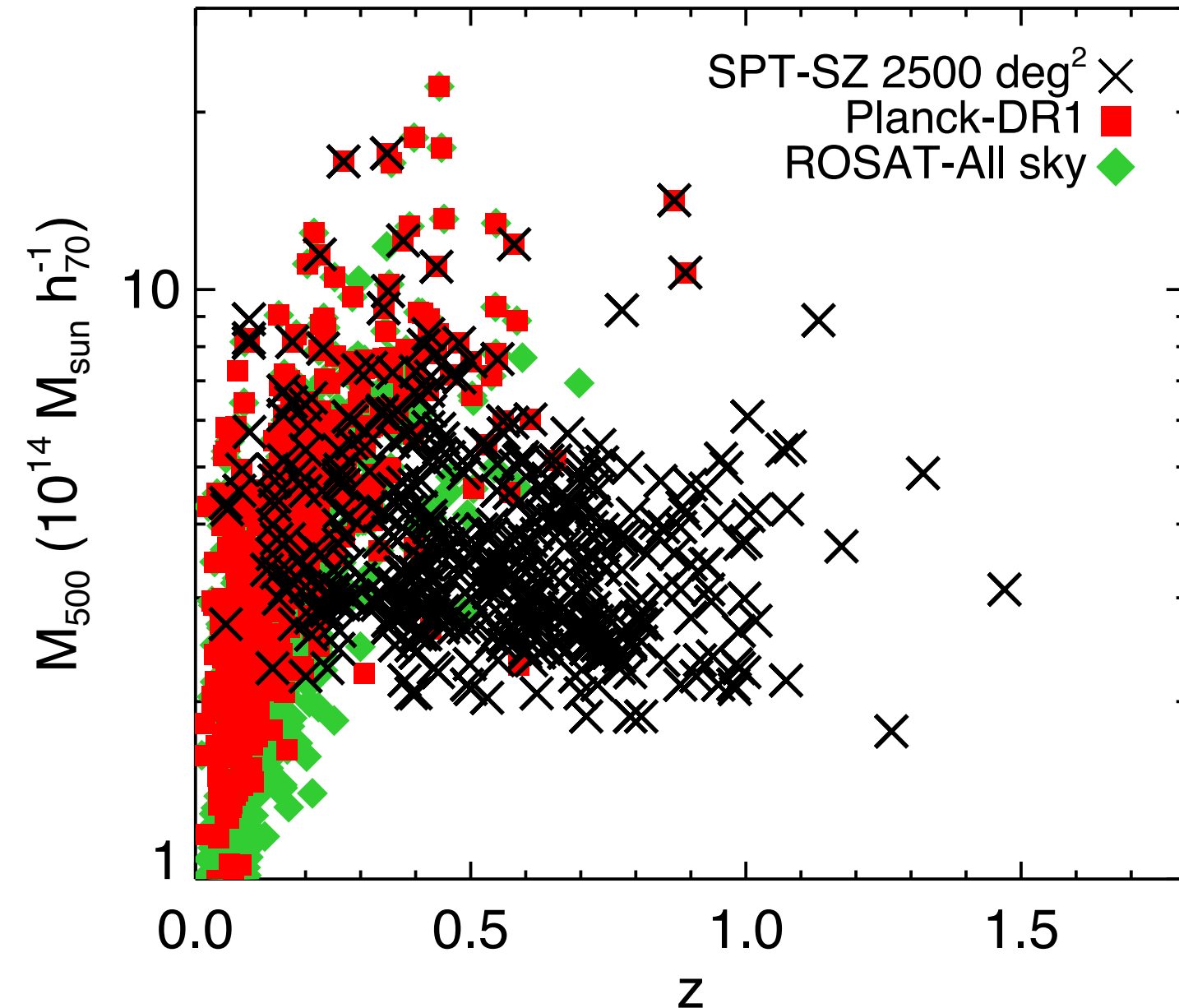
- Adding SPT_{CL} to CMB improves σ_8 and Ω_m constraint by factor of 1.5:

$$-\sigma_8 = 0.795 \pm 0.016$$

$$-\Omega_m = 0.255 \pm 0.016$$

SPT-2500d Cluster Sample

Cluster Mass vs Redshift



- Reichardt et al. 2013 presented a catalog of 158 clusters from first 1/3 of survey

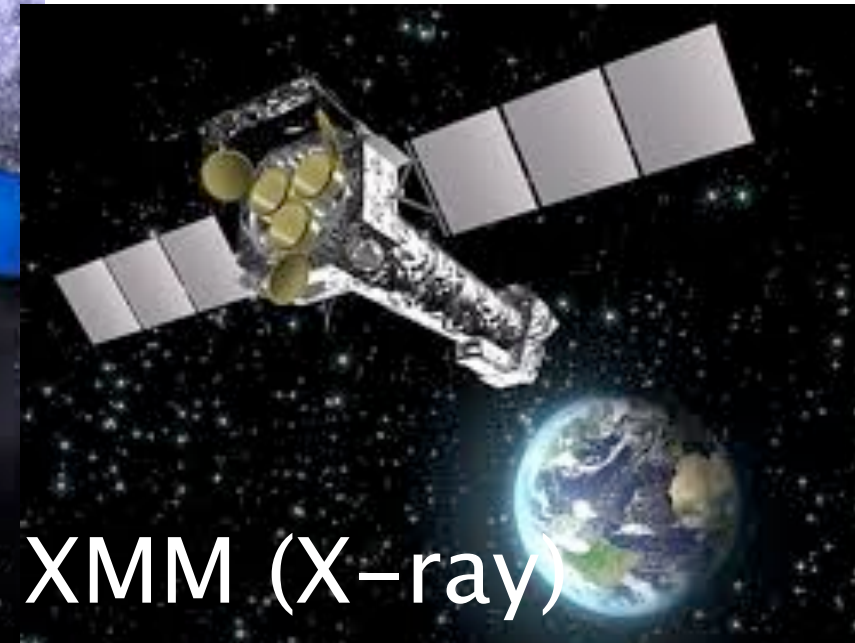
- 80% are newly discovered
- $\langle z \rangle \sim 0.55$
- 20% of sample at $z > 0.8$
- Mass threshold falls with redshift, at $z = 0.6 - M_{500} > 3 \times 10^{14} M_{\text{sol}}/h_{70}$

- ~500 clusters in 2500 deg² catalog; >400 with measured redshifts, analysis on-going

See, Reichardt et al ApJ 763 (2013), 127 for results from first 720d

Multi-wavelength Observations: *Mass Calibration*

- **Multi-wavelength mass calibration campaign, including:**
 1. **X-ray** with Chandra and XMM
 2. **Weak lensing** from Magellan ($0.3 < z < 0.6$) and HST ($z > 0.6$)
 3. **Dynamical masses** from NOAO 3-year survey on Gemini ($0.3 < z < 0.8$), also VLT at ($z > 0.8$)

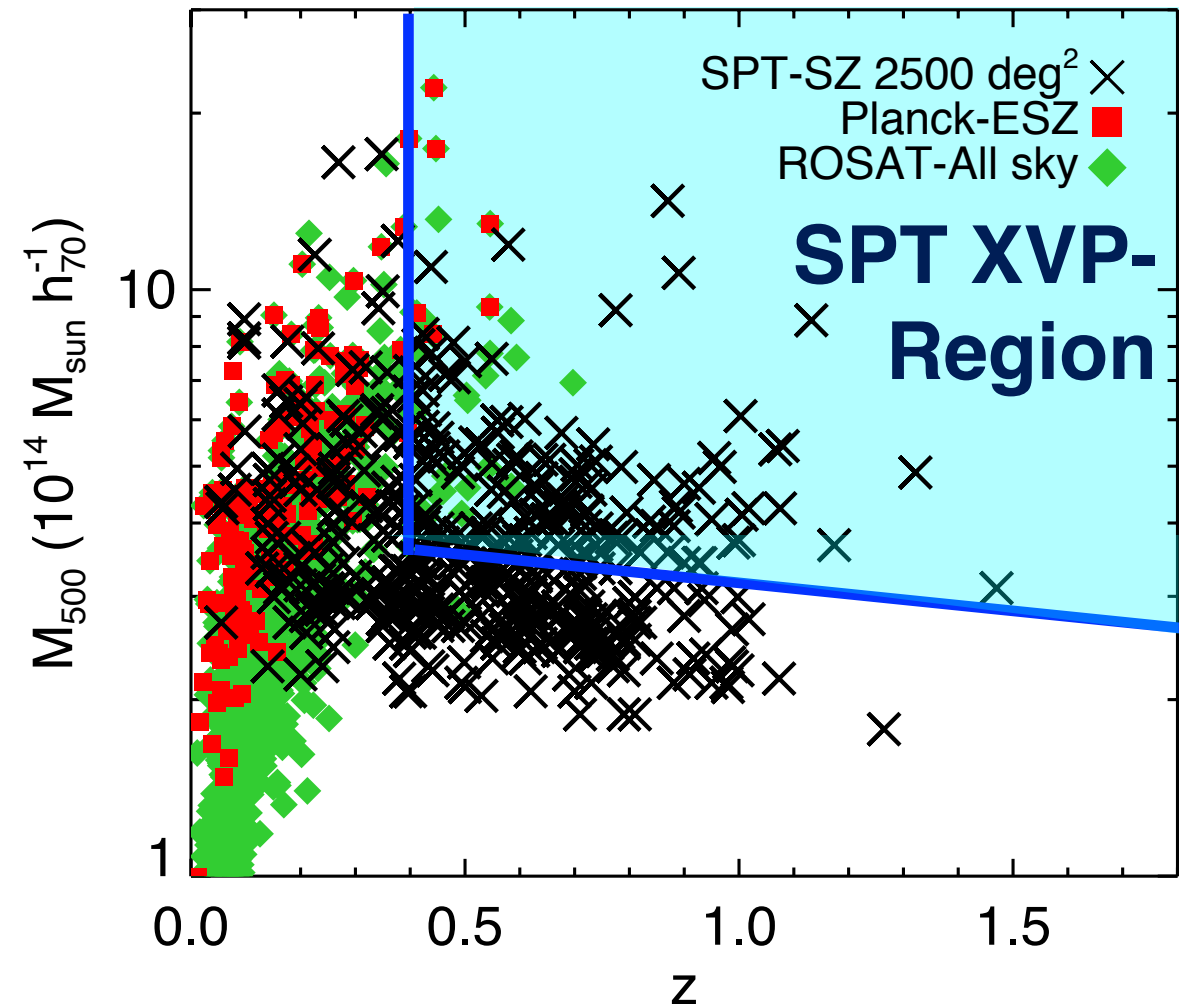


<http://obs.carnegiescience.edu/Magellan/>

Multi-wavelength Observations: *Mass Calibration*

- **Multi-wavelength mass calibration campaign, including:**

1. **X-ray** with Chandra and XMM (**PI:** Benson, Vikhlinin)
2. **Weak lensing** from Magellan ($0.3 < z < 0.6$) and HST ($z > 0.6$) (**PI:** High, Hoekstra, Schrabback)
3. **Dynamical masses** from NOAO 3-year survey on Gemini ($0.3 < z < 0.8$) (**PI:** Stubbs), also VLT at ($z > 0.8$) (**PI:** Bazin, Mohr)



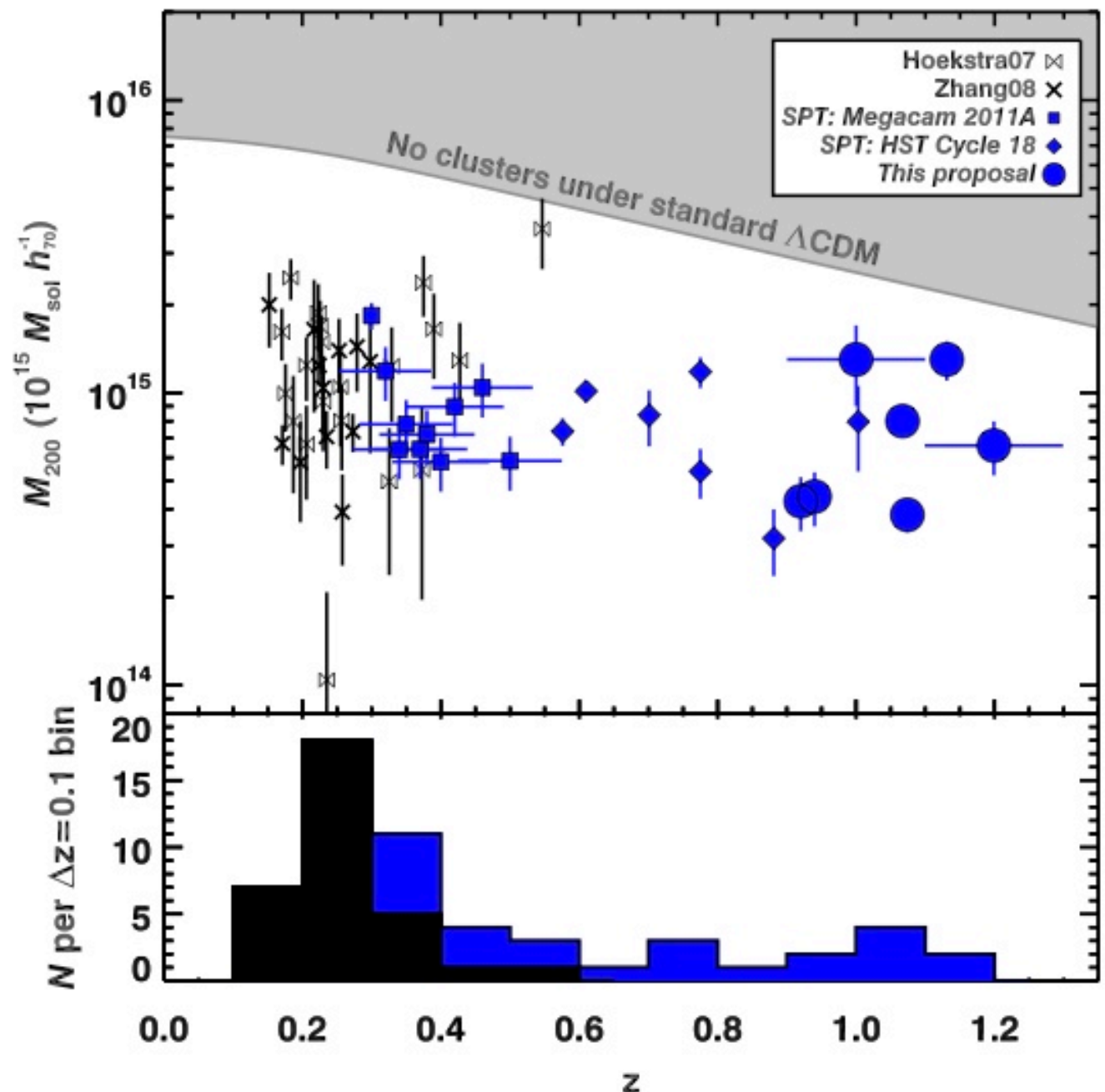
- 90 clusters at $0.3 < z < 1.2$ with $5.7 < \text{SPT-significance} < 43$
- Optical Follow-up complete, analysis on-going. Look for results soon!

Multi-wavelength Observations: *Mass Calibration*

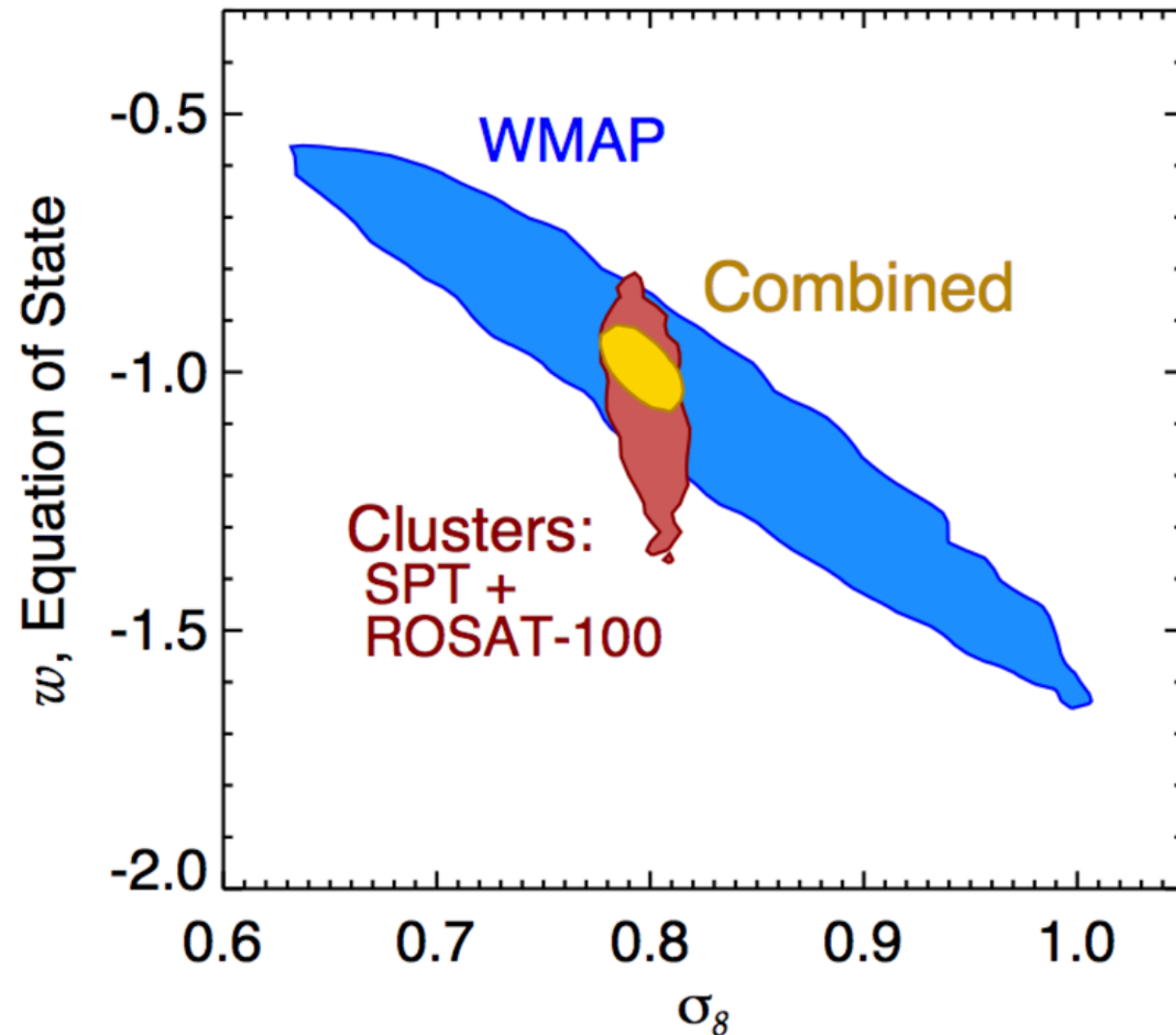
- **Multi-wavelength mass calibration campaign, including:**

1. **X-ray** with Chandra and XMM (**PI:** Benson, Vikhlinin)
2. **Weak lensing** from Magellan ($0.3 < z < 0.6$) and HST ($z > 0.6$) (**PI:** High, Hoekstra, Schrabback)
3. **Dynamical masses** from NOAO 3-year survey on Gemini ($0.3 < z < 0.8$) (**PI:** Stubbs), also VLT at ($z > 0.8$) (**PI:** Bazin, Mohr)

Weak Lensing Sample



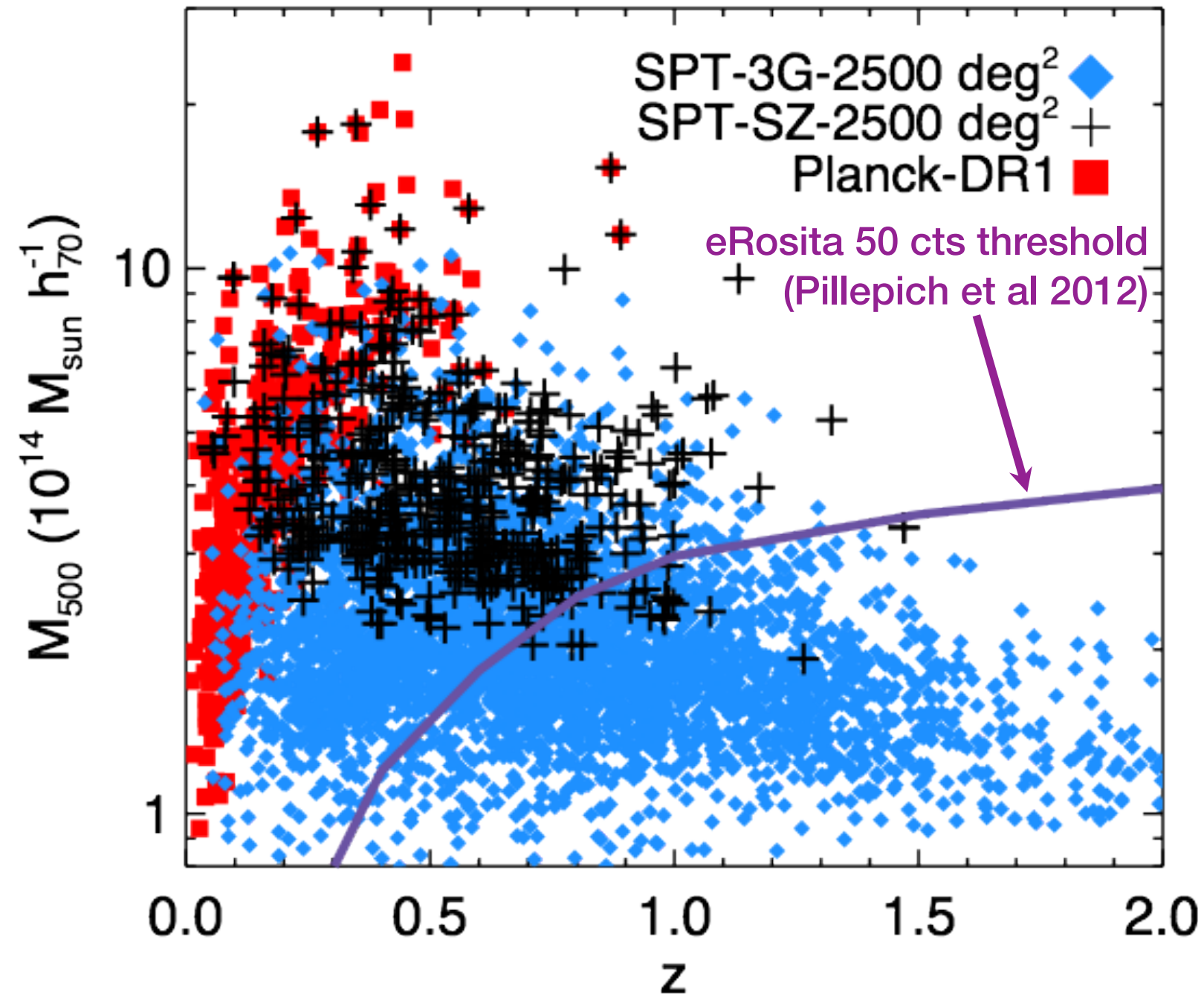
SPT Cosmological Constraints: 2500 deg² (projected)



SPT 2500 deg² survey has detected ~550 clusters, assuming mass calibration expected with X-ray and Lensing programs then:

- **Combined CMB + SPT cluster survey will constrain $dw \sim 7.5\%$, **independent** of constraints from SNe, BAO**

SPT-3G: Cluster Survey



- SPT-3G will survey 2500 deg² to a level 10x deeper than SPT-SZ survey
- >10x increase in number of clusters over SPT-SZ
 - 4000 clusters at 99% purity threshold
- CMB-cluster lensing would provide a 3% cluster mass calibration
 - competitive with stacked weak-lensing (Rozo et al. 2011)

Dark Energy Survey (DES) and SPT



Image credit: Roger Smith/NOAO/AURA/NSF

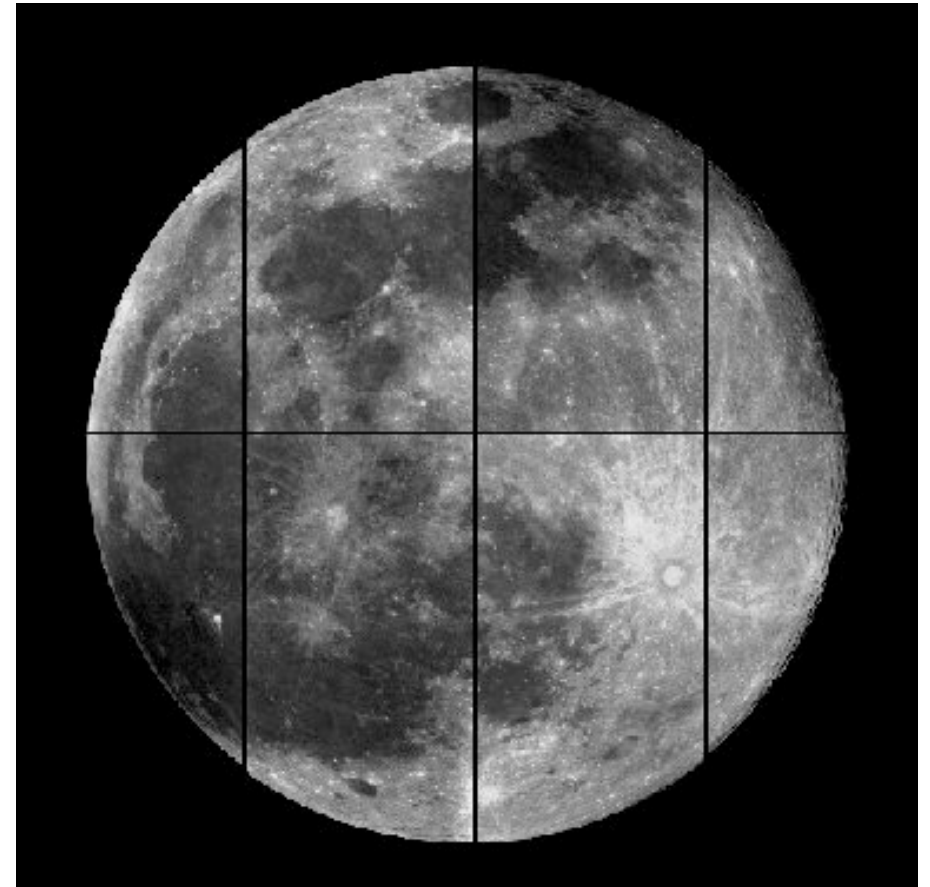
Blanco 4m. Cerro Tololo, Chile

- Wide field (2.2 deg^2) optical camera for 4-meter Blanco telescope (Chile)
- **Optical survey (2012-2016) to cover $\sim 5000 \text{ deg}^2$ which will detect $\sim 100,000$ clusters out to $z \sim 1$**
- Multiple probes of dark energy (cluster survey, weak lensing, BAO, SN)
- Coordinated to overlap with SPT

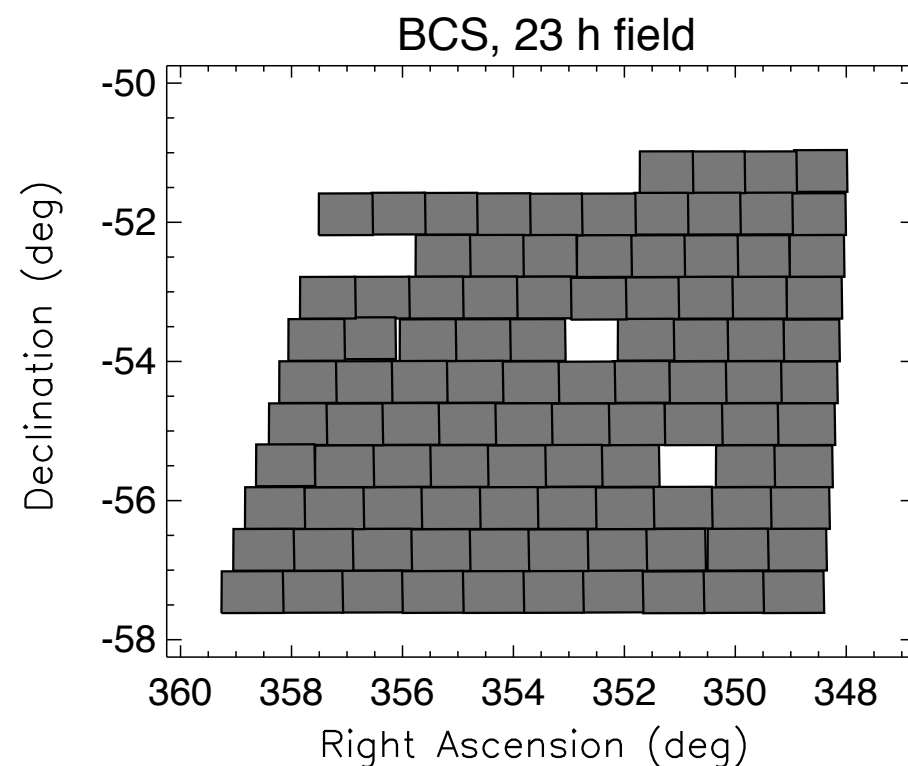
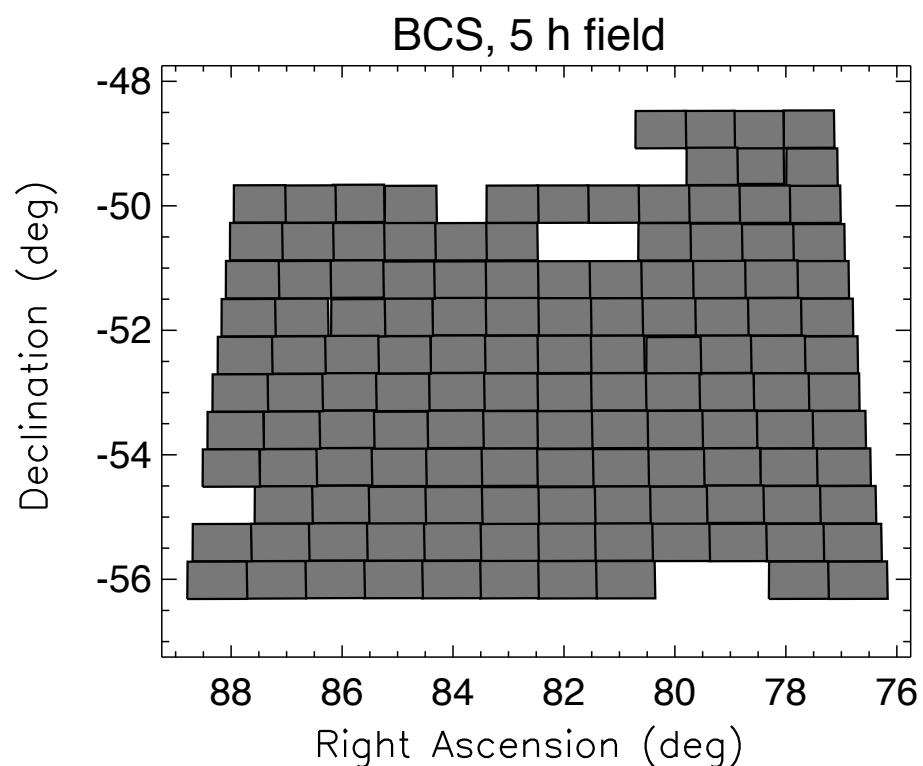
But before there was
DES...

The Blanco Cosmology Survey

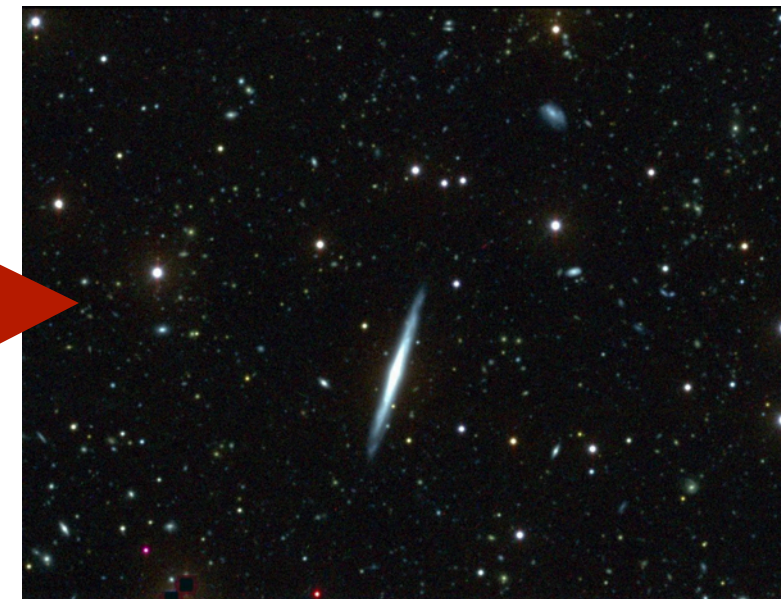
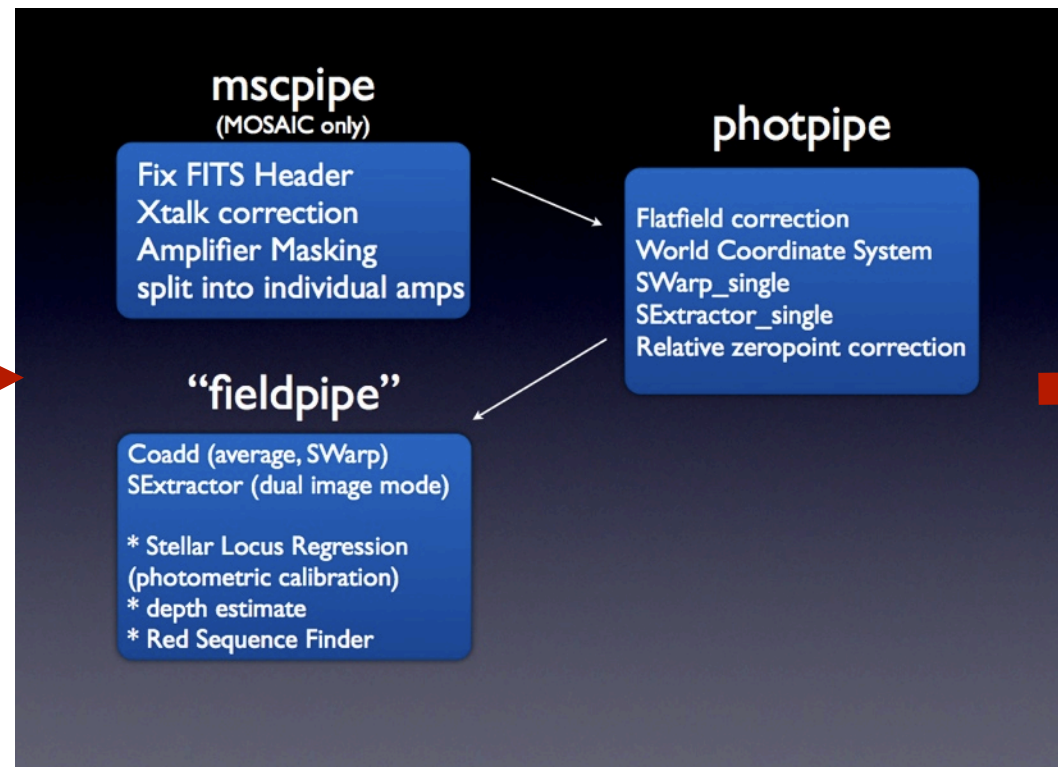
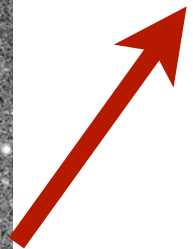
- NOAO Large Survey
- $\sim 80 \text{ deg}^2$ over 2 fields
- 57 nights Nov 2005-2008
- Survey coordinated with SPT



Mosaic-II FOV



Data was reduced with the photpipe algorithm.



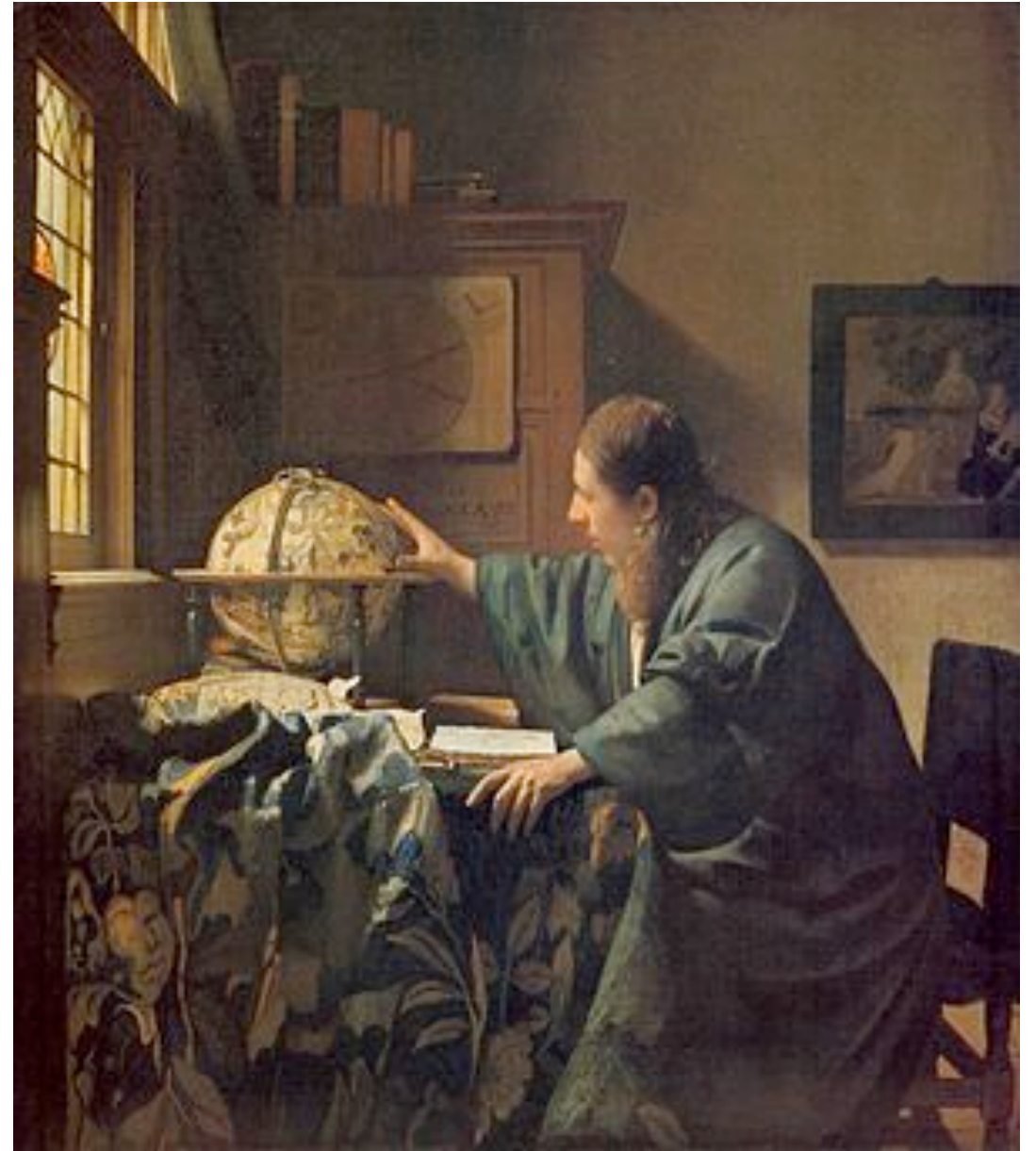
>3000 Individual Exposures
(Including Calibration Files)

A crash course in optical observing

- Observing Considerations
- “Reducing” the images
- Photometry

Planning

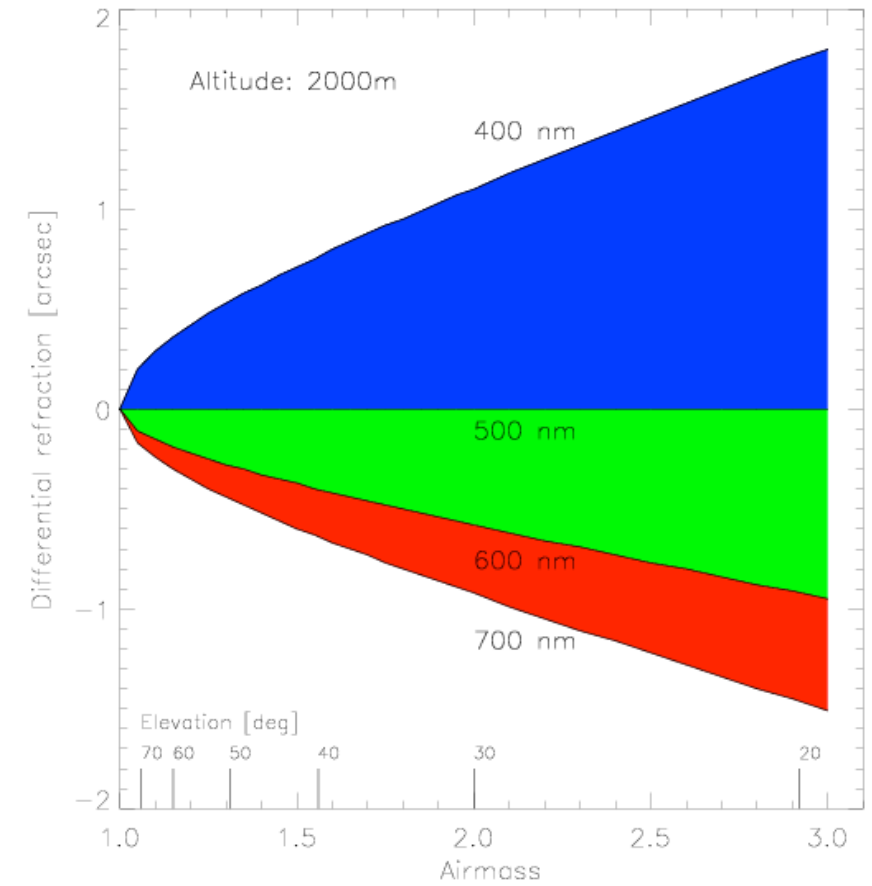
- Target Visibility
- Scientific Objective
 - filter choices
 - lunar phase
 - observation strategy



[Johannes Vermeer](#)

Target Visibility

- Airmass - path length relative to zenith
- Seeing $\sim \text{airmass}^{0.6}$
- Differential Atmospheric Refraction



[HTTP://WWW.ASTRO.UNI-BONN.DE/~MISCHA/OBSTIPS/AIRMASS.HTML](http://www.astro.uni-bonn.de/~misch/obstips/airmass.html)

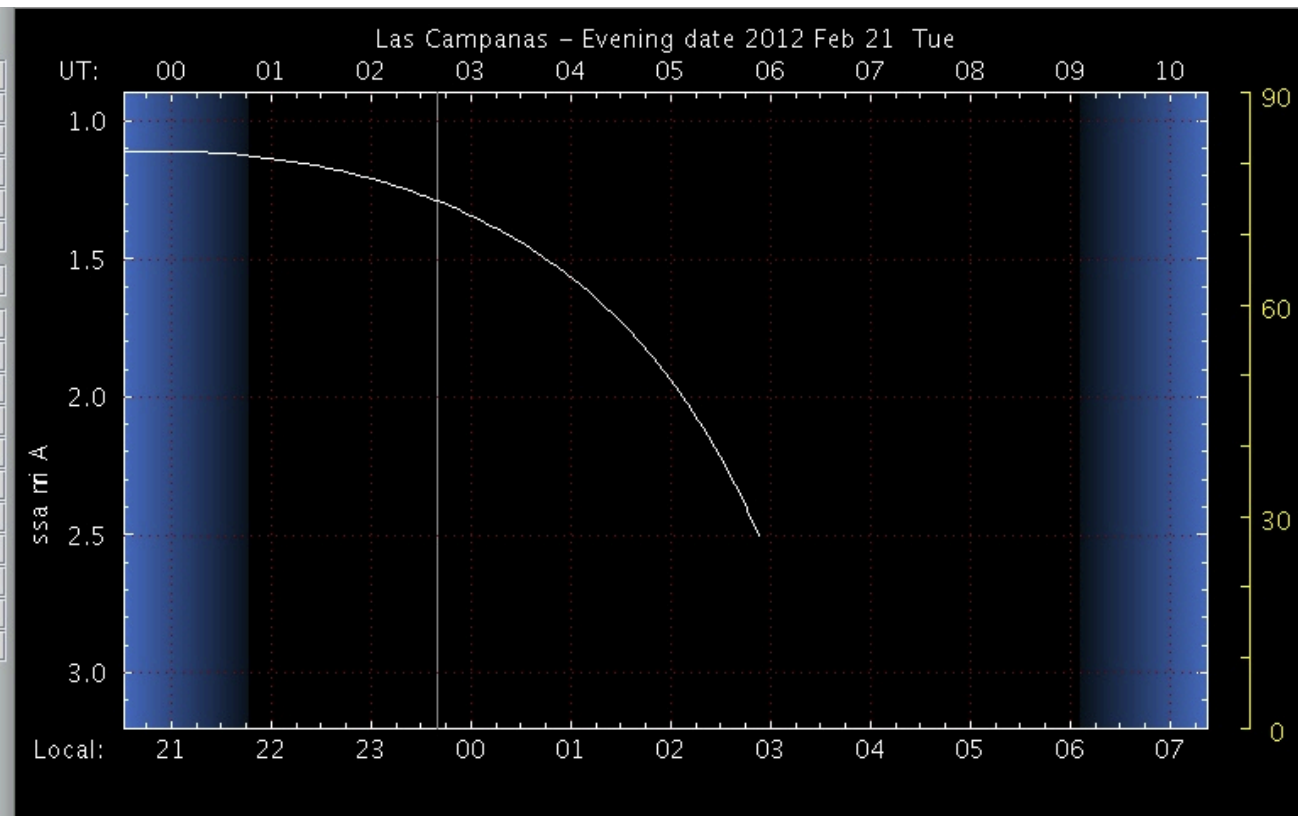
JSkyCalc v1.2.1: John Thorstensen, Dartmouth College

Object:	null	Sidereal	08 02 23
RA:	05 17 00.49	HA	+2 45 07
dec:	-54 30 27.9	Airmass	1.287
equinox:	2000.00	AltAz	50.9 az = 217.4
Date:	2012 Feb 21 Tue	parallactic	66.3 [-113.7] degr.
Time:	23 39 29.2	SunRAdec	22:19:17.8 -10:26:50
Time is:	<input checked="" type="radio"/> Local <input type="radio"/> UT	SunAltAz	-38.5 az = 225.0
timestep:	1 h	ZTwilight	No twilight.
sleep for (s):	2	MoonPhase	0.2 days since new moon.
JD:	2455979.610755	MoonRAdec	22:17:44.2 -04:35:08
Site name:	Las Campanas	MoonAltAz	-43.3 az = 229.7
Longitude:	04 42 47.9 H W	MoonIllumFrac	0.003
Latitude:	-29 00 30	LunSkyBrght	Moon is down.
Time zone:	4.00	Moon-Obj ang.	94.8 deg
DST code:	-1	Bary. JD	2455979.61072 [-2.7 s]
Zone name:	Chilean	Bary. Vcorr.	-6.99 km/s
Elevation:	2282 m	Constellation	Pic
Terrain elev:	2282 m	Planet Warning?	---

Refresh output Set to Now Step Forward Step Back

Auto Update Auto Step Site Menu Planet Table

Hourly Circumstances Nightly Almanac Seasonal Observability



Observing Plan

- Filter Choice
 - Bright v/s Dark Time
 - Air Glow
 - Dither Strategy

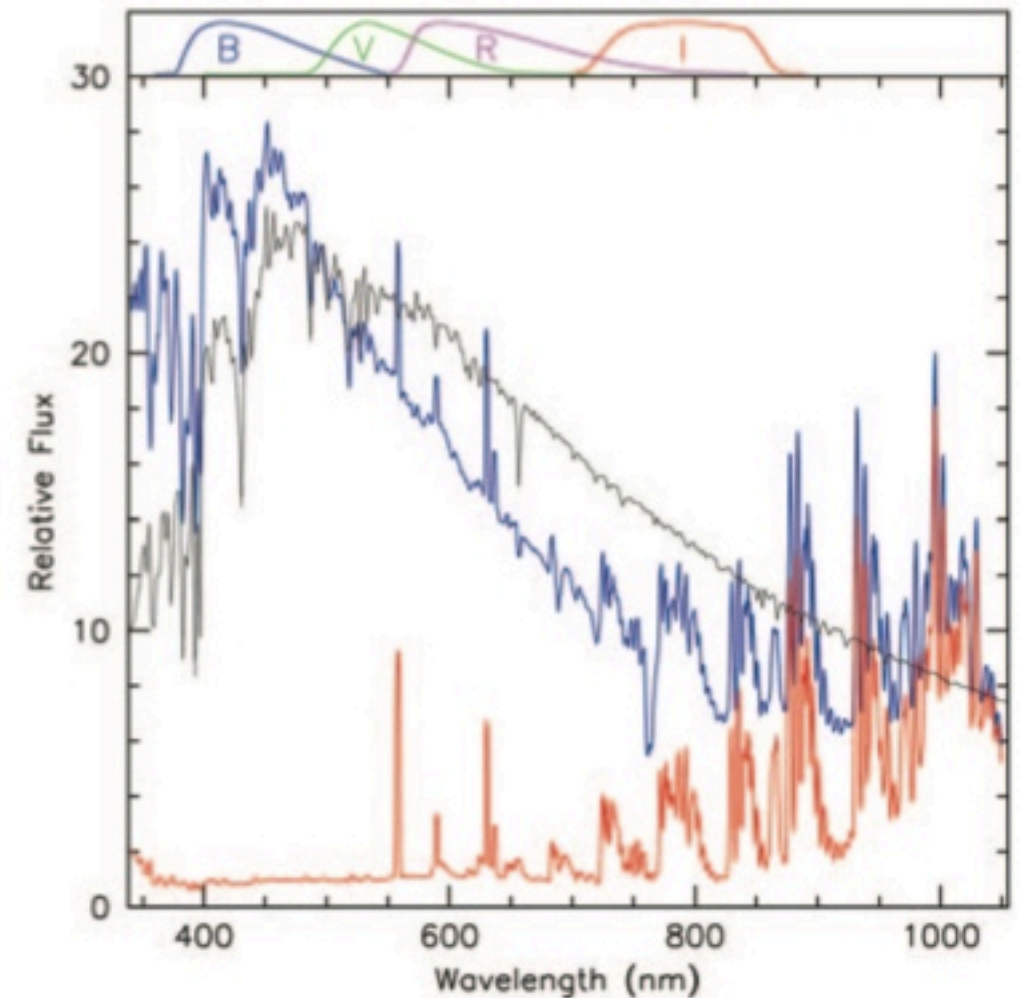
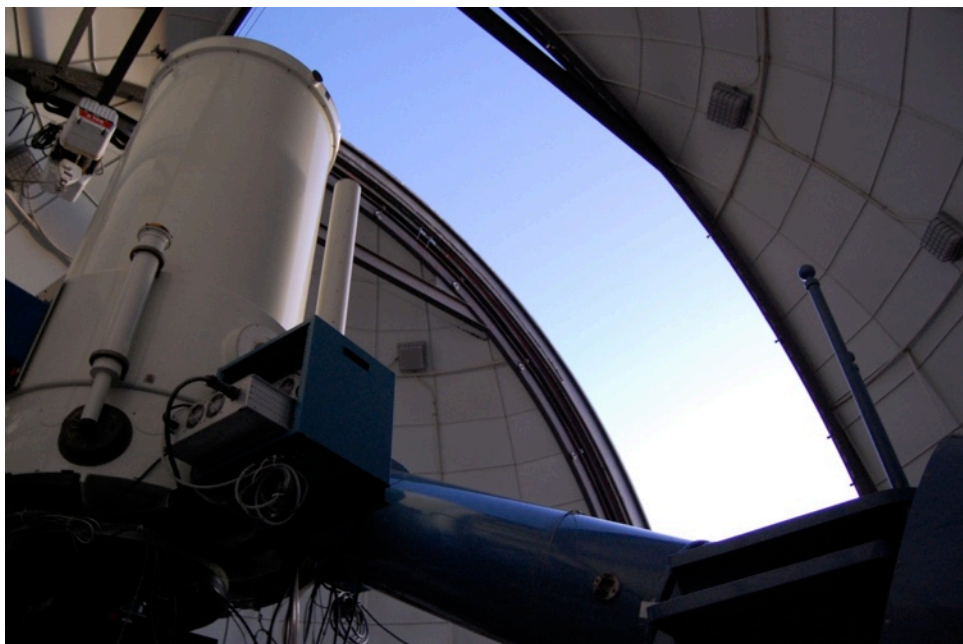
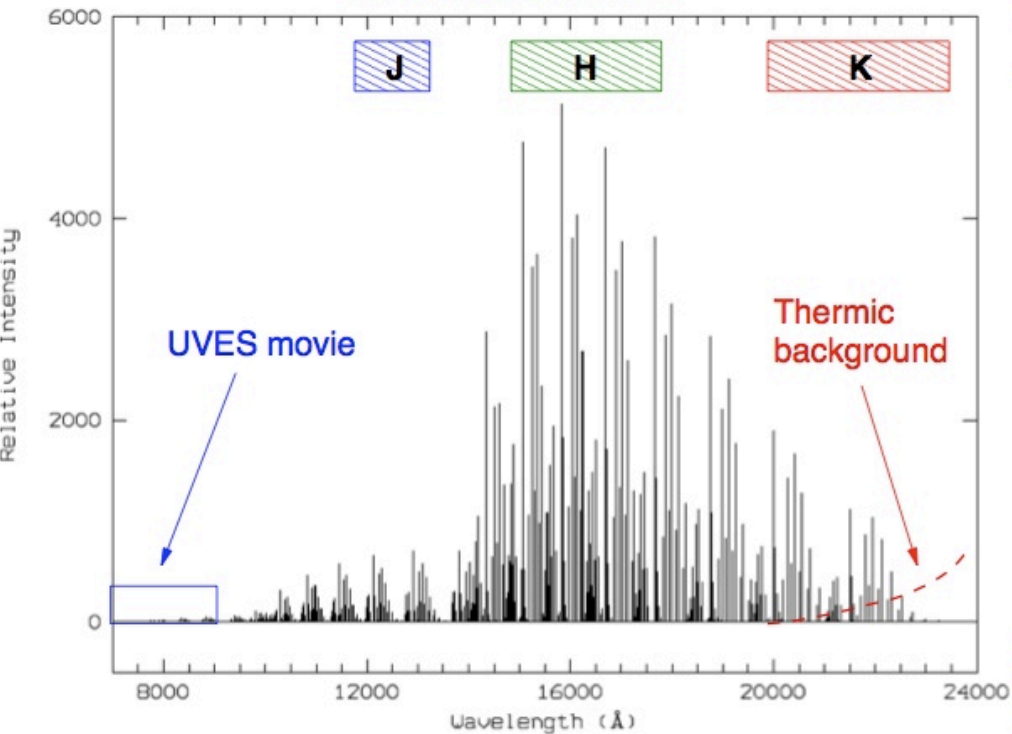


Figure 2: Comparison between the night sky spectrum during dark time (red line, Patat 2003) and bright time (blue line). The latter was obtained with FORS1 on September 1, 2004 using the low dispersion grism 150l and no order sorter filter. Due to the very blue continuum, the spectral region at wavelengths redder than 650 nm is probably contaminated by the grism second order. Both spectra have been normalized to the continuum of the first one at 500 nm. For comparison, the model spectrum of a solar-type star is also plotted (black line). For presentation, this has been normalized to the moonlit night sky spectrum at 500 nm. The upper plot shows the standard *BVR/I* Johnson-Cousins passbands.

Observing Plan

- Air Glow

OH emission lines



Night sky brightness:
[mag / arcsec²]

<i>B</i>	=	22.7
<i>V</i>	=	21.9
<i>R</i>	=	21.0
<i>I</i>	=	20.0
<i>J</i>	=	16.0
<i>H</i>	=	14.5
<i>K</i>	=	13.5

Short exposure times:
30, 20, 10s in J, H, K

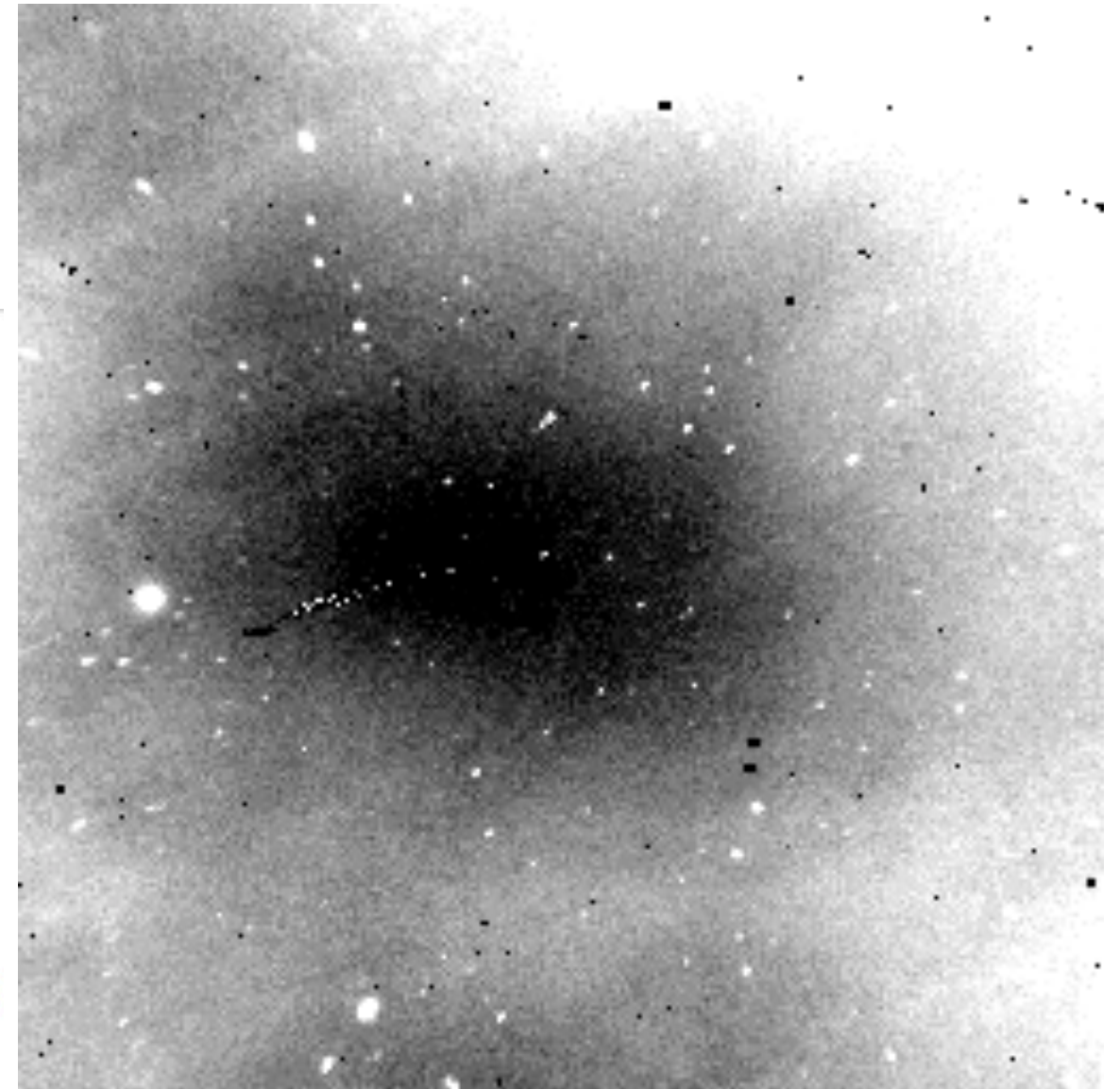
Mischa Schirmer

WIDE-FIELD AIRGLOW EXPERIMENT
FOR THE 2-MICRON ALL-SKY SURVEY
(2MASS)

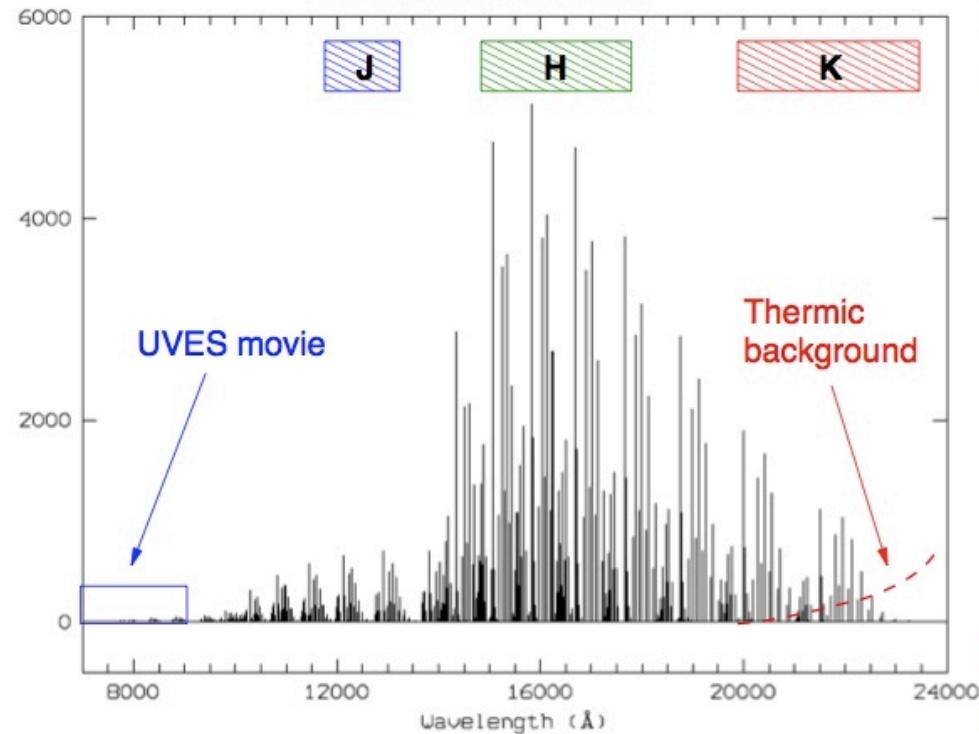
1SEC MOVIE = 7.5 MIN

Observing Plan

- Air Glow



OH emission lines



Night sky brightness:
[mag / arcsec²]

<i>B</i>	=	22.7
<i>V</i>	=	21.9
<i>R</i>	=	21.0
<i>I</i>	=	20.0
<i>J</i>	=	16.0
<i>H</i>	=	14.5
<i>K</i>	=	13.5

Short exposure times:
30, 20, 10s in J, H, K

Mischa Schirmer

WIDE-FIELD AIRGLOW EXPERIMENT
FOR THE 2-MICRON ALL-SKY SURVEY
(2MASS)

1SEC MOVIE = 7.5 MIN

Raw Images -> Science

- Calibration Files
 - Bias
 - X-talk corrections (mosaic cameras)
 - Flat Fielding
 - Fringe Frames
- Distortions
 - WCS, PSF

CCD Operation in a nutshell

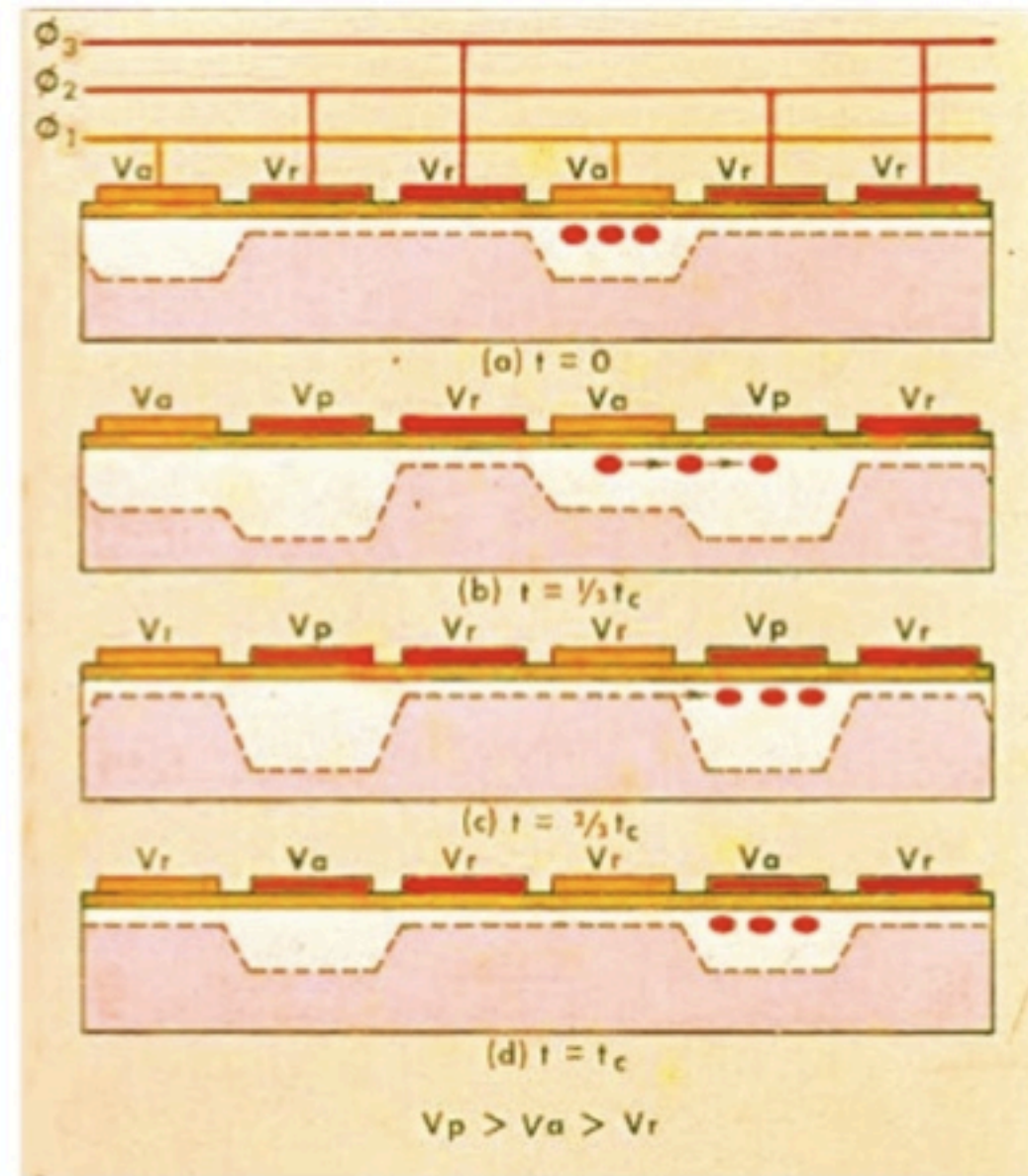
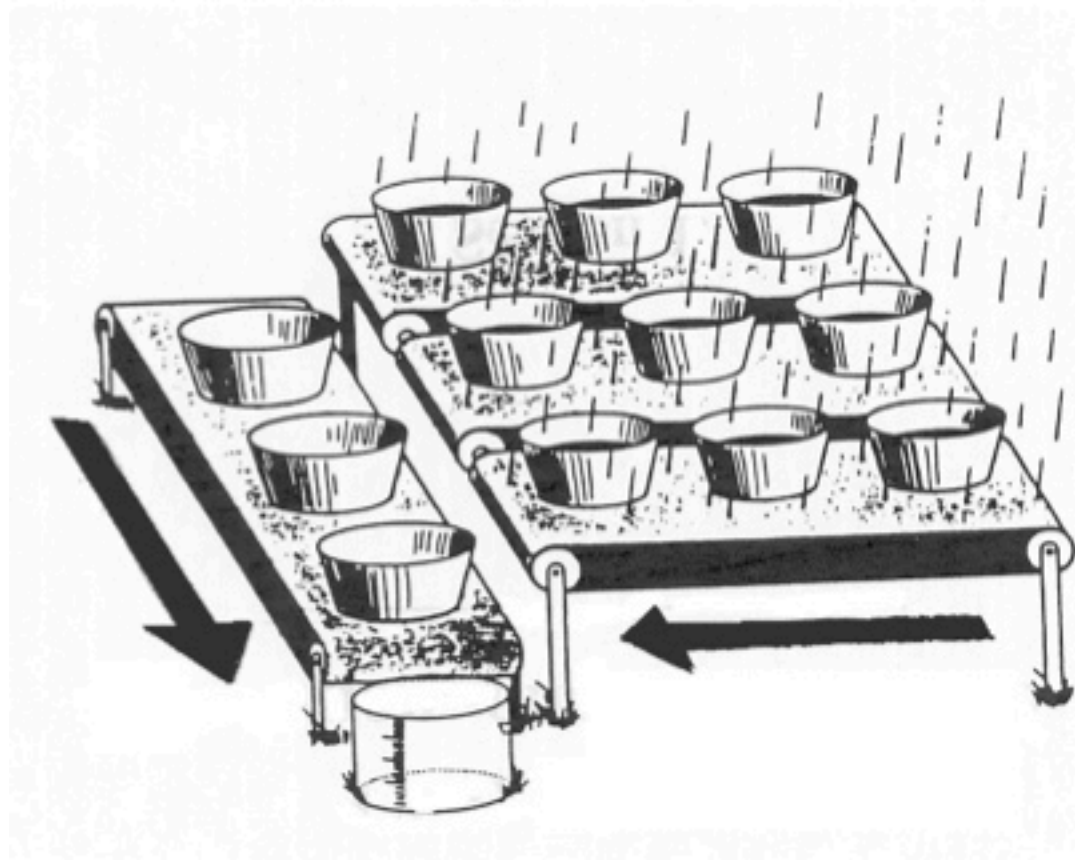
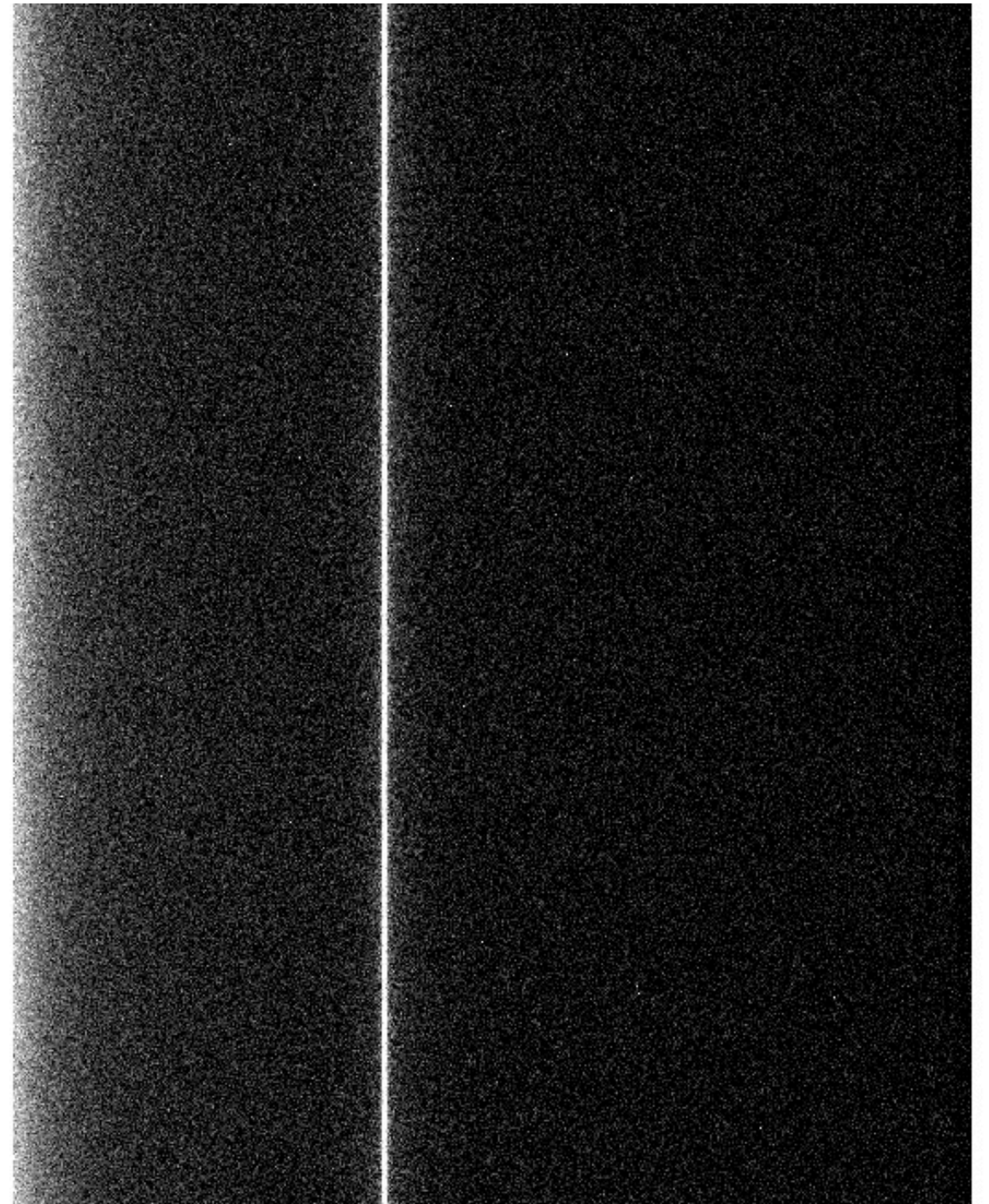


Figure 6. The basic CCD structure.

GEORGE SMITH

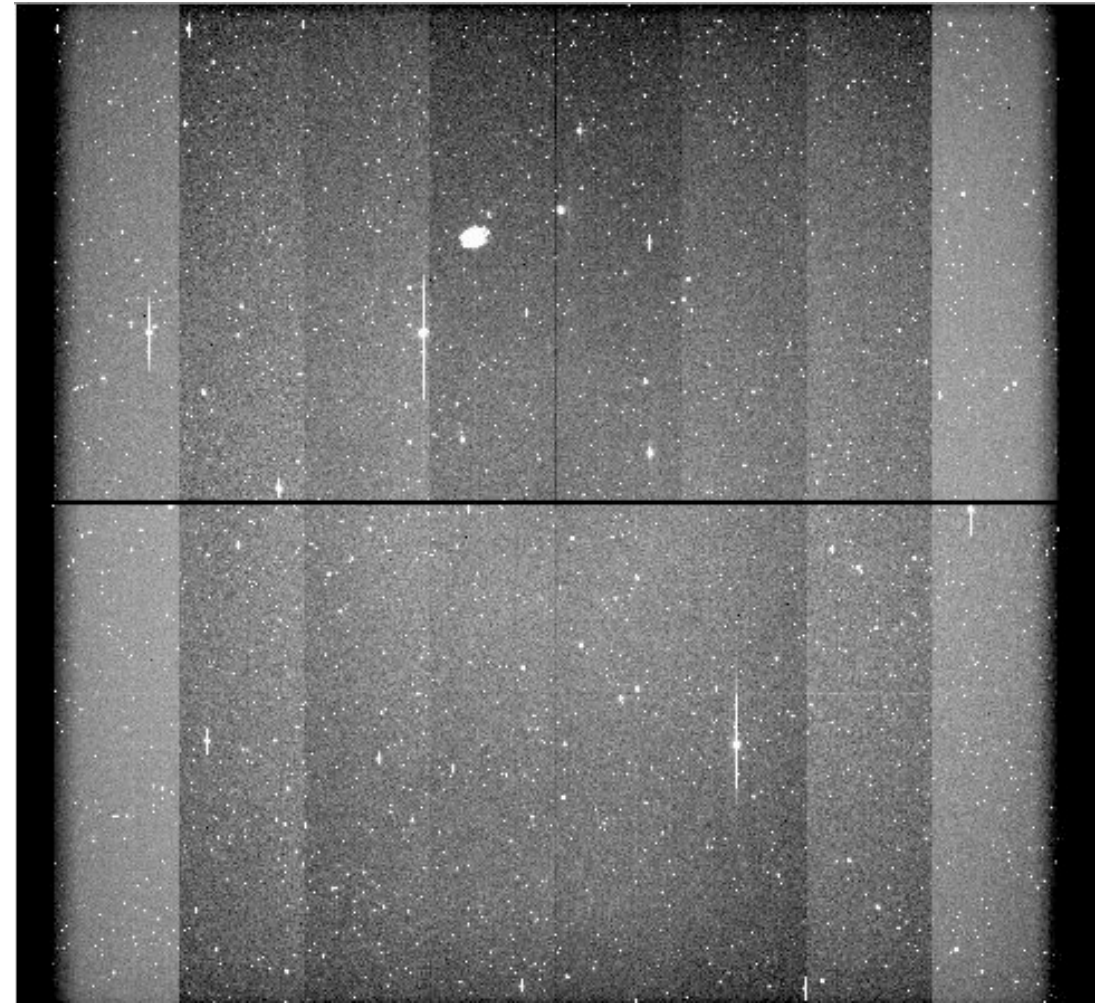
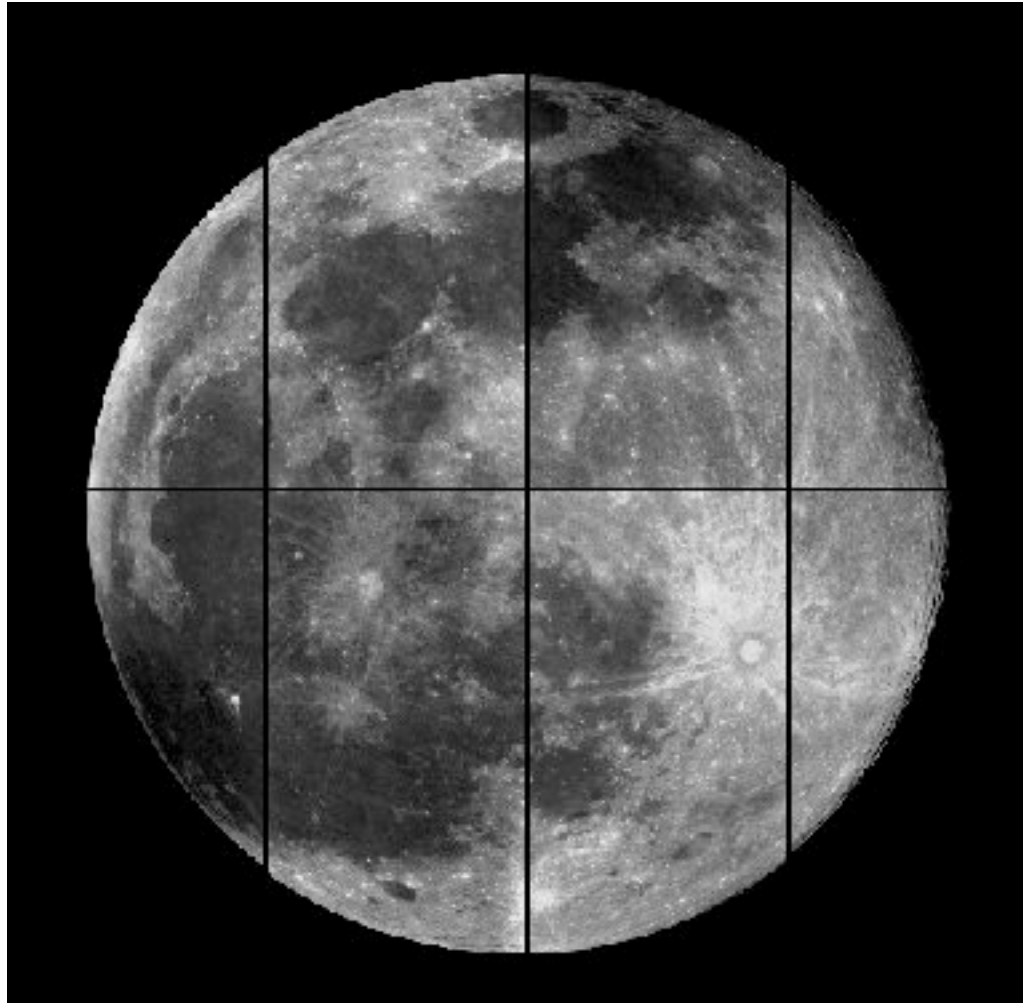
Bias

- 0 second (dark) exposures that allow us to correct for pixel to pixel structure in the read noise of an image
- Take a decent number and average to get a master bias that we will then apply to all images for a night.



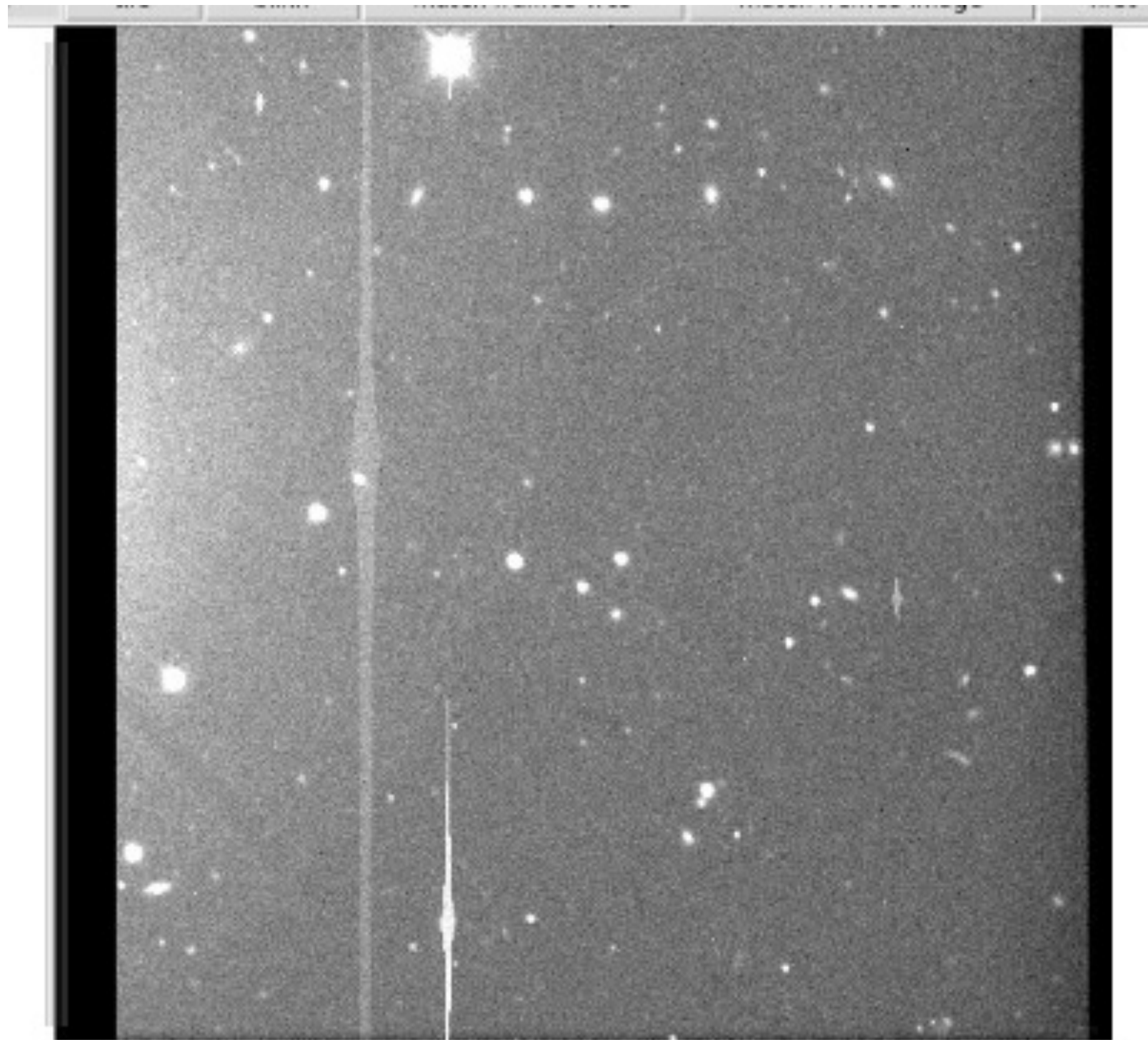
EXAMPLE BIAS SWOPE 0.9M

X-Talk Corrections



NOAO MOSAIC I

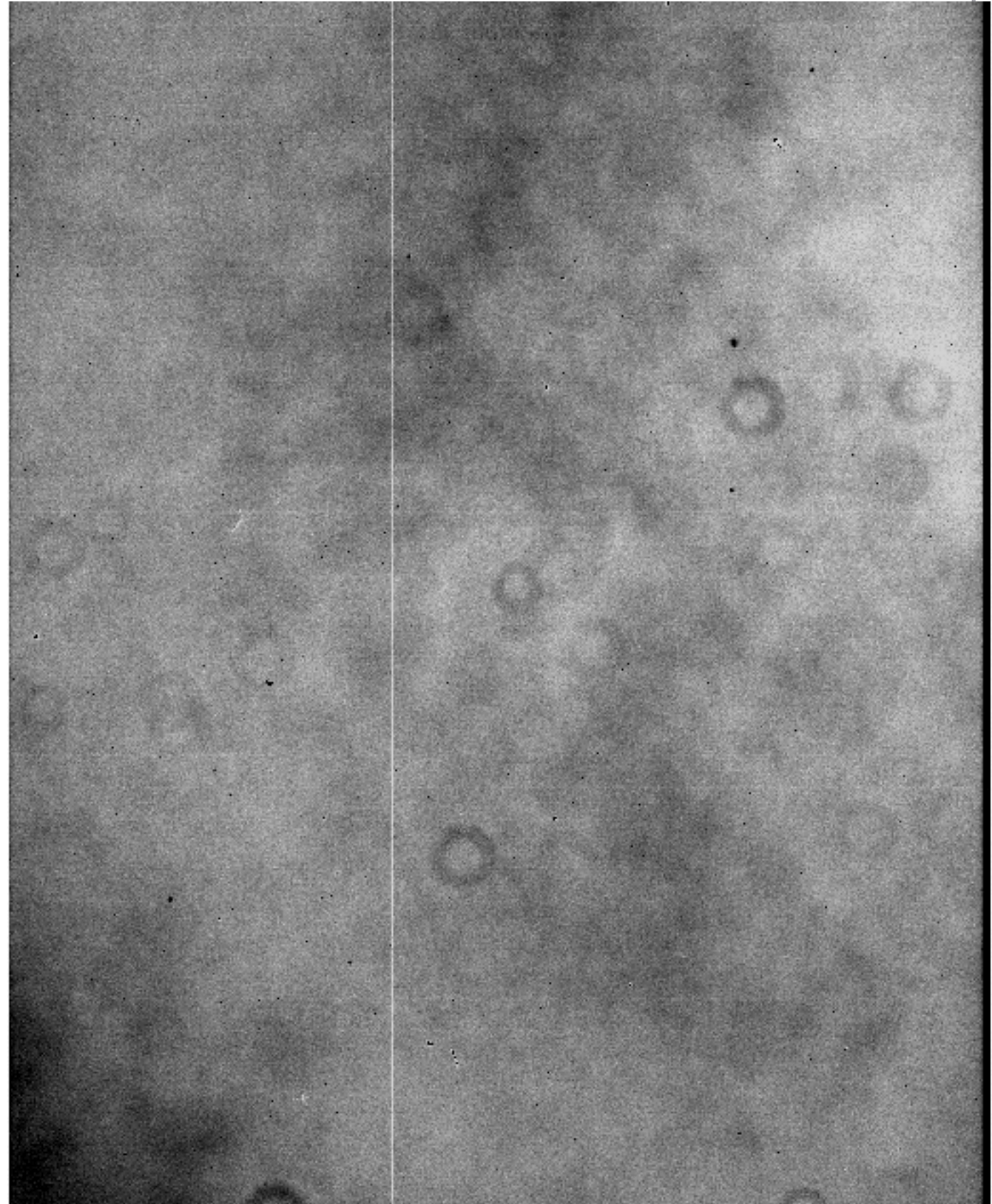
X-Talk Corrections



Blanco 4m g-band

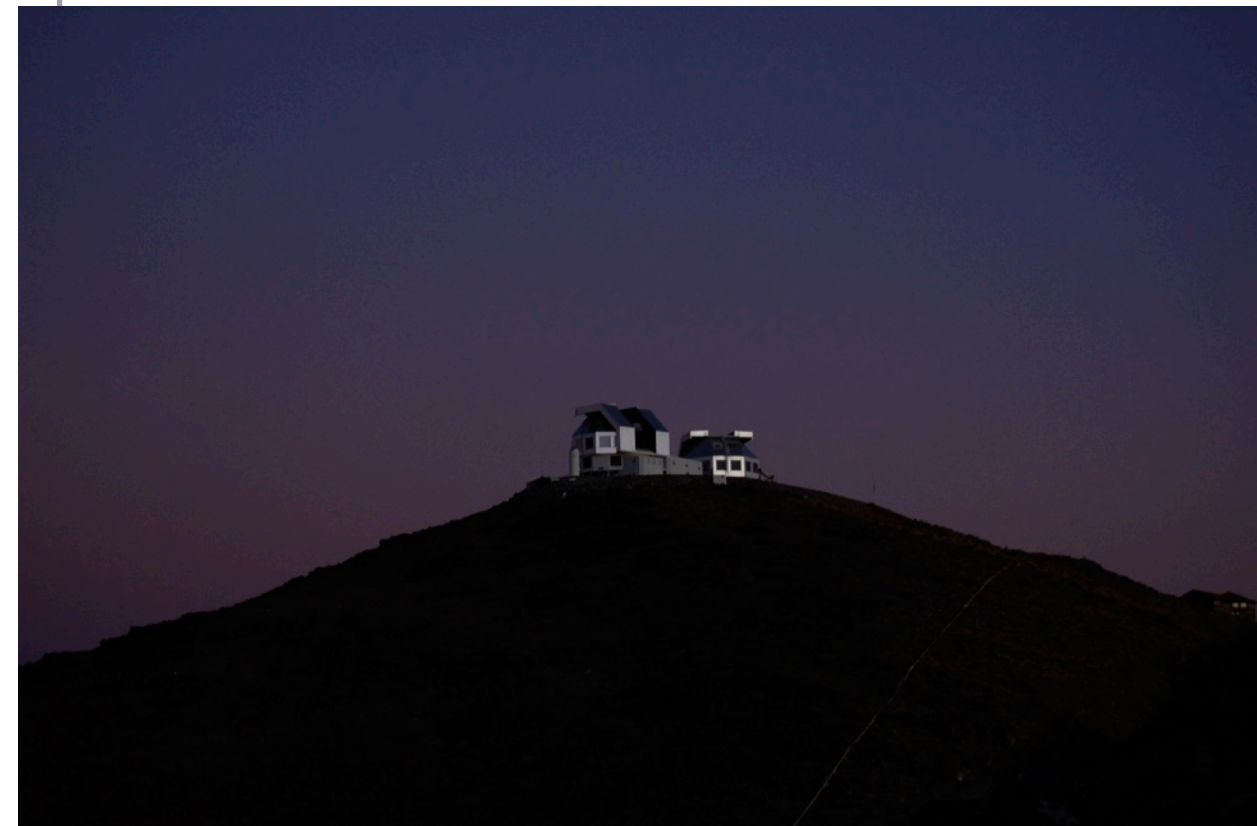
Flat Fielding

- Need to measure relative gain of all of the pixels
- Dome Flats
- Twilight/Sky Flats



Magellan at Twilight

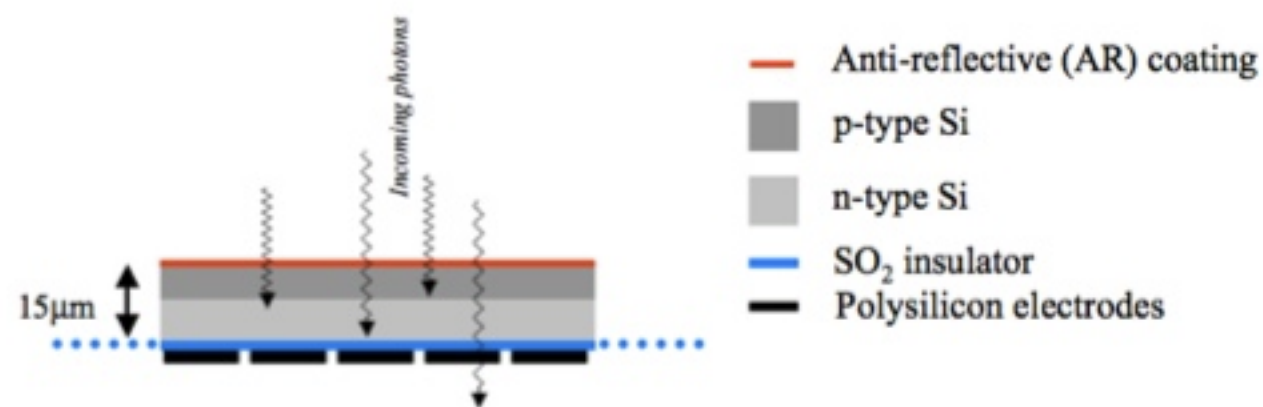
Swope 0.9m Dome flat



Fringe Frames

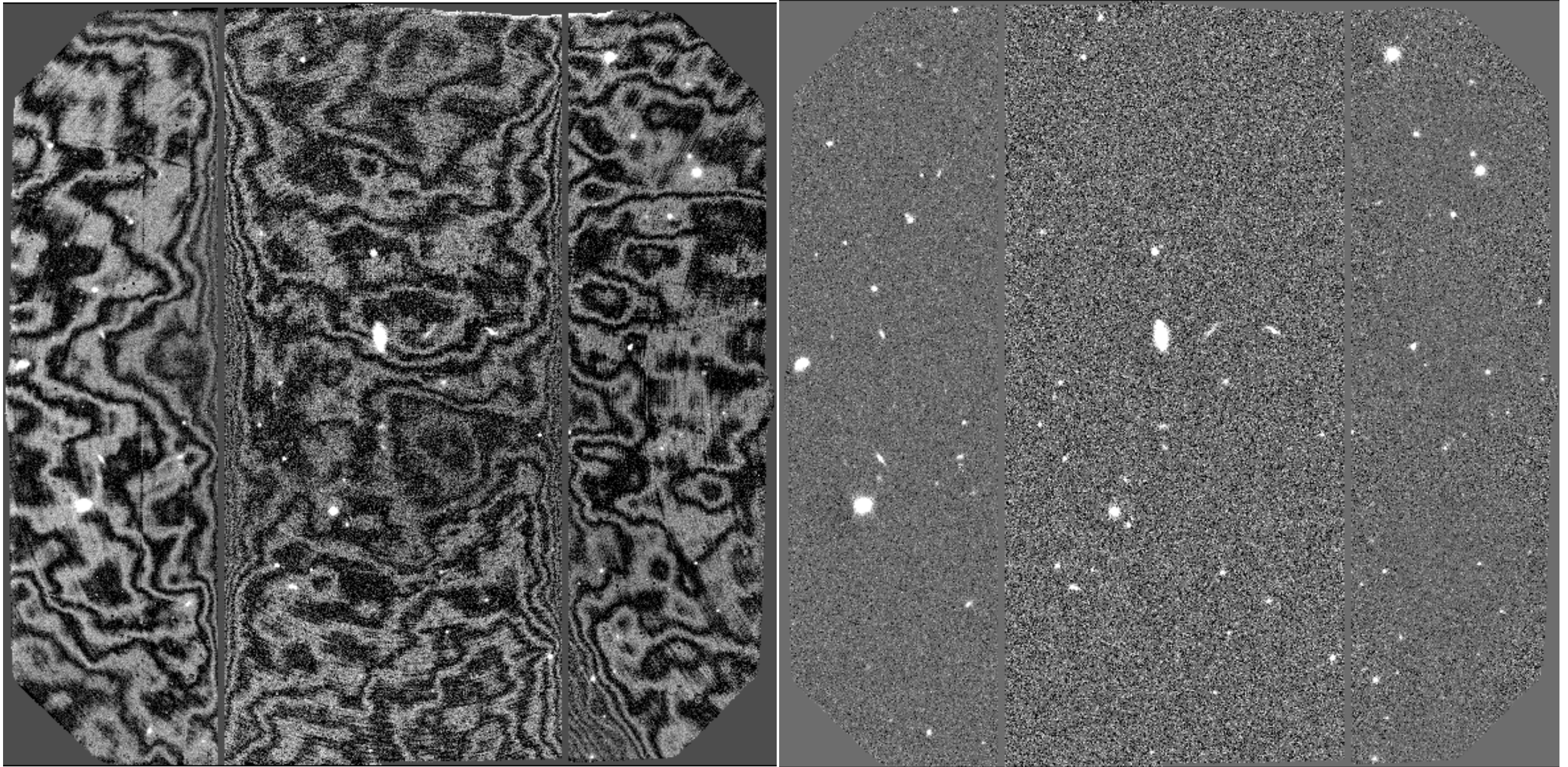
- Caused by thin-film interference effects in the detector
- Mitigate CCD design

Thinned Back-side Illuminated CCD



BLANCO 4M Z-BAND FRINGE FRAME

Fringing: Subtraction



GMOS-N

Distortions - Examples

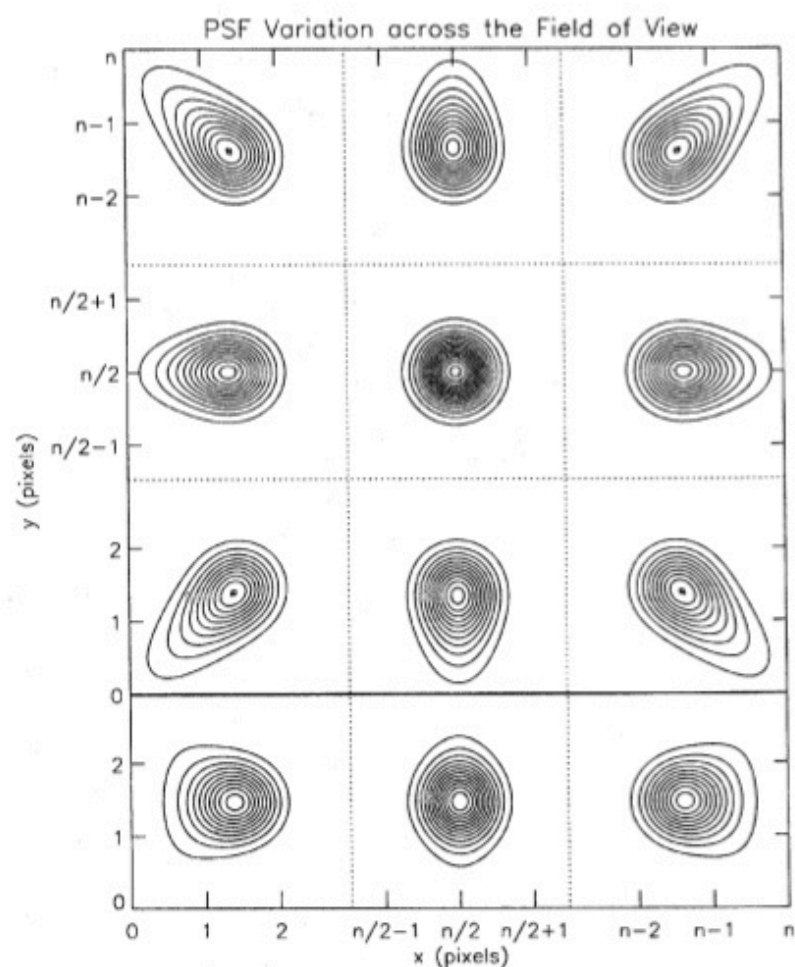
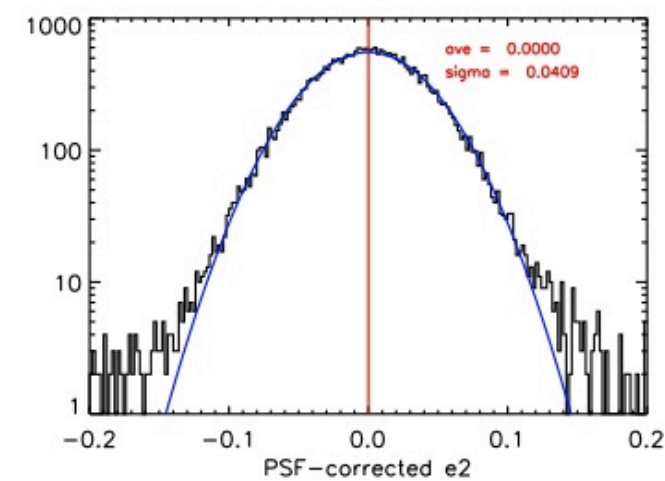
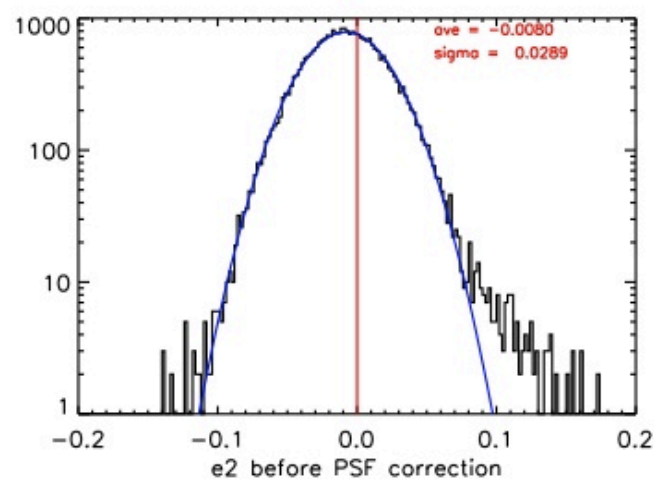
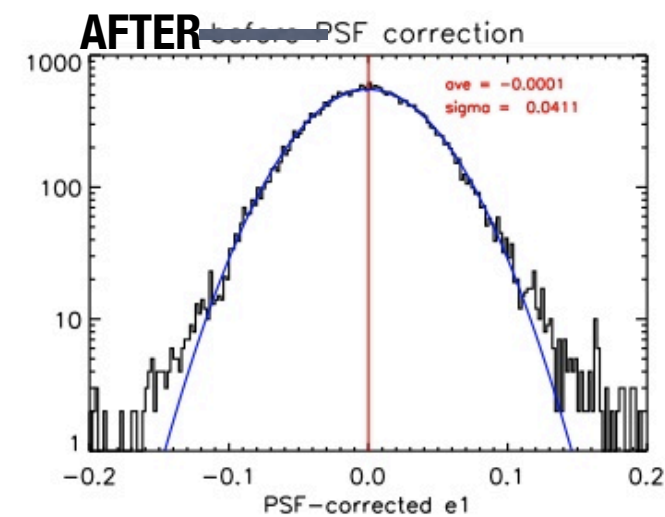
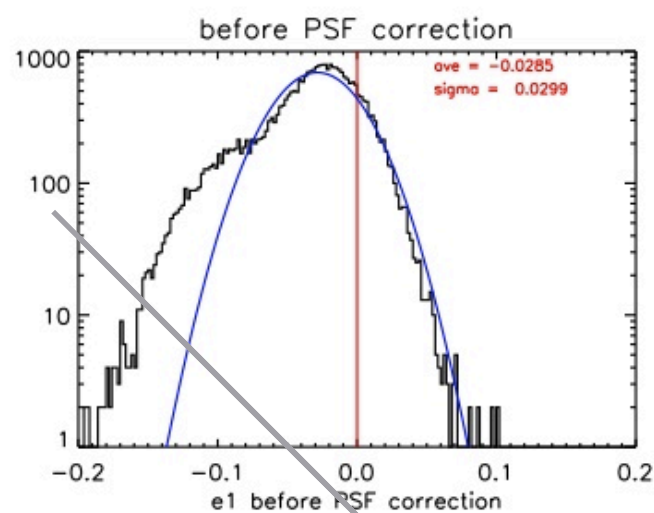


FIG. 3. Contour diagrams indicating schematically how the LONEOS PSF varies over the focal plane of the camera. The 9 PSFs in the top of the diagram indicate the way a star image would appear in a stare-mode frame where n is the total number of pixels in x or y (2048 in this case). As the point-source image approaches the edges of the CCD mosaic, chromatic aberration spreads the PSF. In scan mode, each point source will be transferred across the CCD from top to bottom. The bottom of this figure shows the resulting accumulated PSF as read from the camera. Each is the renormalized sum of the three PSFs above it.

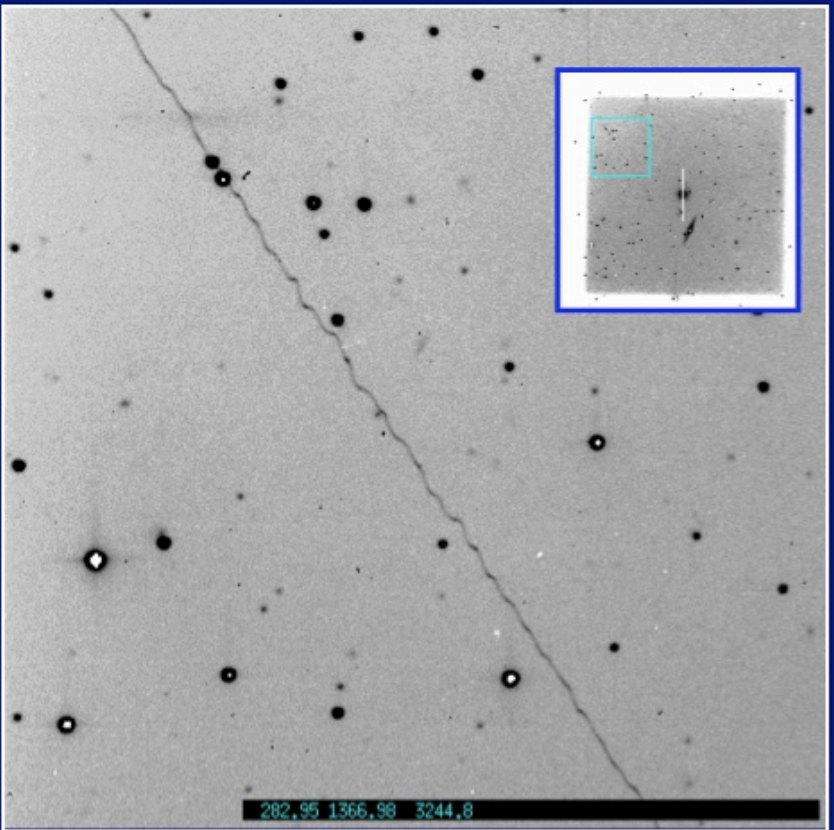


SDSS, LIN ET AL

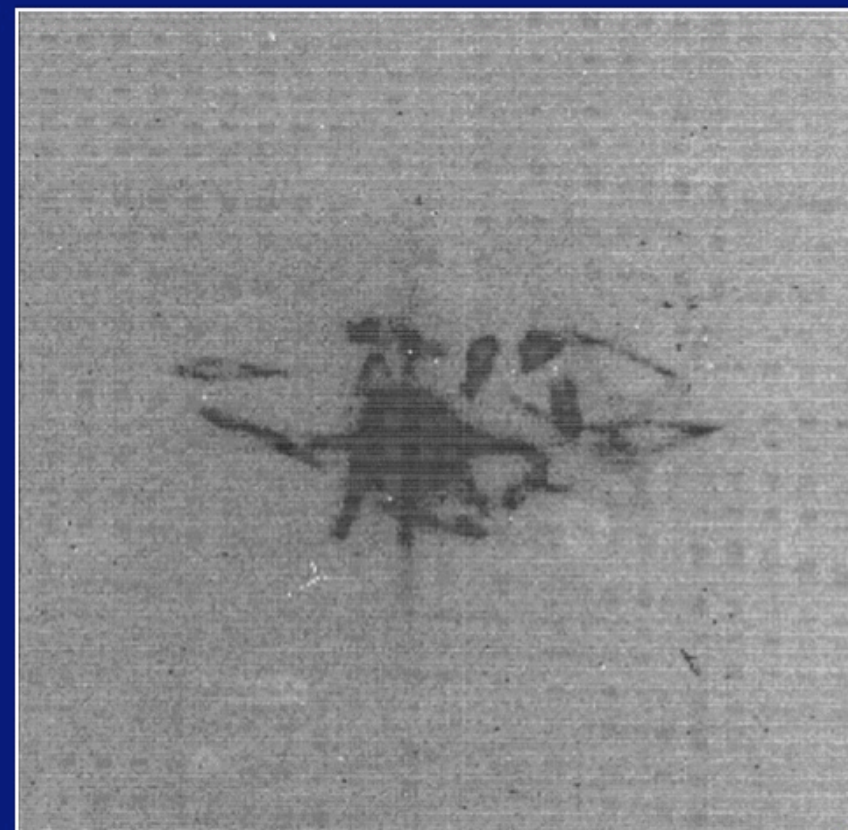
Problems!



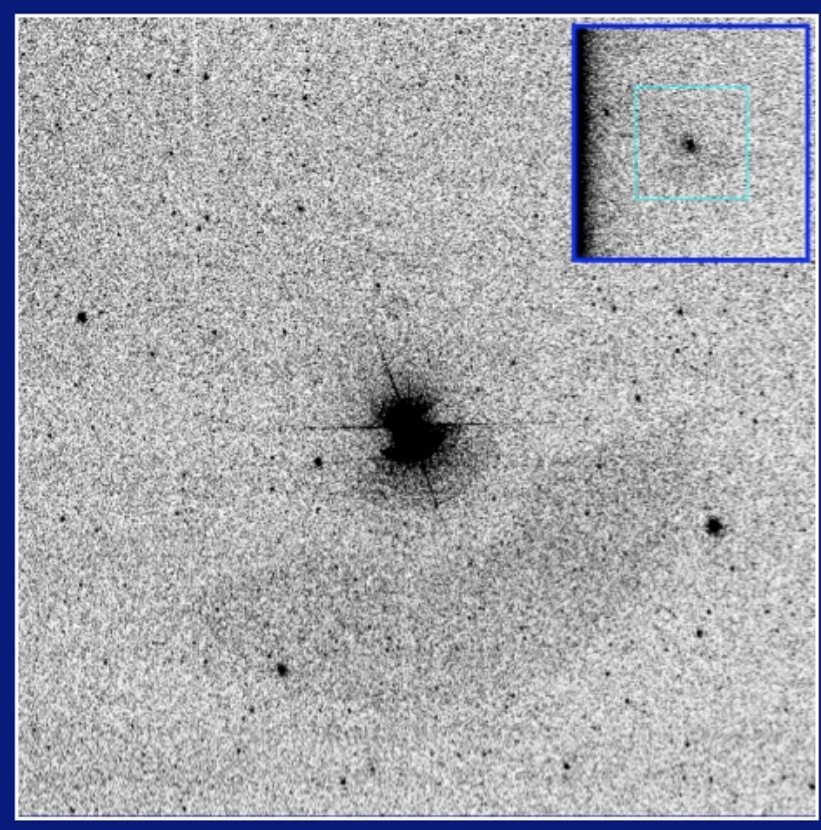
Squiggle



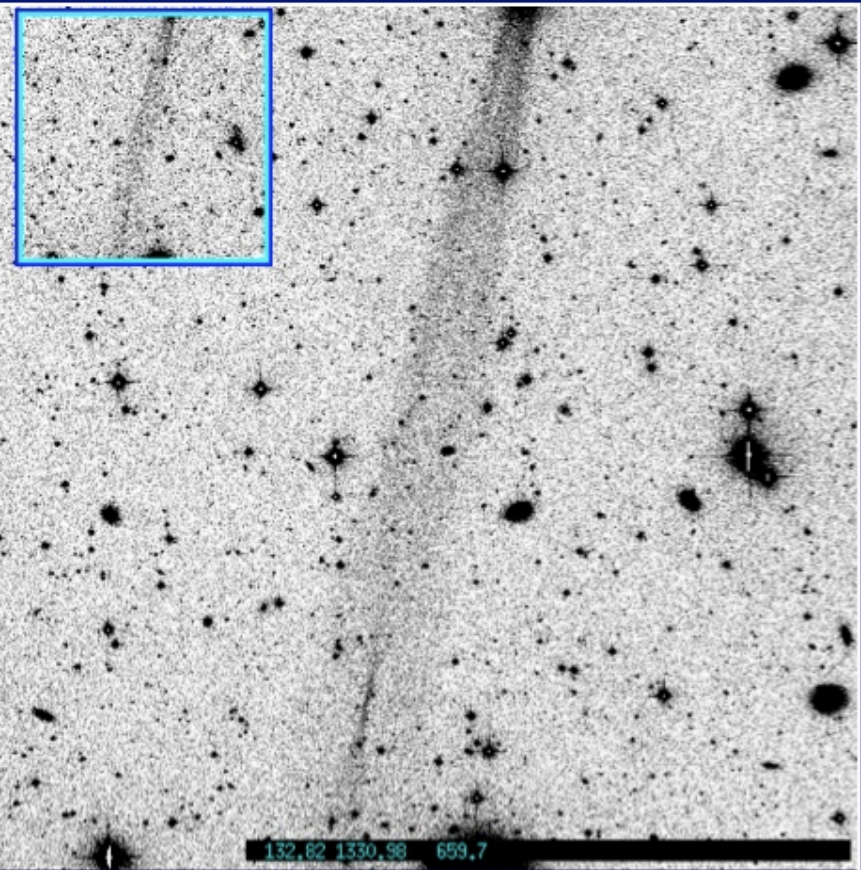
Intergalactic battle



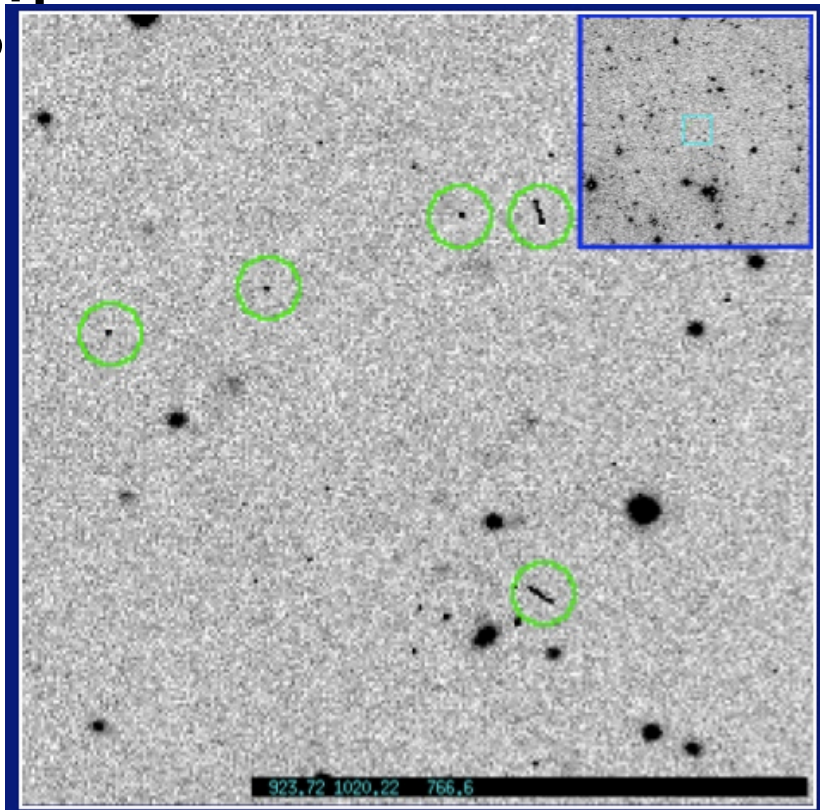
Dome Occulting



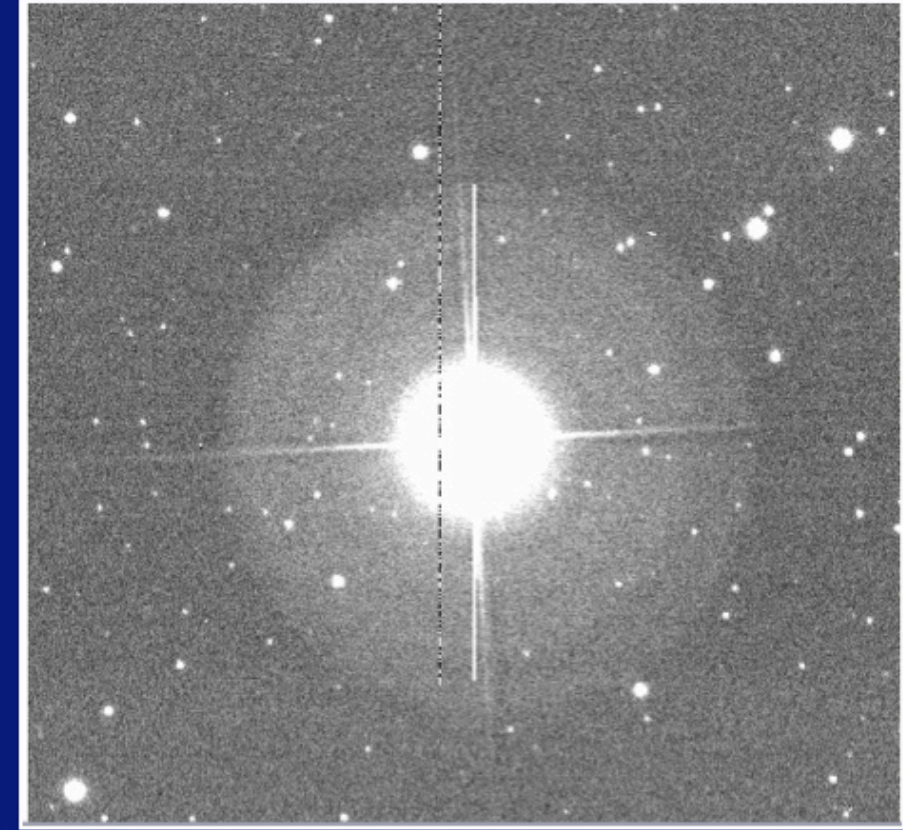
Reflection



COSMIC RAYS

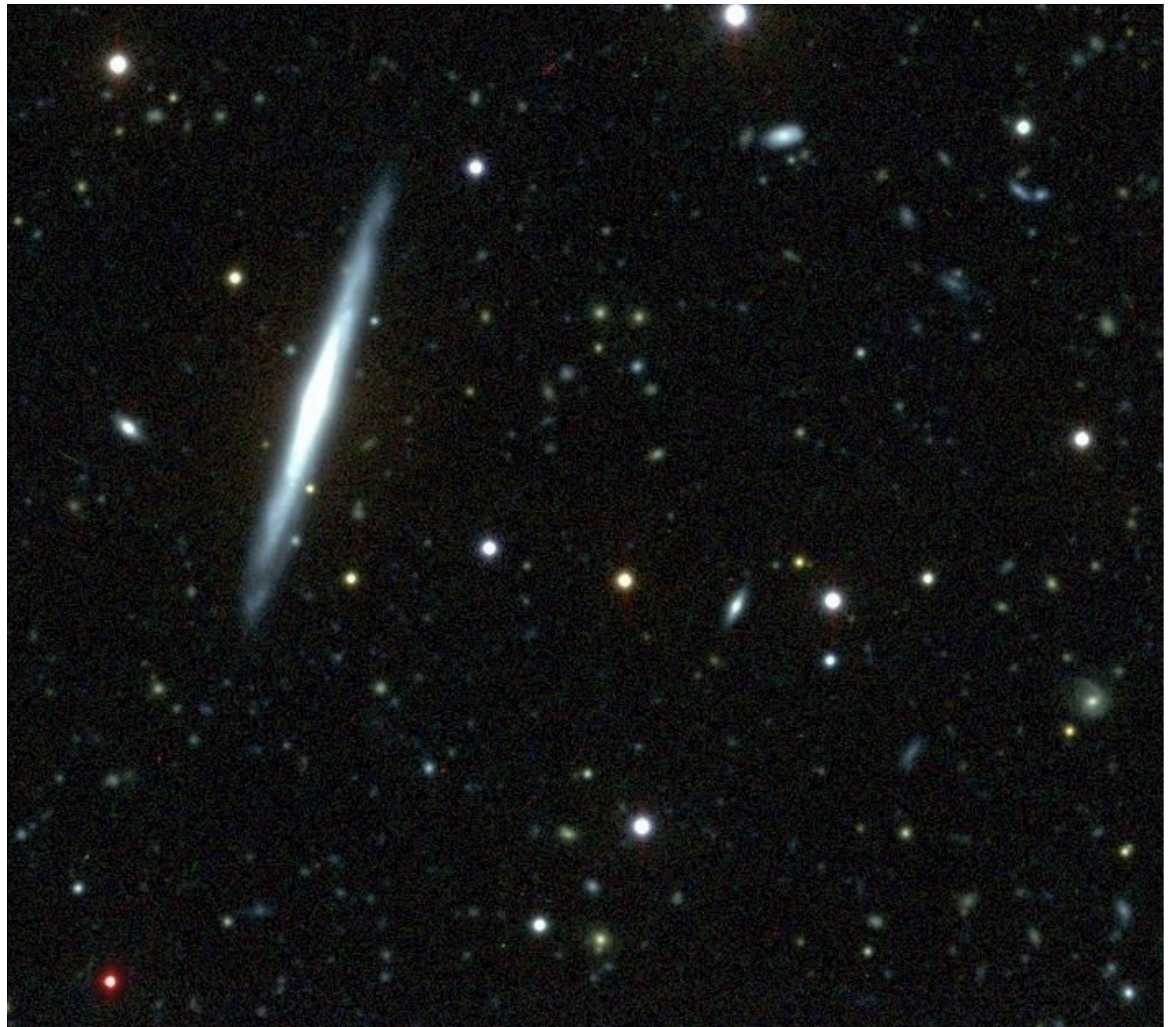


Internal Reflections and Diffraction Spikes



Photometry

- Sextractor
- DAOPhot
- Photo (SDSS)
- And many more!



BCS0508-5223

Sextractor

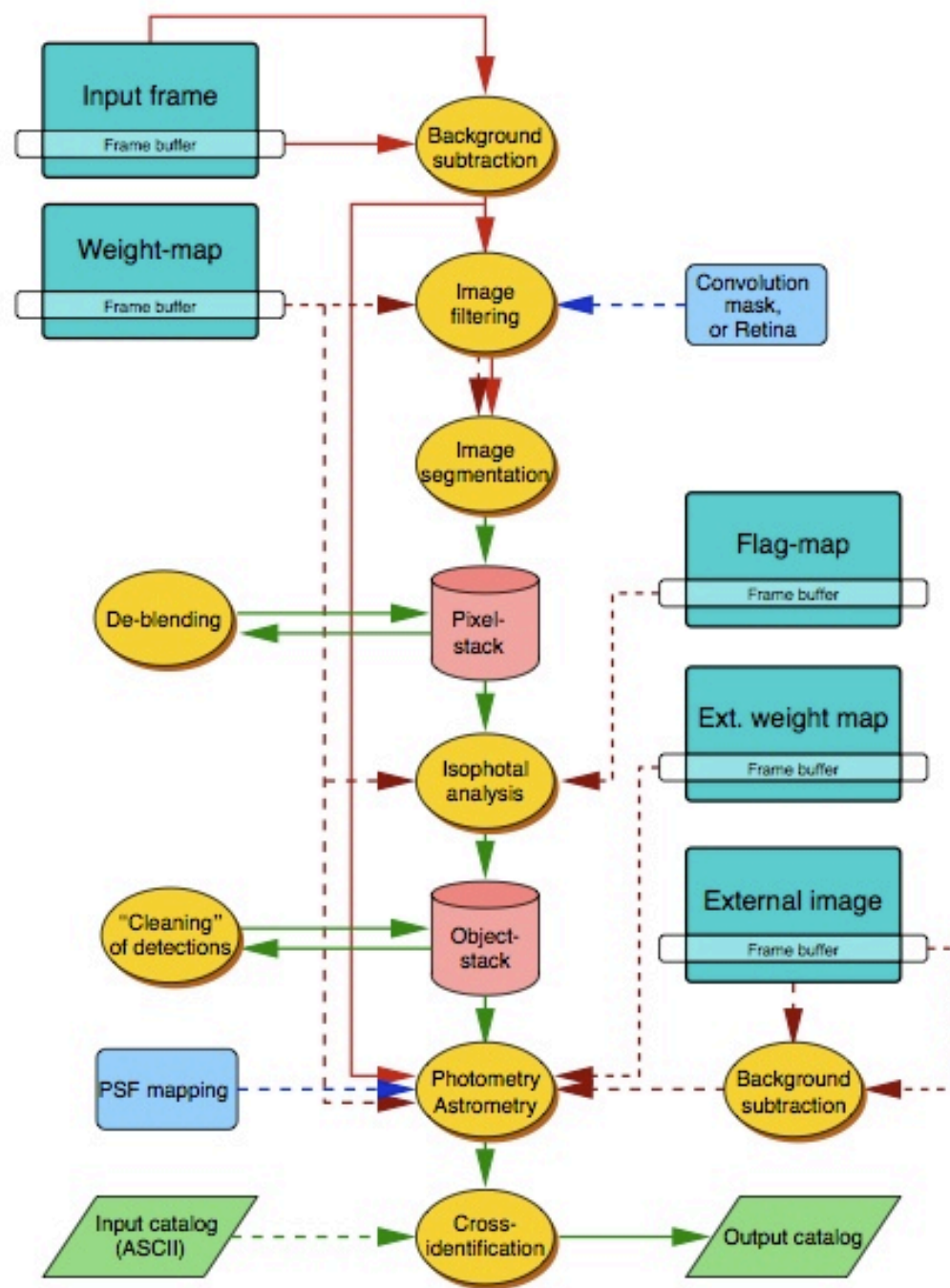
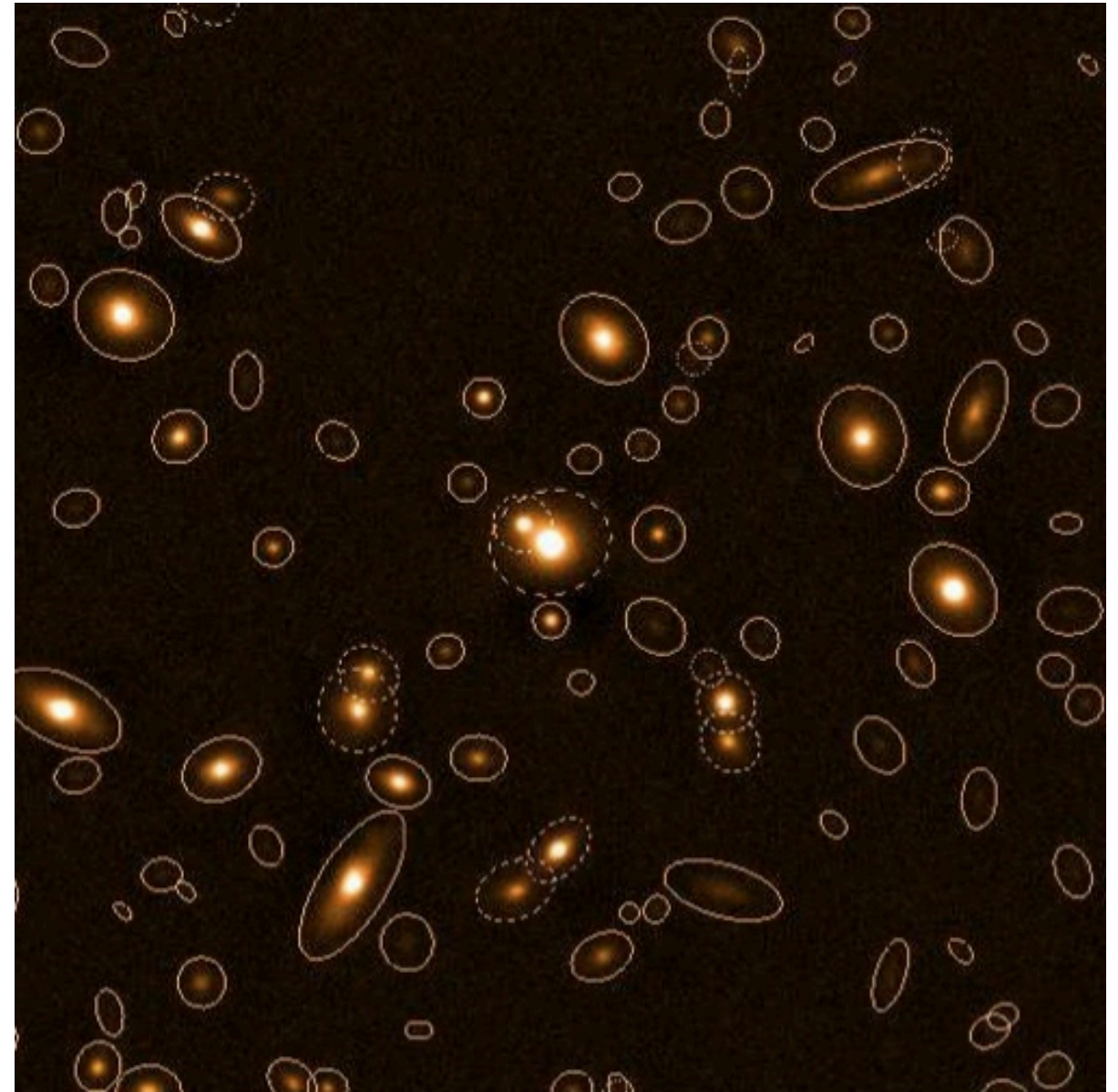
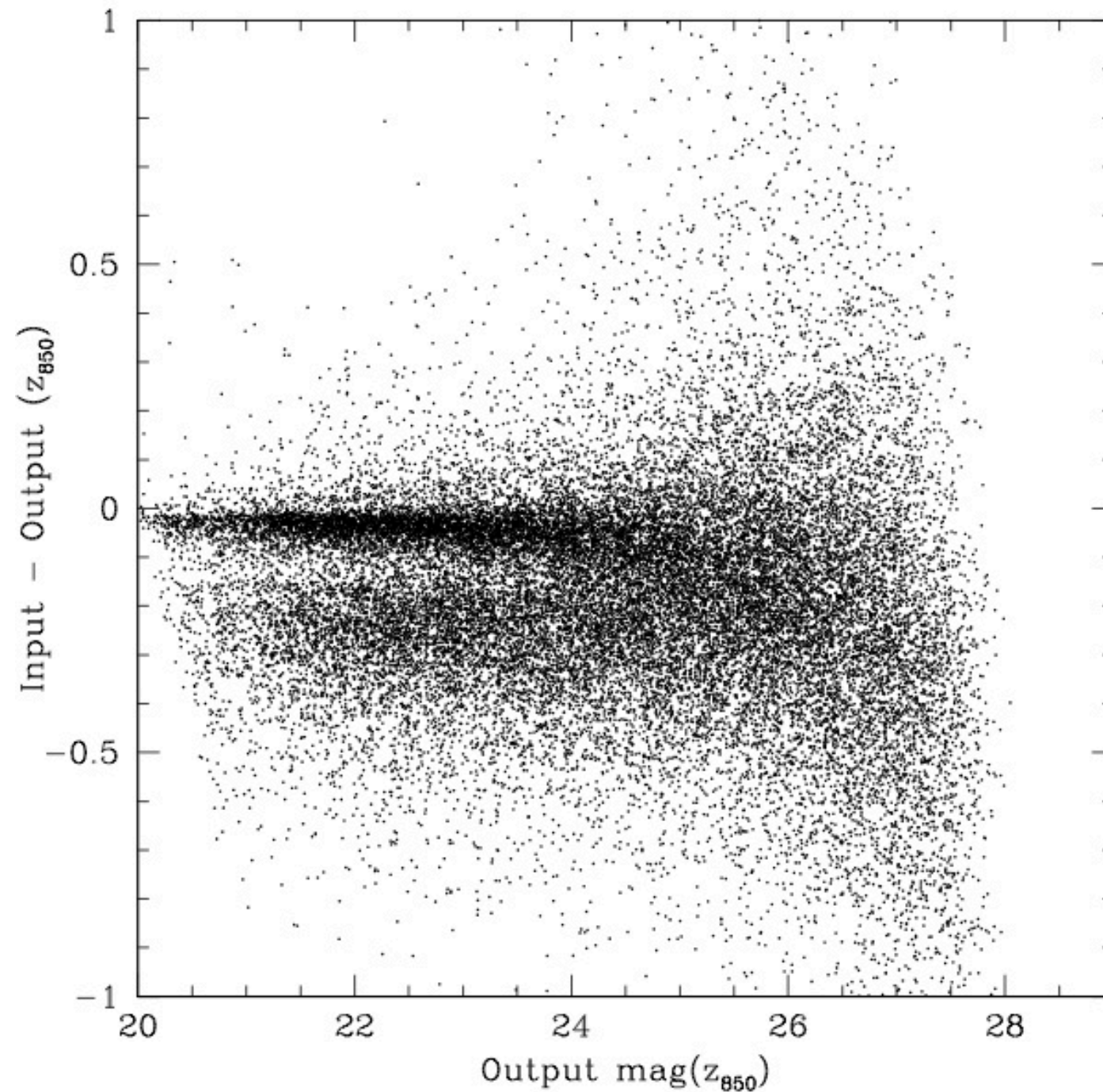


Figure 1: Layout of the main SEXTRACTOR procedures. Dashed arrows represent optional inputs.



E. Bertin

Sextractor



**GOODS SIMULATIONS --
2 POPULATIONS: DISKS AND SPHEROIDS**

Photometric Calibration

- Standard Stars
- Stellar Locus Regression (SLR)

Performing photometric calibrations

- In general, standard stars (usually from the compilations of **Landolt** or **Stetson** should be observed at a variety of zenith distances and colours.
- They should be at approximately the same airmasses at the target field.

$$m_{\text{calib}} = m_{\text{inst}} - A + Z + \kappa X$$

- This is a simple least-squares fit. But in general a system of equations will have to be solved:

$$U = U_{\text{inst}} - A_u + Z_u + C_u(U - B) + \kappa_u X$$

$$B = B_{\text{inst}} - A_b + Z_b + C_b(B - V) + \kappa_b X$$

$$V = V_{\text{inst}} - A_v + Z_v + C_v(B - V) + \kappa_v X$$

ESTIMATED GALACTIC EXTINCTION

ZEROPOINT

COLORTERM

EXTINCTION*AIRMASS

source: Henry Joy McCracken

SLR

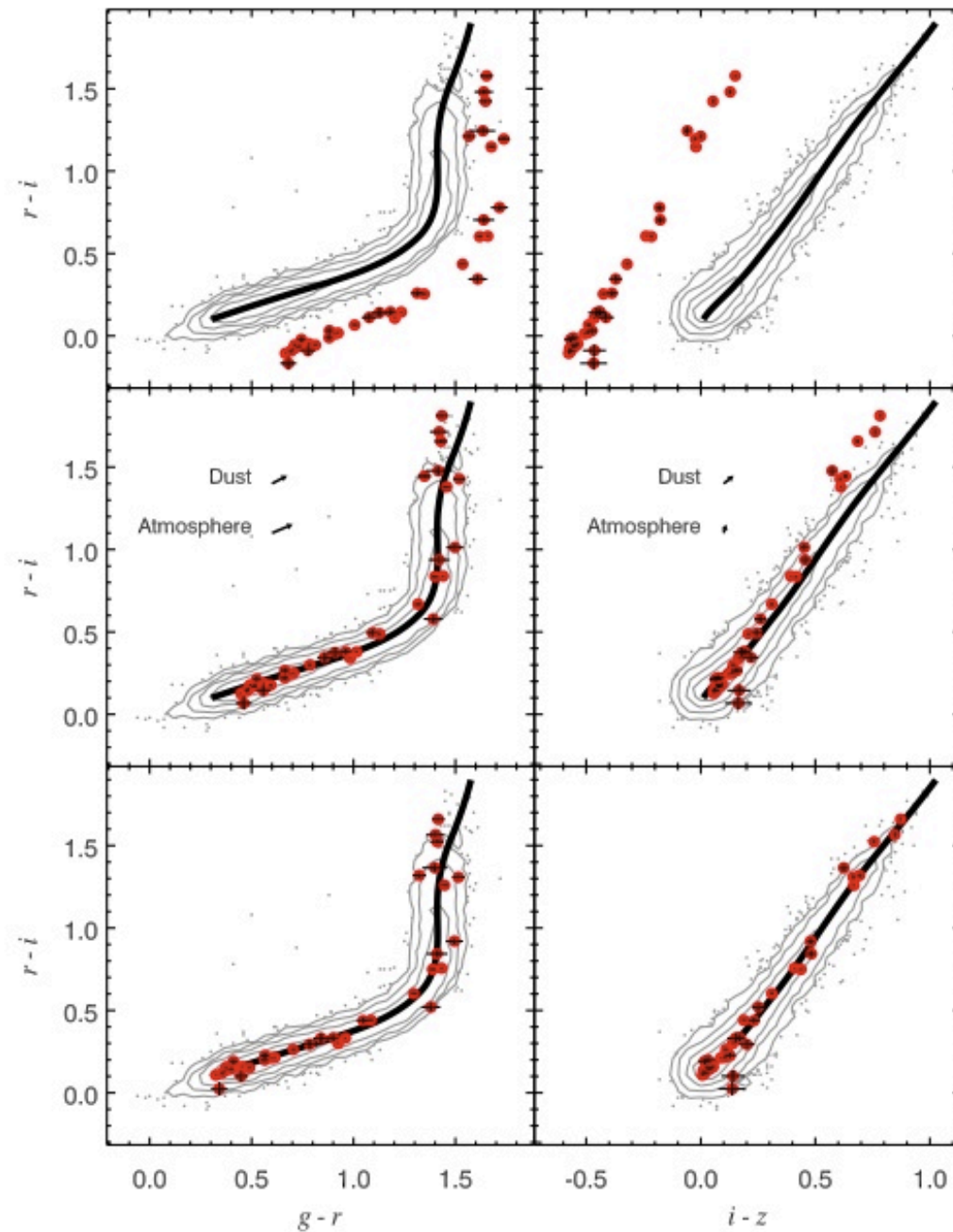
STELLAR LOCUS REGRESSION: ACCURATE COLOR CALIBRATION AND THE REAL-TIME DETERMINATION OF GALAXY CLUSTER PHOTOMETRIC REDSHIFTS

F. WILLIAM HIGH, CHRISTOPHER W. STUBBS, ARMIN REST, BRIAN STALDER, AND PETER CHALLIS

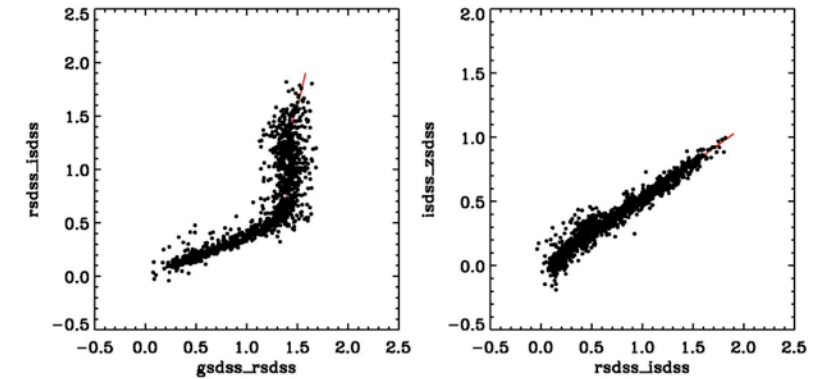
Department of Physics and Harvard-Smithsonian Center for Astrophysics, Harvard University, Cambridge, MA, USA; high@physics.harvard.edu

Received 2009 January 30; accepted 2009 April 24; published 2009 May 27

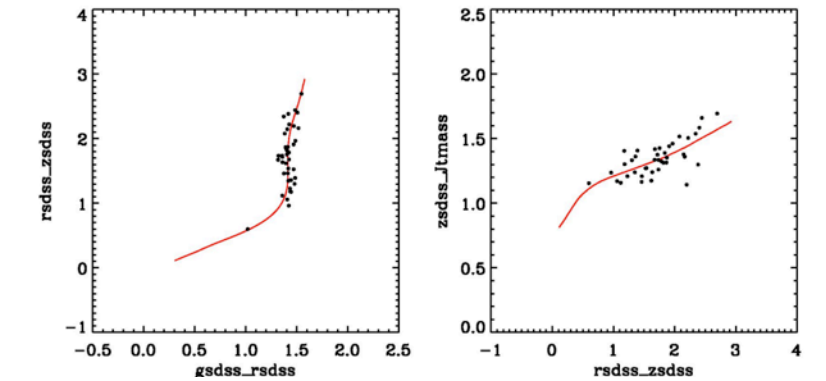
HIGH ET AL.



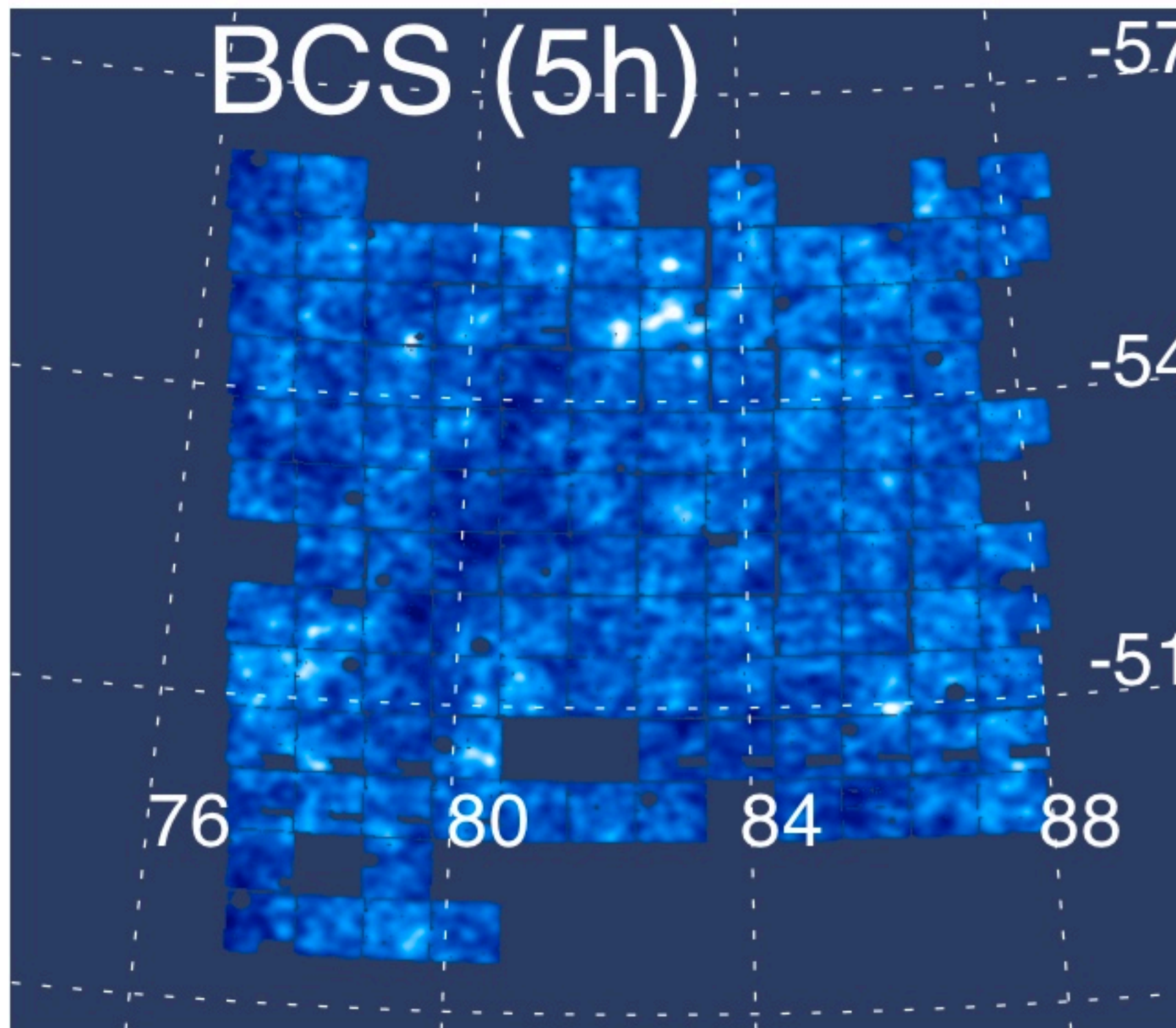
Regression Results



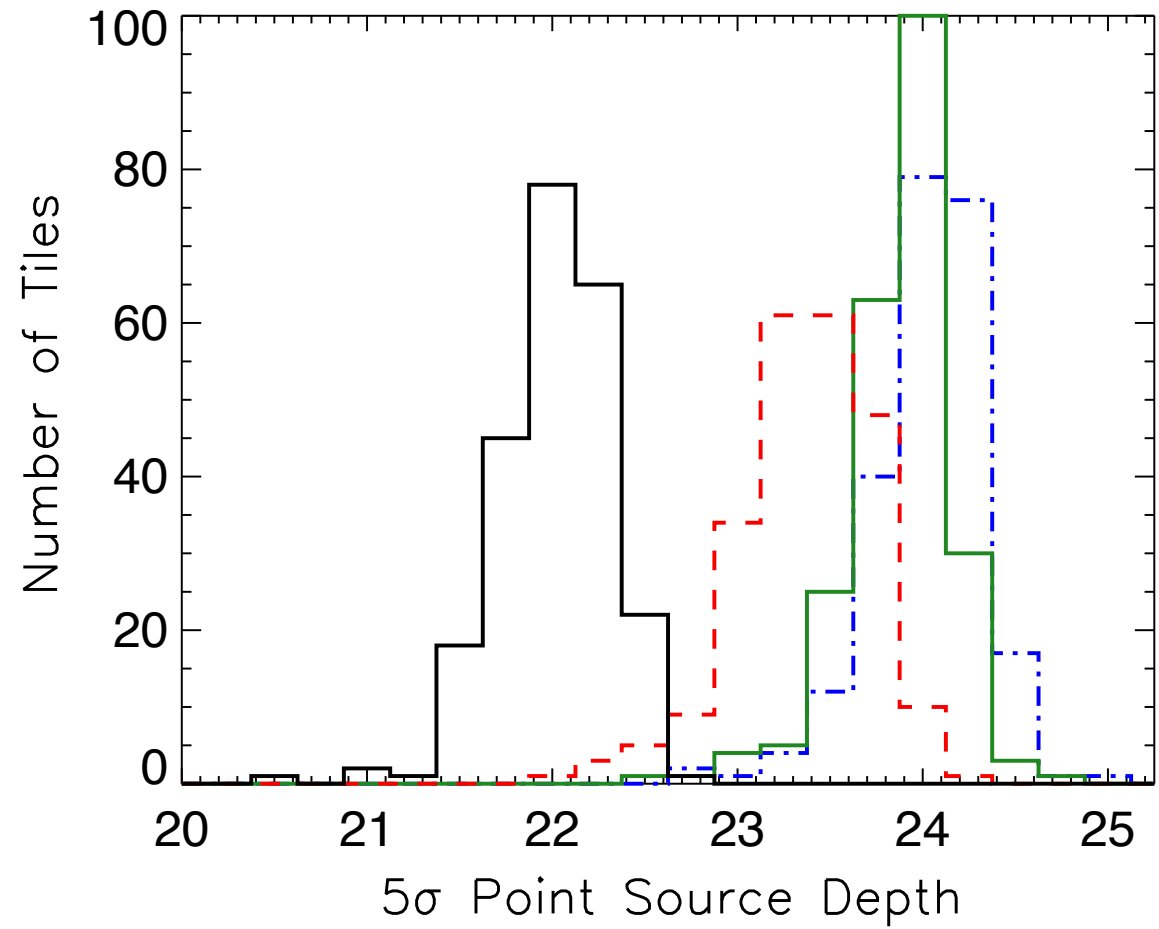
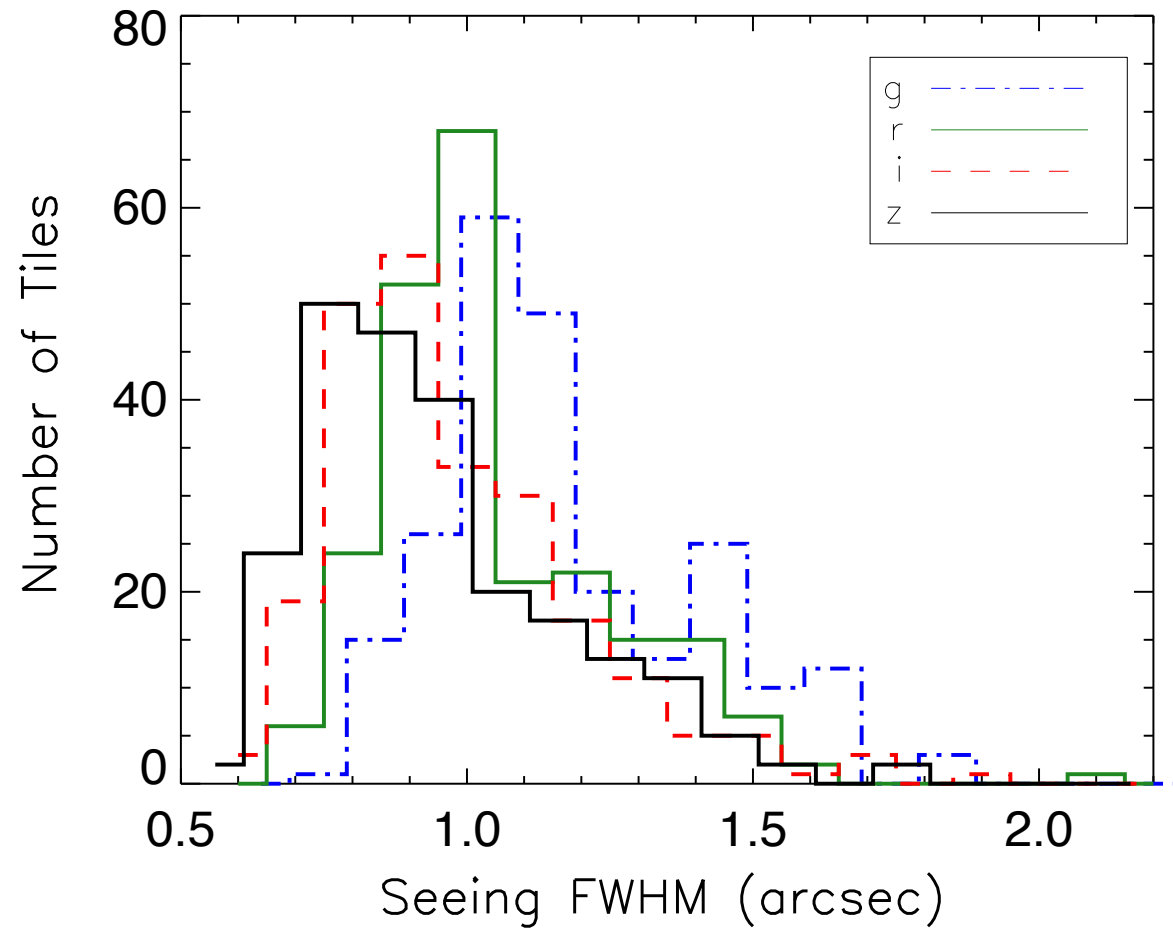
Regression Results



$$(g-r) = (g_0 - r_0) + (a_g - a_r) + (E_g - E_r) + (A_g - A_r) + b_g(g_0 - r_0) - b_r(r_0 - i_0) + c_g X_g(g_0 - r_0) - c_r X_r(r_0 - i_0) \quad (A2a)$$

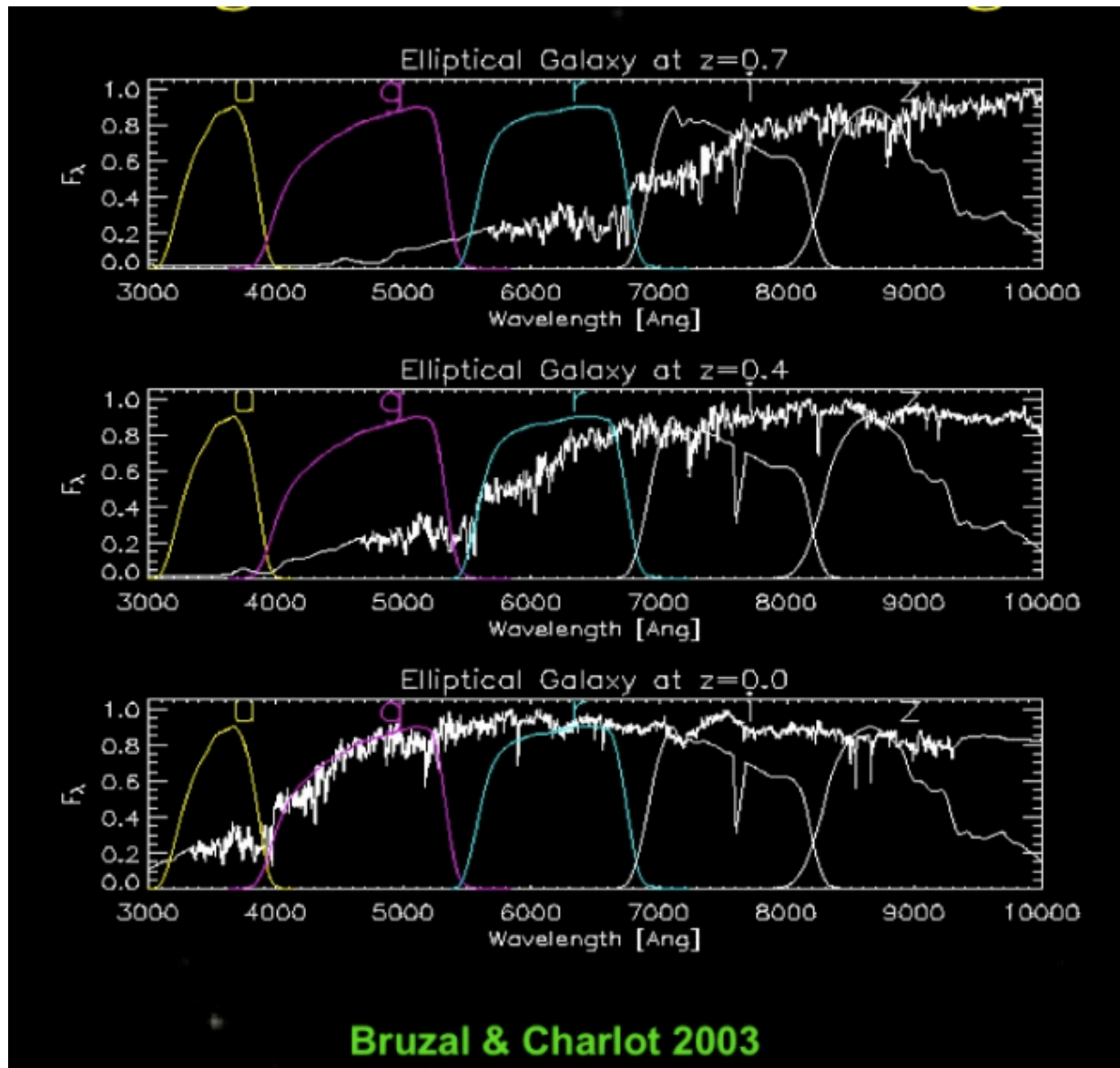


>3000 INDIVIDUAL EXPOSURES (INCLUDING CALIBRATION FILES)

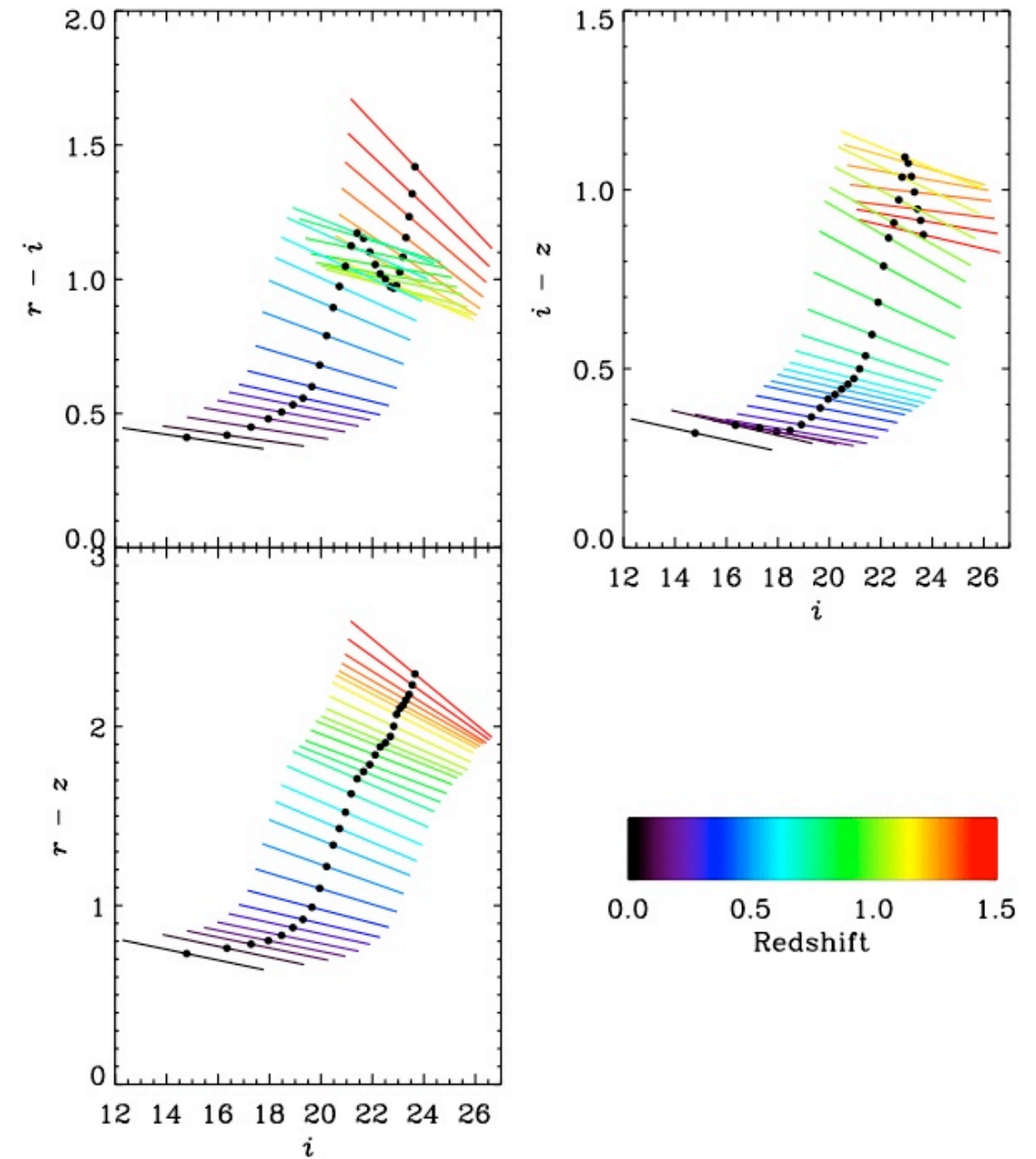


- Data sufficient for detection of L^* galaxies to $z=1$.
But ... heterogeneous depth across the survey

The Red-Sequence provides a tight relation for cluster galaxies in color-magnitude space.



J. Hao

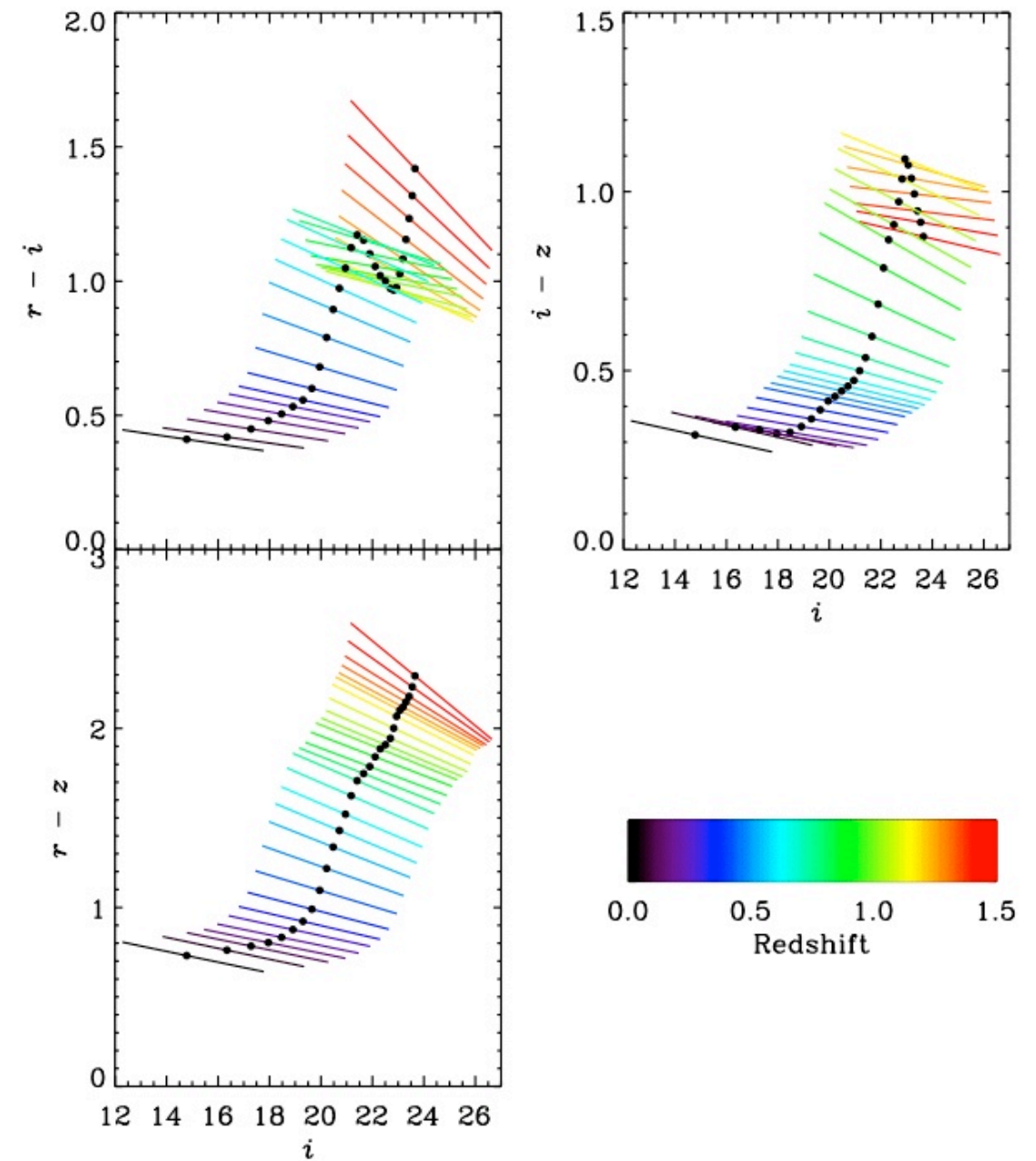


High et al, 2010

The Red-Sequence provides a tight relation for cluster galaxies in color-magnitude space.

Build a filter to pull out clusters based on:

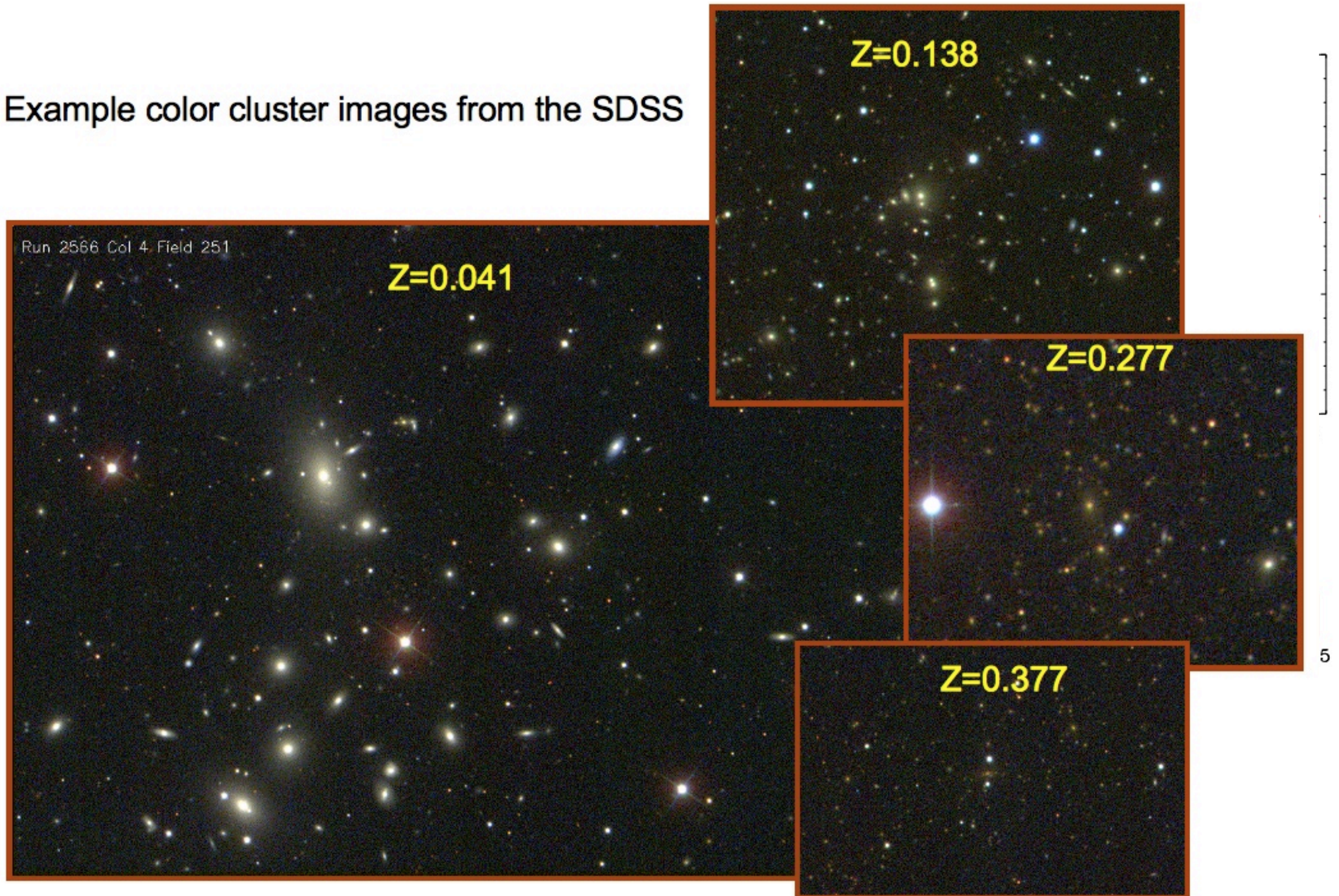
- 1) Color
- 2) Magnitude
- 3) Spatial Profile



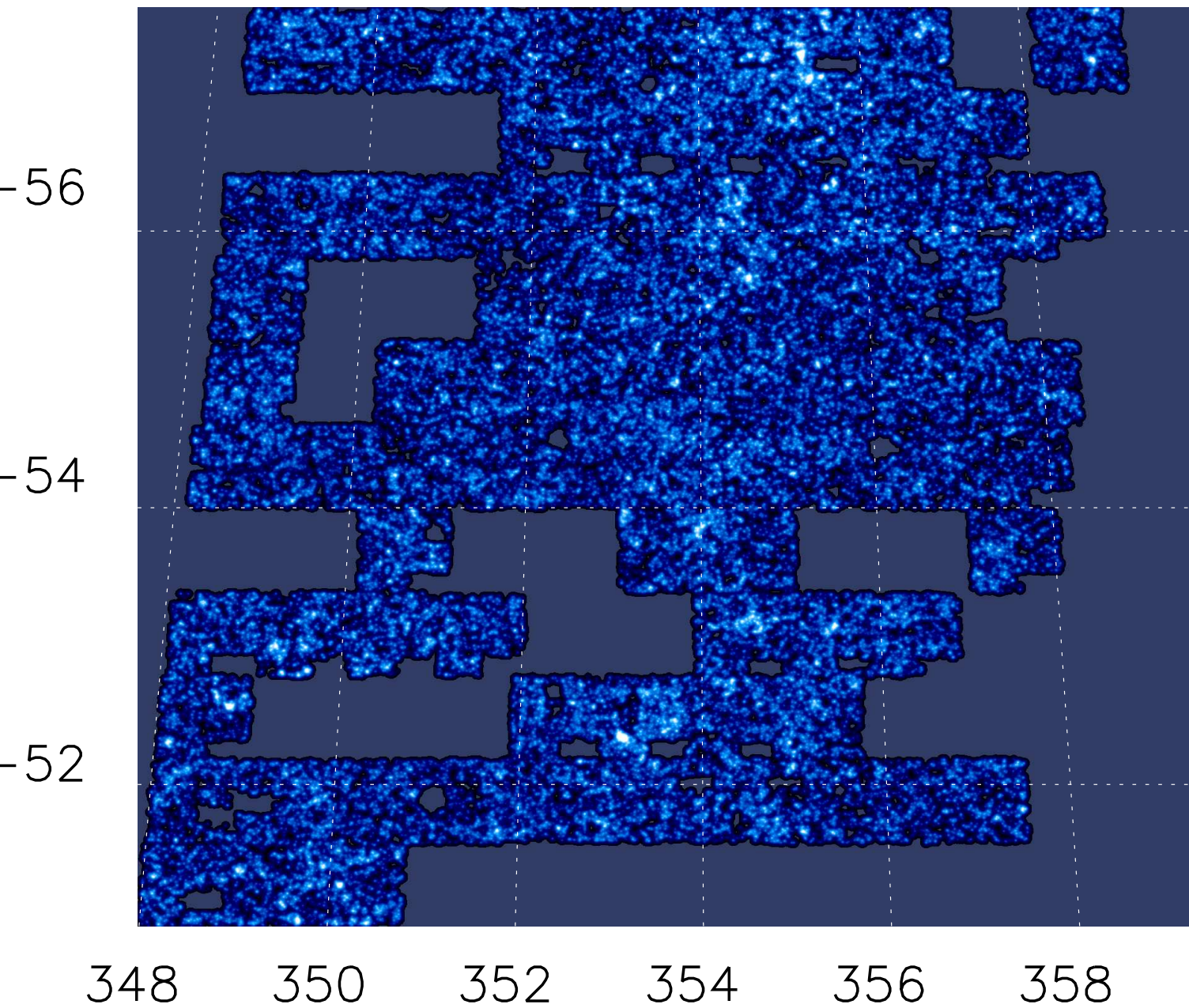
High et al, 2010

The Red-Sequence provides a tight relation for cluster galaxies in color-magnitude space.

Example color cluster images from the SDSS

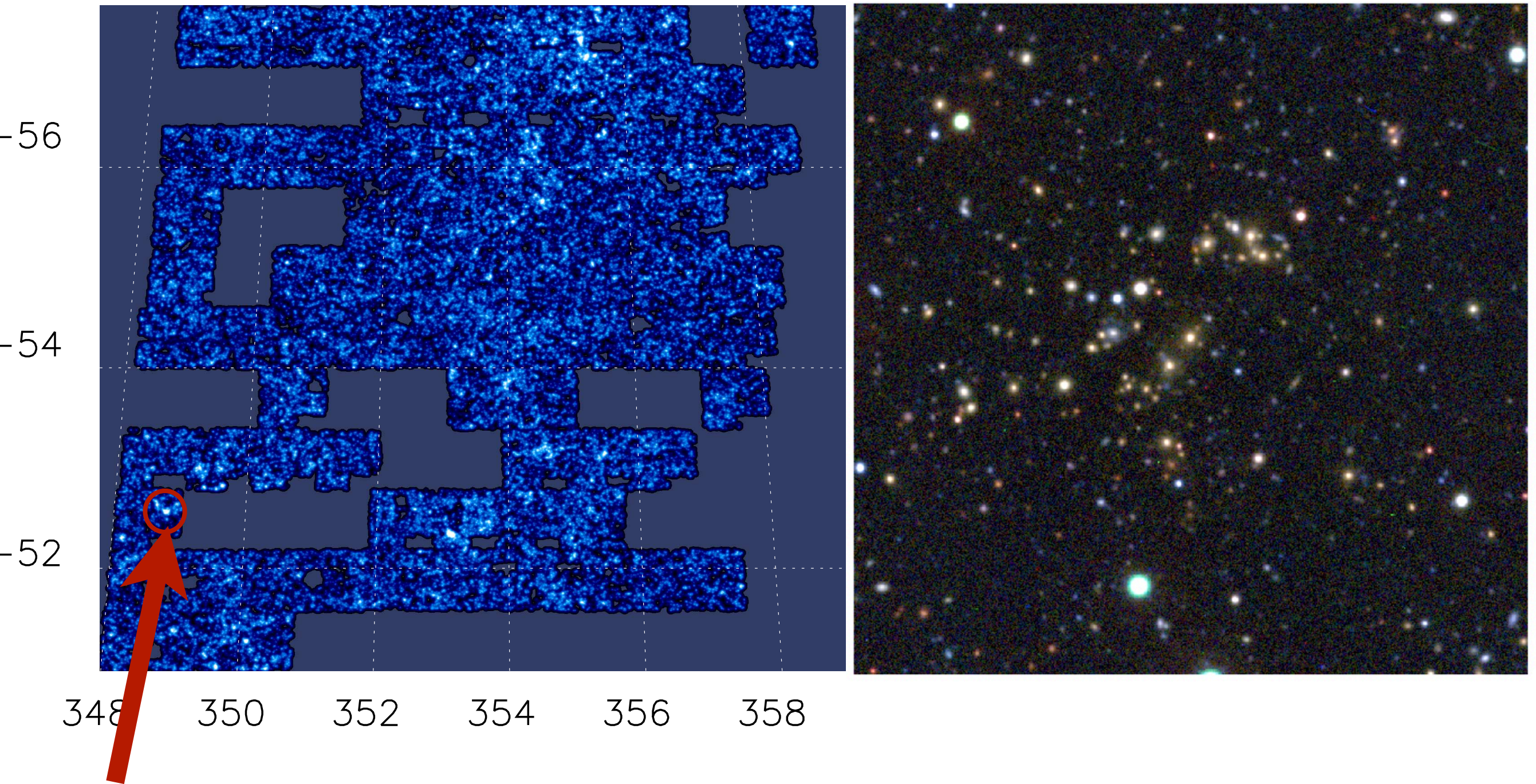


Example Cluster-finder Slice at $z=0.46$



Algorithm based on Gladders & Yee, 2000

Example Cluster-finder Slice at $z=0.46$



The Optical-Richness, λ , is a weighted galaxy count.

$$p(\mathbf{x}) = \frac{\lambda u(\mathbf{x}|\lambda)}{\lambda u(\mathbf{x}|\lambda) + b(\mathbf{x})}.$$

Probability of Cluster membership

Color, magnitude, radial filter

background density

$$\lambda = \sum p(\mathbf{x}|\lambda) = \sum_{R < R_c(\lambda)} \frac{\lambda u(\mathbf{x}|\lambda)}{\lambda u(\mathbf{x}|\lambda) + b(\mathbf{x})}$$

Here lambda is run after the cluster finder.

Rozo et al, 2009;
Rykoff et al 2012

But new cluster finder algorithm
redMaPPer
developed for DES by Rykoff et al

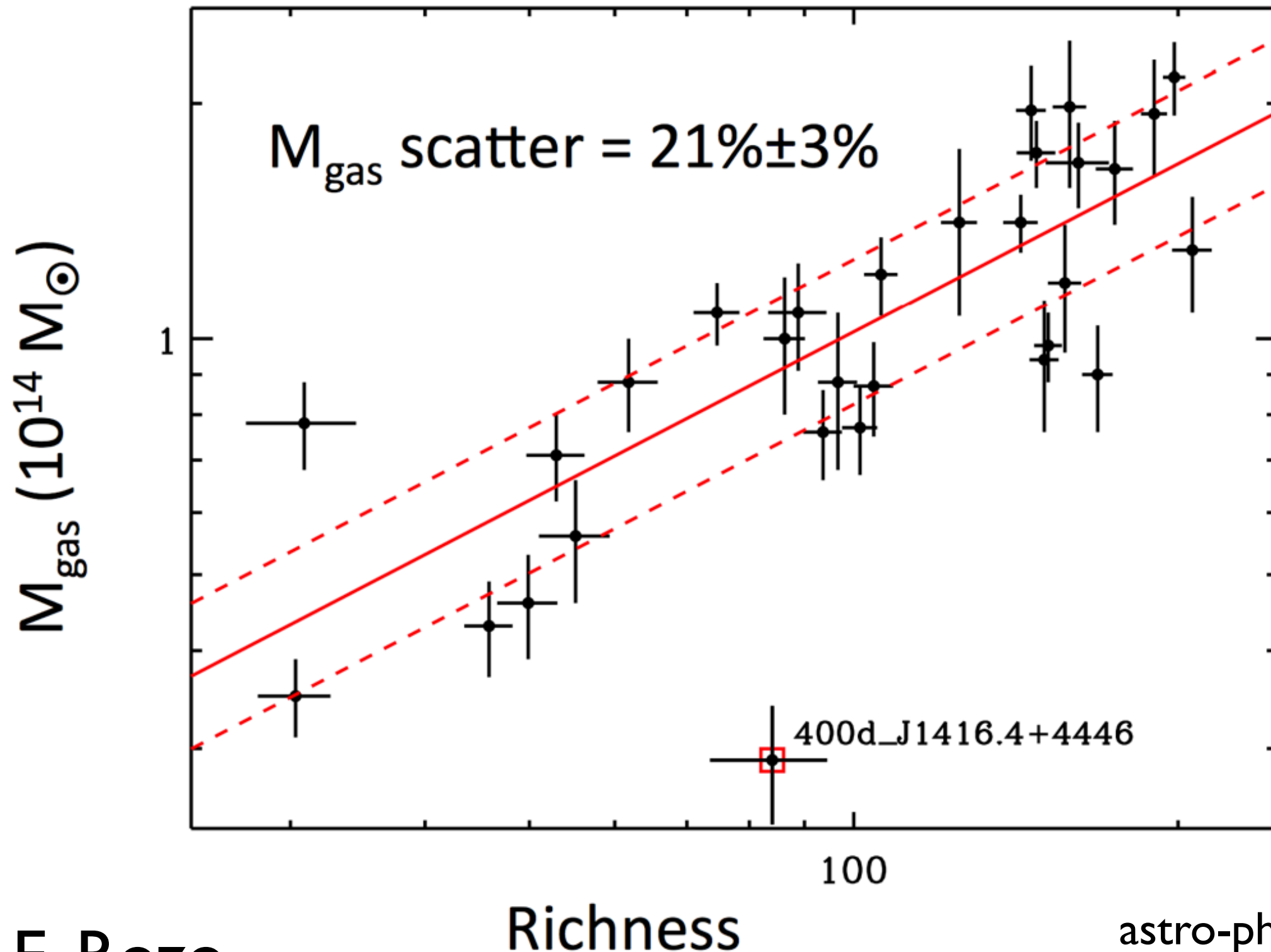


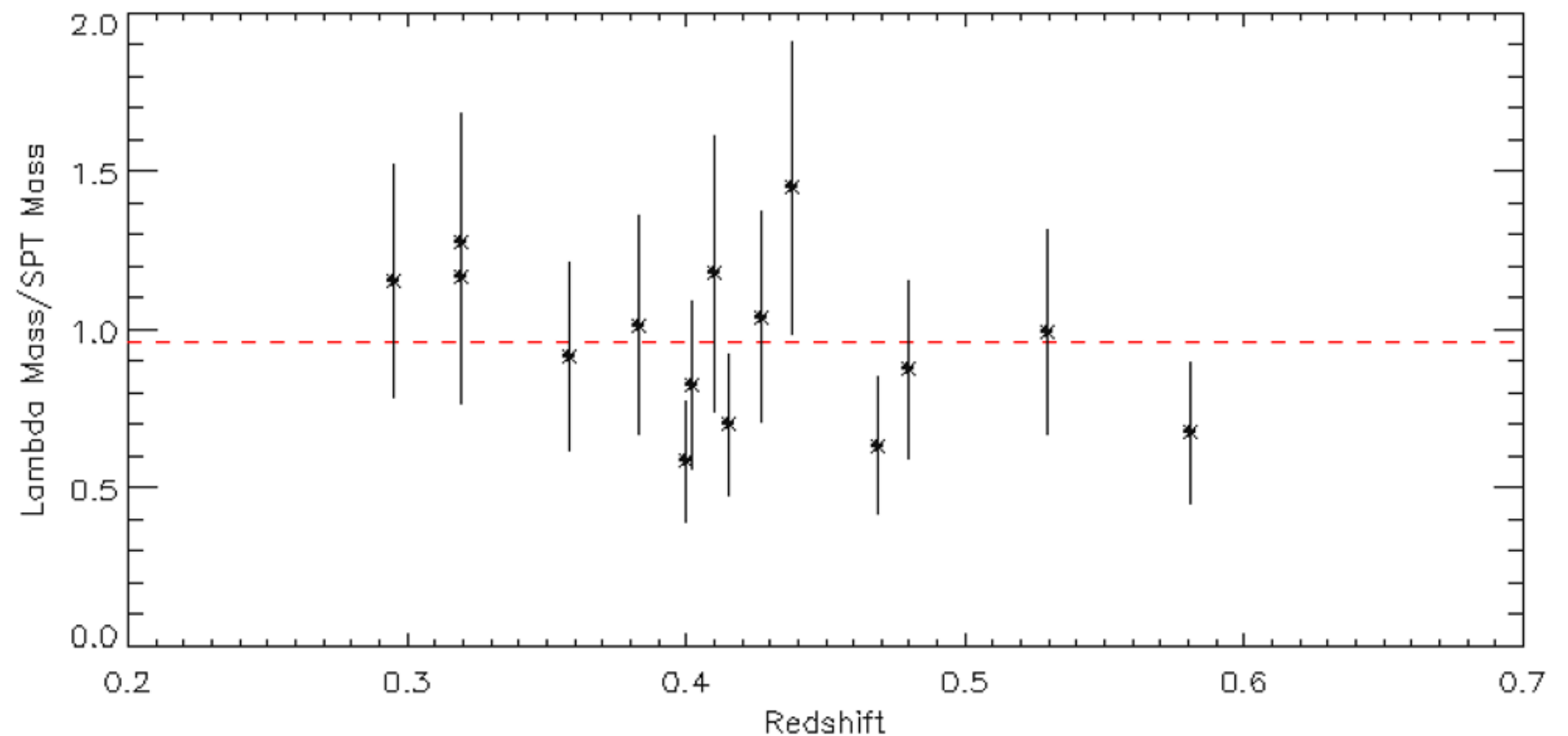
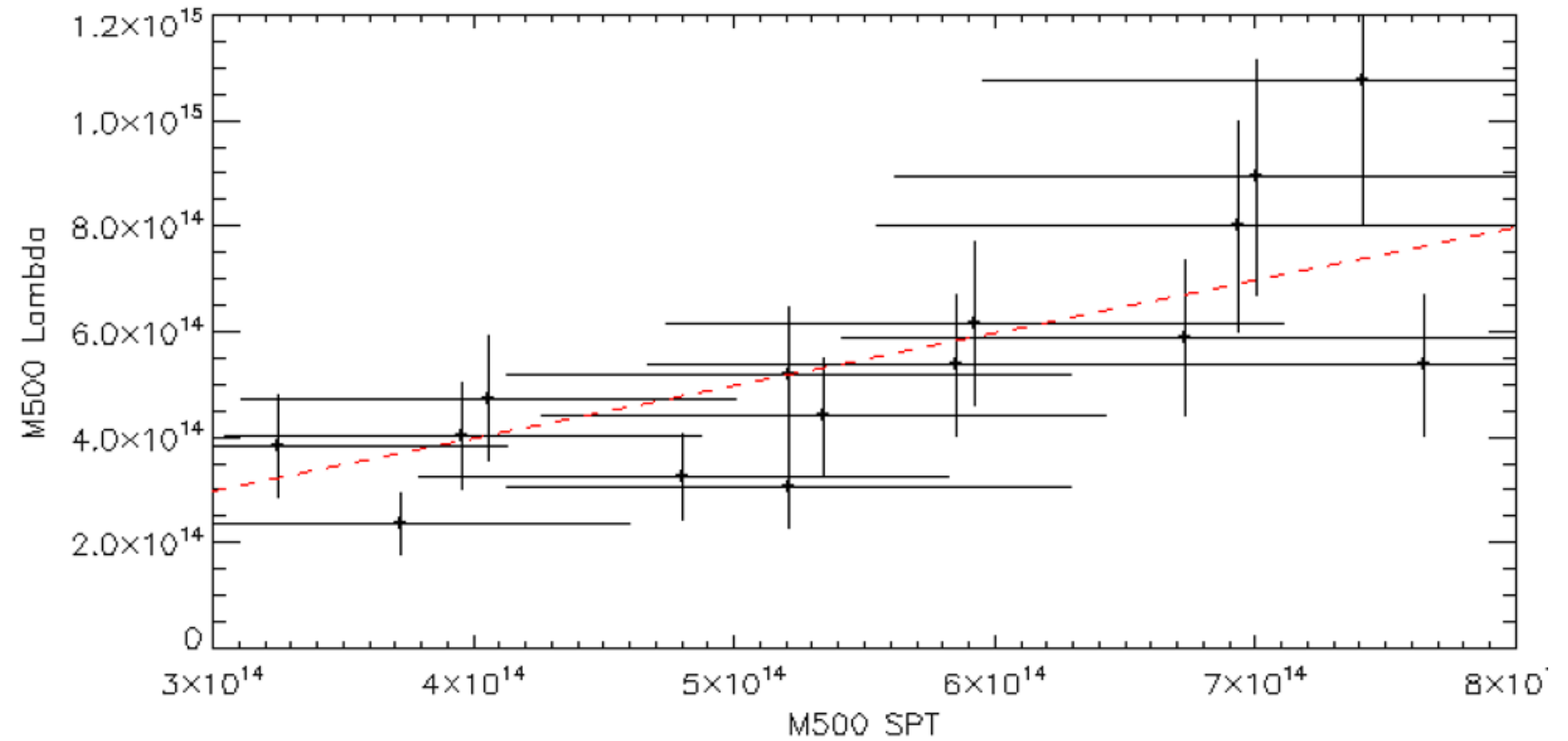
Image: E. Rozo

astro-ph/1303.3562
1303.3373

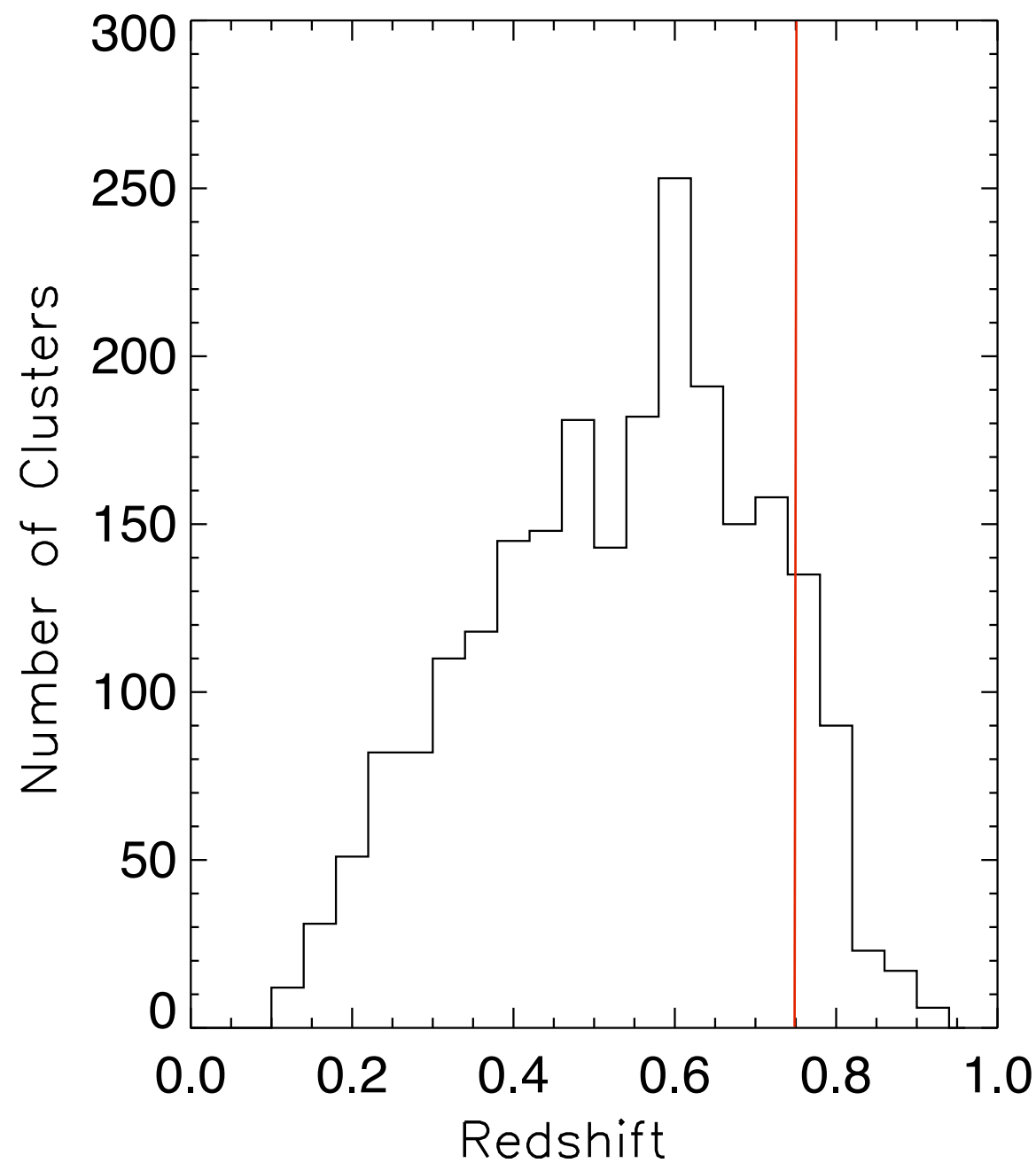
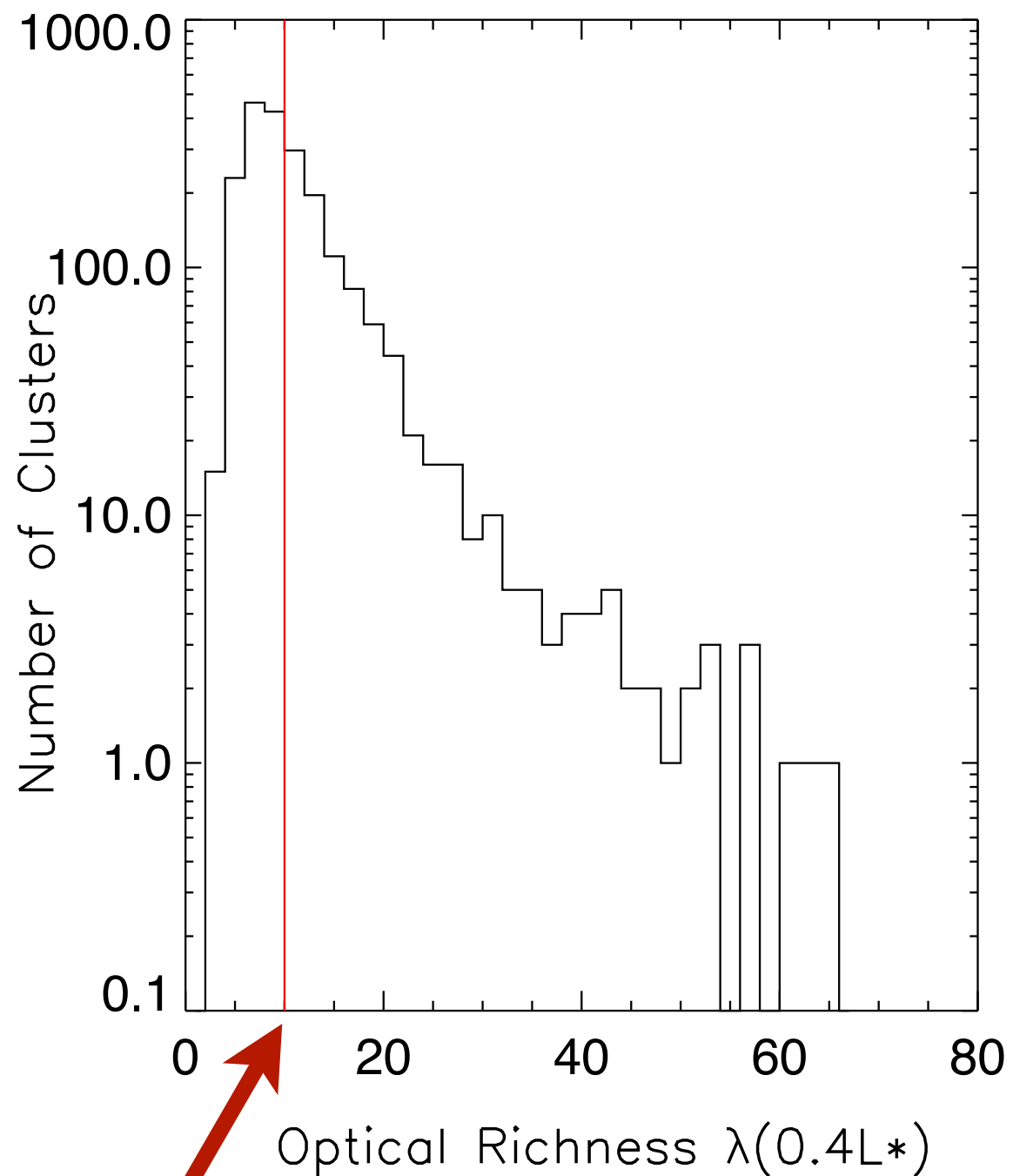
Back to our story ...

Excellent agreement at the high mass end when using the best fit SPT cosmology.

$$\langle M_{\Lambda}/M_{\text{SPT}} \rangle = 0.96 \pm 0.06$$



The BCS Cluster Sample

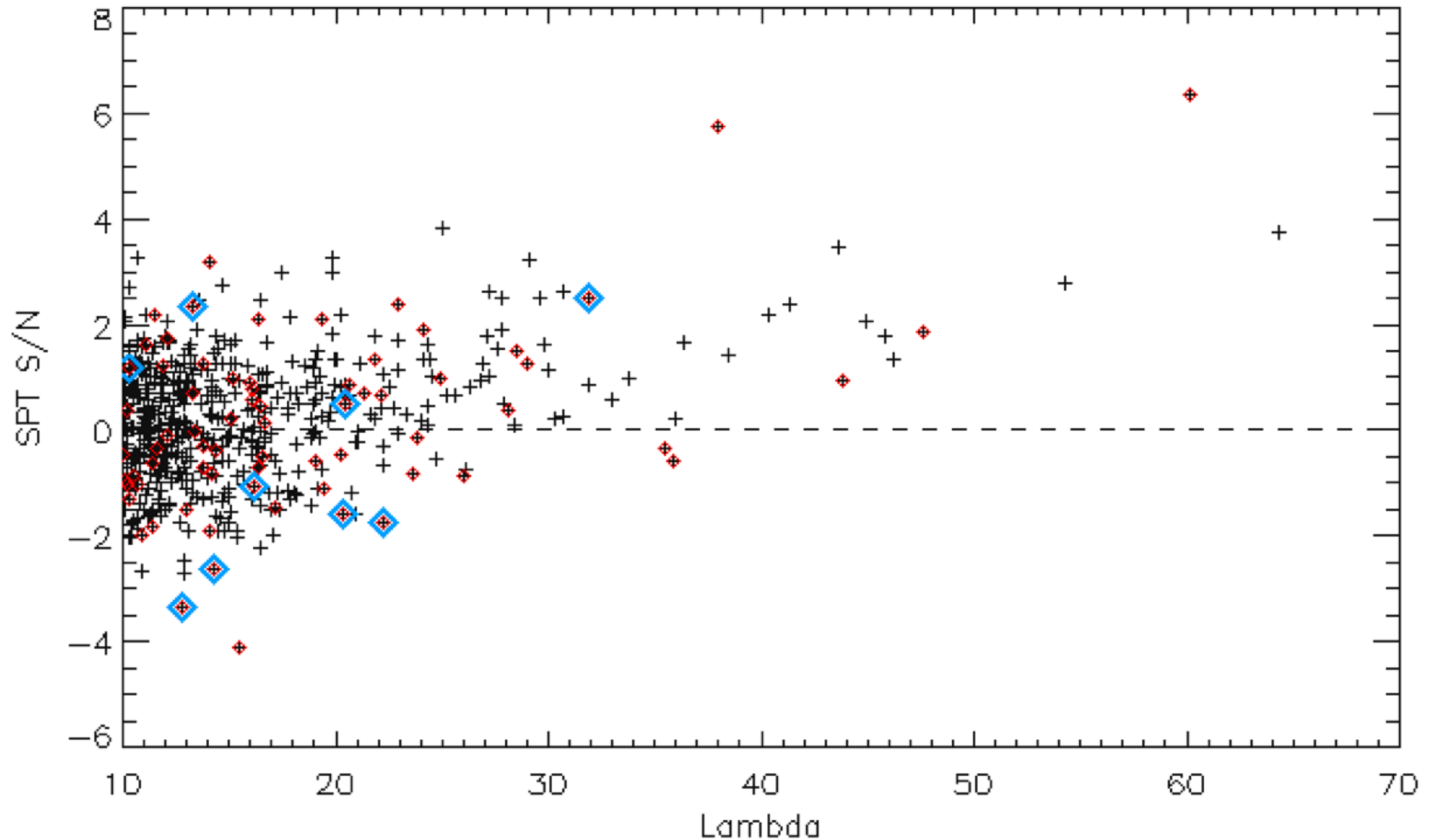


Median redshift: 0.55 and Median λ^* : 13.6

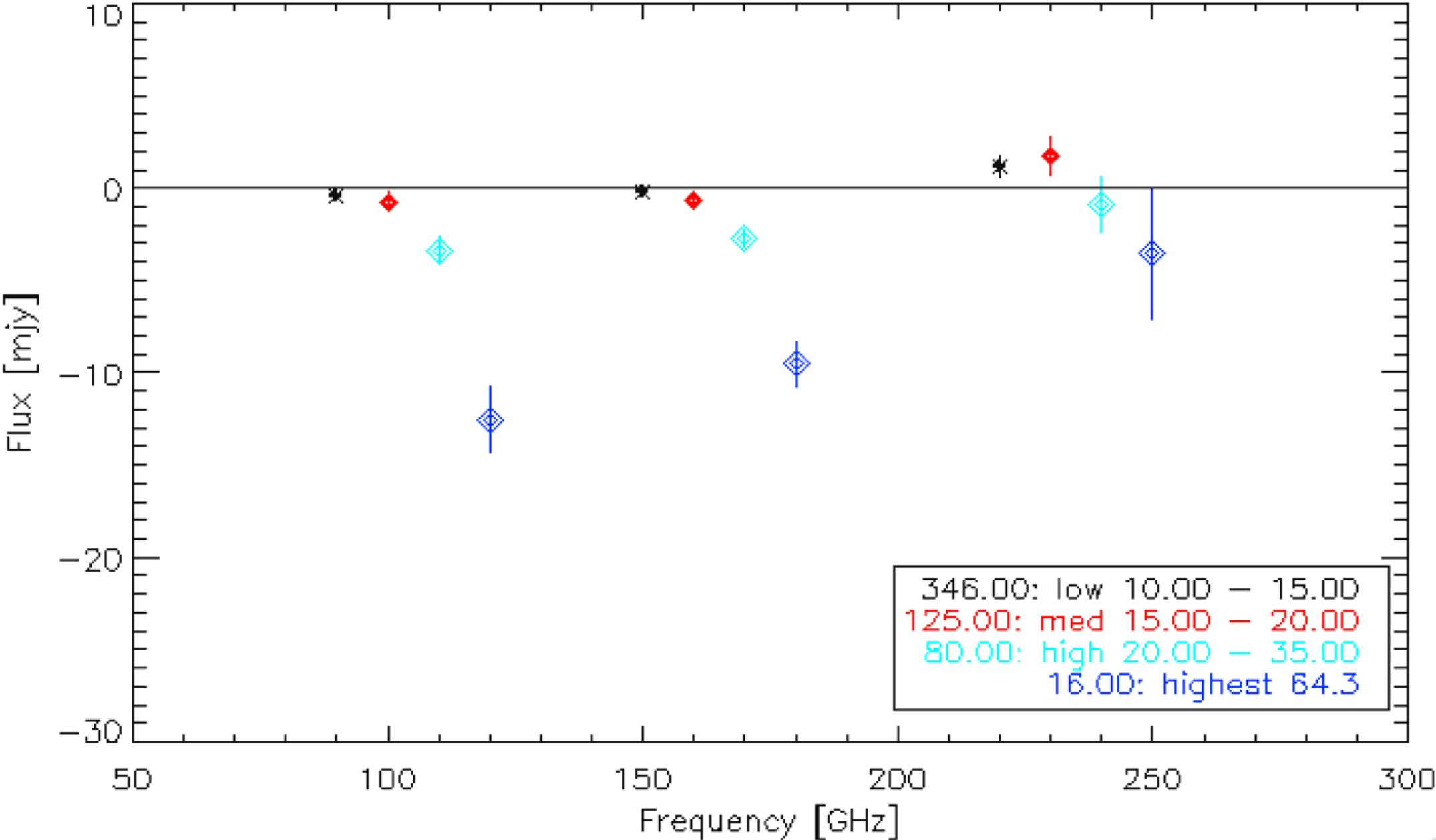
Catalog
Threshold

* $\lambda(0.4L^*)$

We filter the SPT-SZ maps at the cluster locations to extract the cluster signal.



Stacking the data to boost the signal-to-noise



λ -mass



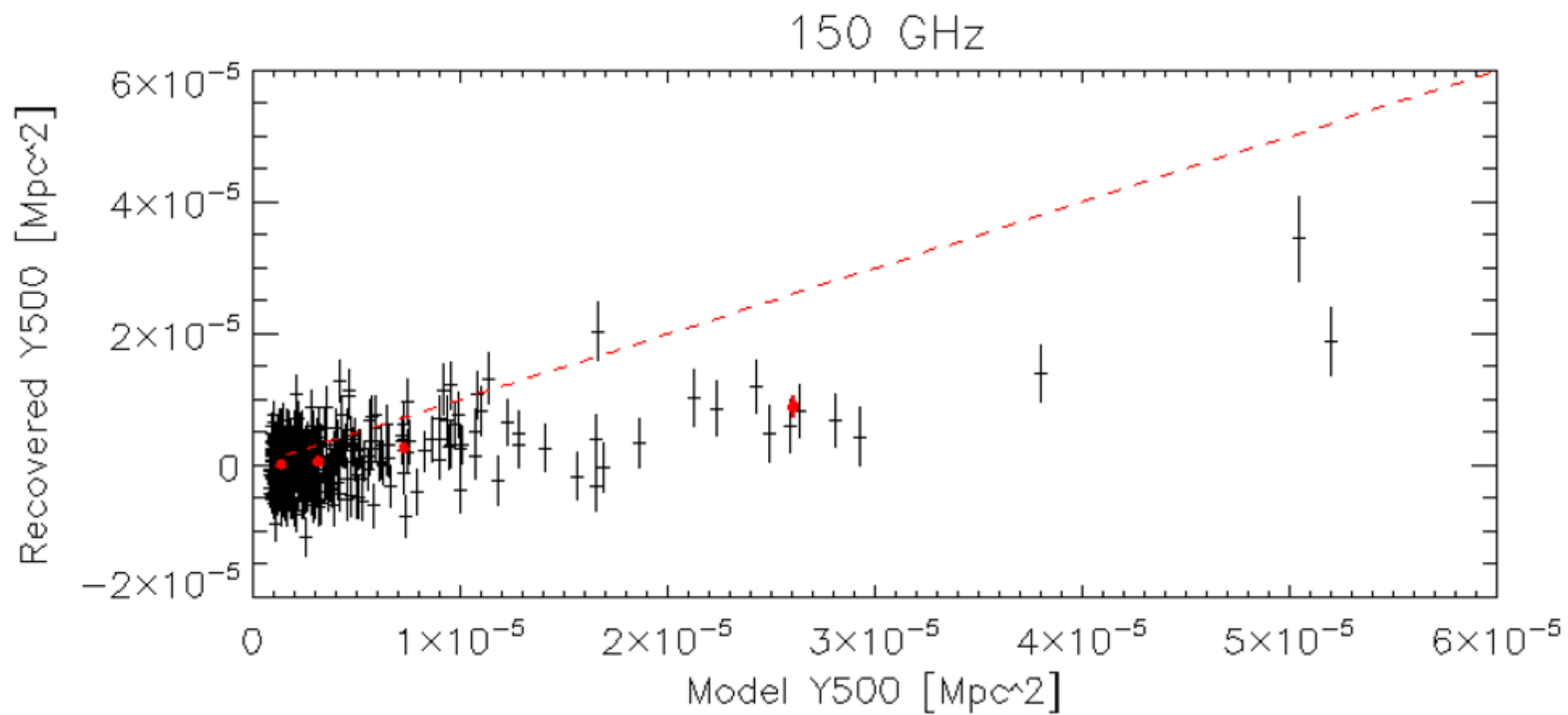
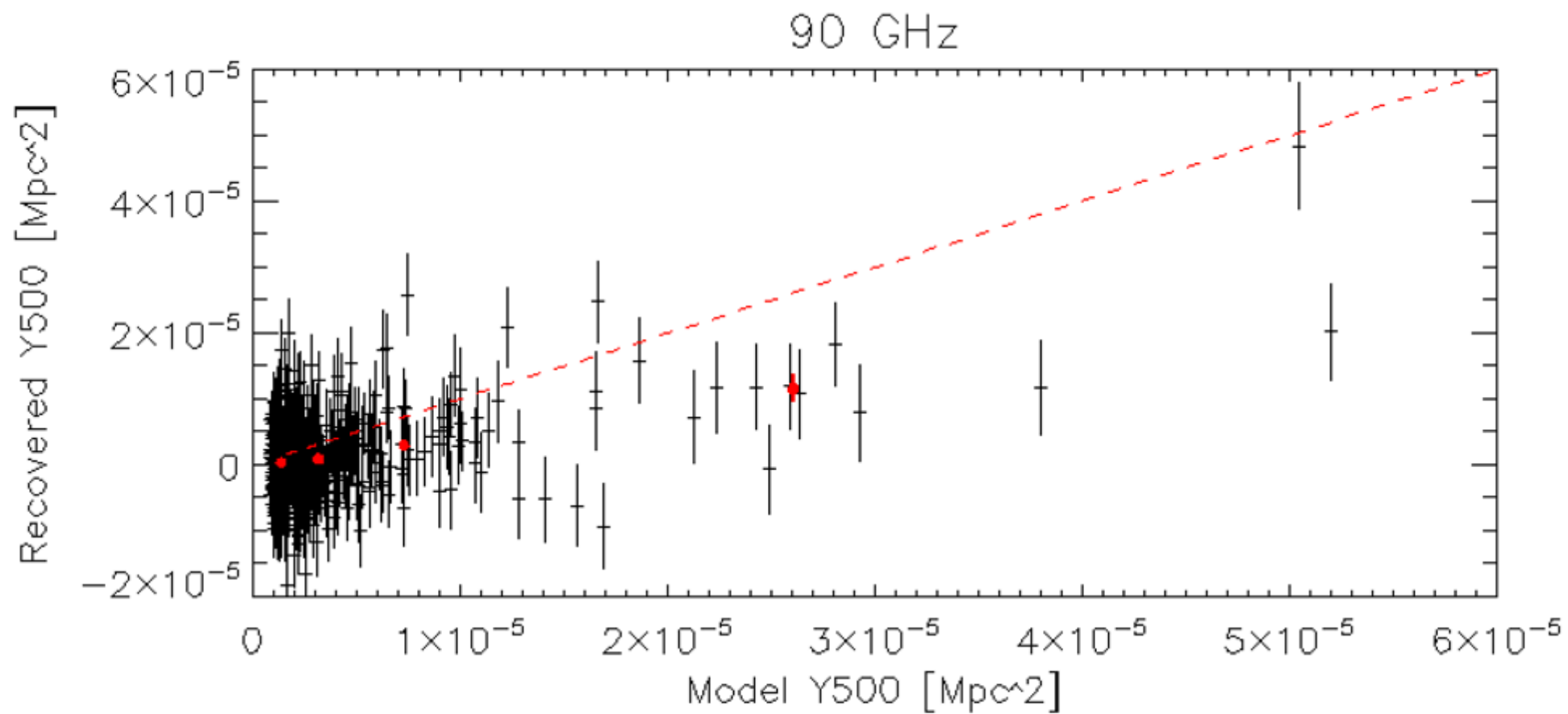
Arnaud Model

$$Y_{500} = h(z)^{2/3} A_x \left(\frac{M_{500}}{3 \times 10^{14} h_{70}^{-1} M_{\odot}} \right)^{\alpha} h_{70}^{-5/2}$$



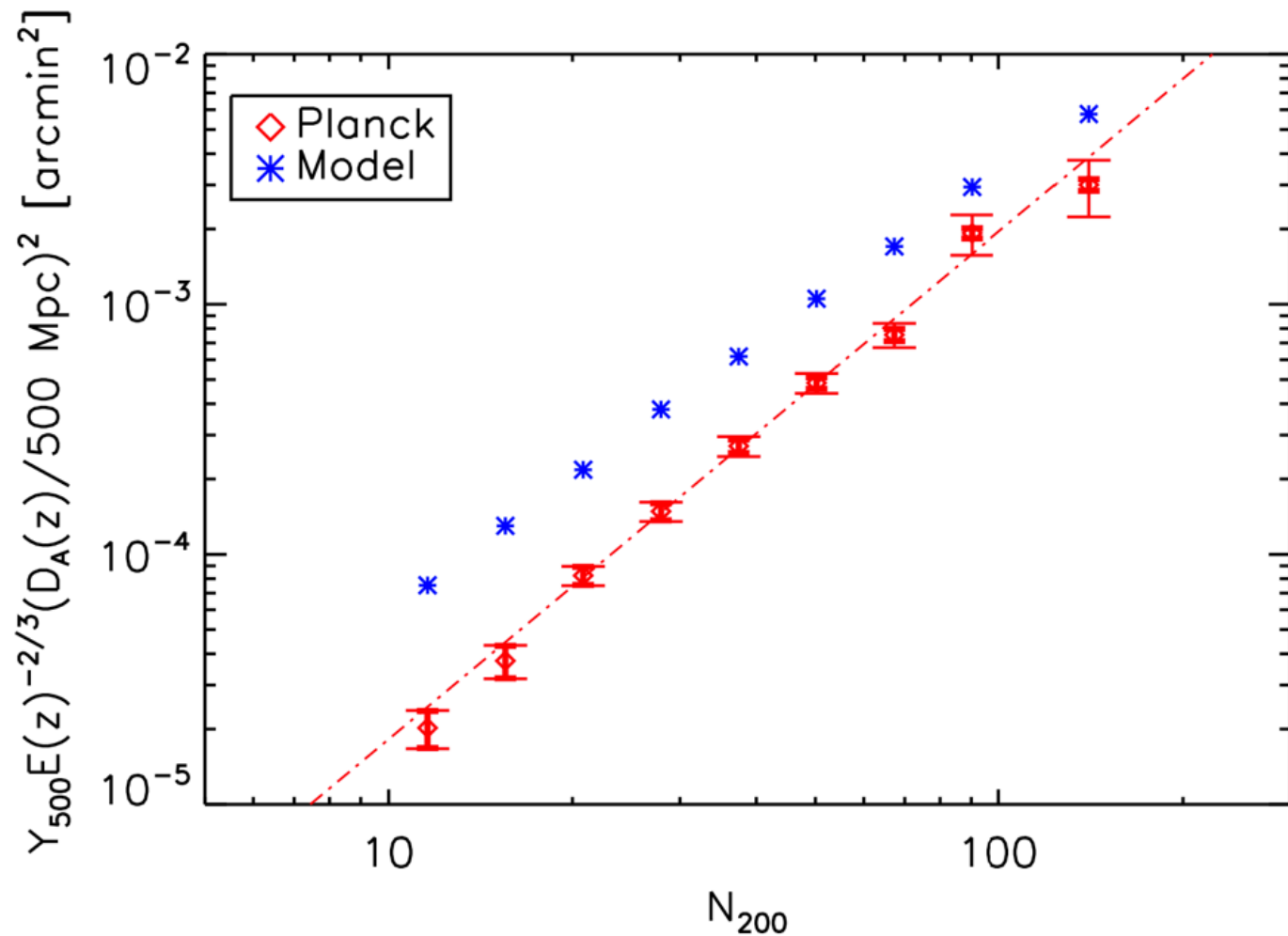
Expected Signal

$$A_x = 10^{-4.739}, \alpha = 1.79, h(z) = H_0 [\Omega_m (1+z)^3 + \Omega_{\Lambda}]^{1/2}, H_0 = 72.5 \text{ km/s/Mpc}$$

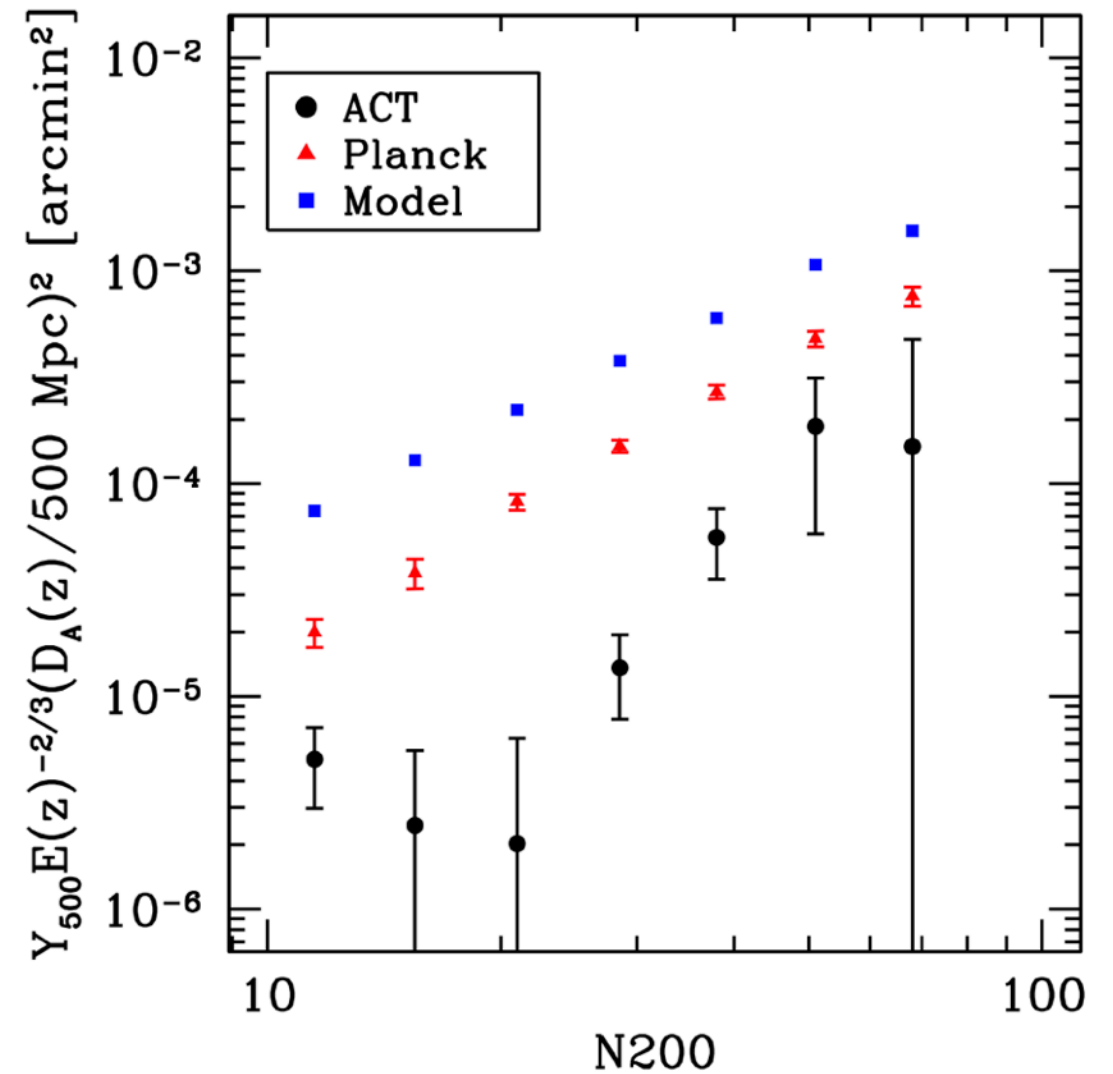


What happened?

We have seen this before (?)

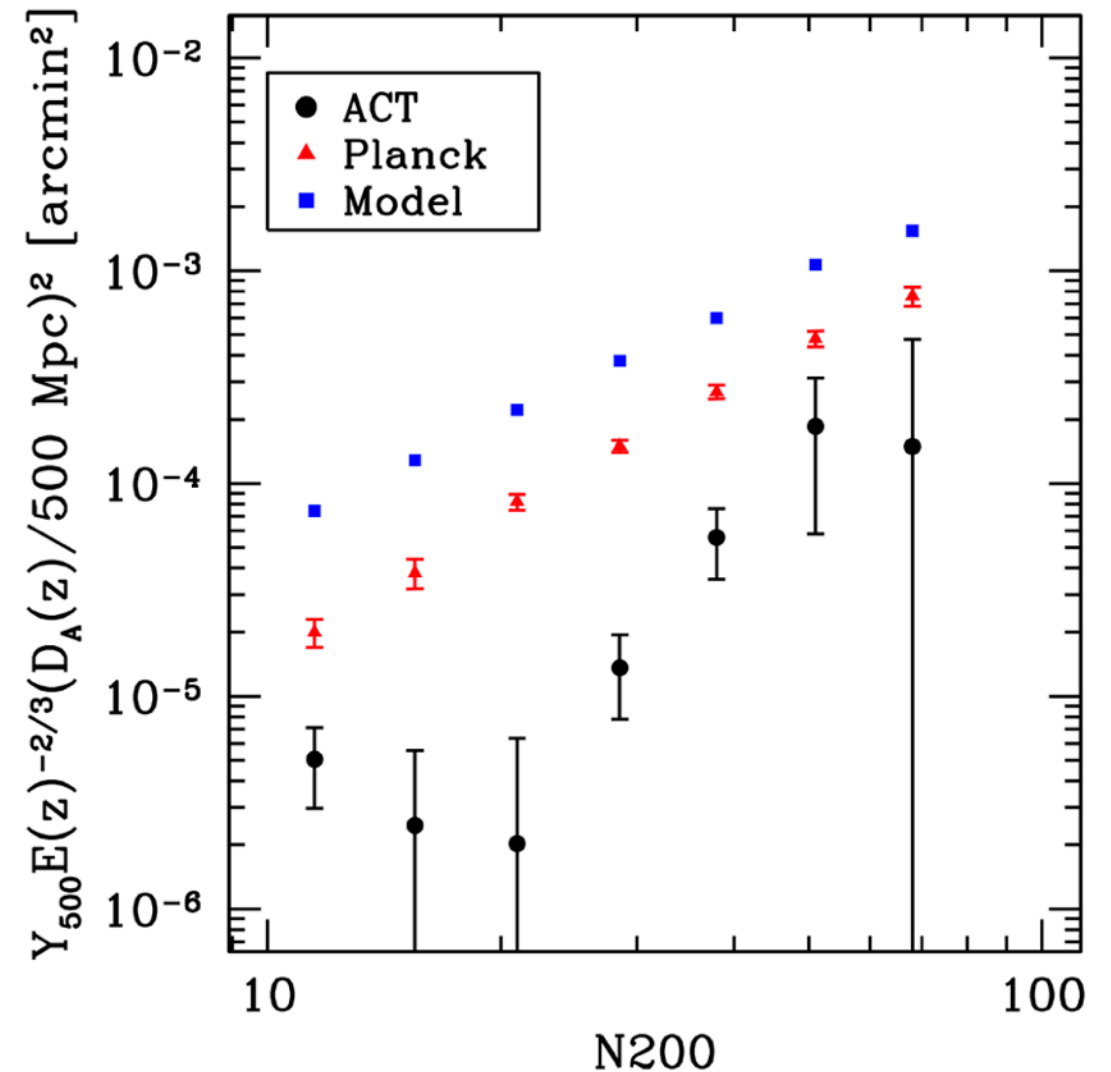
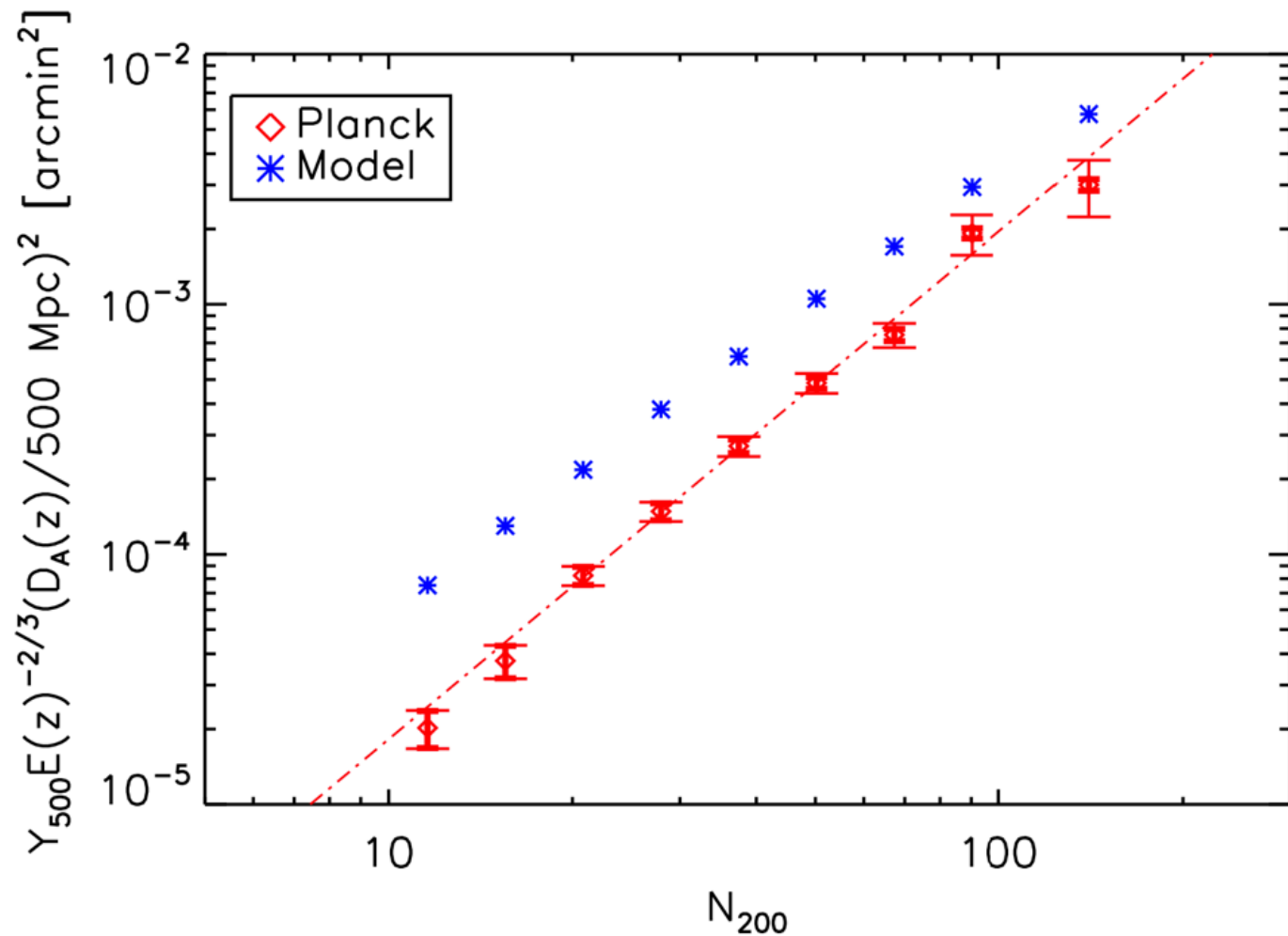


Planck Collaboration,
Planck2011-5.2c



Sehgal et al 2013
(1205.2369)

We have seen this before (?)



See:

Biesiadzinski et al. 1201.1282

Angulo et al. 1203.3216

Rozo et al. 1204.6305

SZ contamination?

Radio Sources? No.

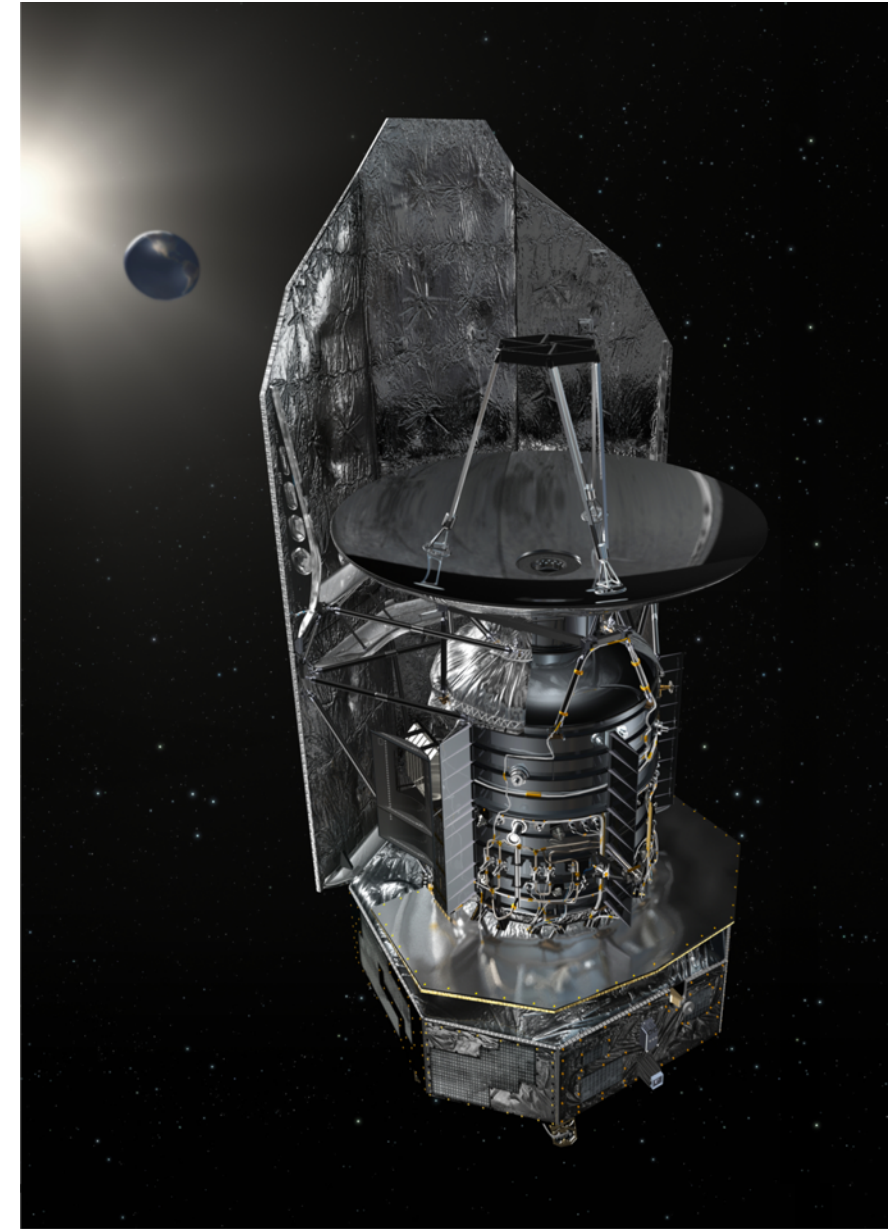
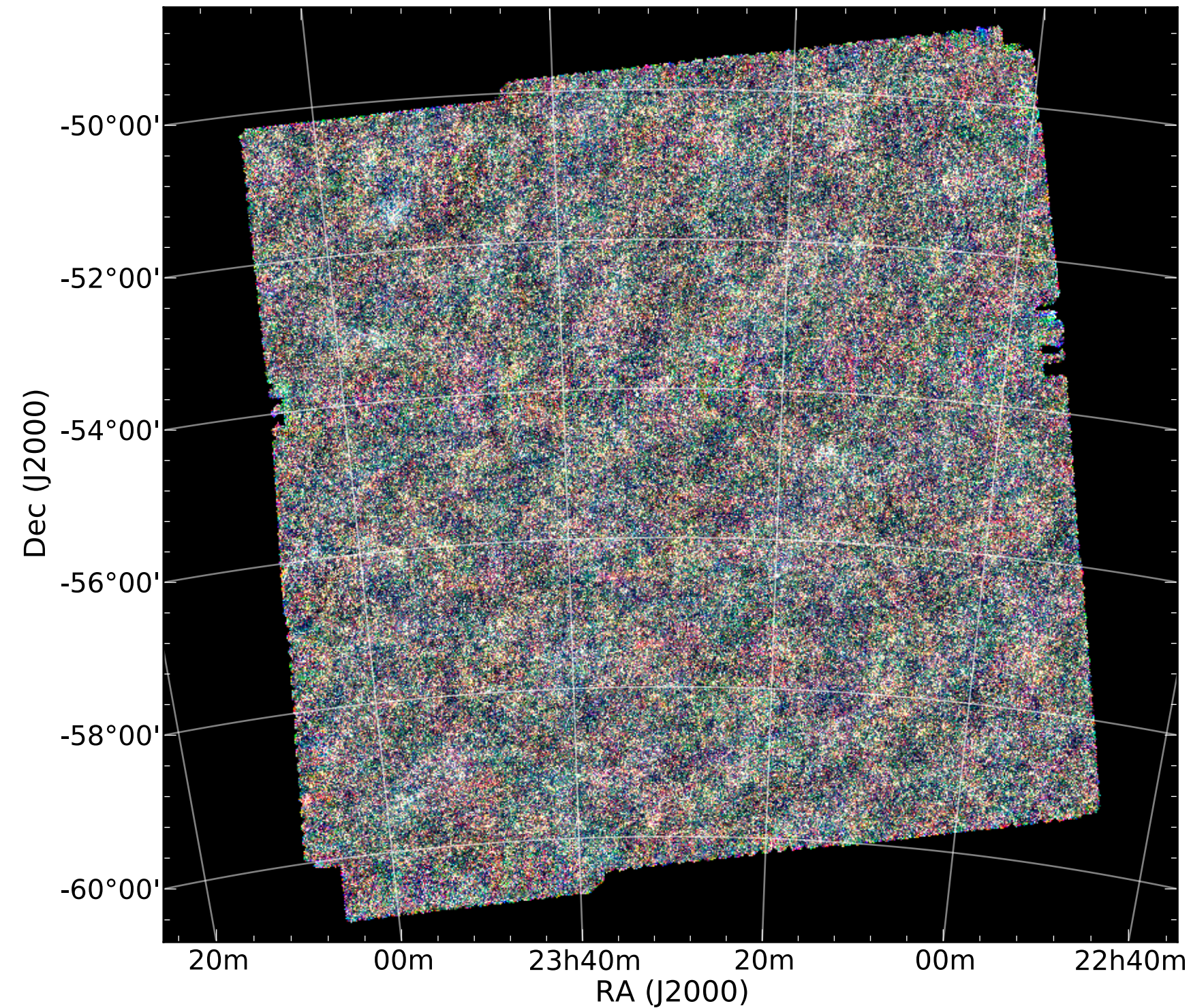
Sydney University Molonglo Sky Survey (SUMSS), (Mauch et al., 2003)

Complete to 8 mJy at 845 MHz

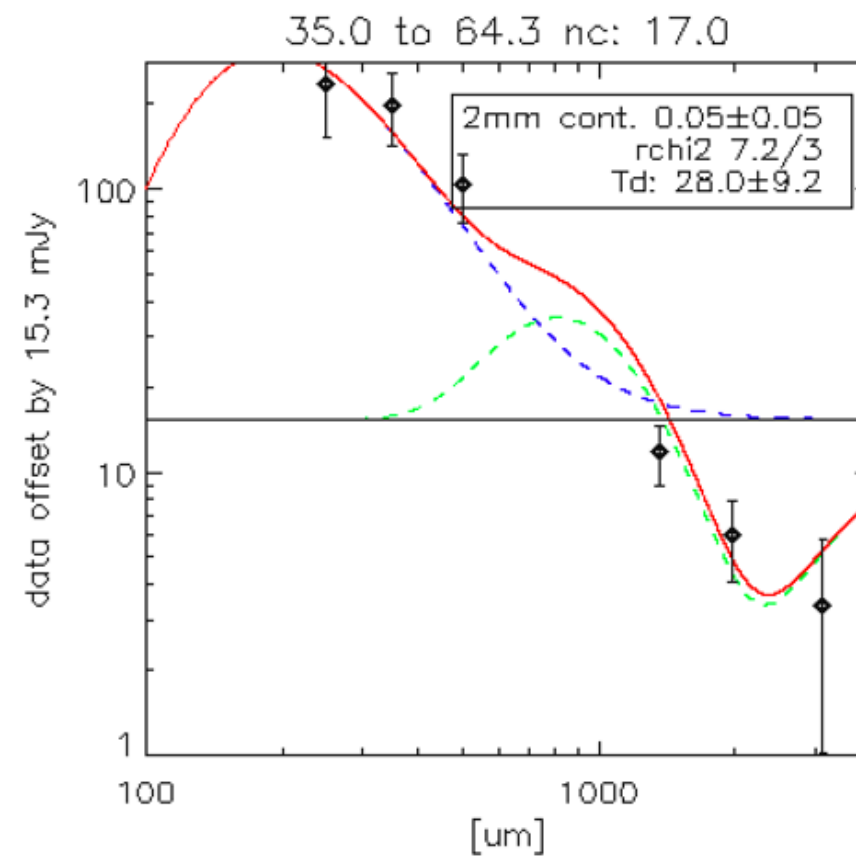
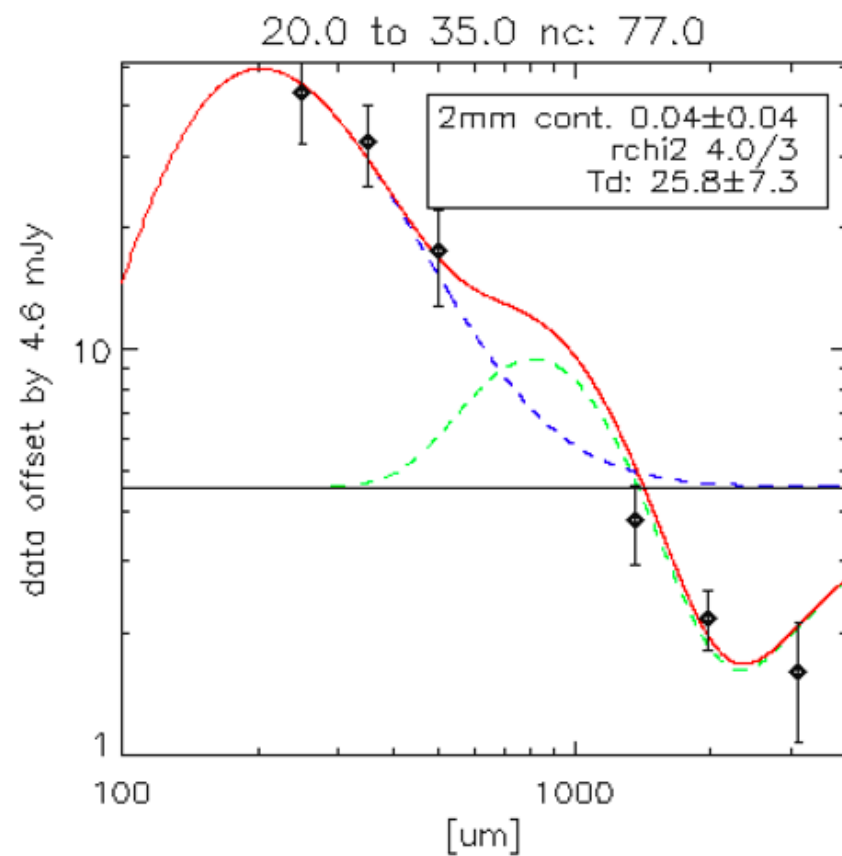
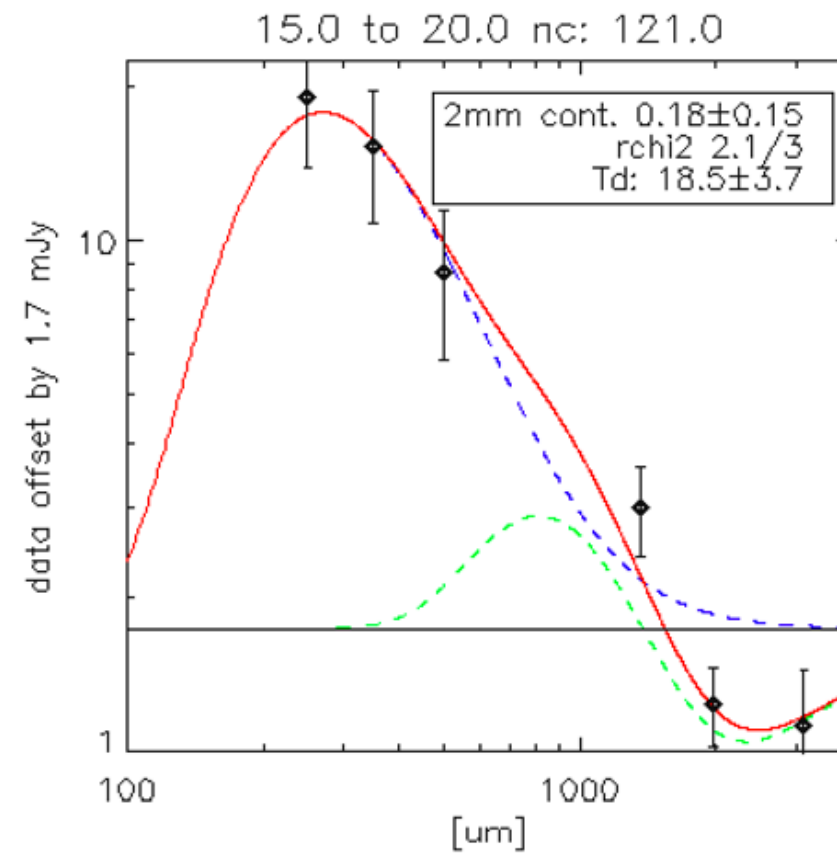
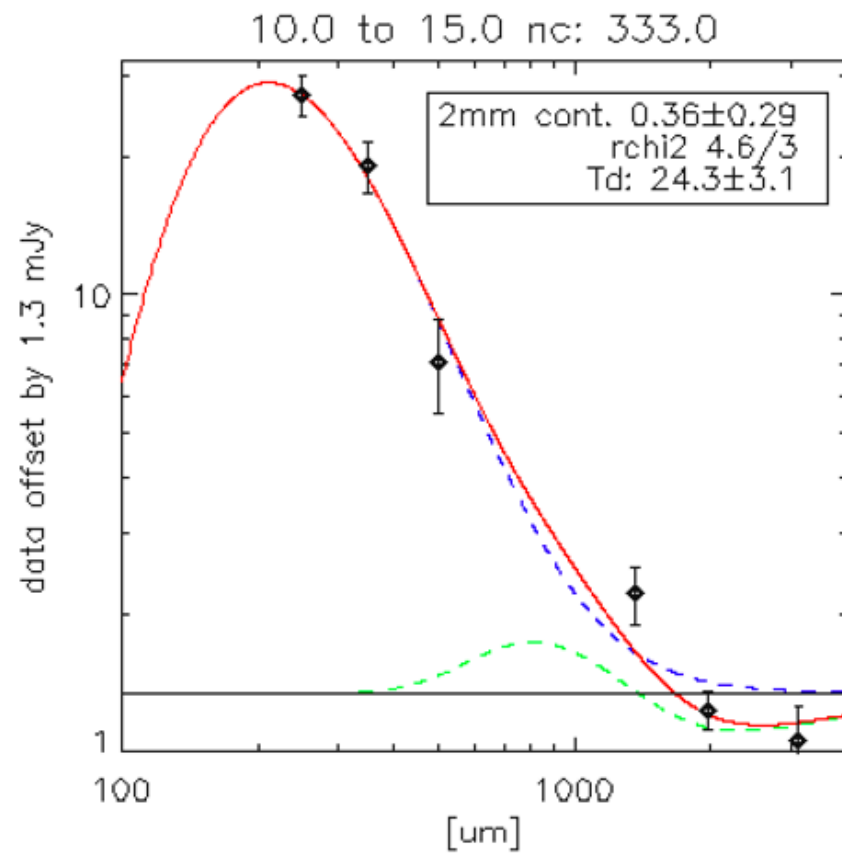
$$S_{96\text{GHz}} = S_{845\text{MHz}} \left(\frac{845 \text{ MHz}}{96 \text{ GHz}} \right)^\alpha$$

λ	M_{500}	N_{sys}	N_{Radio}	845 MHz (mJy)	SPT 96 GHz (mJy)	$\alpha = 1$	$\alpha = 1/2$
10 – 15	6.5e13	333	30	1596	-114 ± 95	13%	62%
15 – 20	1.0e14	121	16	454	-90 ± 62	5%	37%
20 – 35	1.6e14	77	18	1410	-260 ± 55	6%	38%
35 – 65	3.3e14	17	6	241	-224 ± 29	1%	11%

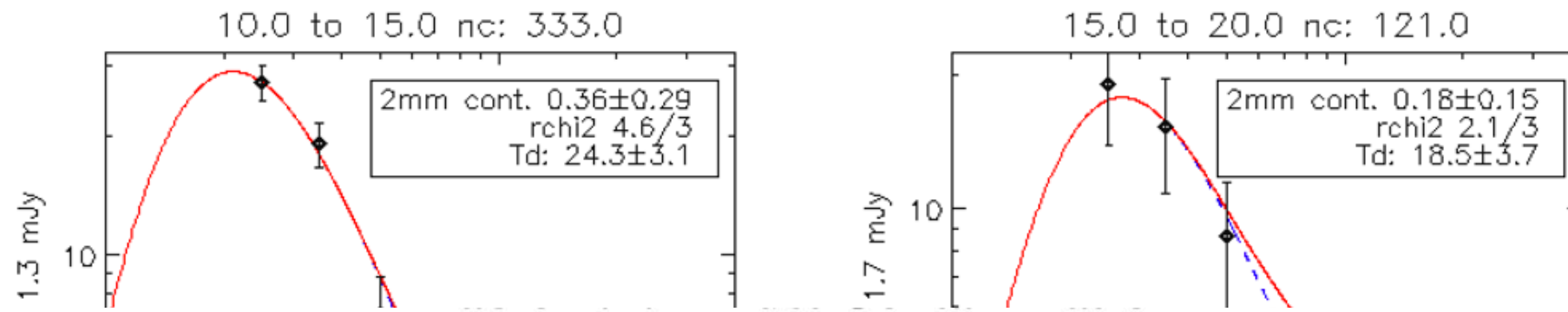
Dust? Check with submm-data from *Herschel*/ SPIRE in the 23 h field



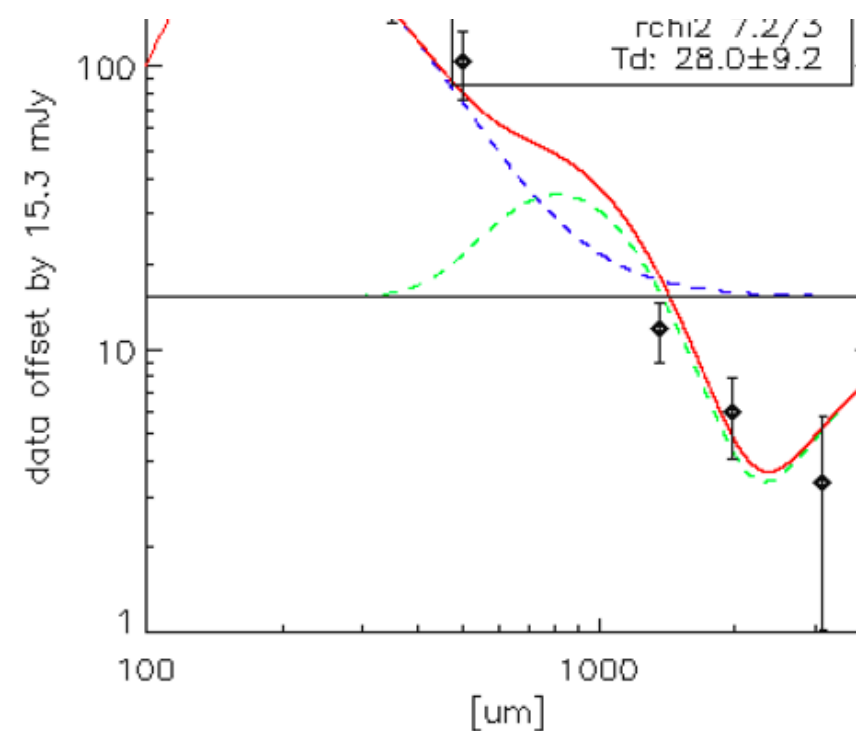
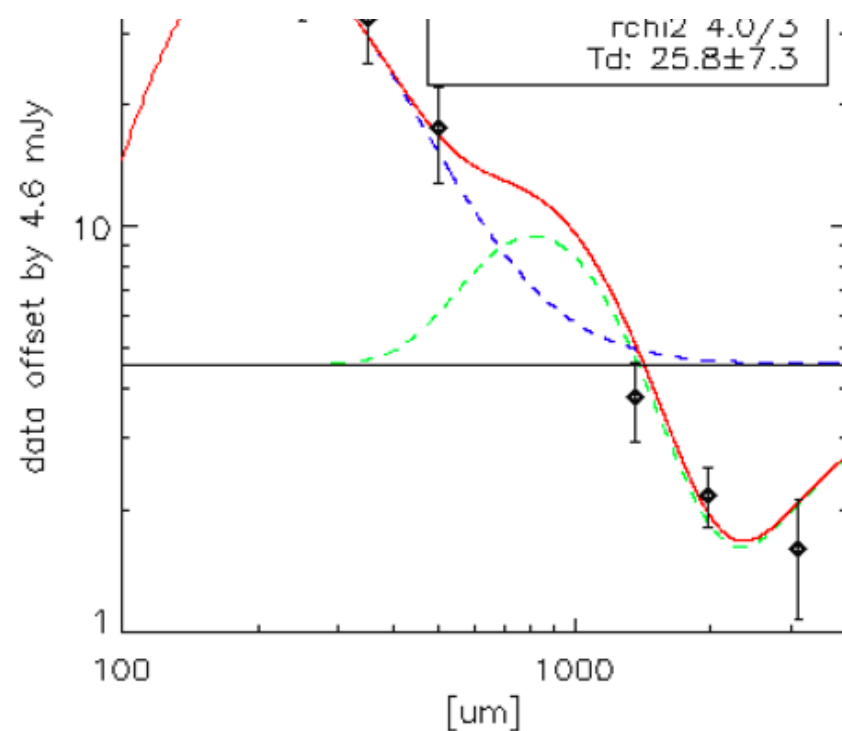
Dust contamination? No.



Dust contamination? No.



λ	M_{500}	N_{sys}	N_{SPIRE}	T_{dust}	Contamination	Contamination _{25K}
10 – 15	$6.5e13$	333	165	24 ± 3	0.4 ± 0.3	0.34 ± 0.26
15 – 20	$1.0e14$	121	51	19 ± 4	0.2 ± 0.15	0.10 ± 0.06
20 – 35	$1.6e14$	77	35	26 ± 7	0.04 ± 0.04	0.04 ± 0.02
35 – 65	$3.3e14$	17	11	28 ± 9	0.05 ± 0.05	0.06 ± 0.03

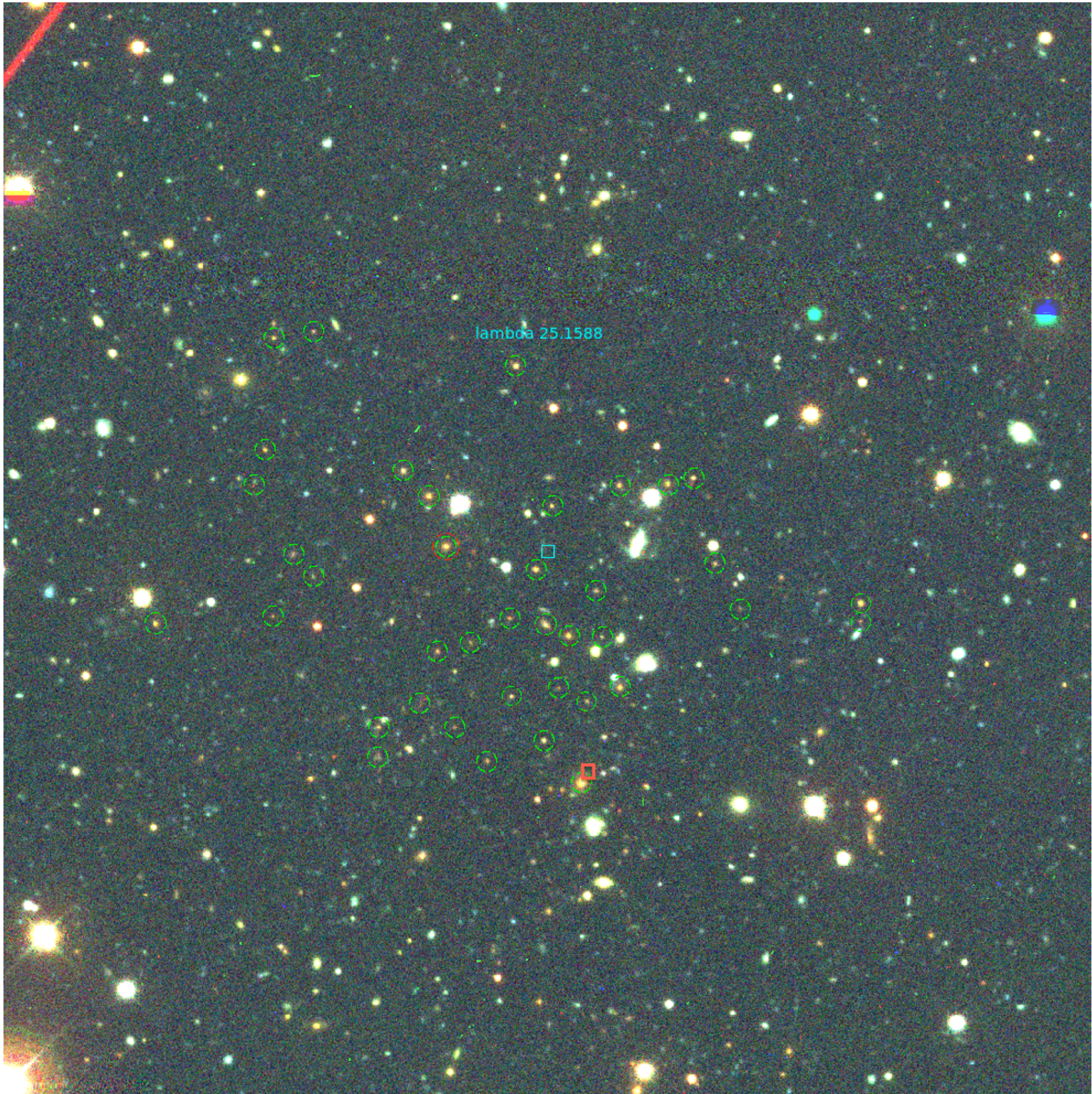


Optical Tracer?

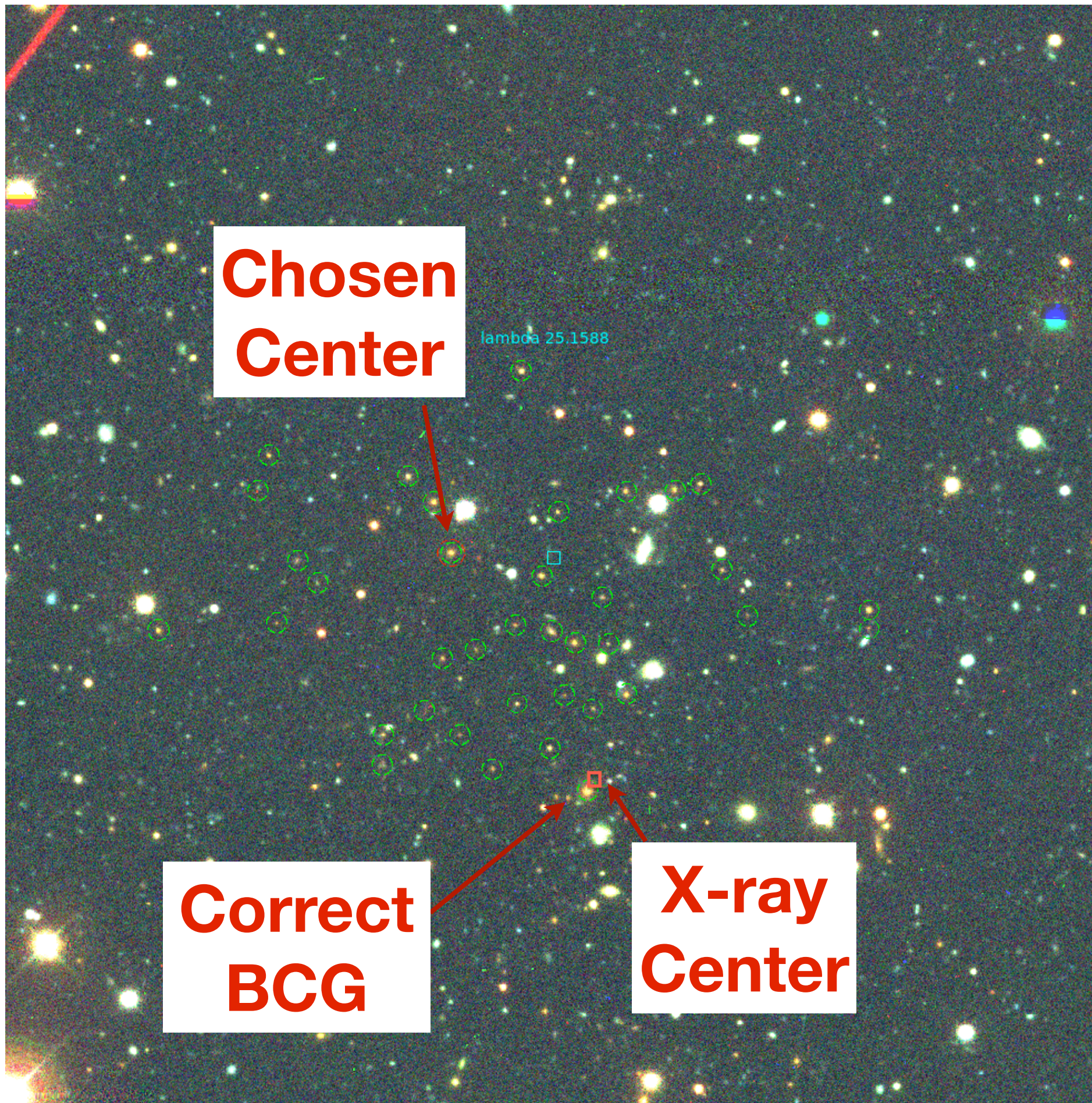
Optical Tracer?

- Mass Calibration?
 - Good agreement at high-mass end and Eddington bias insufficient to explain discrepancy
 - Overall sample is lower mass, higher redshift (and different photometry) than SDSS cluster sample used to calibrate λ
- What about optical centers?
 - ratio of recovered $Y(90\text{GHz})/Y(150\text{GHz}) \sim 4/3$!? ?!
 - for X-ray and SZ samples ratio 1.

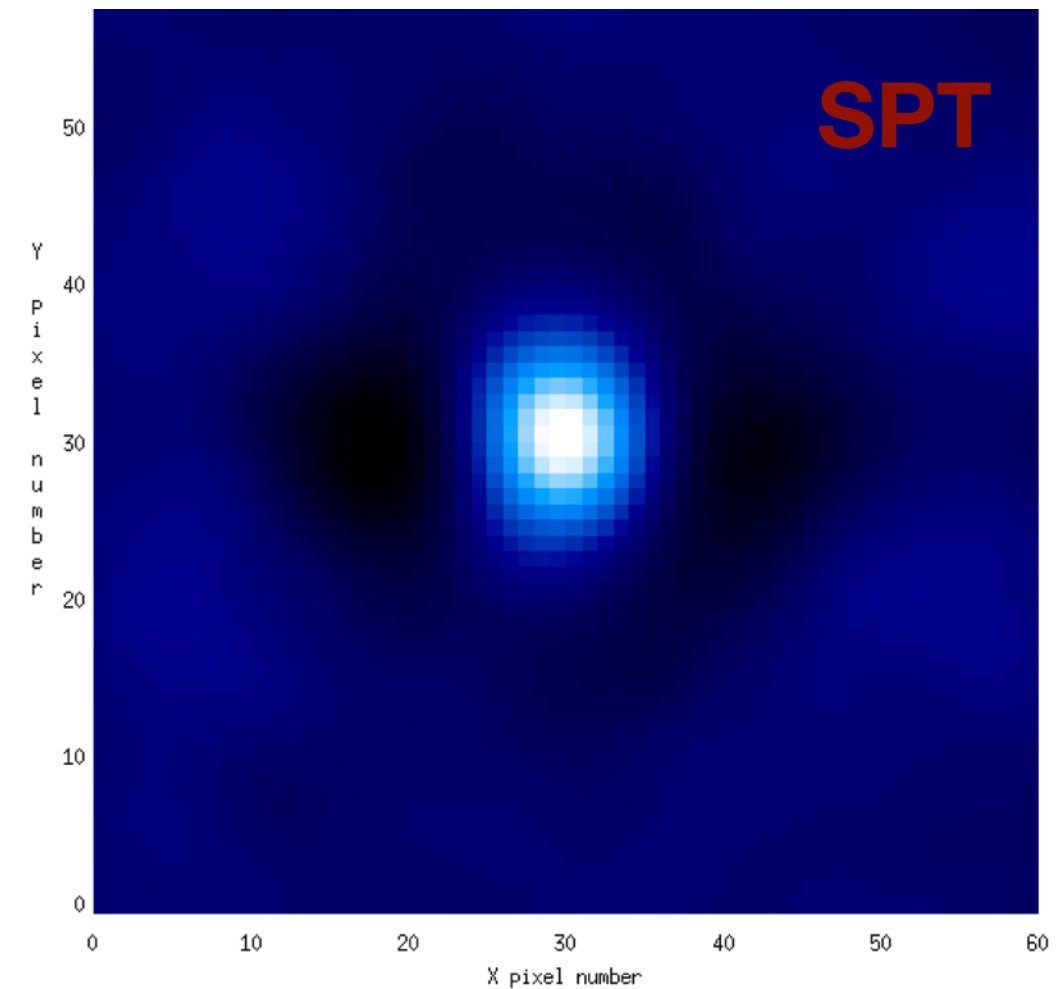
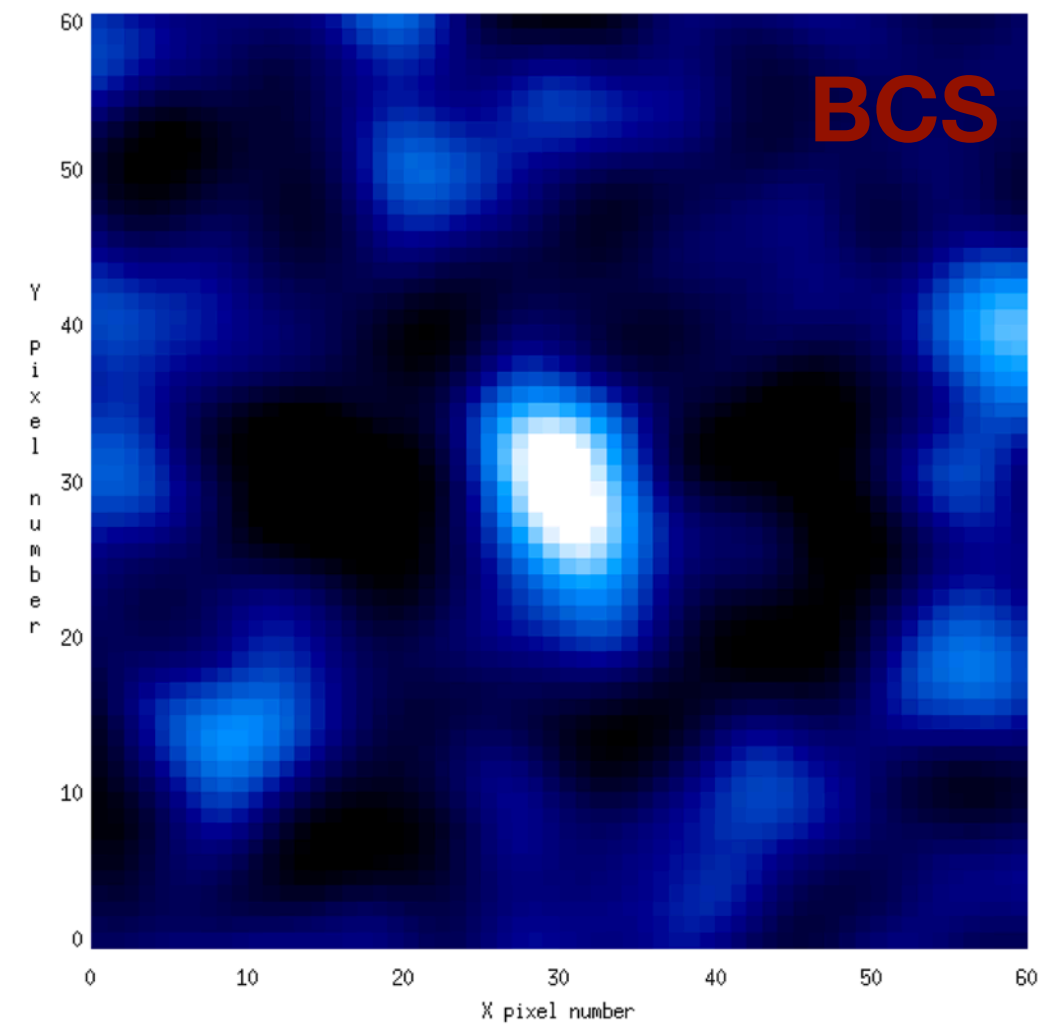
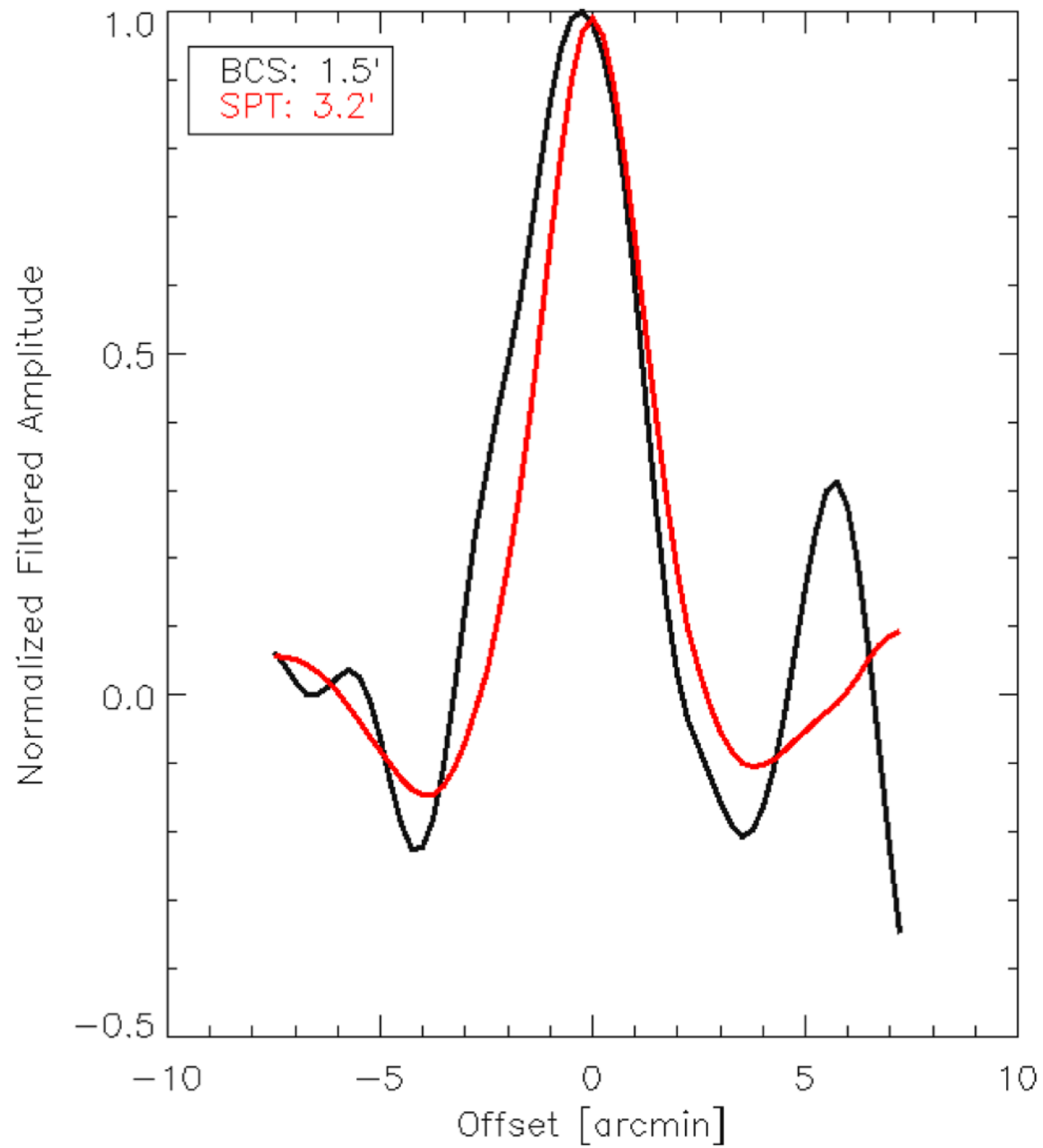
Miscentering: Maybe?



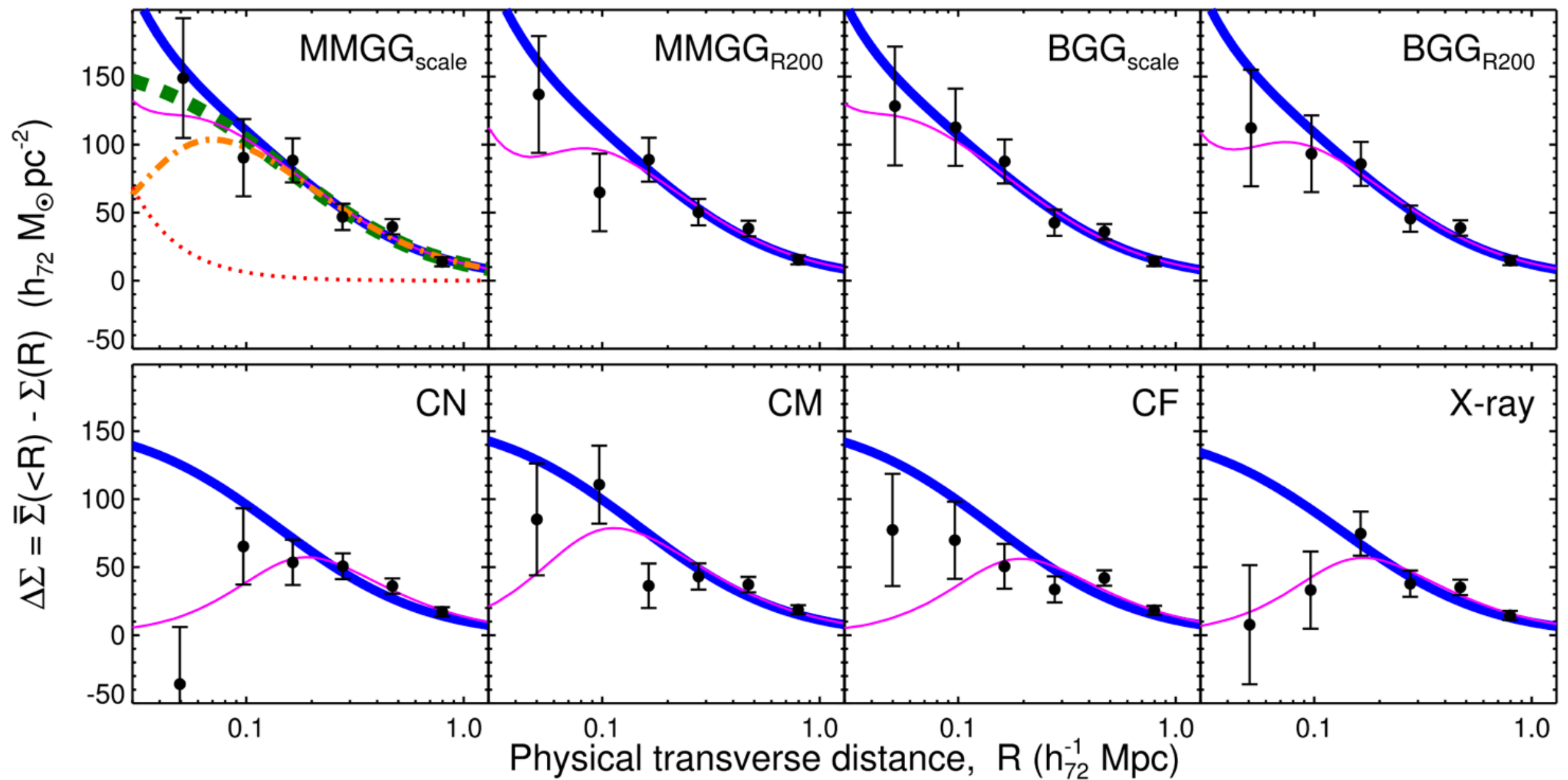
Miscentering: Maybe?



Miscentering: Maybe?



In the future can combine with
weak lensing observations.



George et al. 1205.4262

Conclusions

- Clusters are powerful tools to test models of dark energy.
- Full 2500d SPT-SZ Cluster catalog coming soon!
- Large optically-selected cluster catalogs from DES on the horizon.
- Joint analyses provide important tests for systematics and tighter cosmological constraints.

Thanks!

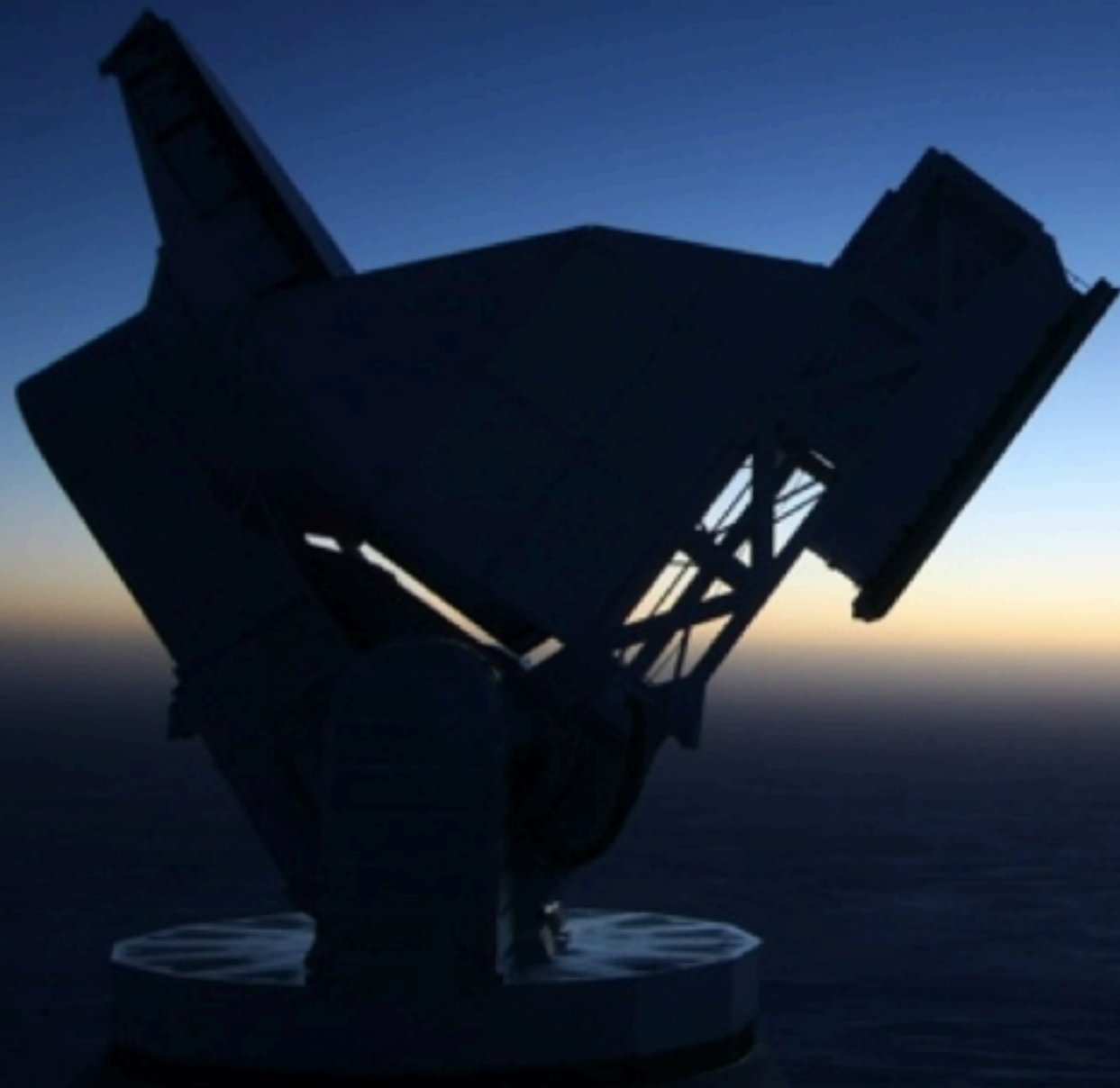


Photo credit: Keith Vanderlinde